Predator diversity and ecosystem functioning: An allometric approach

Vom Fachbereich Biologie der
Technischen Universität Darmstadt
zur Erlangung des akademischen Grades eines

Doctor rerum naturalium

genehmigte Dissertation von

Dipl.-Biol. Florian Dirk Schneider

aus Darmstadt

Berichterstatter: Prof. Dr. Ulrich Brose
Mitberichterstatter: Prof. Dr. Nico Blüthgen
Tag der Einreichung: 07.09.2012
Tag der mündlichen Prüfung: 30.11.2012

Darmstadt, 2012
D17

TECHNISCHE
UNIVERSITÄT
DARMSTADT

Florian Dirk Schneider

"**Predator diversity and ecosystem functioning: An allometric approach**"

Die vorliegende Arbeit wurde unter der Leitung von Prof. Dr. Ulrich Brose am Fachbereich Biologie der Technischen Universität Darmstadt durchgeführt und von der Deutschen Bundesstiftung Umwelt (DBU) durch ein Promotionsstipendium gefördert.

This thesis was conducted at the Department of Biology, Technische Universität Darmstadt, under the supervision by Prof. Dr. Ulrich Brose and was funded by Deutsche Bundesstiftung Umwelt (DBU) with a PhD-fellowship.

printed on 100% recycled paper.

Bitte zitieren Sie dieses Dokument als / Please cite this document as:
Schneider, Florian D. (2012). *Predator diversity and ecosystem functioning: An allometric approach*, Dissertation – Technische Universität Darmstadt, Darmstadt, GER.
URN: urn:nbn:de:tuda-tuprints-32065
URL: http://tuprints.ulb.tu-darmstadt.de/3206

Dieses Dokument wird bereitgestellt von tuprints, E-Publishing-Service der TU Darmstadt.
http://tuprints.ulb.tu-darmstadt.de; tuprints@ulb.tu-darmstadt.de

Predator diversity and ecosystem functioning: An allometric approach

für meine Oma
Maria Roth

"O Deep Thought computer," he said, "the task we have designed you to perform is this. We want you to tell us ..." he paused, "The Answer!"

"The Answer?" said Deep Thought. "The Answer to what?"

"Life!" urged Fook.

"The Universe!" said Lunkwill.

"Everything!" they said in chorus

Deep Thought paused for a moment's reflection.

"Tricky," he said finally.

"But can you do it?"

"Yes," said Deep Thought, "I can do it."

The Hitchhiker's Guide to the Galaxy – Douglas Adams

Contents

Summary

Many services and functions of ecosystems are the achievements of the local food web. Each single species contributes to the system's emergent properties. The highest complexity, however, culminates in food webs with high diversity of predatory generalist species, feeding on many prey species at the same time, including other predators. As a consequence, the net effect of losing a predator species can be positive, negative or neutral, depending on the food-web context and the species-specific properties. These species 'identity effects' render the consequences of random species loss on ecosystem functioning and ecosystem services unpredictable. The estimation of these effects with general models is the primary objective of this thesis. To achieve this aim, I apply allometric theory to estimate numerous properties of the species, including metabolism, population density, prey range and feeding intensity by the easy-to-assess parameter 'body mass'. Especially, two assumptions are applied in the experiments and models: Firstly, allometric feeding rates predict predators to prefer prey of a certain body mass, with declining feeding rates towards larger and smaller prey; Secondly, allometric mass–abundance scaling predicts small species to be more abundant than large species. I show, that by providing this general framework, allometric theory integrates all levels of complexity, from population level over predator-prey systems towards food webs and ecosystems. It thus provides answers to four research questions: (Q1) How can body mass explain the observed feeding rates of a predator on a prey? (Q2) Do these allometric feeding rates predict the effect of a predator in the context of a community? (Q3) How do these predictions scale with increasing predator diversity? (Q4) Can allometrically-defined predator species explain patterns at the ecosystem level?

As an experimental model system, I chose the food web of the litter layer in deciduous forests, which comprises body-mass structured communities of generalist predators. The process of litter decomposition by detritivores, which is important for nutrient recycling and CO_2-release, is the focal ecosystem function.

In Chapter 2, I parameterized a mechanistic model for allometric feeding rates on basis of a comprehensive experimental data-set of feeding experiments. In microcosm experiments, I combined multiple differently-sized, generalist predator species by applying a novel allometric design, which balances the bias by individual density and biomass density. In Chapter 3, I decomposed the nested effects of three predators, which were combined in a full factorial treatment design (the centipede *Lithobius forficatus*, the spider *Pardosa lugubris*, the predatory mite *Hypoaspis miles*), on the lower trophic level springtail population and on microbial biomass.

Here, intraguild predation of the large centipedes dampened the suppressive effect of the small mites on springtails. In Chapter 4, these interactions could be predicted by simulating body-mass dependent feeding of the three species.

In Chapter 5, I tested the predictability of net interaction strength of five generalist predators on seven detritivore species. Predator body mass and target species population density proved to be the best explanatory parameters. Surprisingly, the predictability in complex communities was higher than in simple predator monocultures. This was due to the occurrence of body-mass driven intraguild predation in the complex communities.

Chapter 6 presents a mesocosm study where I manipulated population body-mass structure of the top predator (the shore crab, *Carcinus maenas*) using an allometric design in a subtidal habitat as a simulation of climate change consequences. The community responded to gradually decreasing body mass of the top predator with increasing total biomass and individual body masses. Furthermore, this triggered a gradual trophic cascade.

In Chapter 7, I applied the validated model of allometric feeding rates in a mechanistic simulation of the relationship between predator diversity and ecosystem function. With increasing diversity of predators the biomass stock of the basal trophic level was suppressed although the total predator biomass was low due to high respiration rates and intraguild feeding. This contradicts the expectations of community-level trophic cascades.

In summary, the projects provided the following answers to the research questions (Q1–4):

(A1) The body masses of predator and prey predict the quantitative feeding rates.

(A2) The context dependent positive and negative, weak and strong effects of a predator species on the lower trophic level are resolved by body-mass dependent feeding rates.

(A3) In increasingly complex communities the prediction of interaction strengths becomes simpler.

(A4) A mechanistic model of predator diversity predicts negative effects of diversity on the trophic level below.

Zusammenfassung

Viele Ökosystemdienstleistungen und -funktionen stellen eine Gesamtleistung lokaler Nahrungsnetze dar. Jede einzelne Art trägt zu diesen emergenten Eigenschaften des Systems bei. Die größte Komplexität wird jedoch in Nahrungsnetzen mit hoher Diversität an generalistischen, räuberischen Arten beobachtet. Deren Fraß umfasst zahlreiche Beutearten zugleich und beinhaltet auch andere Räuber. Der Nettoeffekt nach dem Verlust einer Räuberart kann folglich positiv, negativ oder neutral ausfallen, abhängig vom Nahrungsnetzkontext und den artspezifischen Eigenschaften. Diese sogenannten "Artidentitäts-Effekte" haben die Unvorhersagbarkeit der Konsequenzen zufälliger Artverluste auf die Ökosystemfunktionen und –dienstleistungen zur Folge. Das Abschätzen dieser Effekte durch generalisierende Modelle ist das vorrangige Ziel dieser Doktorarbeit. Um dieses Ziel zu erreichen, bediene ich mich der Allometrischen Theorie um vielfältige Arteigenschaften – eingeschlossen den Stoffwechsel, die Populationsdichten, das Beutespektrum und die Fraßintensität – durch den leicht messbaren Parameter "Körpermasse" vorherzusagen. Zwei Annahmen finden in den Experimenten und Modellen Anwendung: (1) Allometrische Fraßraten beschreiben die Präferenz des Räubers für eine bestimmte Beutekörpermasse, wobei die Fraßrate bei kleineren und größeren Beutearten abnimmt; (2) Die allometrische Beziehung von Masse und Abundanz sagt voraus, dass kleine Arten höhere Populationsdichten aufweisen als große Arten. Ich zeige, dass die Allometrische Theorie durch dieses Regelwerk alle Ebenen ökologischer Komplexität abbilden kann – von Populationen über Räuber–Beute Systeme bis hin zu Nahrungsnetzen und Ökosystemen. Daher ermöglicht sie die Beantwortung folgender vier Forschungsfragen: (Q1) Können die beobachteten Fraßraten eines Räubers auf einer Beute durch die beobachteten Körpermassen erklärt werden? (Q2) Können diese allometrischen Fraßraten den Effekt eines Räubers im Kontext einer Artengemeinschaft vorhersagen? (Q3) Wie skalieren diese Vorhersagen mit ansteigender Räuberdiversität? (Q4) Können durch allometrisch definierte Räuber auch Muster auf der Ökosystemebene erklärt werden?

Als experimentelles Modellsystem verwende ich das Nahrungsnetz der Laubstreu in sommergrünen Laubwäldern. Dieses umfasst körpermassenstrukturierte Artengemeinschaften generalistischer Räuber. Der für das Nährstoffrecycling und die CO_2-Freisetzung relevante Prozess des Laubstreuabbaus durch Zersetzer ist dabei die betrachtete Ökosystemfunktion.

In Kapitel 2 parameterisiere ich ein Modell für allometrische Fraßraten auf Basis eines umfangreichen experimentellen Datensatzes von Fraßexperimenten. Unter Anwendung eines

neuartigen allometrischen Designs, das den Einfluss von Populationsdichte und Biomassedichte ausbalanciert, wurden in Mikrokosmen-Experimenten unterschiedlich große, generalistische Räuberarten miteinander kombiniert. In Kapitel 3 konnte ich die ineinander geschachtelten Effekte von drei vollfaktoriel kombinierten Räubern auf eine Springschwanz-Population und die mikrobielle Biomasse statistisch auflösen (als Räuber dienten der Hundertfüßer *Lithobius forficatus*, die Spinne *Pardosa lugubris* sowie die Raubmilbe *Hypoaspis miles*). Intragildeprädation der großen Hundertfüßer dämpfte den unterdrückenden Effekt der kleinen Raubmilben auf die Springschwänze. Diese Interaktion konnte in Kapitel 4 durch eine Simulation körpermasseabhängiger Fraßraten der drei Arten reproduziert werden.

In Kapitel 5 wurde die Vorhersagbarkeit von Interaktionsstärken fünf generalistischer Räuber auf sieben Zersetzer getestet. Die Räuberkörpermasse und die Beutedichte stellten sich dabei als die besten Vorhersageparameter heraus. Überraschenderweise war die Vorhersagbarkeit komplexer Artengemeinschaften besser als in einfachen Monokulturen der Prädatoren. Dies war auf das Vorhandensein von körpermasseninduzierter Intragildeprädation in den komplexen Artgemeinschaften zurückzuführen.

In Kapitel 6 wurde die Körpermassenstruktur einer Räuberpopulation (die Strandkrabbe, *Carcinus maenas*) in einem marinen, subtidalen Habitat graduell manipuliert, um indirekte Folgen des Klimawandels zu simulieren. Die Artengemeinschaft reagierte auf die graduell verringerte Räuberkörpermasse mit zunehmender Gesamtbiomasse und mittlerer Körpermasse. Darüber hinaus wurde eine graduelle trophische Kaskade beobachtet.

In Kapitel 7 wurde das validierte Modell für allometrische Fraßraten angewandt, um die Beziehung von Biodiversität und Ökosystemfunktion mechanistisch zu simulieren. Mit ansteigender Räuberdiversität wurde die Gesamtbiomasse der Basalarten unterdrückt, obwohl die Gesamtbiomasse der Räuberarten von hohen Respirationsraten und Intragildeprädation niedrig gehalten wurde. Dies steht im Widerspruch zu den klassischen Erwartungen an trophische Kaskaden.

Zusammenfassend lassen sich folgende Antworten auf die Forschungsfragen (Q1–4) ableiten:

(A1) Die quantitativen Fraßraten lassen sich durch die Körpermasse von Räuber und Beute vorhersagen.

(A2) Die kontextabhängigen, positiven und negativen, schwachen und starken Effekte von Räubern auf das darunterliegende trophische Level können durch körpermassenabhängige Fraßraten erklärt werden.

(A3) In zunehmend komplexen Artengemeinschaften wird die Vorhersage von Interaktionsstärken einfacher.

(A4) Ein mechanistisches Modell der Prädatorendiversität sagt einen negativen Effekt von Diversität auf das darunterliegende trophische Level voraus.

Contributions to the chapters of this thesis

Chapter 2

Generalized allometric functional responses facilitate predator-prey stability

Gregor Kalinkat, Florian D. Schneider, Anna Schmehl, Thomas Schimmer, Olivera Vucic-Pestic, Christian Guill, Christoph Digel, Ulrich Brose and Björn C. Rall

The authors have made the following declarations about their contributions: G.K. and F.D.S. contributed equally to this study. G.K., F.D.S., U.B., O.V-P., and B.C.R. conceived and designed the experiments. The experiments were performed by G.K., F.D.S., A.S., T.S., O.V-P., and B.C.R.. Data were analyzed by G.K., F.D.S., and B.C.R.. C.D. provided empirical data. B.C.R. and C.G. performed simulations. G.K., F.D.S., U.B., and B.C.R. wrote the paper.

This chapter was printed before in the doctoral thesis of Gregor Kalinkat, submitted at Technische Universität Darmstadt, Department of Biology, April 13th 2012.

Chapter 3

Beyond diversity: how nested predator effects control ecosystem functions

Florian D. Schneider, Ulrich Brose

The authors have made the following declarations about their contributions: F.D.S. and U.B. designed the experiment, analyzed the data and wrote the paper. F.D.S performed the experiment.

This chapter was conditionally accepted for publication in *Journal of Animal Ecology*. It was revised and currently awaits final acceptance.

Chapter 4

Body mass constraints on feeding rates determine the consequences of predator loss

Florian D. Schneider, Stefan Scheu, Ulrich Brose

The authors have made the following declarations about their contributions: F.D.S., S.S. and U.B. conceived and designed the experiment and wrote the paper. F.D.S. performed the experiment. F.D.S. and U.B. analyzed the data.

Published as a letter in *Ecology Letters* volume 15, pages 436–443, doi: 10.1111/j.1461-0248.2012.01750.x

Contributions to the chapters of this thesis

Chapter 5
Size-structured intraguild predation simplifies the prediction of interaction strengths in complex food webs
Florian D. Schneider, Ulrich Brose

The authors have made the following declarations about their contributions: F.D.S. and U.B. conceived the experiment, analyzed the data and wrote the paper. F.D.S. performed the experiment.

Chapter 6
Climate-induced changes in bottom-up and top-down processes independently alter a marine ecosystem
Malte Jochum, Florian D. Schneider, Tasman P. Crowe, Ulrich Brose, Eoin J. O'Gorman

The authors have made the following declarations about their contributions: M.J., F.D.S., T.P.C., U.B. and E.J.O'G. conceived and designed the experiment and wrote the paper. M.J., F.D.S. and E.J.O'G. conducted the experiment. M.J., F.D.S., U.B. and E.J.O'G. analyzed the data.

In press in *Philosophical Transactions of the Royal Society B: Biological Sciences.* doi: 10.1098/rstb.2012.0237

Chapter 7
How predator diversity drives ecosystem functioning in complex food webs
Florian D. Schneider, Ulrich Brose, Björn C. Rall, Christian Guill

The authors have made the following declarations about their contributions: F.D.S., U.B., B.C.R. and C.G. conceived the experiment. F.D.S. and C.G. wrote the simulation code. F.D.S., U.B., and C.G. wrote the paper.

Affiliations of co-authors

Ulrich Brose Georg August University Göttingen
J.F. Blumenbach Institute of Zoology and Anthropology
Berliner Str. 28, 37073 Göttingen, Germany

Tasman P. Crowe School of Biology and Environmental Science
Science Centre West, University College Dublin
Belfield, Dublin 4, Ireland

Christoph Digel Georg August University Göttingen
J.F. Blumenbach Institute of Zoology and Anthropology
Berliner Str. 28, 37073 Göttingen, Germany

Eoin J. O'Gorman School of Biological and Chemical Sciences
Queen Mary University of London
Mile End Road, London E1 4NS., United Kingdom

Christian Guill Georg August University Göttingen
J.F. Blumenbach Institute of Zoology and Anthropology
Berliner Str. 28, 37073 Göttingen, Germany

Technische Universität Darmstadt
Institut für Festkörperphysik
Hochschulstr. 6-8, 64289 Darmstadt, Germany

Malte Jochum Georg August University Göttingen
J.F. Blumenbach Institute of Zoology and Anthropology
Berliner Str. 28, 37073 Göttingen, Germany

Gregor Kalinkat Technische Universität Darmstadt
Department of Biology
Schnittspahnstr. 10, 64287 Darmstadt, Germany

Björn C. Rall Georg August University Göttingen
J.F. Blumenbach Institute of Zoology and Anthropology
Berliner Str. 28, 37073 Göttingen, Germany

Stefan Scheu Georg August University Göttingen
J.F. Blumenbach Institute of Zoology and Anthropology
Berliner Str. 28, 37073 Göttingen, Germany

Thomas Schimmer, Anna Schmehl and Olivera Vucic-Pestic have been members of Technische Universität Darmstadt, Department of Biology, but are without an affiliation at present.

Part I.

General introduction

Chapter 1.

Predator diversity and ecosystem functioning: An allometric approach

Aims and scope of this thesis

The global biodiversity is on decline due to human impacts on ecosystems. Species extinctions threaten functions and services that are relevant for the human wellbeing (Millennium Ecosystem Assessment, 2005; Hooper *et al.*, 2005). But what exactly will happen to ecosystem functioning when species numbers change? The relationship between diversity and functioning are certainly not to be described by simple correlations (Lawton, 1994; Solan *et al.*, 2009). The complexity of this issue reaches a climax in multi-trophic communities, where feeding triggers a multitude of indirect cascading effects, with positive as well as negative net effects on plant productivity (Estes and Palmisano, 1974; Polis *et al.*, 2000; Shurin *et al.*, 2002; Finke and Denno, 2004; Bruno and O'Connor, 2005; Letourneau *et al.*, 2009), causing an utter unpredictability of the effects of particular predator loss (Yodzis, 2000, 2001). These cascading effects may translate to the community level and determine total primary production of an ecosystem (Hairston *et al.*, 1960; Oksanen *et al.*, 1981; Polis and Strong, 1996). It is, however, still unresolved in what direction this effect will develop with declining number of predator species and how the richness of predator species shapes the concerted properties of an ecosystem. Regarding predator species, we must ask the question, what determines their role in the community as a dominant or less dominant species. Do they enhance or decrease ecosystem functioning? Do they propose weak or strong effects?

The aim to predict the net functioning of an ecological system may be approached from the large scale – by describing the consequences of unspecified biodiversity loss on ecosystem functioning – or from the small scale – by setting up communities of defined predator species (Loreau, 2010*a*). The main difficulty in merging those perspectives is caused by the lack of a theoretical framework that bridges the levels of complexity. Particularly, this requires predator-prey models that are able to reproduce the patterns that are found on the ecosystem scale. The mechanistic modelling of predator species in the context of a complex community, however, is

not an easy task. What defines the diet range of a particular predator? Which of the available prey species will it prefer? What determines its feeding rates on a particular prey? How does the feeding depend on prey density? What other predators may interfere with it as a competitor or threaten it as a superior predator? Even in the simplest predator communities, answers to all those questions are necessary to predict the interaction strength of a particular predator on a particular prey. Thus, a model that generates realistic predator effects must provide realistic estimates of the diet ranges and preferences, feeding rates, and vulnerabilities within the community at the same time.

The approach I chose builds upon the framework of allometric theory. This concept describes the dependency of many physiological and ecological properties of a species on its body mass (Peters, 1983; Brown *et al.*, 2004). As one of the most reliable rules in ecology, the metabolic rate of an individual scales with its body mass following a general power law (Kleiber, 1947; West *et al.*, 1997; Brown *et al.*, 2004; Ehnes *et al.*, 2011). Similar relationships were found for the average population body mass and several population-level properties such as abundance (Peters, 1983; White *et al.*, 2007). Most important for the scope of this thesis, allometric rules were shown to apply to predator feeding rates (Brose *et al.*, 2008; Rall *et al.*, 2011) and diet breadth (Petchey *et al.*, 2008*a*; Otto *et al.*, 2007). From these observations we can generalize for species whose properties are unknown. It is a simplifying approach that allows to estimate a species' characteristics from its body mass. Although predator species differ in more respects than body mass, I consider this approach useful to achieve a mechanistic understanding of the complexity inherent to ecosystems.

In this thesis, I synthesize those threads to describe how predator species interact in complex communities aiming at the following research questions:

(Q1) How can body mass explain the observed feeding rates of a predator on a prey?

(Q2) Do these allometric feeding rates predict the effect of a predator in the context of a community?

(Q3) How do these predictions scale with increasing predator diversity?

(Q4) Can allometrically-defined predator species explain patterns at the ecosystem level?

Experimental model system

The model system that I used to answer these questions is the species community of the litter layer in European deciduous forests (see Fig. 1.1). Here, litter decomposition is performed by a community of detritivores – such as earthworms, springtails and isopods – which is under the control of a predator community – including predatory mites, spiders or centipedes. The predators in this system are mainly generalists, which means that they feed on prey within a certain range.

Litter decomposition, the focal ecosystem function, is of high relevance for the global climate, because the rates of decomposition determine the release of carbon dioxide (CO_2) into the atmosphere. Furthermore, the process of nutrient recycling in forest soils is crucial to maintain the primary production. If this process gets imbalanced, it may lead to ecosystem degradation. Knowledge on the predator interactions in the forest-litter food web are of use for many applications in ecosystem management, agroforestry or ecotoxicology, to name but a few.

I used predators and detritivores from this community to parameterize and validate allometric feeding rates in microcosm experiments. I combined multiple predators to measure their species and community effects on the detritivore species and litter decomposition. Additionally, empirical data from a large biodiversity experiment (the 'Biodiversity Exploratories'; Fischer *et al.* 2010) were used to validate the findings. These models were then used in a computer simulation to scale the effects of multiple predators to higher levels of diversity.

Figure 1.1 – The predator community of deciduous forest litter served as a model system for the allometric approach. Predators from that system, like spiders, centipedes and predatory mites, are generalists, which means that they feed on detritivores as well as other predators. Consequently, their net effect on detritivores influences the process rates of litter decomposition and CO_2 release.

Box 1 – Glossary of important terms

Allometry describes the observation of power-law scaling of physiological rates with body mass, usually with fixed exponents of 2/3 or 3/4. These scaling laws were found to also apply on larger scales for ecological rates, such as the species' abundance.

Biodiversity is the variety of life. It includes the richness of species, families, habitats or genes on local, regional and global scale. The common use means number of species on a global scale. In this study, the term is only used in the context of biodiversity–ecosystem functioning research.

Biodiversity–ecosystem functioning evolved as an ecological research tradition, aiming at the description of a causal relationship between species diversity and ecosystem functioning.

Complementarity effects are found, where increased species richness produces an ecosystem function larger than expected by adding the species singular effects.

Complexity of food webs is described by the connectance, C, times number of species, S. Usually, C is defined as the proportion of realized links, L, *vs.* possible links. Commonly it is defined as $C = L/S^2$. In this thesis complexity means the number of interactions per species.

Ecosystem functioning describes the whole system's performance, including stability, stocks and rates, without a statement of quantity. It was generalized from the more specific **ecosystem function**, which describes a particular, quantitative ecosystem process.

Food webs are network-theoretical representations of all feeding interactions in an ecosystem. Species (or species groups) are represented as nodes that are connected by feeding links.

Functional diversity is a metric for biodiversity which 'counts' the different traits that are represented in a local ecosystem. Different trait-based definitions were proposed to quantify the variation in multi-dimensional trait space.

Idiosyncrasy literally describes the properties of a thing (a species) as very specific and unique. The random loss of an idiosyncratic species thus has unpredictable consequences. This is the 'idiosyncratic hypothesis' of the biodiversity–ecosystem functioning relationship.

Indirect effects from one species to another are mediated via third species or abiotic element of the system. In this thesis, I use the term for indirect feeding effects such as trophic cascades.

Interaction strengths are the quantities by which species affect each other. They might be conceived as static rates or as non-linear functions.

Intraguild predation is a three-species food web motif with a predator feeding on both, a prey species and another predator of that prey. The motif is found in food webs more frequently than expected by chance. The motif is structurally equivalent to **omnivory**. In a community context, both terms connote feeding across different trophic levels. Different fields of research prefer either of both terms. A network-theoretical term for the motif would be 'feed-forward loop'.

Sampling effects are found, when with increased species richness the likelihood to include a species with dominant effects on ecosystem function is enhanced. In natural systems, the term **selection effect** was established to describe that the fitness of a particular species in a given environment may lead to its dominance and this species alone may drive ecosystem functioning.

Species identity describes the total effects that a particular species accounts for. This usually can be assessed directly in a presence *vs.* absence comparison and may be – experimentally or statistically – corrected for population abundance or biomass.

Stability of an ecosystem was defined in multiple ways and may describe the long-term survival of the species or community (i.e. persistence), the ability to return to an initial state after a disturbance, or the temporal variation of the populations over time.

Trophic cascades are found, where the feeding of a predatory species reduces the population of a prey species by direct feeding, and thus indirectly releases the prey's resource from a feeding pressure. **Community trophic cascades** are the translation of this concept to whole trophic levels.

Background

In this section, I want to summarize the state of research in the relevant fields of predator-prey theory, food-web theory and biodiversity–ecosystem functioning theory. All these fields investigate predator interactions on different levels of complexity separately (Fig. 1.2), but are connected by many cross-references. This review starts from the smaller scale of predator-prey interactions and ends with the complex ecosystem level.

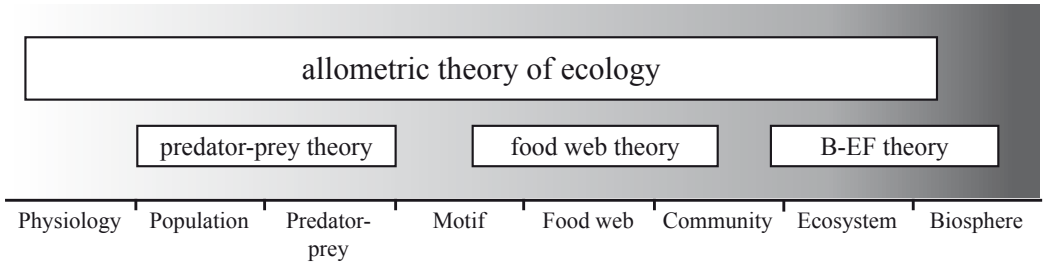

Figure 1.2 – The research on predator interactions is distributed over (at least) three research programmes. The field of predator–prey theory focuses on how predator populations affect one or more prey populations directly. Food-web theory investigates the effect of multiple species interacting by direct feeding links. The correlation between biodiversity and ecosystem functioning is importantly driven by complex predator communities. This thesis discusses how all of these fields connect to the allometric theory of ecology.

Predator-prey populations

Population dynamics. The theoretical backbone of several chapters in this thesis (Chapters 2, 4 and 7) is the simulation of population dynamics. The simulations are tracking the energy bound in biomass through the ecosystem. These 'bioenergetic' models define primary producer species growth as energy uptake from a basal resource, feeding as biomass transfer from one population into another, and finally metabolism as conversion of energy into thermal energy (Yodzis and Innes, 1992; Williams and Martinez, 2000; Brose *et al.*, 2005). The change in population biomass B_j of species j over time is thus defined as

$$\frac{dB_j}{dt} = r_j B_j - \sum_i (B_j B_i f_{ij}) + \sum_k (B_k B_j f_{jk}) e - x_j B_j. \tag{1.1}$$

This general form of the model defines the summed feeding *on* species j by all its predators i, by a rate f_{ij}, and the summed feeding *of* species j on all its prey species k, by a rate f_{jk}. The growth rate r and the metabolic rate x define the intrinsic gains and losses of the species. The assimilation efficiency e is a conversion factor, defining how much predator biomass can grow from a unit of consumed prey biomass and how much is lost as feces.

This model can easily be tailored to any structure of multi-species interactions, from simple two-species predator–prey pairs, over three-species food chains to more complicated networks

with many species and even more feeding links, called food webs. Thus, it provides an important approach in scaling the effects between predator and prey to complex communities. Starting with initial biomass densities, the changes of the species over time can be integrated. To generate realistic feeding rates, the static feeding rate, f, needs to be substituted by density-dependent terms.

Density dependence. The most obvious parameter determining the feeding rate, F, of a predator individual is the available density of prey individuals, N. The concept of density-dependent feeding rates is termed 'functional response' of the predator and dates back to the 1950s (Solomon, 1949; Holling, 1959*a*,*b*). The basic form,

$$F = \frac{aN}{1 + ahN}, \tag{1.2}$$

describes an increase of predator feeding rate with increasing prey density with the factor a, for capture rate (or 'attack rate'), saturating on high prey densities at the inverse of handling time, h. This model concept predicts the number of prey individuals eaten by a predator given a certain prey density on basis of mechanistic assumptions. The premise is, that each predator has to split its time budget into searching and subduing (capture) as well as ingesting and digesting (handling) (Holling, 1959*a*; Brose, 2010*a*; Rall *et al.*, 2010). The parameters of the model, a and h, can be estimated by direct time-budget measurement, or by fitting the model into feeding rates observed in gradients of initial prey density. The fitting procedure is described in detail in chapter 2 of this thesis.

Most importantly, the model can be extended by a density dependent capture rate, which can be perceived as the time a predator needs to find a prey individual (search time) times a likelihood of success in subduing it. The exponential decrease of search time with prey density can be incorporated by substituting bN^q for a, with a capture coefficient b and the capture exponent q. This yields the feeding rate,

$$F = \frac{bN^{q+1}}{1 + bhN^{q+1}}, \tag{1.3}$$

as a general form of functional response (Real, 1977). By adjusting q, the density-dependent feeding rate turns gradually from saturating ($q = 0$, type-II functional response; equivalent to equation 1.2) to sigmoidal shape ($q = 1$, type-III functional response; Real 1977).

The model can be further extended to incorporate multiple prey species (Kalinkat *et al.*, 2011) or interference among predator individuals (Skalski and Gilliam, 2002). All these variants of functional response will find application in the chapters of this thesis. For compatibility with equation 1.1, the feeding rate needs to be redefined in units of predator biomass. Embedded in the differential equation 1.1, the functional response will determine the development of both predator and prey populations over time. Especially the sigmoidal variants will prevent the

predator from over-exploiting its resource into extinction and are highly stabilizing (Murdoch *et al.*, 1975; Hassell *et al.*, 1977; Williams and Martinez, 2004*a*; Sarnelle and Wilson, 2008; Rall *et al.*, 2008).

Trophic cascades. Apart from these mathematical concepts, the field of predator–prey interactions concerns the qualitative effects between populations in nature. A well developed framework is that of biological control of a prey population by a predator. In the simplest case, a predator will constrain the population of its prey to low levels. Taken one step further, this will release the basal resource of the prey from feeding pressure. This pattern termed 'trophic cascade'* causes the indirect effect of a predator on the remote basal resource to be positive (Paine, 1980; Polis, 1994; Polis *et al.*, 2000). The most prominent cascading effects are those of keystone-predators, whose loss will affect most species of an ecosystem (Paine, 1966; Estes and Palmisano, 1974). Examples for trophic cascades were found *en masse* in all types of ecosystems, spanning several fields of ecological research (Schmitz *et al.*, 2000; Shurin *et al.*, 2002; Borer *et al.*, 2005). The concept importantly is applied in biological control of herbivore pests in agricultural systems and radiates into ecosystem ecology. Here, the 'green world'-hypothesis (Hairston *et al.*, 1960) and the 'exploitation ecosystems'-hypothesis (Oksanen *et al.*, 1981) are translations of trophic cascades to the community level.

Multi–trophic complexity. The concept of trophic cascades was extended to the community level on the interactions between distinct 'trophic levels', beginning with primary producers as the first, herbivores as a second and primary predators as a third trophic level (Hairston *et al.*, 1960; Oksanen *et al.*, 1981). Higher level predators might form further trophic levels (Oksanen *et al.*, 1981). The existence of community cascades was proposed and empirically backed in aquatic and some scarce terrestrial habitats (Oksanen *et al.*, 1981; Strong, 1992; Polis, 1999). In terrestrial habitats, however, it was hypothesized that instead of trophic cascades only 'trophic trickles' are to be found (Strong, 1992; Pace *et al.*, 1999; Polis *et al.*, 2000; Halaj and Wise, 2001). The argument was that in terrestrial ecosystems a clear distinction of trophic cascades does not apply. Instead, predators form a trophic continuum due to feeding within and across multiple trophic levels. This pattern of intraguild predation† was discussed intensely as a compensatory mechanism that dampens trophic cascades in nature (Finke and Denno, 2004, 2005). Indeed, meta-analyses revealed variable effects of predator removal on the basal plant productivity (Schmitz *et al.*, 2000; Halaj and Wise, 2001; Letourneau *et al.*, 2009). The value of the trophic-level concept for the prediction of ecosystem level dynamics was reasonably doubted (Persson, 1999; Polis *et al.*, 2000). In this vein, species communities were over the years successively perceived as messy, complex networks (Polis, 1991; Polis and Strong, 1996; Lawton, 1999; Duffy *et al.*, 2007). This fueled a renaissance of food-web theory as a framework for the structure and dynamics of ecological complexity.

*from greek τροφός (trophos): nurse, nourish; 'trophic' is used in ecology for terms that relate to feeding.

†also termed 'omnivory'; in this thesis I use the term intraguild predation.

Food web theory

Food web theory is a network-theoretical approach on ecosystems. Thereafter, network terminology defines populations of species as the 'nodes' which are connected by feeding 'links'. Describing the network of trophic interactions in an ecosystem is a concept that dates back to Charles Elton (1927; Brose 2008). A theoretical approach on the qualitative feeding interactions in species was not born before the early 1970s. Back then, by investigating randomly distributed feeding interactions, Robert M. May (1972; 1973*a*) rejected the tenet that species-rich food webs must be stable. This demanded research on the reasons why natural systems persist in spite of exceedingly high numbers of coexisting species (Cohen 1978; Yodzis 1981; reviewed in McCann 2000).

The first generation of empirical food webs comprised binary information on feeding links (1 = i feeds on j, 0 = i does not feed on j). The sampling of species was far from complete, methodologically inconsistent and feeding interactions often were not observed but guessed (Polis, 1991; Dunne, 2006; Cohen *et al.*, 1993). Therefore, in the 1990s, a new generation of food web data was gathered including quantitative data on species population densities and body masses (Polis, 1991; Martinez, 1991).

Food web structure. Several structural network models were proposed that were used to predict a successively increasing amount of structure and stability of food webs (reviewed by Dunne, 2006). These models distribute L qualitative links into a species matrix of S (i.e. the number of species) rows and columns (usually rows represent predators and columns represent prey) after a set of simple rules and, in some cases, stochastic variation. The cascade model early recognized the importance of body mass in structuring food webs and allowed the stochastic distribution of links only on prey that is smaller than the predator (Cohen, 1990). The niche model, proposed over a decade later, arranges species by a continuous niche value (Williams and Martinez, 2000). Each species feeds on all species within a limited range on this axis with a mid-point below its own niche value. This allows for predators that express cannibalism or feeding loops by feeding on a prey with a higher niche value. Further models proposed were the nested-hierarchy model (Cattin *et al.*, 2004) which adds more specific rules for the link distribution to generate non-interval feeding ranges. A recently proposed food web model is of relevance for this thesis because it explicitly applies allometric rules: the allometric diet breadth model distributes links within a certain body-mass range (Petchey *et al.*, 2008*a*). A noteworthy critique regarding these models is their lack of predicting non-interval feeding of a predator (Allesina *et al.*, 2008). There is an ongoing debate on how to investigate gaps in the niche interval of a predator (Allesina, 2011; Petchey *et al.*, 2011; Stouffer *et al.*, 2011).

All these models were validated by their ability to reproduce the patterns found in empirical food webs. Beside simple metrics of link density (number of links per species) or connectance (proportion of realized links; Dunne *et al.*, 2002*a*,*b*), the frequency of recurring topological

patterns, so called network motifs, became a target for research (Milo *et al.*, 2002; Stouffer *et al.*, 2007). One noteworthy finding was that empirical food webs are characterized by the disproportionate occurrence of three-species food chains and intraguild-predation motifs (Polis and Holt, 1992; Dunne *et al.*, 2004; Stouffer *et al.*, 2007). The latter motif, defined as the pattern of three species, where an intraguild predator species feeds on another predator with which it shares a prey species, is of high relevance for this thesis and deserves further explanation.

Intraguild predation. First, when using this term I have to define it and justify its use prior to the common term of 'omnivory'. Intraguild predation as well as omnivory both describe the feeding pattern where a predator feeds on a competitor for a shared prey, but both have slightly different connotations. 'Omnivory' highlights the feeding on more than one trophic level and is more common in food web theory (e.g., McCann and Hastings, 1997; Stouffer *et al.*, 2007). It derives from the simple food chain by adding one feeding link from the higher level predator to the basal species. 'Intraguild predation' highlights the feeding within the same guild and is preferred in research on biological control and trophic levels. Here, it is perceived as one species prevailing in competition by including the competitor into the prey spectrum (e.g. Finke and Denno, 2004, 2005). Mathematically, the gradual transition between competition, intraguild predation and a food chain is determined by the distribution of feeding rates within the motif (Holt and Polis, 1997; McCann and Hastings, 1997; Vandermeer, 2006). While agreeing with this notion of a continuum, I think the term intraguild predation is more appropriate for the use in my thesis because I focus on the feeding interactions within the predator community.

The motif of intraguild predation became a lasting enigma. On the one hand, in theory it was found to be profoundly unstable over time, meaning that three species connected in an intraguild motif cannot co-exist (Pimm and Lawton, 1978; Pimm, 1982). On the other hand, it was observed more frequently than expected by chance, which allows the deduction that the motif must be stable over time (Polis, 1991; Polis and Strong, 1996; Dunne *et al.*, 2004; Stouffer *et al.*, 2007). Which properties of naturally occurring intraguild predation warrants this long-term persistence? To answer this question, theoretical concepts turned towards a dynamic perspective on food webs by simulating the population dynamics in food web motifs (Yodzis and Innes, 1992; McCann and Hastings, 1997). By using such an approach, McCann and Hastings (1997) found that a relatively weak feeding of the higher level predator on the basal prey can lead to persistence of all three species in the motif. McCann *et al.* (1998) also could show that weak interactions can constitute stability in other network motifs. Interestingly, these models incorporated allometric power laws for species metabolism and type-II functional responses, following an approach described by Yodzis and Innes (1992). Later studies corroborated the potential of intrinsic stability of intraguild predation motifs with weak links under certain conditions and showed that these conditions are granted in empirical food webs (Neutel *et al.*, 2002; Emmerson *et al.*, 2004; Kondoh, 2008).

These food-web approaches focused on stability in motifs and did not address the question

how cascading effects on the basal resource might change in consequence to intraguild predation. They provided, however, a fundamental mechanistic understanding of the dynamics within such motifs. The major outcome was that interaction strengths in persistent motifs are not distributed uniformly. Instead, there are few strong and many weak interactions (Wootton, 1997; McCann *et al.*, 1998; Neutel *et al.*, 2002; Emmerson *et al.*, 2004). Thus, the distribution of interaction strengths is key to an understanding of the stability of food web motifs and thus must be evidently important for the stability of entire food webs.

Interaction strengths. The commonly applied stability criterion by May (1973*b*) includes the quantification of the feeding interactions, termed interaction strength, as a parameter. In early stability analyses, that parameter was assigned randomly to the links and was assumed to be a constant value representing the feeding of populations in equilibrium (McCann, 2000; Dell *et al.*, 2005). However, empirical work revealed that interaction strengths are not distributed randomly and are strongly skewed towards a predominance of weak interactions (Wootton, 1997; Emmerson and Yearsley, 2004). Such distributions of interaction strengths improve stability of food web models significantly, at least after the equilibrium-based criteria of May (McCann, 2000).

To resolve this additional quantitative dimension of food webs, several studies targeted the measurement of interaction strength in field- and microcosm studies (Wootton, 1997; Berlow *et al.*, 1999, 2004; Wootton and Emmerson, 2005). For synthetic species composition experiments, as presented in this thesis (Chapters 3, 4 and 5), densities of the target population, j, in presence and absence of the influencing species, i, are available. This enables the expression of interaction strengths IS_{ij} of species i on species j as log response ratios (Laska and Wootton, 1998; Berlow *et al.*, 1999):

$$IS_{ij} = \log \frac{B_j^{+i}}{B_j^{-i}}. \tag{1.4}$$

In field studies, a multitude of other static metrics are applicable (Berlow *et al.*, 2004; Wootton and Emmerson, 2005). Empirically determined log response ratios, however, do hardly separate direct and indirect trophic effects. They measure a net effect, balancing all direct interactions in the particular food web. Also, they do not capture the dynamic variation of predator and prey population densities over the experimental time. The deduction of feeding rates from interaction strengths that were measured in composition experiments requires a thorough treatment design and may be supported by knowledge of the particular population dynamics (see Box 2 and Chapter 4).

Food web dynamics. As noted above, commonly the population densities were assumed to be in a stable equilibrium state (May, 1973*b*; DeAngelis and Waterhouse, 1987; Allesina and Tang, 2012). This notion is far from the natural dynamics in populations. Similarly, the linear feeding rates, as assumed in the stability criterion of May, are not reflecting the dynamics of

feeding interactions in nature. Theoretical work on food web dynamics adopted more dynamic perceptions of nodes and links in food webs and substituted the constant interaction strengths by non-linear feeding rates as described by the concept of functional responses (see above; Yodzis and Innes, 1992). The density dependence of feeding added more realism to the food web dynamics. Applied to entire empirical food webs to simulate the dynamics in a marine food web (Yodzis, 1998, 2000) it demonstrated a purposeful connection between food web theory and the mathematical framework of predator–prey interactions. The combination of structural food web models with plausible models for predator–prey feeding rates was a fruitful one and yielded insights into the stability of food web motifs (McCann and Hastings, 1997) and entire food webs (Williams and Martinez, 2004*b*; Brose *et al.*, 2003, 2006*a*).

Only very scarcely, simulations of food web dynamics were connected to the question how species number affects functions on the ecosystem level (Ives *et al.*, 2005; Thébault and Loreau, 2005, 2006; Long *et al.*, 2007). Nonetheless, several researchers anticipated the great potential for dynamic food web theory to answer the questions of biodiversity–ecosystem functioning research (Ives *et al.*, 2005; Cardinale *et al.*, 2009; Loreau, 2010*a*,*b*).

Biodiversity and ecosystem functioning

Mechanisms of ecosystem functioning. Research on biodiversity and ecosystem functioning evolved in the 1990s with the formulation of the paradigm that ecosystem functioning is a consequence of species richness (Lawton, 1994; Naeem *et al.*, 2002; Solan *et al.*, 2009). From that point, the hypotheses about the true shape of the correlation radiated describing it to be linear, logistic, log-linear or idiosyncratic (Lawton, 1994; Naeem *et al.*, 2002; Schmid *et al.*, 2009; Solan *et al.*, 2009). This research tenet lasted for a decade and successfully identified 'niche complementarity' and 'sampling effects' as the general natural mechanisms behind the correlation (Huston, 1997; Loreau *et al.*, 2001; Loreau and Hector, 2001; Ives *et al.*, 2005). Niche complementarity is found where species cover complementary parts of niche space which allows a joint exploitation of basal prey which is more than additive (Huston, 1997; Tilman, 1999; Loreau *et al.*, 2001; Ives *et al.*, 2005). This gave rise to a research on species traits, as a multi-dimensional measure for species diversity beyond the mere species richness. The concept of trait-based ecology is discussed in one of the following paragraphs.

Sampling effects are found if the likelihood to include a dominant species increases with species richness, which alone may drive the community net functioning (also 'selection effects'; Huston, 1997; Loreau and Hector, 2001). An experiment that combines different numbers of species from a species pool and measures the effect of these assemblages on an ecosystem function would necessarily increase the likelihood of including a particular species identity. The separation of complementarity and identity effects from a general diversity effect can be achieved by applying thorough experimental design and statistical modelling (see Box 2).

The question arises, which parameters shape the species-specific 'identity' effect (Duffy, 2002; Bruno and O'Connor, 2005). This connects to the species-traits concept that is described further below. Both mechanisms provide explanation for the change in ecosystem functioning with increasing plant species richness. The concepts, however, are limited to the change of diversity *within* one trophic level ('horizontal' diversity; Duffy *et al.*, 2007; Reiss *et al.*, 2009).

Predator diversity. Apparently, the role of species richness is more complicated in systems with multiple trophic levels (Duffy, 2002; Naeem *et al.*, 2002). The inclusion of predators into classic biodiversity–ecosystem functioning experiments revealed the importance of 'indirect effects', like the triggering of a species-level cascade by a higher level consumer or antagonistic and synergistic effects between consumers (Sih *et al.*, 1998; Finke and Denno, 2004; Ives *et al.*, 2005; Schmitz, 2007). Indeed, the findings of experiments differ widely documenting negative and positive effects of predator species loss on the trophic level below (Halaj and Wise, 2001; Shurin *et al.*, 2002; Bruno *et al.*, 2008; Letourneau *et al.*, 2009) and on ecosystem functioning in general (Balvanera *et al.*, 2006; Bruno *et al.*, 2008; Schmid *et al.*, 2009). In this thesis, I focus on the ability of intraguild predation in predator communities to generate apparently idiosyncratic, negative as well as positive net effects of predator loss (Finke and Denno, 2004, 2005; Chapter 3).

In the early 2000s, the debate on community trophic cascades was on a new climax (see above; Chapter 7). Research on this topic targeted the response of ecosystem functions with changing number of trophic levels ('vertical' diversity; Duffy, 2002; Duffy *et al.*, 2007; Loreau, 2010*a*). As pointed out above, this debate struggled with the insight that diverse and highly interconnected predator communities do not shape distinct trophic levels (Pace *et al.*, 1999; Shurin *et al.*, 2002). The community effects on the lower trophic level become difficult to predict.

Merging the notions of 'vertical' and 'horizontal' diversity to produce a more realistic understanding of multi-trophic diversity is a highly acute issue in biodiversity research (Loreau, 2010*b*). The proposed approaches use functional traits and functional groupings of species to reduce the complexity to a tractable level (Hooper *et al.*, 2005; Reiss *et al.*, 2009).

Functional Diversity. From the concept of sampling effects that assign a proportion of the change in functional diversity to a particular predator species arises the question what determines the species-specific effects in nature. What determines species identity? The concept of functional species traits tries to solve this issue by assigning a set of traits to each species (McGill *et al.*, 2006; Reiss *et al.*, 2009). From these, a simple metric for functional diversity could be derived by counting the different traits present in the local ecosystem. More sophisticated definitions of functional diversity are based on the distribution of species in multi-dimensional trait-space, comprising the clustering in functional groups or the length of branches in a dendrogram (Petchey and Gaston, 2006; Petchey, 2007; Petchey *et al.*, 2009; Laliberté and Legendre, 2010). Functional diversity was found to be a better predictor of ecosystem functioning than mere species richness, because it corrects for redundant species and highlights complementary species (Hooper *et al.*, 2002; Griffin *et al.*, 2009). Even in systems with multiple trophic levels, knowledge on species traits may predict intraguild predation (Werner and Peacor, 2003; Schmitz *et al.*, 2004). Thus, the concept of trait-space connects to the concept of 'horizontal'

Box 2 – Experimental design for biodiversity–ecosystem functioning research

The first experiments that varied species number and measured the consequences for a particular ecosystem process, like primary productivity (Tilman and Downing, 1994; Naeem *et al.*, 1994), were criticized for including hidden treatments (Huston, 1997; Tilman *et al.*, 1998; Loreau *et al.*, 2002). Sampling effects and niche complementarity (see Box 1) were discussed as experimental bias, that must be accounted for in experiments and statistical analysis (Huston, 1997). This notion triggered a debate on experimental design and data analysis in biodiversity research. The confounding effects, however, were soon accepted as part of the natural mechanism that shapes the correlation between biodiversity and ecosystem functioning (Wardle, 1999; Loreau and Hector, 2001). To resolve the role of sampling effects on ecosystem functioning, subsequent research targeted the statistical separation of single species' effects from a *per se* biodiversity effect (Loreau *et al.*, 2001; Fox, 2005, 2006; Bell *et al.*, 2009; Fox and Kerr, 2012).

The research on trophic cascades and biological control joined into this debate to investigate the consequences of predator diversity on ecosystem functions. Therefore, a wealth of synthetic composition experiments (SCEs) were carried out to investigate predator-diversity effects on herbivore suppression (Schmitz, 2007; Bruno *et al.*, 2008; Letourneau *et al.*, 2009). The effect of species 'identity' was hardly ever provided with a clear definition but mostly is used for the total effect on ecosystem function caused by a particular species' presence. (Steiner, 2001; Duffy, 2002; Bruno *et al.*, 2005).

In SCEs, communities are assembled from scratch, and must therefore contain an implicit or explicit decision about initial numbers of individuals. Thus, SCEs provide a sharp control of species presence and absence and enable a separate addition of behaviourally similar species, which is not possible in removal experiments. The initial density can be controlled by applying an additive or substitutive design (see Figure; Schmitz, 2007; Byrnes and Stachowicz, 2009). While the first keeps the density of each species constant over all treatments, the latter will reduce population density in higher diversity levels to keep the community density constant over all treatments. Thus, additive SCEs control for intra-specific interference effects, while substitutive SCEs control for inter-specific individual interference (Schmitz, 2007). Byrnes and Stachowicz (2009) suggest therefore to combine both treatment designs to yield reliable information on density-dependent per capita effects.

A second problem is caused by the type of density controlled for in SCEs. Each type of design can be applied to abundance or biomass density (see Figure). It is inevitable that taxonomic differences coincide with differences in average individual body mass, m. Controlling abundance, N, creates variation in biomass density, B, and vice versa, due to the simple relationship $B = m \cdot N$ (Schneider *et al.*, 2012). The measured effect of species identity is biased. Although obvious, this bias is ignored in all but very few predator composition studies (Griffin *et al.*, 2008; Reiss *et al.*, 2011).

Alternatively to these restricted composition experiments, researchers perform removal experiments from field communities (e.g. O'Connor *et al.*, 2008). In contrast to SCEs, the initial population densities in removal experiments represent natural levels which must be considered as the outcome of dynamic, bioenergetic processes. Therefore, it is very likely that identity effects measured in removal experiments provide a better estimate for the consequences of species loss.

To resolve these issues and make experimental results comparable, a universal definition of 'identity effects' would be of great value.

Finally, the combination of predators of multiple trophic levels bears great difficulties in estimating single species effects, due to the possibility of indirect effects which lead to negative and positive net effects likewise, rendering species identity intangible (Sih *et al.*, 1998; Finke and Denno, 2004; Ives *et al.*, 2005; Reiss *et al.*, 2009, 2011). Thus, identity effects of predators are strongly context dependent (Worsfold *et al.*, 2009). This context dependency could be resolved in full-factorial treatment combinations, an option that is limited to not more than 4 predator species.

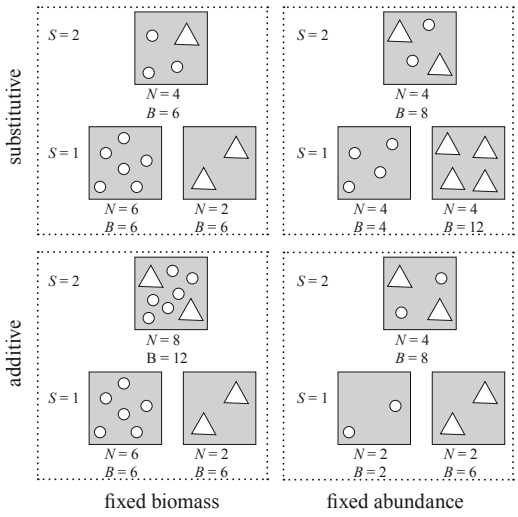

Options for experimental design with two species. Species 'circle' has a body mass of 1 while 'triangle' weighs 3. Standardizing either for abundance or biomass density inevitably will cause treatment bias by the other.

ecological niche (McGill *et al.*, 2006) and redundancy (Reiss *et al.*, 2009), as well as 'vertical' diversity (Schmitz *et al.*, 2004). In this concept, two predators are redundant if they occupy similar positions in trait-space and are complementary if they carry entirely different traits.

One important trait – if not the most important – is species body mass. It determines many other species traits and thus may be perceived as a 'super trait' (Brown *et al.*, 2004; Jacob *et al.*, 2011). The relationships between body mass and the properties of predators in the context of a community are a major topic of this thesis and will be illuminated in the following section.

Trait-based ecology recently experiences a leap towards individual-based traits, targeting to integrate intra-specific variation for the prediction of ecosystem processes (Savage *et al.*, 2007). Analogue, to that critique, population-averaged body mass is recently discussed to misrepresent the natural individual variation (Raffaelli, 2007; Woodward *et al.*, 2010). In this vein, individual-based ecology might be better suited to reflect ontogenetic differences and realistic niche occupation over time, but this also would require a much higher resolution of data. On the contrary, recent modelling approaches used functional groups to model ecosystem functioning. But these approaches tend to extend either the 'vertical' or the 'horizontal' diversity perspective in direction of the other (Loreau, 2010*a*; Wollrab *et al.*, 2012) and are loaded with *a priori* assumptions of the own perspective which limits the validity of the results. Some researchers demand therefore that a novel theoretical approach, which merges population dynamics and food webs, is required to overcome the separation of vertical and horizontal diversity research (Ives *et al.*, 2005; Cardinale *et al.*, 2009; Loreau, 2010*a*). Thus, in this thesis the approach of choice sets its focus on the population as the smallest entity.

Stability of ecosystem functioning. A last topic of biodiversity–ecosystem functioning research that needs some introduction is the stability of ecosystem functioning. Beyond May's criterion for the ability of the system to return to equilibrium, multiple criteria of stability of ecosystems were formulated (Pimm, 1984; Loreau *et al.*, 2002; Ives and Carpenter, 2007). Usually in the context of ecosystem functioning, stability is discussed either in terms of temporal variation or resistance and recovery of an ecosystem process after perturbations and primary extinctions (Loreau *et al.*, 2002; Griffin *et al.*, 2009). Referring to this, increasing species richness is expected to cause what was termed the 'insurance effect' of biodiversity: a functionally diverse community will be able to buffer functioning after environmental variations better than a less diverse community, resulting in a reduced coefficient of variation over time (Naeem and Li, 1997; Yachi and Loreau, 1999). The insurance effect was reproduced in simulations of simple multi-trophic communities (Thébault and Loreau, 2005). Many studies aimed to find such consolidating effects of species richness (Petchey and Gaston, 2002; Romanuk *et al.*, 2006; Griffin *et al.*, 2009 and references therein). However, the hypothesis turned out difficult to falsify or corroborate, since this requires long experimental duration and cautious design (Cottingham *et al.*, 2001; Petchey and Gaston, 2007).

A more general concept of ecosystem stability is the 'robustness' against secondary extinctions as a consequence to induced disturbance or primary extinction events (Loreau *et al.*, 2002). This is a topic that was investigated by food web theory, where the importance of single species was weighed by the impact of their loss (Sole and Montoya, 2001; Dunne *et al.*, 2002*a*). It translates in experimental ecology as the search for species traits that are correlated with extinction risk. Certainly, species are not lost randomly from ecosystems, but as a consequence of their capabilities to cope with environmental change of and insufficient energetic supply. Interestingly, experimental evidence was found that predators of high trophic position (Purvis *et al.*, 2000*a*,*b*) are most prone to extinction, which was corroborated and generalized by theoretical results (Eklöf and Ebenman, 2006; Dunne and Williams, 2009; Binzer *et al.*, 2011). This spotlights the importance of predatory species for the stability of ecosystems. While the topic was raising high interest of theoreticians, experimental data on this topic remain scarce. Recent experiments in micro- and mesocosms indicated that species with unique sets of traits are at higher risk than redundant species (Petchey *et al.*, 2008*b*; O'Gorman and Emmerson, 2010). Most interestingly, the topic is characterized by neglecting a unidirectional relationship between diversity and functioning. In contrast to most topics within biodiversity–ecosystem functioning research, in the notion of robustness functioning *begets* diversity.

The concepts summarized in this section developed in separate research programmes with mutual exchange between the topics. As an example, consider the relatedness between cascading effects of populations (predator–prey interactions), the motif of intraguild predation (food web theory) and indirect effects in predator communities (biodiversity–ecosystem functioning). Another topic present in all research fields is the question of stability: What warrants long-term co-existence of species in predator–prey pairs, food web motifs, communities and ecosystems?

The range of ecological research on predator interactions described in this section appears to be comprehensive. Surprisingly, there exists a theoretical framework to unify all these levels of eco-complexity (Fig. 1.2). In the following section, I will summarize the achieved integration of allometric principles into the three fields and suggest allometric theory as an approach to merge concepts from all three fields.

The allometric approach

The allometric theory developed as a generalizing framework for physiological characteristics such as physiology, metabolism, reproduction or movement (Kleiber, 1947; Peters, 1983). Hereafter, an individual biological rate, Y, depends on individual body mass, M, following a power law with exponent α, yielding $Y = aM^{\alpha}$ (Peters, 1983; Brown *et al.*, 2004). The allometric exponent, α, for many rates was found to approximate $^3/_4$ (Peters, 1983; West *et al.*, 1997, 1999). Therefore, the allometric theory of ecology proposes that patterns on physiological and population level relate to those individual-based, physiological rules (Brown *et al.*, 2004). The 'metabolic theory' extends this physiological model by temperature dependency (Brown *et al.*, 2004). Interestingly, power laws on average body mass are good descriptors for ecological parameters as well, with astonishingly similar exponents, as in the case of the distribution of species abundances (White *et al.*, 2007). Body mass was subsequently used as a determinant for a wide variety of ecological parameters, such as feeding rates (Brose *et al.*, 2008), diet selection (Otto *et al.*, 2007; Petchey *et al.*, 2008*a*), food web structure (Petchey *et al.*, 2008*a*) and dynamics (Brose, 2010*b*). With regard to ecosystem functioning, body mass was described as a 'super trait' (Jacob *et al.*, 2011) that indirectly determines many species traits and thus is collapsing many dimensions of species variability in one single parameter (see Fig. 1.3). This marks the starting point for my own research. I subsequently describe the concepts of allometric theory and experimentation that are applied in the chapters of this thesis.

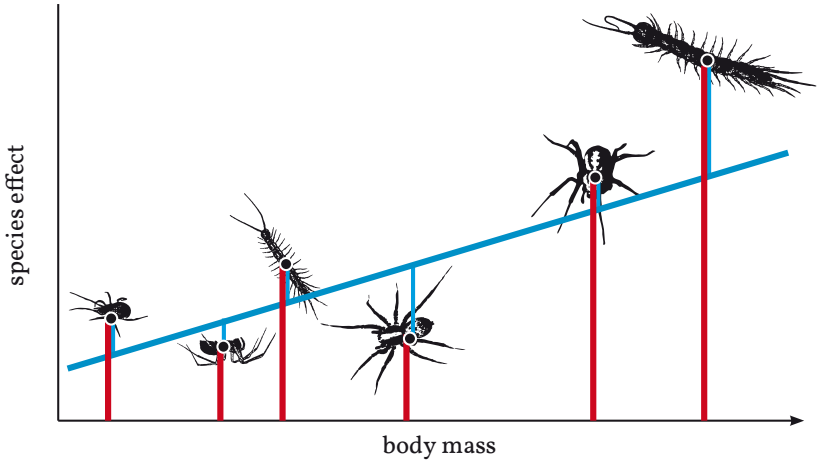

Figure 1.3 – The definition of a particular predator species in trait space, here collapsed to a one-dimensional species identity effect, can be described by taxonomy (red vertical lines) or by an allometric model (blue model line & residuals). The taxonomic model explains all of the variation in the species identity, but uses one defining coefficient per species. The allometric model explains only a fraction of the variation, but uses only few coefficients. Allometry is a parsimonious way to differentiate the species' feeding characteristics and effects on ecosystem functioning.

Allometric theory of ecology

A variety of physiological and ecological parameters scales exponentially with body mass (Peters, 1983). Primarily, allometric scaling takes action on the individual level as a direct consequence of metabolic scaling (see above). Allometric theory describes patterns on different levels of ecological complexity (Fig. 1.2). Therefore, I want to propose it as a framework to connect the issues of predator–prey interactions, food web theory and biodiversity–ecosystem functioning research. In the following paragraphs I recapitulate the state of science with regard to allometric theory and introduce how this thesis adds to the research in this field.

Allometric mass–abundance scaling. The power-law correlation of species abundance, N, with average species body mass, m, is well documented (Peters, 1983; Damuth, 1987; White *et al.*, 2007). The exponent of the relationship $N = am^{\alpha}$ differs widely on local scales but is consolidated on the global scale, where it approximates $-3/4$ (Damuth, 1987; White *et al.*, 2007). From this observation derives the allometric design for predator-composition experiments, that I propose further below. More generally, the allometric mass–abundance scaling provides a static estimate of relative population size of multiple predator and prey species. This is of importance when connecting the population level interaction strengths to per capita interaction strengths (Chapter 4).

Allometric foraging theory. The density dependent feeding of predators on prey, the functional response, was successively related to the body masses of predator and prey. The parameters that determine the predators' feeding rates were described mechanistically by biological components which can be substituted by allometric power laws. Three parameters define the shape of the functional response (equation 1.3) of a predator: the handling time h, the capture coefficient b, and the capture exponent q.

For handling time, h (equation 1.3), a power law dependency on the body mass of predator, m_i, and of prey, m_j, can be assumed yielding

$$h_{ij} = h_0 m_i^{\eta_i} m_j^{\eta_j}. \tag{1.5}$$

The exponents take negative values for η_i, describing an exponential decrease in handling time with increasing predator body mass, and positive values for η_j, increasing the handling time for large prey. This is reasoned biologically because predators will handle and digest relatively small prey in shorter time than relatively large prey (Rall *et al.*, 2008; Brose, 2010*b*).

The capture coefficient, b (equation 1.3), is modelled phenomenologically, as a hump-shaped function (Ricker's function) with predator–prey body-mass ratio (Persson *et al.*, 1998; Vonesh and Bolker, 2005; Vucic-Pestic *et al.*, 2010; Brose, 2010*a*; Rall *et al.*, 2011). This curve follows the concept of optimal foraging theory (Brose, 2010*a*), in which a predator should specialize to capture prey of energetically optimal properties. For a predator, a small prey takes more

time to find and catch while yielding little energy, whereas a large prey will be harder to subdue, may escape or bears a higher risk of injury for the predator. Foraging on prey of an optimal body size ratio, R_{opt}, is a consequence of this trade-off (Brose, 2010*a*). This property of optimal foraging connects to structural models that predict the link distribution on basis of niches on the body-mass axis (Beckerman *et al.*, 2006; Petchey *et al.*, 2008*a*). In Chapter 4, I discuss how this produces the intraguild predation motif.

The capture exponent, q, is commonly defined independent from body mass. Only few experiments were able to detect a capture exponent significantly different from 0, a classic type-II functional response (Holling, 1959*a*; Rall *et al.*, 2010). The lack of experimental evidence, however, could be due to insufficient replication of very low densities (Sarnelle and Wilson, 2008). Biological mechanisms for a decrease in the capture rate at low prey densities are found in the limited refugial space that can be accessed by small prey species, but not by large predators (Hassell, 1978; Crawley, 1992). In chapter 2, the defining parameters of handling time, capture coefficient and capture exponent are quantified by fitting the model into an extensive data-base of empirically measured feeding rates. This also aims at corroborating the hypothesis of a body mass scaling of q with predator–prey body-mass ratio. Similar assumptions on the quantity of the coefficients and exponents, all derived from empirical observations, are applied in the other chapters of this thesis (Chapters 4 and 7).

Interaction strengths. The concept of allometrically-defined feeding rates provides a plausible model for differentiated, weak and strong direct feeding interactions within a community (Brose, 2010*a*; Vucic-Pestic *et al.*, 2010). As described further above, interaction strengths derived from microcosm or field experiments as log response ratio are net effects, balancing direct and indirect effects of a removed species on a target species (Berlow *et al.*, 2009). The knowledge of direct feeding rates would be required to achieve a full understanding of the processes in the entire community. Feeding rates derived from generalized allometric-foraging models could provide this knowledge (Chapter 2). Even in more complex communities allometric feeding rates determine the net effect of the predator on the target species qualitatively and quantitatively. The species identity effect of a particular predator becomes fully resolvable. In such a simulation of niche-model food webs with allometrically defined feeding rates, Berlow *et al.* (2009) found that the net interaction strengths become more consolidated as the species number and complexity of the food webs increase. I tested this hypothesis in a microcosm experiment with simple and complex predator communities (Chapter 5).

Allometric food web structure. Feeding links in food webs are strongly determined by body mass structure (Woodward and Hildrew, 2002). Most structural models – the early cascade model, the niche model and finally the allometric diet breadth model – are based on this observation (Williams and Martinez, 2000; Dunne, 2006; Petchey *et al.*, 2008*a*). The allometric diet breadth model builds upon the assumption that only those species are included in the prey range that yield the most profitable trade-off between energy yield per handling time and rate

of an encounter (Beckerman *et al.*, 2006; Petchey *et al.*, 2008*a*). These parameters, energy yield, handling time and encounter rate, all can be assumed to depend on body mass by allometric power laws (Petchey *et al.*, 2008*a*). These models provide a realistic quantity of connectance, and therefore intraguild predation, in food webs (Beckerman *et al.*, 2006). The phenomenological, hump-shaped capture rate of the allometric foraging model (Brose, 2010*a*; Vucic-Pestic *et al.*, 2010) is based on the same assumptions of profitability. However, the latter model additionally provides quantitative feeding rates, which can be used in dynamic simulations.

Allometric food web dynamics. As pointed out above, food webs can be modelled as dynamical systems of individuals, populations or functional groups. The approach chosen in this thesis focuses on populations as nodes (Yodzis and Innes, 1992; Brose *et al.*, 2006*a*). The feeding links can as well be modelled in different ways, e.g. as constant proportions of prey biomass (Kondoh, 2003), or as non-linear functions of predator and prey biomass (Brose *et al.*, 2006*a*) as does the allometric foraging model – the approach chosen in this study. The allometric foraging model uses non-linear, allometric functional responses to define the feeding rate of a predator on a prey under given biomass densities and under given body masses. Therefore, the allometric foraging model can be used to predict qualitative feeding links and quantitative feeding rates at the same time. The intraguild predation motifs generated from these models vary in the distribution of feeding rates. Thus, the net effect may be positive or negative, depending on the body mass structure. In Chapter 2, I test whether the allometric functional response model predicts feeding links in empirical food webs correctly. Furthermore, I evaluate the ability of the model to generate negative and positive net effects on the lower trophic level as expected from differentiated feeding within intraguild predation motifs (Chapter 4). The model is then applied to generate qualitative structure and quantitative feeding rates of model food webs in Chapter 7. These food webs comprise stochastically assembled networks of species that interact on basis of allometric rules and in doing so emerge higher level properties.

Emergent ecosystem functioning. In this thesis, I want to provide a theoretical framework to approach the higher level properties of predator communities on basis of a mechanistic model that defines interactions on the population level. The final species biomass levels arise from the population dynamics and approximate an attractor in phase space. This model includes the possibility of species extinction. In contemplation of this highly dynamic system, ecosystem functioning may not be perceived as the consequence of diversity but as its cause.

This framework imitates the bi-directional relationship between ecosystem functioning and biodiversity with unprecedented realism. Perceiving ecosystem functioning as the product of allometrically defined species, interacting in the context of a food web can help anticipating the consequences of the threatening erosion of biodiversity.

Allometric design for biodiversity experiments

Combination of multiple predators in species diversity experiments requires cautious experimental design (Box 2). This thesis includes reports on two synthetic composition experiments where I manipulated species richness in microcosms (Chapters 3, 4 and 5). Two problems are eminent for these experiments: (1) the target species identity effects belong to species of variable body mass, and (2) the species are generalist predators and are therefore expected to exert intraguild predation upon each other. The feeding effects within the predator community should trigger indirect cascading effects and thus render the measured net identity effect to be highly variable in quality and quantity (Finke and Denno, 2004). Thus, the experiments are not aiming at measuring direct interaction strengths, but indirect net interaction strengths. The theoretical compound of the thesis (see above) will address the resolution of these indirect effects and estimate direct feeding rates (Chapter 4).

A thought experiment will illustrate that the measured net effects are highly sensitive to the starting conditions of the experiment. Given the high difference in the species body masses, the application of a classic additive or substitutive design with standardized densities would cause disproportionately high biomass for the large species, causing a diversity-treatment bias (see Fig. 1.4a). The large predators direct intraguild feeding on the other predators might be unduly amplified, which may cause the net effect on the basal prey to switch from negative to positive. A standardization for species biomass would cause equally arbitrary results (see Fig. 1.4c). This lack of realism has the potential to distort the very sensitive measurement of net interaction strengths beyond recognition. Therefore, balanced starting conditions for the predator treatments need to be warranted.

In this thesis, I apply two slightly different solutions to this problem. The easiest, and probably most representative composition design is applied in Chapter 5 and initializes the experiment

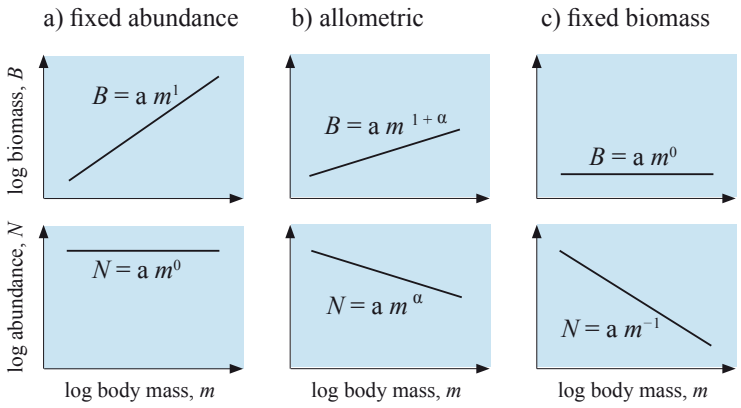

Figure 1.4 – Body mass, abundance and biomass density are strictly coupled. An unwarily experimental standardization of either (a) abundance or (c) biomass of treatments with variable body mass might cause coinciding bias in the other. (b) An intermediate compromise is achieved by applying allometric mass–abundance scaling.

with field densities (e.g. Finke and Denno, 2004). This would also enable comparison with effects measured in removal experiments (see Box 2) but requires knowledge about the habitat. The alternative is more general in assumptions and initializes the predator populations with densities that derive from an allometric mass–abundance scaling (e.g. Griffiths *et al.*, 2008; see Fig. 1.4b). Such an 'allometric design' is proposed in the experiment in Chapters 3 and 4. The rationale behind this is that empirically observed mass–abundance scaling laws of the form $N = am^{\alpha}$ represent energetically balanced communities. The measured interaction strengths can be assumed to reflect this energetically balanced state.

Finally, in a mesocosm experiment performed in the subtidal of a marine habitat I manipulated the average body mass of a predator species gradually (Chapter 6). This treatment has the same impediments as the composition experiments, because manipulation of average body mass under constant individual densities would cause a treatment bias in biomass. Therefore, the initial densities in this experiment were thoroughly adjusted to scale allometrically.

Outline of this thesis

This thesis discusses aspects of predation in the context of multi-trophic networks by using a unifying allometric approach. In the following chapters, I will present several studies that illuminate the complexity of interactions within diverse predator communities.

(Q1) How can body mass explain the observed feeding rates of a predator on a prey?

Starting with **Chapter 2**, page 29, I introduce the concept of a body mass determined model for feeding rates between predator and prey. A collection of feeding experiments combined differently-sized prey individuals with a wide range of predators of variable body mass. On basis of these data, a model was parameterized which defines the predator capture rate, handling time and capture exponent as dependent on average body mass of predator and prey. The study illustrates, how allometric constraints on feeding are valid without regard for the taxon of the species and can serve as a generalized model to predict feeding.

(Q2) Do these allometric feeding rates predict the effect of a predator in the context of a community?

In **Chapter 3**, page 53, in a study of three predators on a single basal prey, I illustrate the consequences of predator loss as nested sampling effects of different predator identities. While the consequences of random species loss must remain unpredictable, the consequences of a particular predator loss depends on the context of the remaining community. The predators' net effects are well defined by species body masses, as I show in **Chapter 4**, page 67, in a study on the same data set. Here, the simple assumptions of an optimal foraging on prey of a certain relative

size (i.e., a hump-shaped capture rate) and of body mass dependent population densities (i.e. allometric mass–abundance scaling) are employed to predict the interaction strengths of three differently sized predators. These allometric constraints on predators reproduce the smooth transition between competition, weak and strong intraguild predation towards a tri-trophic food chain (Fig. 4.1 on page 70). I tested whether this concept of allometrically constrained predator species explains the existence of positive and negative interaction strengths in complex multi-predator communities.

The experiment of Chapters 3 and 4 was performed using a novel allometric design that defines the initial population densities of the additive predators following a power law with their average body mass. This design avoids an unrealistic bias of per capita interaction strengths by extreme population biomasses, as would be the case in classical fixed-density designs.

(Q3) How do these predictions scale with increasing predator diversity?

In **Chapter 5**, page 83, I present a second microcosm study where I tested the validity of allometric constraints on interaction strengths in a more complex community. Here, population level parameters are used to predict interaction strengths of five predators on a detritivore community in simple monocultures and embedded into a complex community. This study uses a design with adjusted initial population densities. Furthermore, this study tested whether the prediction of interaction strengths becomes more consolidated with increasing complexity.

(Q4) Can allometrically-defined predator species explain patterns at the ecosystem level?

Chapter 2 applies the achieved model for allometric feeding rates in a dynamic simulation to estimate the coexistence under given predator and prey body mass combinations. I compare this predicted stability domain to thousands of empirically observed predator–prey pairs of forest litter ecosystems and evaluate the match.

In **Chapter 6**, page 105, I demonstrate how allometric concepts can be applied for investigations of altered body mass structure of predator populations, as it can be observed under changing climate conditions. I report the *in situ* manipulation of a marine top predator's average body mass and the response of the subtidal ecosystem. The study also investigated how such top-down effects interact with coinciding bottom-up effects of nutrient enrichment.

I performed a dynamic simulation of allometrically defined predator species over a large gradient of initial species richness, which is reported in **Chapter 7**, page 127. In these model food webs, I investigate the emergent stability properties of the species assemblage and of its functioning. Furthermore, these simulations provide a picture how different ecosystem functions, such as biomass stocks and rates, are interacting.

In the final **Chapter 8**, page 145, I synthesize the findings of the research chapters and provide answers to the central research questions. I discuss the allometric approach on the correlation between biodiversity and ecosystem functioning with special regard to theory and experimental design.

Part II.

Research chapters

Chapter 2.

Generalized allometric functional responses facilitate predator-prey stability

Gregor Kalinkat, Florian D. Schneider, Anna Schmehl, Thomas Schimmer, Olivera Vucic-Pestic, Christian Guill, Christoph Digel, Ulrich Brose and Björn C. Rall

Abstract

The stability of ecological communities depends critically on the distribution and strength of interactions as quantified by non-linear functional responses. Two major approaches in community ecology have highlighted the importance of (1) classic functional-response types and (2) systematic constraints of body sizes on interaction strengths. Merging these two aspects of current food-web ecology we present a novel framework with allometric constraints on all functional-response parameters including their type. To empirically test this framework we gathered the largest dataset on laboratory feeding rates of terrestrial invertebrates compiled so far. The predators and their prey cover a wide range of body-size ratios. Our results demonstrate that all functional-response parameters (i.e., handling times, capture coefficients and capture exponents) scale with predator and prey body masses. In consequence, our generalized functional responses replace the conventional functional-response types by an allometrically defined continuum from type II to type III with increasing predator-prey body-mass ratios. Subsequently, we implemented the new generalized and the traditional functional responses in a bioenergetic model of population dynamics, which suggested stable coexistence for entirely different combinations of predator and prey body masses. Interestingly, an independent dataset on terrestrial predator-prey interactions provided strong support for the predictions of the new generalized functional-response models. Together, these results suggest that the traditional functional-response types represent extremes of continuous allometric scaling functions. The novel generalized functional-response models presented here will allow a deeper understanding of quantitative interactions and their implications for the stability of food webs.

Keywords | Allometry, body size, predator-prey interactions, functional response, interaction strength

Introduction

The stability of populations, communities, and ecosystem functions depends critically on the strengths, distributions and characteristics of the interactions connecting species in complex food webs (de Ruiter *et al.*, 1995; McCann *et al.*, 1998; Neutel *et al.*, 2002, 2007; Rooney *et al.*, 2006). Traditionally, consumer-resource interactions have been categorized according to their functional response which mostly describes hyperbolic (type II) or sigmoidal (type III) increases in the consumer's per capita feeding rate with the resource density (Holling, 1959*a*; Oaten and Murdoch, 1975; Hassell *et al.*, 1977; Jeschke *et al.*, 2002, 2004; Sarnelle and Wilson, 2008). While type-II functional responses generally lead to unstable, oscillatory dynamics, density-dependent per capita predation rates of type-III functional responses cause stable equilibria of population densities (Oaten and Murdoch, 1975; Williams and Martinez, 2004*b*; Fryxell *et al.*, 2007; Rall *et al.*, 2008). However, characterizing these functional-response types for each of the myriads of interactions in natural communities by tedious individual experiments is infeasible which renders a generalized understanding of natural population dynamics impossible.

An alternative approach employs body sizes and their "allometric" relationships with ecologically important traits of species and their interactions (Elton, 1927; Sheldon *et al.*, 1972; Peters, 1983; Brown *et al.*, 2004). This allometric approach predicts the biological rates of populations such as respiration, death and growth by population-averaged body masses (Peters, 1983; Brown *et al.*, 2004) that are often easily available for all consumer-resource pairs (Brose *et al.*, 2006*a*). Moreover, this constrains the universe of possible combinations of biological rates to those that are probable, given that they all scale with species' body masses (Brose, 2010*b*). Allometric models demonstrated that variance in consumer and resource body masses has profound effects on population dynamics (Yodzis and Innes, 1992; Weitz and Levin, 2006; Otto *et al.*, 2007) and food-web persistence (Loeuille and Loreau, 2005; Brose *et al.*, 2006*b*; Brose, 2008; Rall *et al.*, 2008). However, they could not explain the radical dynamic shifts associated with differences between functional-response types, which limits their predictive accuracy.

Here, we present a novel approach merging allometric scaling models with functional-response types. These entirely allometric functional responses go beyond the traditional functional-response types by including allometric scaling relationships for the capture exponent, enabling a smooth transition between functional-response types. After parameterizing these allometric functional responses to a database of empirical predator-prey interactions, dynamical analyses demonstrate that these modifications of the functional responses cause severe differences in population dynamics. Note, that the principles in this study were exercised on terrestrial invertebrate predators and prey in the classical sense (i.e., consumers that subdue and feed on a heterotroph resource) but are suitable for other types of consumer–resource interactions. For reasons of clarity we will adhere to the predator–prey terminology. The resulting possible combinations of predator and prey body masses allow stable coexistence. Finally, these differ-

ences are successfully tested against empirical predator–prey body-size data from an entirely independent database.

Material and methods

Functional responses

While there are various measures of interaction strengths (Berlow *et al.*, 2004) the functional response model framework established by Solomon (1949) and Holling (1959*a*) has been used in a plethora of studies (reviews in Jeschke *et al.*, 2004; Englund *et al.*, 2011; Rall *et al.*, 2012), where the per capita consumption rate of the predator, F, depends on the density of the prey, N:

$$F = \frac{aN}{1 + ahN}, \tag{2.1}$$

with the handling time, h, needed to kill, ingest and digest one prey individual (Holling, 1959*a*; Hassell, 1978) and the attack rate, a (hereafter: "capture rate"). Although there is only a limited number of functional-response studies that were focusing on body-size relationships we know today about the nature of capture rates and handling times. Capture rates follow hump-shaped relationships with predator-prey body-mass ratio (e.g., Hassell *et al.*, 1976; Wahlström *et al.*, 2000; Aljetlawi *et al.*, 2004; Vonesh and Bolker, 2005; Vucic-Pestic *et al.*, 2010; Rall *et al.*, 2011). Handling times generally decrease with increasing body mass ratios (Brose, 2010*b*), although different relationships have been reported (linear relationships e.g., Hassell *et al.*, 1976; Spitze, 1985, exponential or power law relationships e.g., Hassell *et al.*, 1976; Aljetlawi *et al.*, 2004; Vucic-Pestic *et al.*, 2010; Rall *et al.*, 2011). These relationships can be explained by allometric arguments provided by bioenergetic constraints (Yodzis and Innes, 1992) and metabolic theory (Brown *et al.*, 2004; Brose, 2010*b*). The type-II functional response with a constant capture rate (Eq. 1) can be modified to account for capture rates that vary with prey density, $a = bN^q$ (Real, 1977; Williams and Martinez, 2004*b*; Rall *et al.*, 2008; Vucic-Pestic *et al.*, 2010), which yields type-III functional responses:

$$F = \frac{bN^{1+q}}{1 + bhN^{1+q}}, \tag{2.2}$$

where b is a capture coefficient (sometimes also referred to as search coefficient), and q is a scaling exponent (hereafter: "capture exponent") that converts hyperbolic type-II ($q = 0$) into sigmoid type-III ($q = 0$) functional responses (note that some authors refer to intermediate or modified type-II functional responses for values $0 < q < 1$; e.g., Williams and Martinez, 2004*b*). Historically, the quest for type-III functional responses has been fuelled by its far-reaching consequences on population dynamics, i.e., its ability to promote stable equilibrium states as increasing predation risks under sigmoid functional responses can yield an effective per capita top-down control while at low population densities the prey is released from predation risk

(Oaten and Murdoch, 1975; Yodzis and Innes, 1992; Williams and Martinez, 2004*b*; Rall *et al.*, 2008). On the other hand the empirical and statistical documentation of type-III functional responses has been difficult (Sarnelle and Wilson, 2008) and type-II functional responses prevail in the vast majority of laboratory studies (Jeschke *et al.*, 2004). However, Sarnelle and Wilson (2008) showed that type-III functional responses might be more common than previously assumed and the lack of evidence for the existence of type-III responses might often be due to scanty replication at low prey densities. Another reason for a possible underrepresentation of type-III responses in laboratory studies might stem from oversimplified environment in experimental arenas lacking habitat structure that provides prey refuges especially for relatively small prey (Hassell *et al.*, 1977; Crawley, 1992). This concept has been confirmed by the study of Vucic-Pestic and colleagues (2010) where functional responses of predatory beetles and hunting spiders were tested for one large and one small prey species, respectively. This study showed that more sigmoid type-III functional responses occur when the predators feed on the smaller prey species (flightless fruit flies in experiments with beetles and springtails in experiments with spiders, respectively). Furthermore, the authors suggested a general allometric scaling of the capture exponent: increasing predator–prey body-mass ratios coincide with increasing values for q. Since only two prey sizes (that simultaneously represented two different prey species) per predator group where deployed in this study and a significant allometric relationship of the capture exponent was only documented for the beetles, the findings of Vucic-Pestic and colleagues (2010) still have to be verified in a more generalized study including more predator and prey groups and especially an extended prey-size range. In the present study we therefore investigated the allometric effects on the functional response based on the methods and the model framework developed in earlier studies (Brose *et al.*, 2008; Vucic-Pestic *et al.*, 2010; Rall *et al.*, 2011). While in these studies only the predator size was varied on a uniform prey, we now performed a series of experiments where predator and prey sizes were varied systematically. Subsequently, we analyzed the resulting dataset combining results from previous and novel experiments for allometric relationships of the parameters of capture rate, a, and capture coefficient, b, handling time, h, and the capture exponent q.

Feeding rate experiments

The basic experimental setup mainly follows prior functional-response experiments (Brose *et al.*, 2008; Rall *et al.*, 2010, 2011; Vucic-Pestic *et al.*, 2010, 2011). We studied the per capita feeding rates of 25 species of generalist arthropod predators (carabid and staphylinid beetles, lycosid, pisaurid and salticid spiders and centipedes) on eight differently-sized prey species varying prey densities from one to 1000 individuals of prey per arena (0.04 m^2). Different life stages of some of the predators were used to extend the body mass range (particularly those of *Trochosa terricola*, Aranaea and *Lithobius* spec., Chilopoda). For most predators we included

only imagines, and for adult spiders only female individuals were used (see supplementary material Table 2.1 on page 46, for a complete list of predator-prey pairs, their body-mass ratios and references to prior studies). We measured the body masses of each predator individually for each replicate. However, most replicates contained multiple prey individuals. Hence, we sorted prey individuals to minimize within-replicate variance in body mass and used the average prey body mass for each replicate (see supplementary material Table 2.2 on page 48, for predator and prey species with body masses). Prey density levels were replicated up to eight times resulting in a total number of 2820 experimental units. The predators were sampled from the field and only a small fraction of juvenile centipedes and lycosid spiders were reared in the laboratory until they reached the designated size class.

The predator individuals were kept separate in plastic jars dispersed with water and were deprived of food for at least 48 hours before starting the experiments. The experiments were performed in Perspex® arenas (0.2 × 0.2 × 0.1 m) covered by lids with holes to allow gas exchange. The arena floor was covered with moist plaster of Paris (200 g dry weight) to provide constant moisture during the experiments. Habitat structure in the arenas was provided by moss (*Polytrichum formosum*, 2.35 g dry weight) that was first dried for several days at 40°C to exclude other animals and then re-moisturized prior to the experiments. Prey individuals were placed in the arenas 30 minutes in advance of the predators, to allow them to disperse in the arenas. The experiments were run for 24 hours with a day/night rhythm of 12 hours each and a temperature of 15°C. Initial and final prey densities were used to calculate the number of prey individuals eaten. Predators were weighted before and after the experiments to calculate mean body mass. Control experiments without predators showed that prey mortality or escape was negligible.

Statistical analyses

Our general approach was based on fitting three different allometric functional-response models to the feeding-rate data that were evaluated according to their ΔAIC (difference in Akaike Information Criterion, AIC, to the model with lowest AIC). The first model was a type-II functional response with fixed allometric-scaling exponents according to Yodzis and Innes (1992) where the capture rate

$$a = a_0 m_r^{-1} m_c^{0.75} \tag{2.3}$$

as well as the handling time

$$h = h_0 m_r m_c^{-0.75} \tag{2.4}$$

are described with h_0 and a_0 as constants and the body masses [g], m_c and m_r, of the predator c, and the prey r, respectively. These null models of allometric relations are based on the simplified assumption that interaction parameters should scale with metabolic rate, which follows a $^3/_4$

power law with body mass (Peters, 1983; Brown *et al.*, 2004; Brose, 2010*b*, see supplementary material page 48, for a detailed description of the derivation from the models in Yodzis and Innes (1992) into the allometric-scaling relations for Holling type-II functional-response parameters). Subsequently, we will refer to this first model as traditional type-II functional response. In the second model, allometric relationships were included according to prior studies (Vucic-Pestic *et al.*, 2010; Rall *et al.*, 2011) where handling time, h, follows power law relationships with predator and prey body mass:

$$h = h_0 m r^{c_r} m_c^{c_c}, \tag{2.5}$$

where c_c and c_r are allometric exponents (Rall *et al.*, 2011). As capture rates follow hump-shaped relationships with predator-prey body-mass ratios (Wahlström *et al.*, 2000; Aljetlawi *et al.*, 2004; Vucic-Pestic *et al.*, 2010) we estimated the allometry of the capture rate, a, using a combined equation comprising a power-law relationship with prey body mass and an exponential Ricker function that describes a humped curve with increasing body-mass ratios of the predator to the prey:

$$a = a_0 m_r^{\beta_r} \frac{m_c}{m_r} \mathrm{e}^{\varepsilon \frac{m_c}{m_r}}, \tag{2.6}$$

where a_0 is a constant, β_r is the exponent for the scaling of m_r, and e is the exponential parameter determining the decrease of attack rates at high body-mass ratios (Rall *et al.*, 2011). This pattern of decreases and increases in attack rates at low and high prey body mass yields a hump-shaped attack model (Wahlström *et al.*, 2000; Aljetlawi *et al.*, 2004; Vucic-Pestic *et al.*, 2010). The capture exponent is not included in this model, yielding a strict type-II functional response. We will refer to this second model as hump-shaped functional response.

Finally, we extended the second model by including sigmoidal scaling of the capture exponent, q, with the predator-prey body-mass ratio R:

$$q = \frac{q_{max} R^2}{q_0^2 R^2}, \tag{2.7}$$

where q_{max} and q_0 are scaling exponents defining the sigmoid relationship. The definition of the capture coefficient b (Eqn. 2.2) then follows that of the capture rate (Eqn. 2.6) substituting the constant b_0 for a_0:

$$b = b_0 m_r^{\beta_r} \frac{m_c}{m_r} \mathrm{e}^{\varepsilon \frac{m_c}{m_r}}. \tag{2.8}$$

Accordingly, the insertion of equations 2.5, 2.7 and 2.8 into equation 2.2 yielded our third model (hereafter: generalized allometric functional response) accounting for hyperbolic as well as sigmoid forms of the response in dependence of predator and prey body masses.

To account for decreasing prey densities during experiments we used the integrated form of the functional response, also known as Rogers' 'Random Predator Equation' (Royama, 1971;

Rogers, 1972), for all three models:

$$N_e = N_0 - N_0 e^{(ahN_e - aT)}, \tag{2.9}$$

where N_e is the number of the prey individuals eaten during the experiment, T is the experimental time and all other parameters are as given in equation 2.2 (with $a = bN^q$ in the generalized allometric functional response model scenario; Vucic-Pestic *et al.*, 2010). We solved this recursive function of N_e using the Lambert W function (see Bolker, 2008 and references therein for a detailed description):

$$N_e = N_0 - \frac{W(ahe^{(ahN_e - aT)})}{ah}. \tag{2.10}$$

The parameters in equation 2.10 and respective substitutes were estimated by fitting it to the dataset of experimentally observed feeding events at different prey densities and predator and prey body masses, using a non-linear least squares method ("nls") using the package "emdbook" for the statistical software R (Bolker, 2008; R Development Core Team, 2011). See supplementary material for a description of the substitution of parameters into equation 2.10 for the three different models.

Model analyses

To illustrate the consequences of these allometric relationships on population dynamics, we performed a series of simulations following a bioenergetic predator-prey model where the three scenarios of allometric relationships in the feeding interactions (the traditional type-II, the hump-shaped and the generalized allometric functional response, respectively) were realized and other components of the model were also adjusted according to allometric constraints (Yodzis and Innes, 1992; Rall *et al.*, 2008; see Supplementary Material page 51 for methodological details of the model simulations). Finally, we compared the resulting persistence domains of the model simulations (i.e., the range of prey and predator sizes at which the predator is able to persist) with a novel database on the body masses of predator–prey pairs in terrestrial soil food webs from a large biodiversity research project in Germany (the Biodiversity Exploratories; Fischer *et al.*, 2010; see Supplementary Material on page 52 for methodological details of database assembling).

Results

The comparison via AIC revealed that the generalized allometric functional response model with allometric scaling of all parameters including q was the best fitting model (ΔAIC = 0.0; degrees of freedom, df = 9) compared to the simpler, hump-shaped functional response (ΔAIC = 645.52; df = 7) and the traditional type-II functional response (ΔAIC = 1703.74; df = 3;

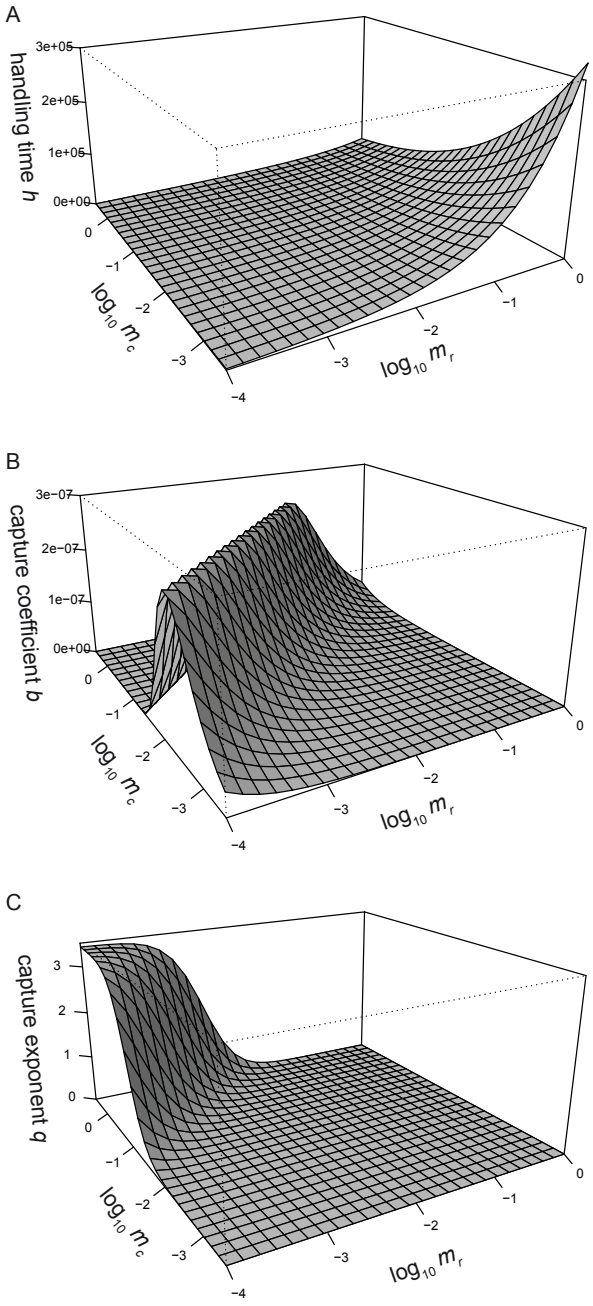

Figure 2.1 – Relationship between the three fundamental functional response parameters handling time h (A), capture coefficient b (B) and the capture exponent q (C) with $\log_{10}$ predator mass m_c [g] on the z- and $\log_{10}$ prey mass m_r [g] on the x-axis.

see supplementary material for an overview of all parameters of the three fitted models). Together, these results imply that the generalized allometric functional-response model provides a substantially better fit to the functional-response data, and all subsequent results will be based on this model.

We found a negative power-law scaling relationship for handling time h with predator body mass ($h_0 = 35,960$; standard error = 6,986; $p < 0.001$; $c_c = -0.2738$; *s.e.* = 0.0213; $p < 0.001$;

Fig. 2.1A), while h scaled positively with prey mass following a power-law relationship ($c_r = 0.544$; *s.e.* = 0.021; $p < 0.001$; Fig. 2.1A). Hence, handling times followed power-law relationships with predator as well as prey masses resulting in highest handling times at very low predator-prey body-mass ratios (i.e., the prey is larger than the predator, Fig. 2.1A). Furthermore, we found hump-shaped relations for the capture coefficient b with the predator-prey body-mass ratio ($b_0 = 1.212 \cdot 10^{-8}$; *s.e.* = $2.912 \cdot 10^{-9}$; p < 0.001; $\varepsilon = -0.0189$; *s.e.* = 0.0008; $p < 0.001$; Fig. 2.1B) although the scaling factor β_r was not significant ($\beta_r = -0.0065$; *s.e.* = 0.0342; $p = 0.844$) meaning that the capture coefficient did not scale explicitly with prey mass (besides the body-mass ratio scaling). Finally, the capture exponent q scaled positively with the predator-prey body-mass ratio R following a sigmoid relationship ($q_0 = 996.5$; *s.e.* = 19.83; $p < 0.001$; $q_{max} = 3.422$; *s.e.* = 0.144; $p < 0.001$; Fig. 2.1C) implying that the higher the body-mass ratio the more sigmoid the functional response. This translates into type-II-like responses for small predators on relatively large prey, while large predators should be feeding on smaller prey following type-III-like responses.

In Figure 2.2 (C and D) we illustrate how these allometric constraints on functional-response parameters translate into specific feeding rates at fixed prey (functional-response plane as a function of $\log_{10}$ predator mass, Fig. 2.2C) and predator masses (functional-response plane as a function of $\log_{10}$ prey mass, Fig. 2.2D). Figure 2.2A illustrates the location of these fixed body masses relative to the other data. In both graphs, the hump-shaped curvature of the feeding rates and the sigmoid behaviour at low densities and high body-mass ratios can be observed (Fig. 2.2C, D). Additionally, Figure 2.2B provides an overview of the observed feeding rates in the experimental replicates versus the feeding rates predicted by the best fitting model.

The results of the dynamic population model simulations under the three allometrically constrained feeding-rate scenarios are depicted in Figure 2.3. Here we show the persistence domains of the consumer as a function of predator and prey body masses defined as the area with individual-density minima of the predator larger than 10^{-30} [g m^{-2}]. While the predator in the traditional type-II functional response model scenario only persisted with very low prey masses (Fig. 2.3A), the other two model scenarios produced a more band-shaped persistence domain across the predator–prey masses (Fig. 2.3B, C). However, these two domains exhibit pronounced differences including that under the hump-shaped functional response scenario large predators can persist across a wide range of prey body masses (Fig. 2.3B), whereas the generalized allometric functional response scenario produces a cone-shaped persistence domain where the largest predators can only persist on a very small range of prey body masses (Fig. 2.3C).

Subsequently, we compared the persistence domains predicted by the dynamic population models with empirical body-mass data of forest soil invertebrates. These data were chosen, because they include the same predator and prey groups as the functional-response experiments. We evaluated the models according to the percentage of natural predator-prey links

(black dots in Fig. 2.3A, B, C) that fall within the persistence domains. Interestingly, this comparison revealed that the fixed allometric-scaling relations following Yodzis and Innes (1992) yielded a persistence domain that included only 25.42 % of the natural body-mass combinations (Fig. 2.3A), which is considerably less than the persistence domain of the hump-shaped functional-response model including 78.64 % of the interaction pairs (Fig. 2.3B). The generalized allometric functional-response model performed best yielding a persistence domain matching 95.57 % of the links in the food-web data base (Fig. 2.3C).

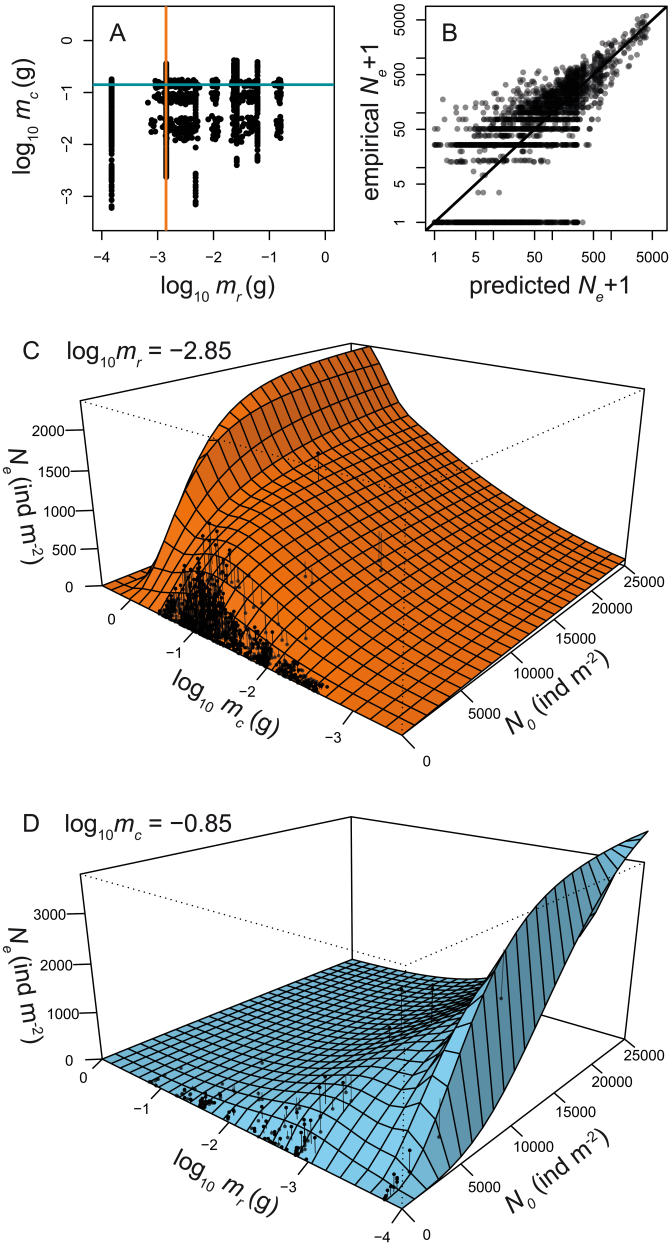

Figure 2.2 – (A) Overview of the range of predator body masses, m_c, versus prey body masses,m_r, in the experimental replicates. The vertical, orange line (at $\log_{10} m_r = -2.85$) corresponds to the orange plane in C while the blue horizontal line (at $\log_{10} m_c = -0.85$) corresponds to the plane in D. (B–D) generalized allometric functional response. (B) predicted feeding rates versus observed feeding rates. (C) functional response as a function of prey densities and $\log_{10}$ predator mass m_c at a fixed prey mass of $\log_{10} m_r = -2.85$. (D) functional response as a function of prey densities and $\log_{10}$ prey mass m_r at a fixed predator mass of $\log_{10} m_c = -0.85$.

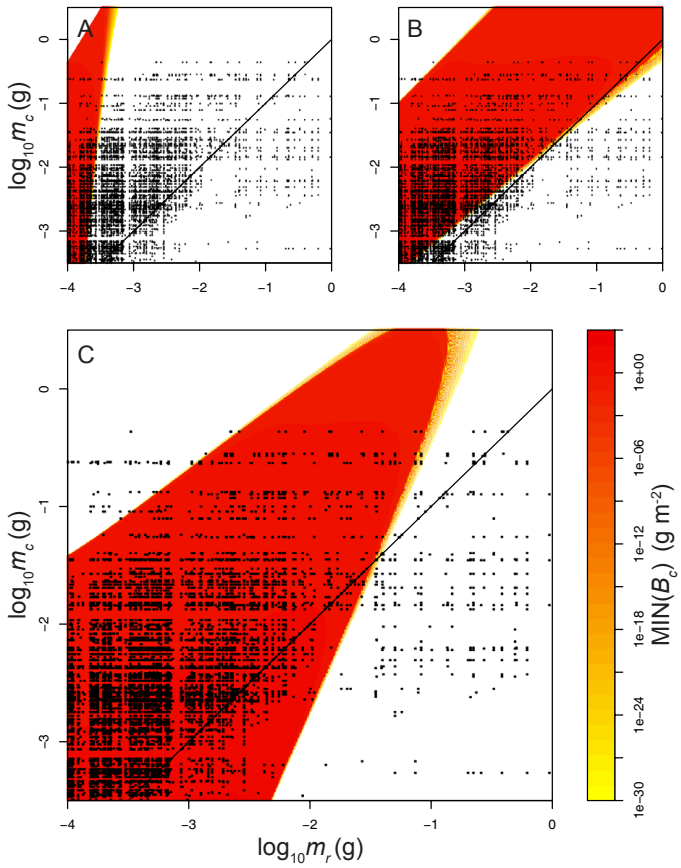

Figure 2.3 – Results of the bioenergetic model simulations following three different functional response models: (A) traditional type-II; (B) hump-shaped functional response; (C) generalized allometric functional response (see supplementary material page 48 for parameters of the three models and page 51 for details on model simulations). Colour represents the persistence domain of the predator shown as minima of biomass density [ind. m^{-2}] depending on $\log_{10}$ prey mass, m_r, and $\log_{10}$ predator mass, m_c. Black dots represent body masses from empirical predator–prey pairs observed in the Biodiversity Exploratories meta–food-web. Black diagonal represents the body-mass ratio $R = 1$ (i.e., where m_c equals m_r).

Discussion

In the present study, we examined how the body masses of predators and prey constrain their interaction strengths. Corroborating prior functional-response studies (Wahlström *et al.*, 2000; Aljetlawi *et al.*, 2004; Vonesh and Bolker, 2005; Vucic-Pestic *et al.*, 2010; Rall *et al.*, 2011), we found power-law relationships between handling time and predator as well as prey mass and hump-shaped relationships between capture rates and predator-prey body-mass ratios. In addition, our results add a dependency for the capture exponent on predator and prey body mass, converting hyperbolic type-II into sigmoid type-III functional responses. Strikingly, this suggests that there are no discrete functional-response types. Instead, our generalized functional response model proposes gradual shifts from type-II predation of small predators on equally sized prey to type-III functional responses of large predators on small prey. This new concept of generalized allometric functional responses thus bridges lingering gaps between prior allometric models predicting quantitative interaction strengths and approaches based on functional-response types addressing constraints on population dynamics. Our bioenergetic model simulation illustrate mechanistic constraints of predator and prey body masses on population dynamics and persistence that deviate significantly from prior models. This new

understanding of intrinsic population persistence is strongly supported by independent food-web data. Our results emphasize biological mechanisms that might be responsible for the regularities in body-size distributions across food webs (Brose *et al.*, 2006*a*; Riede *et al.*, 2011) with their critical importance for stability (Otto *et al.*, 2007; Berlow *et al.*, 2009).

General approach

In the present study we have chosen an allometric approach by evaluating a large functional-response data base (more than 2,800 replicates) without accounting for the phylogenetic or taxonomic variance in the dataset, which comprises 72 taxonomically different predator-prey pairs (supplementary material Table 2.2, page 48). However, previous work has shown how allometric functional-response models can (1) explain a large part of variation in predatory feeding rates with a minimal number of parameters as well as (2) be easily extended to account for taxonomic differences (Rall *et al.*, 2011). We emphasize that this kind of model must be considered as a mechanistic null-model for our understanding of predator–prey interactions and their implications for food-web stability. While the traditional approach in research on interaction strengths has been to look at body-size constraints within the framework of taxonomic entities (e.g., Hassell *et al.*, 1976; Spitze, 1985; Aljetlawi *et al.*, 2004; Vonesh and Bolker, 2005) we suggest to take allometry as a baseline and add taxonomic (or phylogenetic) information atop. Until recently, this approach was exclusively used in the aquatic sciences ("size spectra", e.g., Sheldon *et al.*, 1972; Jennings and Mackinson, 2003) but food-web ecologists have been calling lately for a more universal application (Raffaelli, 2007).

Handling time and hump-shaped capture rates

Corroborating prior studies (Hassell *et al.*, 1976; Wahlström *et al.*, 2000; Aljetlawi *et al.*, 2004; Vonesh and Bolker, 2005; Vucic-Pestic *et al.*, 2010), we found (1) power-law increases in handling time with prey mass, (2) power-law decreases in handling time with predator mass, and (3) hump-shaped relationships between capture rates (i.e., capture coefficients) and predator–prey body-mass ratios. Metabolic arguments suggest that maximum consumption rates that are proportional to the inverse of handling time (Yodzis and Innes, 1992; Koen-Alonso, 2007) should follow the same scaling relationships with body mass as metabolic rates (Yodzis and Innes, 1992; Brown *et al.*, 2004). Interestingly, our results suggest that the power-law exponent of the relationship between handling time and predator mass (–0.27) is much shallower than the negative $^3/_4$ exponent expected by metabolic theory. Moreover, the power-law increase in handling time with prey mass is also shallower (0.54) than the expected isometric scaling. These shallow scaling relationships of handling time with predator and prey masses are corroborated by prior studies (Rall *et al.*, 2012; Vucic-Pestic *et al.*, 2010). Together, these results suggest that handling time is constrained by more complex processes than metabolism. For instance,

the scaling relationship for predator mass might be biased by different feeding modes such as sucking or chewing that shifts with increasing body masses (within our dataset) when comparing the feeding mode of liquid-feeding spiders (mean body mass: 0.036 g; $n = 618$) and centipedes (m.b.m.: 0.082 g; $n = 903$) on the one hand and the chewing beetles (m.b.m.: 0.124 g; $n = 1299$) on the other. Therefore small liquid feeders that ingest less unpalatable parts of their prey (e.g., sclerotized cuticle) than larger chewers ingesting whole prey items could account for shallower relationships.

Moreover, our results support previous studies showing a hump-shaped relationship between capture rates and predator-prey body-mass ratios (Wahlström *et al.*, 2000; Aljetlawi *et al.*, 2004; Vucic-Pestic *et al.*, 2010; Rall *et al.*, 2011). Altogether, the qualitative check of the model with the observed versus predicted feeding rates (Fig. 2.2B) shows that the model performs well at high feeding rates that are characterized by the handling time (i.e., proportional to the maximum ingestion rate; Koen-Alonso, 2007) whereas the model predictions overestimate especially the zero-consumption events (empirical $N_e + 1 = 1$, Fig. 2.2B). Naturally, the model can hardly predict these cases where individuals do not feed at all. Although we controlled the most important factors that might cause the refusal of feeding (e.g., we standardized the hunger levels) there might be other biological mechanisms causing lowered foraging activity. For instance, spiders stop feeding several days before starting to moult (Foelix, 1996).

Functional-response types

Historically, the majority of studies on sigmoid functional responses have been associated with prey switching (Murdoch *et al.*, 1975; Kalinkat *et al.*, 2011) whereas our study corroborates prior findings that type-III responses can occur in simple one predator–one prey systems (Hassell *et al.*, 1977; Sarnelle and Wilson, 2008; Vucic-Pestic *et al.*, 2010). There are diverse biological mechanisms that might be responsible for these allometrically-fostered sigmoid response curves. First, our experiments included habitat structure provided by moss to avoid overestimation of consumption rates that has been observed in unstructured artificial systems (Munyaneza and Obrycki, 1997; Hohberg and Traunspurger, 2005). It has been proposed that such conditions might provide prey refuges and that the existence of such refuges is suited to promote type-III responses (Crawley, 1992, see Supplementary Material, p. 48) particularly for large predator-prey body-mass ratios (Vucic-Pestic *et al.*, 2010). This concept is based on the assumption that large predators cannot follow their smaller prey into interstices provided by the moss. While a previous study (Vucic-Pestic *et al.*, 2010) demonstrated higher scaling exponents for larger predators, we generalized this concept across a wider range of predator and prey species with an extended range of prey sizes resulting in predator-prey body-mass ratios spanning roughly five orders of magnitude ($R_{min} = 0.08$; $R_{max} = 1199.50$). Further mechanisms creating more sigmoid response curves might be explained by optimal foraging theory: Evolu-

tionary fixed active enhancement (or reduction) in search effort at certain threshold levels of prey densities (Sih, 1984) seem to be energetically reasonable. Especially at high predator-prey body-mass ratios it might not be profitable to pursue relatively small prey individuals at very low densities. This means that a predator would not "activate" its "foraging mode" aimed at small prey individuals if their overall density was relatively small. Moreover, our approach of merging data on a wide range of predator-prey pairs to the unidimensional information of body masses together with the outstanding assemblage of the dataset (almost 3000 experimental units) and an adequate replication at low initial prey densities assured detection of type-III behaviour following the suggestions of Sarnelle and Wilson (2008).

Previous theoretical studies have shown that slight changes in the capture exponent converting hyperbolic (i.e., type-II) into sigmoid (i.e., type-III) functional responses may have far-reaching consequences for population dynamics (Williams and Martinez, 2004*b*; Rall *et al.*, 2008) but a link between these concepts and allometrically constrained interaction strengths has been lacking so far. Hence, we present an allometric scaling of the capture exponent that is entirely novel. Interestingly, our results suggest that this capture exponent increases with predator-prey body-mass ratios thus suggesting hyperbolic and sigmoid functional responses at low and high body-mass ratios, respectively. This allometric concept goes beyond simple types of functional responses by relating a continuous distribution of functional-response shapes to the body masses of predators and their prey. Instead of fixed types, the shape of the functional response becomes an emergent property of predator and prey sizes.

Dynamic model

Consequences of these patterns on the level of populations are illustrated in Figure 3 where the results of the dynamic simulation module are shown for the complex model with the sigmoid scaling of q and the two simpler models: Firstly, the allometric null model of Yodzis and Innes (1992), where both capture rates and handling times follow power-law relationships with globally fixed scaling exponents results in a relatively small persistence domain where neither small nor large predators can persist on medium or large sized prey (within the size ranges investigated in the present study; Fig. 2.3A). Meanwhile both allometric models with hump-shaped relation of the capture rates and capture coefficients, respectively, result in a persistence band within the predator-prey mass space (Figs. 2.3B and C). Above all the comparison with the empirical food-web data shows that both the hump-shaped functional response (78.64 % of empirical predator-prey pairs within persistence domain) as well as the generalized allometric functional response (95.57 %) perform by far better than the traditional type-II functional response (25.42 %). The notable differences between the hump-shaped model of Rall *et al.* (2011) and our novel, generalized model highlight the importance of the introduction of the additional, allometrically constrained component allowing for sigmoid response curves. This

result is even more striking when taking into account that the persistence domain is smaller in the generalized allometric model. Interestingly, this also coincides with a particular pattern of body-size relations for the smallest predators: while the empirical data includes only a limited number of predator-prey pairs with a body-mass ratio $R < 1$ (i.e., the predator is smaller than the prey; black dots beneath the black diagonal, Fig. 2.3) the majority of these pairs are to be found for the smaller predators. This is the region within the predator-prey body-mass space where the hump-shaped functional-response model predicts significantly less of the natural predator-prey pairs than the generalized allometric functional response model.

Altogether, our analyses demonstrate how sigmoid response curves at high body-mass ratios contribute critically to the persistence of predator-prey relations. Moreover, we strongly suggest a replacement of the traditional view of functional response types by a concept of gradual transition between hyperbolic and sigmoid response curves framed by allometric constraints.

Conclusions

Within this study we add an essential upgrade to existing knowledge about how allometric effects on interaction strengths structure and stabilize ecological communities (i.e., food webs). Our approach included laboratory feeding-rate experiments, statistical modelling of allometric relations in the experiments, simulations of population dynamics according to our empirical findings and, finally, a comprehensive test of the theoretical implications based on an independent dataset of predator-prey interactions. The core message of our results comprises the advise to outstrip traditional functional-response types and rather replace this categorical thinking by an allometrically defined continuum of hyperbolic and sigmoid response curves. This suggestion has far-reaching consequences for our understanding of structure and stability of food webs as smaller predators feed with hyperbolic responses on their similarly sized prey whereas large predators feed on small prey according to sigmoid response curves. We outline the consequences of our findings with analyses of predator-prey population dynamics under different allometrically constrained interaction models. The persistence domain we found in these bioenergetic population simulations is of striking accordance with the empirical predator-prey pairs from an extensive and independent database. This underlines the importance of this missing link between stability-promoting characteristics and allometric structuring of non-linear interaction strengths.

Acknowledgements

F.D.S. was funded by Deutsche Bundesstiftung Umwelt (www.dbu.de). We thank Petra Hosumbek for rearing the organisms and Lucia Carillo and Theodora Volovei for contributing to the experimental work.

Supplementary material to Chapter 2

Gregor Kalinkat, Florian D. Schneider, Anna Schmehl, Thomas Schimmer, Olivera Vucic-Pestic, Christian Guill, Christoph Digel, Ulrich Brose and Björn C. Rall

Predator and prey species and their body masses

Table 2.1 – Species list with mean, minimum and maximum body masses [gram]

Species	*n*	mean mass [g]	min. mass [g]	max. mass [g]
Predators				
Chilopoda				
Lithobius forficatus	903	0.08215	0.00657	0.20391
Coleoptera				
Carabidae				
Abax ovalis	105	0.16790	0.12151	0.24280
Abax parallelepipedus	176	0.30149	0.22000	0.41916
Anchomenus dorsalis	107	0.01448	0.00810	0.02160
Calathus fuscipes	36	0.07152	0.04525	0.11184
Calathus melanocephalus	6	0.01725	0.01145	0.02125
Calathus piceus	12	0.04492	0.03605	0.05625
Harpalus affinis	56	0.05078	0.03680	0.06590
Harpalus rufipes	142	0.11942	0.07635	0.19025
Nebria brevicollis	57	0.06589	0.04234	0.10365
Notiophilus biguttatus	44	0.00559	0.00400	0.00675
Notiophilus laticollis	40	0.00688	0.00459	0.00835
Poecilus cupreus	8	0.08784	0.08220	0.09740
Poecilus versicolor	140	0.06058	0.04015	0.08215
Pterostichus burmeisteri	27	0.10595	0.08495	0.12620
Pterostichus melanarius	110	0.15953	0.10984	0.26120
Pterostichus oblongopunctatus	122	0.06917	0.04765	0.08685
Staphylinidae				
Ocypus olens	70	0.30597	0.21644	0.40833
Ocypus ophtalmicus	18	0.08858	0.05198	0.11696
Philonthus fuscipennis	20	0.02250	0.01785	0.02970
Staphylinidae	3	0.02980	0.02005	0.03910
Aranaea				
Lycosidae				
Alopecosa spec.	34	0.01974	0.00060	0.07115
Pardosa lugubris	139	0.02975	0.02000	0.09430
Pardosa palustris	12	0.02922	0.01945	0.06825
Pirata spec.	25	0.02669	0.01400	0.05905
Trochosa terricola	388	0.03983	0.00200	0.15425
Pisauridae				
Pisaura mirabilis	13	0.10242	0.07050	0.17025
Salticidae				
Salticus scenicus	7	0.00676	0.00150	0.03030
Prey				
Isopoda				
Trichorhina tomentosa	108	0.00268	0.00067	0.00561
Collembola				
Heteromurus nitidus	526	0.00015	0.00015	0.00015
Ensifera				
Acheta domesticus	242	0.06303	0.00077	0.15987
Gryllus sigillatus	54	0.00478	0.00478	0.00478
Coleoptera				
Tenebrio molitor (Larvae)	118	0.06116	0.06116	0.06116
Alphitobius diaperinus (Larvae)	363	0.01652	0.00104	0.03046
Diptera				
Lucilia caesar (Larvae)	402	0.02604	0.02604	0.02604
Drosophila hydei (Imago, flightless)	1007	0.00143	0.00143	0.00143

Table 2.2 – Predator-prey pairs with mean body-mass ratios

Predator	Prey	*n*	mean *R*	published in
Alopecosa spec.	*Heteromurus nitidus*	16	141.167	Brose et al 2008
Alopecosa spec.	*Gryllus sigillatus*	18	3.791	Brose et al 2008
Abax ovalis	*Drosophila hydei* [1]	60	112.830	unpublished
Abax ovalis	*Lucilia caesar* [2]	39	6.849	unpublished
Abax ovalis	*Tenebrio molitor* [2]	6	2.802	unpublished
Abax parallelepipedus	*Drosophila hydei* [1]	67	200.318	Vucic-Pestic et al 2010
Abax parallelepipedus	*Lucilia caesar* [2]	55	12.042	unpublished
Abax parallelepipedus	*Tenebrio molitor* [2]	12	5.092	unpublished
Abax parallelepipedus	*Alphitobius diaperinus* [2]	42	13.259	Vucic-Pestic et al 2010
Anchomenus dorsalis	*Drosophila hydei* [1]	72	10.150	Vucic-Pestic et al 2010
Anchomenus dorsalis	*Tenebrio molitor* [2]	35	0.386	unpublished
Calathus fuscipes	*Alphitobius diaperinus* [2]	36	3.075	Vucic-Pestic et al 2010
Calathus melanocephalus	*Drosophila hydei* [1]	6	12.107	Brose et al 2008
Calathus piceus	*Drosophila hydei* [1]	6	31.772	Brose et al 2008
Calathus piceus	*Lucilia caesar* [2]	6	1.711	Brose et al 2008
Harpalus affinis	*Tenebrio molitor* [2]	17	0.857	unpublished
Harpalus affinis	*Drosophila hydei* [1]	24	34.383	unpublished
Harpalus affinis	*Lucilia caesar* [2]	15	1.989	unpublished
Harpalus rufipes	*Tenebrio molitor* [2]	18	2.009	unpublished
Harpalus rufipes	*Drosophila hydei* [1]	78	81.471	Vucic-Pestic et al 2010
Harpalus rufipes	*Lucilia caesar* [2]	46	4.750	unpublished
Lithobius forficatus	*Acheta domesticus*	242	21.162	unpublished
Lithobius forficatus	*Alphitobius diaperinus* [2]	220	15.554	unpublished
Lithobius forficatus	*Drosophila hydei* [1]	144	54.354	Rall et al 2011
Lithobius forficatus	*Heteromurus nitidus*	189	515.711	Rall et al 2011
Lithobius forficatus	*Trichorhina tomentosa*	108	37.748	unpublished
Nebria brevicollis	*Drosophila hydei* [1]	21	42.363	Brose et al 2008; unpublished
Nebria brevicollis	*Lucilia caesar* [2]	36	2.654	Brose et al 2008; unpublished
Notiophilus biguttatus	*Drosophila hydei* [1]	37	3.981	Brose et al 2008; unpublished
Notiophilus biguttatus	*Lucilia caesar* [2]	3	0.177	Brose et al 2008
Notiophilus biguttatus	*Tenebrio molitor* [2]	4	0.090	unpublished
Notiophilus laticollis	*Drosophila hydei* [1]	33	4.989	Brose et al 2008; unpublished
Notiophilus laticollis	*Lucilia caesar* [2]	3	0.198	Brose et al 2008
Notiophilus laticollis	*Tenebrio molitor* [2]	4	0.103	unpublished
Ocypus olens	*Drosophila hydei* [1]	36	200.008	Brose et al 2008; unpublished
Ocypus olens	*Lucilia caesar* [2]	34	12.603	Brose et al 2008; unpublished
Ocypus ophtalmicus	*Drosophila hydei* [1]	6	57.840	unpublished
Ocypus ophtalmicus	*Lucilia caesar* [2]	12	3.520	unpublished
Pardosa lugubris	*Drosophila hydei* [1]	63	22.245	Vucic-Pestic et al 2010
Pardosa lugubris	*Heteromurus nitidus*	70	181.076	Vucic-Pestic et al 2010
Pardosa lugubris	*Gryllus sigillatus*	6	8.281	Brose et al 2008
Pardosa palustris	*Heteromurus nitidus*	6	174.444	Brose et al 2008
Pardosa palustris	*Gryllus sigillatus*	6	6.752	Brose et al 2008

Predator	Prey	n	mean R	published in
Philonthus fuscipennis	*Drosophila hydei* [1]	9	16.840	Brose et al 2008
Philonthus fuscipennis	*Lucilia caesar* [2]	5	0.815	Brose et al 2008
Philonthus fuscipennis	*Tenebrio molitor* [2]	6	0.349	unpublished
Pirata spec.	*Heteromurus nitidus*	13	159.641	Brose et al 2008
Pirata spec.	*Gryllus sigillatus*	12	6.205	Brose et al 2008
Pisaura mirabilis	*Heteromurus nitidus*	6	665.476	Brose et al 2008
Pisaura mirabilis	*Gryllus sigillatus*	7	22.062	Brose et al 2008
Poecilus cupreus	*Drosophila hydei* [1]	6	59.932	unpublished
Poecilus cupreus	*Lucilia caesar* [2]	1	3.569	unpublished
Poecilus cupreus	*Tenebrio molitor* [2]	1	1.593	unpublished
Poecilus versicolor	*Drosophila hydei* [1]	70	41.450	Brose et al 2008; unpublished
Poecilus versicolor	*Lucilia caesar* [2]	53	2.375	Brose et al 2008; unpublished
Poecilus versicolor	*Tenebrio molitor* [2]	17	1.027	unpublished
Pterostichus burmeisteri	*Drosophila hydei* [1]	21	72.815	unpublished
Pterostichus burmeisteri	*Lucilia caesar* [2]	3	4.338	unpublished
Pterostichus burmeisteri	*Tenebrio molitor* [2]	3	1.870	unpublished
Pterostichus melanarius	*Drosophila hydei* [1]	36	102.725	Vucic-Pestic et al 2010
Pterostichus melanarius	*Lucilia caesar* [2]	38	6.660	Brose et al 2008, unpublished
Pterostichus melanarius	*Alphitobius diaperinus* [2]	36	6.794	Vucic-Pestic et al 2010
Pterostichus oblongopunctatus	*Drosophila hydei* [1]	45	46.651	Vucic-Pestic et al 2010
Pterostichus oblongopunctatus	*Lucilia caesar* [2]	37	2.753	Brose et al 2008, unpublished
Pterostichus oblongopunctatus	*Tenebrio molitor* [2]	11	1.151	unpublished
Pterostichus oblongopunctatus	*Alphitobius diaperinus* [2]	29	2.994	Vucic-Pestic et al 2010
Salticus scenicus	*Heteromurus nitidus*	5	20.667	Brose et al 2008
Salticus scenicus	*Gryllus sigillatus*	2	3.326	Brose et al 2008
Staphylinidae	*Drosophila hydei* [1]	3	20.916	unpublished
Trochosa terricola	*Heteromurus nitidus*	218	254.102	Vucic-Pestic et al 2010; Rall et al 2011
Trochosa terricola	*Gryllus sigillatus*	6	20.258	Brose et al 2008
Trochosa terricola	*Drosophila hydei* [1]	164	28.090	Vucic-Pestic et al 2010; Rall et al 2011

n number of replicates; R: Body mass ratio between predator and prey; [1] Imago, flightless; [2] Larvae

Functional response models

Overview of functional response models and the parameter estimates that were (1) derived from the model fittings to our feeding rate data and (2) afterwards used in the population dynamic simulations. All subsequent equations refer to the basic Holling type-II functional response where the per capita consumption rate of the predator, F, depends on the density of the resource, N

$$F = \frac{aN}{1 + ahN}, \tag{2.11}$$

with handling time h and capture rate a.

Traditional Type-II functional response

The basic assumption of allometric scaling according to the metabolic theory of Brown *et al.* (2004) is that metabolic rates scale with a 3/4 power law with the body mass of the organism (Yodzis and Innes, 1992 refer to Peters, 1983 as reference for their use of the 3/4-exponent). As the predator has to balance its metabolic rate the maximum possible feeding rate, F_{max}, should also scale with a 3/4 power law:

$$F_{max} = F_{max0} m_c^{0.75}, \tag{2.12}$$

where m_c is the body mass of the predator and F_{max0} is a constant. As F_{max} is the inverse of handling time (Koen-Alonso, 2007) it can be written as

$$h = \frac{1}{F_{max}} = \frac{1}{F_{max0} m_c^{0.75}} = h_0 m_c^{-0.75}. \tag{2.13}$$

Furthermore, following general allometric and energetic assumptions for the null model, the handling time for the prey should scale positively and linearly with its mass, m_r (e.g., a double amount of food needs double the time to be consumed). Therefore, equ. (2.13) can be extended to

$$h = h_0 m_r^1 m_c^{-0.75}. \tag{2.14}$$

To parameterize the entire functional response model according to Yodzis and Innes (1992) we assume the following relationship, where B_0 is the half saturation density:

$$B_0 = \frac{1}{ah}. \tag{2.15}$$

As Yodzis and Innes (1992) used constant half saturation densities independent of species' body masses it follows that the body-mass dependency of the capture rate a has to be inverse of that of the handling time h that they can cancel each other out:

$$a = a_0 m_r^{-1} m_c^{0.75}. \tag{2.16}$$

coefficient	estimate	*s.e.*	*t*	*p*
a_0	$1.684 \cdot 10^{-10}$	$7.127 \cdot 10^{12}$	23.62	< 0.0001 ***
h_0	$4.106 \cdot 10^{5}$	$1.791 \cdot 10^{4}$	22.93	< 0.0001 ***

Hump-shaped functional response

$$a = a_0 m_r^{\beta_r} \frac{m_c}{m_r} \mathrm{e}^{\varepsilon \frac{m_c}{m_r}} \tag{2.17}$$

$$h = h_0 m_r^{c_r} m_c^{c_c}. \tag{2.18}$$

coefficient	estimate	*s.e.*	*t*	*p*
a_0	$5.449 \cdot 10^{-8}$	$1.511 \cdot 10^{-8}$	3.61	0.0003 ***
h_0	$5.511 \cdot 10^{4}$	$1.500 \cdot 10^{4}$	3.67	0.0002 ***
ε	$-1.889 \cdot 10^{-3}$	$1.101 \cdot 10^{-4}$	−17.16	< 0.0001 ***
β_r	$4.463 \cdot 10^{-1}$	$3.746 \cdot 10^{-2}$	11.91	< 0.0001 ***
c_r	$6.498 \cdot 10^{-1}$	$3.265 \cdot 10^{-2}$	19.90	< 0.0001 ***
c_c	$-3.156 \cdot 10^{-1}$	$5.48 \cdot 10^{-2}$	−5.76	< 0.0001 ***

Generalized allometric functional response

$$a = bN^q \tag{2.19}$$

$$h = h_0 m_r^{c_r} m_c^{c_c}. \tag{2.20}$$

$$b = b_0 m_r^{\beta_r} \frac{m_c}{m_r} \mathrm{e}^{\varepsilon \frac{m_c}{m_r}} \tag{2.21}$$

$$q = \frac{q_{max} R^2}{q_0^2 + R^2} \tag{2.22}$$

coefficient	estimate	*s.e.*	*t*	*p*
b_0	$1.212 \cdot 10^{-8}$	$2.912 \cdot 10^{-9}$	4.16	< 0.0001 ***
β_r	$-6.747 \cdot 10^{-3}$	$3.420 \cdot 10^{-2}$	−0.20	0.844
ε	$-1.891 \cdot 10^{-2}$	$7.897 \cdot 10^{-4}$	−23.95	< 0.0001 ***
q_{max}	3.422	$1.444 \cdot 10^{-1}$	23.71	< 0.0001 ***
q_0	$9.965 \cdot 10^{2}$	$1.983 \cdot 10^{1}$	50.25	< 0.0001 ***
h_0	$3.596 \cdot 10^{4}$	$6.986 \cdot 10^{3}$	5.15	< 0.0001 ***
c_r	$5.440 \cdot 10^{-1}$	$2.187 \cdot 10^{-2}$	24.87	< 0.0001 ***
c_c	$-2.738 \cdot 10^{-1}$	$2.128 \cdot 10^{-2}$	−12.87	< 0.0001 ***

Model comparison

Model	AIC	Δ AIC	*df*
Traditional type-II functional response	39069.89	1703.74	3
Hump-shaped functional response	38011.67	645.52	7
Generalized allometric functional response	37366.14	0	9

Model simulation

We performed a simulation of population dynamics to assess the persistence domain of a predator in dependence on its own and its prey's body mass. Persistence of the predator was assumed, if the minima of its population density did not fall below 10^{-30} (individuals m^{-2}). The changes in population density per second of prey, N_r, and predator, N_c, were defined as ordinary differential equations (Yodzis and Innes, 1992; Otto *et al.*, 2007):

$$\frac{dN_r}{dt} = rN_r(\frac{1-N_r}{K}) - FN_c, \tag{2.23}$$

$$\frac{dN_c}{dt} = eFN_c - xN_c. \tag{2.24}$$

Here, the prey followed a logistic growth. The growth rate ($ind_r\ m^{-2}\ s^{-1}$),

$$r = 8.703 \times 10^{-8} m_r^{-0.25}, \tag{2.25}$$

scaled negatively with body mass, based on empirical parameters for growth rate (Savage *et al.*, 2004) adjusted to a temperature of 15 °C. The carrying capacity ($ind_r\ m^{-2}$),

$$K = 1 m_r^{-0.72}, \tag{2.26}$$

was defined to be one $ind_r\ m^{-2}$ for a prey of body mass one gram, scaling negatively with body mass with an empirically derived exponent (Meehan, 2006). The prey was consumed by each predator individual with the dynamic feeding rate, F (equation 2.23), which is a function of prey density. Here, the three allometric functional-response models, which were parametrized to the experimentally observed feeding rates (see supplementary material, page 52, for the respective parameter estimates), are substituted. This yielded three different, model-specific predictions of the persistence domain. The predator's density increased each second with the density lost from the prey population, FN_c, times the assimilation efficiency,

$$e = 0.85 \frac{m_r}{m_c}, \tag{2.27}$$

which comprises the increase in predator density from one consumed prey individual, using the assimilation factor 0.85 for biomass conversion of predators (Peters, 1983). The predator's energetic demands are modelled as

$$x = 4.083 \cdot 10^{-8} m_c^{-0.31}, \tag{2.28}$$

scaled negatively with body mass, based on empirical parameters for metabolic rate (Ehnes *et al.*, 2011) adjusted to a temperature of 15°C.

The differential equations were implemented in C and solved by using procedures from the GNU Scientific Library (4th order Runge-Kutta-Fehlberg method with 5th order error estimate; Galassi *et al.*, 2011). The population density at the start of the simulation was set to $N_c = 0.01$ ($\text{ind}_c\ \text{m}^{-2}$) and $N_r = 1$ ($\text{ind}_r\ \text{m}^{-2}$). Predator and prey body masses, $\log_{10} m_c$ and $\log_{10} m_r$, were varied systematically in the ranges from –3.5 to 0.5 for predators and –4 to 0 for prey with a step width of 0.005. Population dynamics ran over 10^{10} seconds into a steady state. Only the minimal values of the predator population density were saved (Figs. 2.3A,B,C).
Subsequently we extracted all predator-prey pairs within the body mass range covered by the simulation from the Biodiversity Exploratories meta-food-web (see Supplementary Material, p. 52). For each predator-prey pair and each of the three models substituted for F, a link was predicted, if the minimum of the model simulation at this point was larger than 10^{-30}. This allowed calculation of the percentage of those empirical links which lie within the area of persistence predicted by the model.

Soil food web data assembling

The meta-web used to extract predator-prey pairs for this study was assembled based on 48 sub-webs sampled in the spring of 2008 at 48 forest sites in three geographical regions within the research project Biodiversity Exploratories in Germany (Fischer *et al.*, 2010). Soil samples were taken with soil cores and heat extraction following the methods described by Macfadyen (1961) and Kempson *et al.* (1963). Subsequently species were determined and the length of each individual was measured. The body masses were calculated using mass length regressions based on an unpublished database on soil invertebrate body sizes from Roswitha Ehnes (Technische Universität Darmstadt).
We used available data on stable isotope signatures (e.g., Oelbermann and Scheu, 2010; B. Klarner, Georg-August University Göttingen, unpublished data) to sort all species into trophic groups (e.g., fungivores, herbivores). Furthermore, the predators could be assigned to different trophic levels. Feeding interactions were then estimated by literature research to detect possible links (Moulder and Reichle, 1972; Dunger, 2008; McLaughlin *et al.*, 2010) but also those that could be excluded according to other sources (e.g., oribatid mites are not eaten by macrofauna generalist predators; Peschel *et al.*, 2006). If available data was not sufficient to establish whether there was a link or not we used molecular gut content analysis to verify the interaction (B. Eitzinger, Georg-August University Göttingen, unpublished data). Some of the species were divided into size classes because they differed significantly in mean body sizes between different plots. For the model test in Fig. 3 we extracted every predator-prey pair together with the corresponding body-mass information resulting in an interaction matrix with 8446 links.

Chapter 3.

Beyond diversity: how nested predator effects control ecosystem functions

Florian D. Schneider and Ulrich Brose

Summary

1. The global decline in biodiversity is especially evident in higher trophic levels as predators display higher sensitivity to environmental change than organisms from lower trophic levels. This is even more alarming given the paucity of knowledge about the role of individual predator species in sustaining ecosystem functioning.

2. The effect of predator diversity on lower trophic level prey is often driven by the increasing chance of including the most influential species. Furthermore, intraguild predation can cause trophic cascades with net positive effects on basal prey. As a consequence, the effects of losing a predator species appear to be idiosyncratic and it becomes unpredictable how the community's net effect on lower trophic levels changes when species number is declining.

3. We performed a full factorial microcosm experiment with litter layer arthropods to measure the effects of predator diversity and context-dependent identity effects on a detritivore population and microbial biomass.

4. We show that major parts of the observed diversity effect can be assigned to the increasing likelihood of including the most influential predator. Further, the presence of a second predator feeding on the first predator dampens this dominant effect. Including this intraguild predator on top of the first predator is more likely with increasing predator diversity as well. Thus, the overall pattern can be explained by a second identity effect, which is nested into the first.

5. When losing a predator from the community the response of the lower trophic level is highly dependent on the remaining predator species. We mechanistically explain the net effects of the predator community on lower trophic levels by nested effects of predator identities. These identity effects become predictable when taking the species' body masses into account. This provides a new mechanistic perspective describing ecosystem functioning as a consequence of species composition and yields an understanding beyond simple effects of biodiversity.

Keywords | Biodiversity - ecosystem functioning, body size, multi-trophic, sampling effect, species identity, trophic cascade, species richness

Introduction

The relationship between biodiversity and ecosystem functioning (B-EF) has become a major topic of ecological research (Hooper *et al.*, 2005; Balvanera *et al.*, 2006), and its economic consequences have gained attention at a global-political scale (Kumar and United Nations Environment Programme (UNEP), 2010). Research addressed this topic early in plant diversity-productivity experiments (Tilman and Downing, 1994) and subsequently included the effects of predator communities on lower trophic levels (Finke and Denno, 2004; Schmitz, 2007). The latter, however, is still underrepresented in experimental and theoretical studies (Balvanera *et al.*, 2006; Letourneau *et al.*, 2009). Some previous studies have been aimed at partitioning B-EF into three types of effects: the fixed effect of a particular species ("identity effect"), the effect of losing a particular species in the context of a particular community ("composition effect"), and the effect of altering the continuous parameter species richness *per se* ("diversity effect") (Sih *et al.*, 1998; Loreau and Hector, 2001; Fox, 2005, 2006; Bell *et al.*, 2009). This descriptive approach can help to quantify the partitioned effects well for competitive plant communities, but is limited in explanatory power when including multi-trophic interactions, where indirect effects among species render direct contributions of single species intangible (Sih *et al.*, 1998; Reiss *et al.*, 2009). To standardize the three types of effects in multi-predator communities, recent approaches apply elaborate experimental designs accounting for individual and biomass density (Byrnes and Stachowicz, 2009; Bell *et al.*, 2009; Reiss *et al.*, 2009, 2011) and develop theory to connect underlying trophic mechanisms and ecosystem patterns (Thébault and Loreau, 2003; Ives *et al.*, 2005). In a recent study, however, Reiss *et al.* (2011) could show that fundamental different linear modelling approaches are required to separate the effects of consumers in diversity experiments.

Here, we apply a mechanistic perspective and assume that the B-EF pattern emerges only from the trophic interactions of the predator species. From this mechanistic viewpoint, identity effects manifest as systematic sampling probability effects, as the chance of including a particular species identity increases systematically with species diversity (Duffy, 2002; Ives *et al.*, 2005). In this way, a single species with strong influence on ecosystem functioning, might shape the observed overall B-EF relationship (also "sampling effects"; Huston, 1997; Tilman *et al.*, 1997). However this concept fails to predict ecosystem functioning by species diversity if multiple predator species interact antagonistically or synergistically to yield a community effect which is smaller or larger than the sum of their individual effects (Ives *et al.*, 2005). This phenomenon occurs commonly in communities of generalist predators, where indirect effects among species are caused by intraguild predation (Sih *et al.*, 1998; Finke and Denno, 2004; Worsfold *et al.*, 2009; Bell *et al.*, 2009). Predators may control the biomass and abundance of their direct prey species, but they can also consume each other, which dampens the net effect on the basal prey species (Finke and Denno, 2004). This results in indirect cascading effects: A predator feeds on

the population of another predator and therefore releases the basal prey of a feeding pressure. Depending on the relative feeding strength within this three-species motif this yields indirect cascading effects of variable intensity (Halaj and Wise, 2001; Borer *et al.*, 2005). The net effect of a predator on a basal prey is the sum of its direct feeding and the positive indirect effects mediated by intraguild predation. Therefore, the sign of a predator's net effect should depend on the food web context. For generalist consumer communities, the number of intraguild predation motifs should increase with diversity rendering predictions of effects on ecosystem functions highly uncertain. As a consequence, positive and negative net effects of increasing predator diversity on the lower trophic level were observed empirically, with a skew towards positive effects (Schmitz, 2007; Letourneau *et al.*, 2009). How these trophic mechanisms interact in concert to shape the net effect of the whole predator community remains a fundamental gap in our knowledge.

Interestingly, in previous studies the mechanisms determining feeding rates (Brose *et al.*, 2008; Vucic-Pestic *et al.*, 2010; Rall *et al.*, 2011), intraguild predation (also "omnivory" ; Digel *et al.*, 2011; Riede *et al.*, 2011), and food-web structure (Petchey *et al.*, 2008*a*) were all related to the species body masses. In a prior study, we integrated these concepts to show that the feeding rates and the resulting net effects of losing single predators on lower trophic levels can be explained by simple allometric constraints (Schneider *et al.*, 2012). These constraints predict the identity effect of each predator within a species community only based on body mass, by differentiating diet breadth and determining feeding rates. Thus, depending on the species body mass and the food web context, the identity effect of the added species may be negative (if feeding directly on the basal prey), positive (if triggering a trophic cascade via intraguild predation) or neutral (if direct and indirect effects cancel each other out; Schneider *et al.*, 2012). In the present study, we now adopt this mechanistic perspective to decompose the effects of multiple predators on the lower trophic levels while systematically varying consumer diversity. We carried out a full factorial microcosm experiment with three generalist predators of the litter layer of deciduous forests and hypothesized that predator diversity effects can be explained by nested identity effects of the predator species. Thus, we assume that the net effect of consumer diversity is emerging only from the identities of the interacting species instead of from species richness *per se*. With this approach, we go beyond a simple description of the relationship between species diversity and ecosystem functioning by unravelling nested levels of predator composition and providing a mechanistic understanding of multiple trophic effects in a predator community.

Materials and methods

Experiment

Our experiment focused on the predator community of the litter layer of terrestrial ecosystems which comprises generalist arthropods. We set up an experimental microcosm system with three predator species of different body masses: the large centipede *Lithobius forficatus* Linnaeus, 1758, the intermediately-sized spider *Pardosa lugubris* (Walckenaer, 1802), and the small mite *Hypoaspis miles* (Berlese, 1892). The population of the detritivore springtail *Heteromurus nitidus* (Templeton, 1835) and the microbial biomass on the litter served as a proxy for the ecosystem function of decomposition.

The acrylic-glass microcosms were sized 30 × 30 × 15 cm. A layer of dental cast containing activated charcoal was added to buffer the moisture. The filling of soil (1,000 g dry weight) and dry grassland litter (12 g) was defaunated and inoculated twice with a population of 50 springtails at four and two weeks before initiation of the predators. The experiment took place in a controlled greenhouse climate chamber, with temperature varying between 15°C at night and up to 22°C during the day (total average 16.2°C). Humidity was automatically regulated to approximately 70 %.

The centipedes and spiders were caught by hand in the field and weighed individually (average body mass: $\mu_{spiders} = 0.026$ g ±0.006 Std. Dev., $n = 42$; $\mu_{centipedes} = 0.125$ g ±0.041, $n = 84$). The mites were purchased at Katz Biotech AG (Baruth, Germany). The springtails were reared in laboratory cultures. Average body masses of mites and springtails were obtained by pooled weighing ($\mu_{mites} = 0.00016$ g, $n = 366$; $\mu_{springtails} = 0.00010$ g, $n = 553$; obtained from dry weight, multiplied by water-fraction factor 4 after Peters, 1983).

The three predators were combined in a full factorial treatment design, i.e. each possible combination of predators was realized, yielding a gradient from 0 to 3 predator species. An additive allometric design was applied (Schneider *et al.*, 2012).Therefore, for each predator i the initial population density, N_i, was defined from a negative 3/4 power law with average body mass, m_i ($N_i = 74.8 m_i^{-0.75}$). This yields two individuals of centipedes, four spiders and 350 mites per microcosm. These densities were combined additively in the different diversity treatment levels. The negative 3/4 exponent is an *a priori* definition which affects the biomasses and consequently the energetic balance between the predator species during the experiment, and thus affects the measured identity effect (Griffiths *et al.*, 2008; Schneider *et al.*, 2012). It is a conservative estimate from naturally observed mass-abundance relationships (Peters, 1983) which may be much shallower on local scales (around 1/4; White *et al.*, 2007). Nonetheless, classical fixed-density or fixed-biomass designs would imply exponents of 0 or –1, respectively, which most certainly would bias the measured identity effects. Therefore, the allometric design produces identity effects much closer to those measured in

removal experiments or in experiments using field densities (e.g. Finke and Denno, 2004).

The centipedes and spiders were weighed individually before and after the experiment. At the end of the experiment, the mites and springtails were extracted by heat (Macfadyen, 1961) from one quarter of the microcosm content into saline solution to count their abundances. The biomass was estimated by multiplying abundances with their average body mass. Microbial biomass on the litter layer was estimated from a fresh sample (2.8 g) taken at the end of the experiment by measuring substrate induced O_2-consumption in an electrolytic micro-respirometer (Scheu, 1992; Beck *et al.*, 1997).

Linear modelling

Data analyses were performed with R 2.14.0 (R Development Core Team, 2011). To account for heteroscedasticity the abundance of springtails (ind. microcosm^{-1}) was $\log_{10}$-transformed before analyses. An explorative linear modelling approach was chosen to test whether a significant effect of the continuous parameter predator diversity on $\log_{10}$ springtail abundance (subsequently: springtail density) can be detected within different subsets of predator composition. First, we assumed a linear null model which explains springtail density, N, just by predator species diversity S (subsequently 'null model'). The model equation,

$$N = a + bS + \varepsilon, \tag{3.1}$$

is defined by the intercept a, the slope b and the normally distributed residual error ε. This equation was fitted to the observed data using least squares regression. The slope b was tested for significance by applying a two-tailed Student's t-test. Insignificance would indicate a lack of any diversity effect. Alternatively, the linear effect of predator diversity was nested into different levels of a factorial parameter predator composition, C:

$$N = a_C + b_C S + \varepsilon, \tag{3.2}$$

generating a model predicting N within composition by one intercept a and one slope b for each level of C. This procedure is equivalent to the fit of an ANCOVA, but instead of testing the overall significance of the parameters, it was testing the significance of the obtained coefficients (slopes and intercepts) by t-tests (Crawley, 2007). Significant slopes would indicate unexplained diversity effects within the subsets; e.g. if a diversity effect in the null model emerged only from an identity effect of species i, then the slopes in the compositional subsets with species i, b_{+i}, and without i, b_{-i}, would be insignificant.

In a first step, three identity models were fitted to the data to test if any predator identity exerts a dominant effect on springtail density. Therefore, for each predator i, C either takes the value '$+i$' for a replicate containing i, or the value '$-i$' for a replicate lacking i. The three identity

models and the null model were compared via Akaike's Information Criterion (AIC). Among these the best explanatory identity model (with lowest AIC) was chosen for further analyses. If any b_C was significant, this level of composition was further extended by adding a second predator identity j; e.g. if b_{-i} is insignificant and b_{+i} is significant, C was extended to take one of the three levels '$-i$', '$+i-j$', or '$+i+j$'. In case of the two latter subsets, the slope describes the difference in means of the two treatments included in this particular composition level.

This analysis targeted the question of which composition model of the three predators could remove (and thus explain) the overall diversity effect from the null model. A model that lacks significance in all b_C allowed discarding the parameter diversity from the model. Thus,

$$N = a_C + \varepsilon \tag{3.3}$$

would be assumed as the most parsimonious model explaining variance in the springtail population only by the different levels of predator composition. Subsequently, differences in springtail density and litter microbial biomass across these levels of predator composition were tested by Tukey's HSD post-hoc comparison of means.

Results

A full factorial experimental design of all possible predator combinations allowed identification of the composition effects by nesting linear models within different subsets of predator composition. First, a null model that did not include predator identity as an explanatory parameter indicated a significant negative effect of predator diversity on springtail density, explaining 12.7 % of the variation (probability of b being different from 0: p = 0.024, Std. Error = 0.087, two-tailed t-test, AIC = 55.20, Table 3.1; Fig. 3.1A). The direct AIC-based model comparison of the null model with the three single predator models indicated whether the use of predator identity as an explanatory parameter for the prediction of springtail density was justified (Ta-

Table 3.1 – The null model describes $\log_{10}$ springtail density, N, as a linear function of species number, S ($N = a + bS$). The t-statistic gives the probability of the estimates equalling zero (two-tailed t-tests).

	Estimate	Std. Error	t-value	p-value
Intercept a	3.728	0.145	25.62	<0.001 ***
Slope b	−0.204	0.087	−2.35	0.024 *
d.f. / R^2 / AIC	3 / 12.7 % / 55.20			

d.f.: number of parameters used by the model; R^2: coefficient of determination; AIC: Akaike's Information Criterion; * $p < 0.05$; ** $p < 0.01$; *** $p < 0.001$

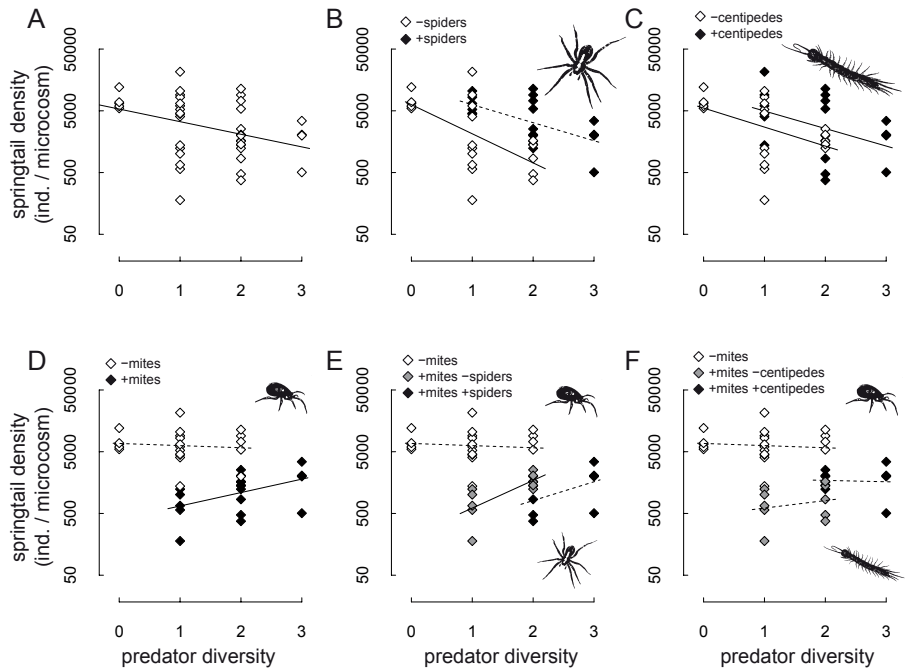

Figure 3.1 – Linear models describe springtail density in dependence of predator diversity and predator composition: A) Null model; diversity effect within subsets B) with and without spiders, C) with and without centipedes, D) with and without mites. The mites explain most of the variance in springtail density. The subset with mites is further divided into subsets E) with and without spiders, and F) with and without centipedes. The latter explains all observed diversity effects. Broken lines have insignificant slopes ($p > 0.05$; two-tailed t-test).

bles 3.1 and 3.2). The single predator model with spiders explained more variation than the null model, but the higher AIC renders the use of this predator composition variable unwarranted (R^2 = 18.2 %, AIC = 56.60). Furthermore, the effect of diversity within the treatments without spiders remained significantly negative (p = 0.040, Std. Error. = 0.361, Table 3.2; Fig. 3.1B). Including the centipedes in the model improved the prediction (R^2 = 38.1 %, AIC = 45.45), although the diversity effects remained significantly negative (Table 3.2; Fig. 3.1C). Finally, the composition model including the presence and absence of mites scored better than all previous models (R^2 = 69.5 %; AIC = 17.09). In addition, there was no significant diversity effect in treatments without mites (p = 0.694, Std. Error = 0.088, Table 3.2; Fig. 3.1D, open symbols). However, there was a positive diversity effect within the subset of experimental units containing mites (p = 0.025, Std. Error = 0.093, Table 3.2; Fig. 3.1D, filled symbols). This implies that predator diversity increased the detritivore abundance in treatments with mites present.

To further explore the positive diversity effect in the subset including mites we nested a second predator j (either spiders or centipedes) into the model and tested for diversity effects within three levels of predator composition C: '−mites', '+mites − j', '+mites + j'. If including the spider as a second predator j, there remained a significant unexplained diversity effect within the composition subset '+mites − spiders' (p = 0.013, Std. Error = 0.172, Table 3.3; Fig. 3.1E). Subdividing

Table 3.2 – Springtail density, N, as linear effect of predator species number, S, within the subsets of predator composition, C ($N = a_C + b_C S$). Here, C can take the value '$+i$', for replicates containing species i, and '$-i$' for replicates lacking species i. The tables were generated with the R-function `summary.lm()`, showing the probability of a_{-i} to be equal zero, of a_{+i} to be equal a_{-i}, and of b_{-i} and b_{+i} to be equal zero (two-tailed t-tests).

	i = centipedes					i = spiders					i = mites				
	Est.	Std. Er.	t-value	p-value		Est.	Std. Er.	t-value	p-value		Est.	Std. Er.	t-value	p-value	
a_{-i}	3.798	0.154	24.69	< 0.001	***	3.743	0.176	21.34	<0.001	***	3.833	0.107	35.80	<0.001	***
a_{+i}	0.293	0.300	0.98	0.335		0.236	0.361	0.65	0.517		−1.231	0.220	−5.59	<0.001	***
effect of S within C															
b_{-i}	−0.471	0.126	−3.75	0.001	***	−0.308	0.144	−2.13	0.040	*	−0.035	0.088	−0.40	0.694	
b_{+i}	−0.292	0.127	−2.30	0.027	*	−0.284	0.153	−1.86	0.071		0.217	0.093	2.33	0.025	*
d.f./R^2/AIC	5 / 38.1 % / 45.45					5 / 18.2 % / 56.60					5 / 69.5 % / 17.09				

d.f.: number of parameters used by the model; R^2: coefficient of determination; AIC: Akaike's Information Criterion; * $p < 0.05$; ** $p < 0.01$; *** $p < 0.001$

Table 3.3 – Extended linear model within predator composition. Here, C can take the value '–mites', '+mites $-j$', for replicates containing species j beside mites, and '+mites $-j$' for replicates lacking species j while containing mites.

	j = centipedes					j = spiders				
	Estimate	Std. Error	t-value	p-value		Estimate	Std. Error	t-value	p-value	
$a_{-\text{mites}}$	3.833	0.104	36.76	< 0.001	***	3.833	0.104	36.76	< 0.001	***
$a_{+\text{mites}-j}$	–1.169	0.291	–4.02	< 0.001	***	–1.495	0.291	–5.14	< 0.001	***
$a_{+\text{mites}+j}$	–0.554	0.466	–1.19	0.243		–1.534	0.466	–3.29	0.002	**
effect of S within C										
$b_{-\text{mites}}$	–0.035	0.086	–0.41	0.686		–0.035	0.086	–0.41	0.686	
$b_{+\text{mites}-j}$	0.122	0.172	0.71	0.483		0.449	0.172	2.61	0.013	*
$b_{+\text{mites}+j}$	–0.022	0.182	–0.12	0.904		0.305	0.182	1.67	0.103	
d.f. / R^2 / AIC	7 / 72.7 % / 16.69					7 / 72.7 % / 16.69				

d.f.: number of parameters used by the model; R^2: coefficient of determination; AIC: Akaike's Information Criterion; * $p < 0.05$; ** $p < 0.01$; *** $p < 0.001$

Table 3.4 – Final model describing springtail density, S, by three levels of predator composition, C, omitting predator species number ($N = b_C S$).

	Estimate	Std. Error	t-value	p-value	
$a_{-\text{mites}}$	3.798	0.057	66.23	< 0.001	***
$a_{+\text{mites}-\text{centipedes}}$	–0.951	0.101	–9.42	< 0.001	***
$a_{+\text{mites}+\text{centipedes}}$	–0.573	0.105	–5.47	< 0.001	***
d.f. / R^2 / AIC	5 / 72.2 % / 11.48				

d.f.: number of parameters used by the model; R^2: coefficient of determination; AIC: Akaike's Information Criterion; * $p < 0.05$; ** $p < 0.01$; *** $p < 0.001$

the set of replicates containing mites by the presence and absence of centipedes yielded a model lacking significant diversity effects ($b_{+\text{mites}+\text{centipedes}}$: $p = 0.904$; $b_{+\text{mites}-\text{centipedes}}$: $p = 0.483$, Table 3.3; Fig. 3.1F). Note that both models ended up with the same coefficient of determination ($R^2 = 72.7$ %, AIC = 16.69) because the slopes within the subsets equal the difference in means of the two included treatments within each composition subset.

What validates the model with mites and centipedes over the model with mites and spiders is the lack of any significant diversity slope b_C in the first. This means, all effects of increasing diversity can finally be attributed to the difference in the three levels of species composition. Hence, the most parsimonious model explained 72.2 % of the variation in springtail density by the three levels of predator composition '–mites', '+mites –centipedes', and '+mites +centipedes' while discarding predator diversity (AIC = 11.48; Fig. 3.2A). Describing springtail density by model equation 3.3, using one mean value, a, for each level of predator composition, C, yielded highly significant parameters ($a_{+\text{mites}-\text{centipedes}}$: $p < 0.001$, Std. Error = 0.101; $a_{+\text{mites}+\text{centipedes}}$: $p < 0.001$, Std. Error = 0.105). A Tukey HSD post-hoc test showed that all levels of predator composition differed significantly in pair-wise comparison (Fig. 3.2A). This indicates two nested predator effects: First, mites reduced springtail density. Second, if mites were present, centipedes enhanced springtail density. The effect of predator diversity on springtail density (Fig. 3.1) emerges from these nested predator effects.

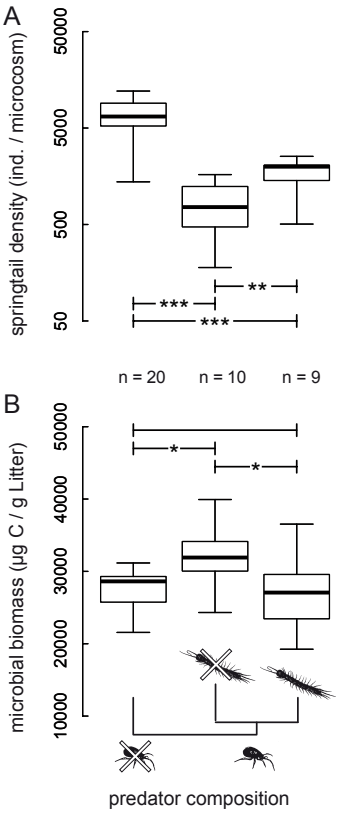

Figure 3.2 – A) The most parsimonious model describes springtail density by three levels of predator composition '–mites', '+mites –centipedes' and '+mites +centipedes'. B) The microbial biomass responds anti-parallel to the predator composition levels. Asterisks show p-values from Tukey HSD test: * $p < 0.05$, ** $p < 0.01$, *** $p < 0.001$. n: number of replicates contained in the subsets of predator composition.

Interestingly, the predator effects on springtails cascaded to the next lower trophic level composed of microorganisms: The composition level '+mite –centipede' resulted in significantly higher microbial biomass than the treatments without mites and treatments containing both predators ($p < 0.05$, Tukey's HSD; Fig. 3.2B). The latter two did not differ significantly. This indicates that microbial biomass responded significantly to the composition of the predator community.

Discussion

There is a need for an integrated understanding of the multiple mechanisms that drive the correlation between biodiversity and ecosystem functioning. In this study, we investigated the interactive nature of single species' identity effects in producing the community's net effect on lower trophic levels. The apparent effect of predator diversity on springtail density in our experiment was due to counteracting effects of differing predator identities. As a first identity effect, the probability of randomly drawing a replicate including mites increased with predator diversity, which caused the overall negative relationship. As a second effect, in replicates including mites, the likelihood of drawing a replicate containing centipedes increased with predator diversity yielding a reduction of the overall net effect. Thus, we found that changes in predator diversity affect ecosystem functioning via nested effects of predator identity.

With our explorative modelling we unravelled the distinction in predator composition that most effectively describes the variation in ecosystem functioning. The final model explained 72.2 % of the variation in the springtail density. In contrast to other modelling approaches (Fox, 2005, 2006; Bell *et al.*, 2009), our linear modelling approach does not assume a diversity effect *per se*. Instead, all of the non-random variation in ecosystem function is assigned to few nested composition levels. In this approach, any unexplained diversity slope in a composition level would finally be explained by sub-dividing the composition level into further sub-levels. For example, in the case of the model with mites and spiders there remains a positive slope in the subset '$b_{+\text{mites}-\text{spiders}}$' (Table 3.3) which would finally be explained by a model which further sub-divides into five explanatory levels of predator composition and omits diversity as an explanatory variable. However, this model would be less efficient (*d.f.* = 6; R^2 = 70.3 %; AIC = 16.03) than the final model. The analyses presented here provide a mechanistic insight into the nested and interdependent effects of the predators reaching beyond diversity effects.

From an ecosystem perspective, the loss of one randomly selected predator species from the experimental three-predator food web has unpredictable consequences: If spiders become extinct, no significant changes in detritivore abundance will be expected; if centipedes become extinct, detritivores should decrease in abundance, because mites are released from a top-down pressure; if the mites become extinct, detritivores will be enhanced in abundance. In a prior study, these apparently idiosyncratic effects were assigned to the predators' body masses

(Schneider *et al.*, 2012). Simple allometric constraints differentiate the predators' prey range and preference for intraguild feeding in two ways. First, predators feed preferably on prey of a certain body mass, with decreasing intensity towards smaller as well as larger prey (Brose *et al.*, 2008; Vucic-Pestic *et al.*, 2010). Second, small predators are present in higher abundances than large predators due to individual metabolism (White *et al.*, 2007; Ehnes *et al.*, 2011). As a consequence, relatively small predators should diminish the shared resource, whereas large predators should affect the resource positively due to intraguild predation.

Our study disentangles the interplay of differently-sized predator species with increasingly complex food web structures. The experiment required a full factorial manipulation of predator composition to provide a mechanistic insight into the effect of predator species assemblages on lower trophic levels. In this vein, the community net effect emerged from the body-mass structure of the increasingly diverse food web. On the one hand, increasing diversity increased the net effect on the lower trophic level by direct feeding of small predators but on the other hand this dampened the effect of direct feeding by enhancing intraguild predation by large predators. These effects triggered down to the basal microbial resource.

The logistic limitations of full factorial designs inhibited a wider range of species diversity, but future studies will need to scale up the mechanistic understanding obtained here to higher levels of predator diversity. Currently there are, to our knowledge, no multi-trophic diversity experiments that cover a much wider range of species richness (Cardinale *et al.*, 2009), but model simulations may provide a tool for scaling up small scale experiments to natural diversity levels (Ives *et al.*, 2005; Cardinale *et al.*, 2009; Loreau, 2010*b*). Our results suggest that it will be necessary to model the indirect effects that are inherent to multi-trophic food webs, to achieve a realistic prediction of ecosystem functioning.

Interestingly, our results are consistent with prior field studies of the forest litter layer, where detritivores were shown to be bottom-up regulated (Scheu and Schaefer, 1998; Oelbermann *et al.*, 2008) despite the presence of a diverse generalist predator community. Community-level trophic cascades (*sensu* Polis, 1999; Polis *et al.*, 2000) appear to be of minor relevance in litter food webs (Mikola and Setälä, 1998; Scheu and Setälä, 2002). However, Ponsard, Arditi, and Jost (2000) point out that bottom-up control by detritus availability indicates the presence of an effect-reducing mechanism within the predator community. Our finding of a four-level cascading effect (species-level cascade *sensu* Polis, 1999; Polis *et al.*, 2000) implies that intraguild predation provides a mechanism that suppresses top-down control on decomposers in the litter food web. Since predators within the litter layer are predominantly generalists, intraguild predation is widespread, which has been shown by stable isotope analyses (Ponsard *et al.*, 2000; Scheu and Falca, 2000). Therefore, with increasing predator diversity the number of intraguild predation motifs – and thus the strength of four-level cascading effects – increases as well.

In general, the net effect on the lower trophic level might be reduced with increasing number of large, higher-level predators. The community-level trophic cascade should be "trickling"

(Strong, 1992; Halaj and Wise, 2001). Similarly, this mechanism has also been validated for above ground systems (Finke and Denno, 2004, 2005). Its maintenance is crucial, since its loss could switch the regime from bottom-up to top-down control and in consequence may profoundly disrupt ecosystem functioning.

Conclusion

In our experiment, the apparent effect of predator diversity emerged from the effects of two predators that were nested into each other. We anticipate that diversity effects *per se* are unlikely to be detected in predator diversity experiments. Instead, all variation of the focal ecosystem function can be assigned to nested levels of predator composition. Apparently, when losing a predator from the community the response of the lower trophic level is highly context sensitive, but taking body masses into account may solve this puzzle. We experimentally restrict the bias by biomass or density on the measured identity effects to a minimum by defining both as a consequence of body mass. By applying allometric constraints, the body mass structure of a community explains properties that were described as important mechanisms of the B-EF relationship: niche differentiation, intraguild predation and, as highlighted in the present paper, sampling effects. Complementary to the paradigmatic search for a biodiversity effect *per se* (Naeem, 2002; Loreau, 2010*a*), this allometric perspective provides a new understanding for the multiple mechanisms that drive ecosystem functioning.

Acknowledgements

We are grateful to Stefan Scheu who contributed to the experimental conception. We thank Andrew D. Barnes, Malte Jochum and one anonymous reviewer for comments on the manuscript; Theodora Volovei for help with respiration measurements; Gregor Kalinkat and Roswitha B. Ehnes, M. Kandziora, A. König, F. Grischkat, S. Mohr and all the other helpers for assistance with experimental work. F.D.S. has been funded by Deutsche Bundesstiftung Umwelt (DBU, http://www.dbu.de). U.B. is funded by the German Research Foundation (BR 2315/13).

Chapter 4.

Body mass constraints on feeding rates determine the consequences of predator loss

Florian D. Schneider, Stefan Scheu and Ulrich Brose

published in *Ecology Letters* volume 15, pages 436–443

doi: 10.1111/j.1461-0248.2012.01750.x

Abstract

Understanding effects of species loss in complex food webs with multiple trophic levels is complicated by the idiosyncrasy of the predator effects on lower trophic levels: direct and indirect effects intermingle and may increase, decrease or not affect ecosystem functioning. We introduce a reductionist approach explaining a predator's trophic effect only by empirically well-founded body-mass constraints on abundance, diet breadth, and feeding strength. We demonstrate that this mechanistic concept successfully explains the positive, negative and neutral net effects of predators on decomposers in a litter microcosm experiment. This approach offers a new perspective on the interplay of complex interactions within food webs and is easily extendable to include phylogenetic and other body-mass independent traits. We anticipate that allometry will substantially improve our understanding of idiosyncratic predator effects in experiments and the consequences of predator loss in natural ecosystems.

Keywords | Allometry, body size, biodiversity-ecosystem functioning, food web, identity effects, interaction strength, intraguild predation, predator-prey interactions, species traits, trophic cascade.

Introduction

Although seminal studies have unraveled the consequences of losing plant species and primary consumers for ecosystem functioning, the trophic group of predatory carnivores (subsequently: predators) is underrepresented in these diversity studies (Balvanera *et al.*, 2006 and references therein), even though they are most prone to extinction (Cardillo *et al.*, 2005). In multi-predator communities, it remains notoriously difficult to predict effects of losing a single species, which are often referred to as 'identity effects' (Sih *et al.*, 1998; O'Connor *et al.*, 2008; Byrnes and Stachowicz, 2009; Worsfold *et al.*, 2009). In complex food webs, consequences of species loss result from direct feeding effects as well as indirect effects via intraguild predation leading to positive, neutral or negative impacts on lower trophic levels (Finke and Denno, 2005; Schmitz, 2007). Thus, the effects of predator loss or gain were perceived as idiosyncratic (Lawton, 1994): consequences of random species loss are not predictable, because each species has a characteristic set of traits. In consequence, the relationship between predator diversity and ecosystem functioning remained rarely explored and mostly unpredictable (Balvanera *et al.*, 2006; Letourneau *et al.*, 2009).

In this article, we argue that species traits and the food-web context are strongly influenced by species body masses. This argument is based on the well-documented allometric scaling of species traits, such as metabolism and movement speed (Peters, 1983; Brown *et al.*, 2004; Ehnes *et al.*, 2011). Moreover, body mass affects various ecological traits such as phenology patterns (McNab, 2002), inter- and intraspecific niche differentiation (Sinclair *et al.*, 2003; Dial *et al.*, 2008; Kohda *et al.*, 2008), vulnerability to predation (Sinclair *et al.*, 2003; Otto *et al.*, 2007; Digel *et al.*, 2011) and intervality in prey size ranges (Zook *et al.*, 2010; Stouffer *et al.*, 2011). Hence, substantial parts of the direct and indirect predator effects within the context of a local food web may be explained when considering body-mass constraints on their physiological and ecological characteristics.

We base this study on the following findings of allometric theory: First, predators most efficiently exploit prey of a certain body-mass range, usually one to two orders of magnitude smaller than themselves, with decreasing feeding strength towards smaller and larger prey (Brose, 2010*b*). This yields a hump-shaped relationship between *per capita* feeding rates and predator-prey body-mass ratios (Brose *et al.*, 2008) driven by allometric dependencies of handling time and attack rate (Vucic-Pestic *et al.*, 2010) as well as interference competition (Lang *et al.*, 2011). Second, large predators are less abundant than small predators (Peters, 1983; White *et al.*, 2007) because of their higher metabolic demands (Brown *et al.*, 2004; Ehnes *et al.*, 2011).

As a simplified conceptual example, we illustrate how allometric theory predicts effects of predator loss in a hypothetical community with two generalist predators and a basal prey (Fig. 4.1). With increasing top-predator size, as in the sequence from the top to the bottom panel of Fig. 1a, the relative *per capita* feeding rates vary systematically. The larger the top

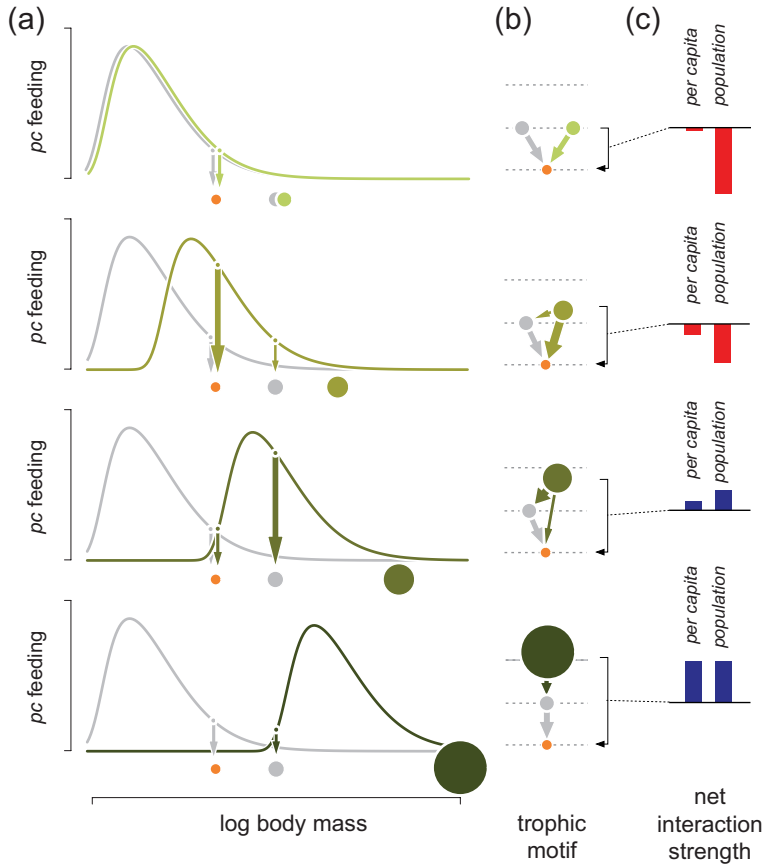

Figure 4.1 – Allometrically constrained feeding rates for two predators (grey and green) and one basal prey (orange). Hump-shaped *per capita* feeding rates (*pc* feeding) are described by an allometric model. (a) Relative *pc* feeding of the larger predator (green curves) shifts with increasing body mass (top to bottom) from the basal prey towards the intraguild prey. (b) Change from an exploitative competition motif towards a trophic-cascade motif (relative *pc* feeding = arrow weight). (c, left) Net interaction strength, IS, of top predator on basal prey switches from negative to positive with increasing body mass. (c, right) Population IS for small predators emerges from high abundance; effects of large predators arise from individual properties. Species density, N_i, scales with body mass, m_i ($N_i = 74.8 \cdot m_i^{-0.75}$).

predator, the stronger the *per capita* feeding rate on the larger prey species compared to the *per capita* feeding rate on the basal prey (Fig. 4.1b). In consequence, the motif switches from exploitative competition over intraguild predation to a food chain with an increase in top-predator body mass. Hence, a small top predator imposes a direct negative effect on the basal prey, whereas larger top-predators cause a trophic cascade resulting in a net positive effect on the basal prey (Fig. 4.1c, left bars). Multiplying these *per capita* interaction strengths with predator abundances yields population-level interaction strengths (Fig. 4.1c, right bars). For this three-species module, allometric theory predicts weak, negative *per capita* effects but strong, negative population-level effects of small predators due to their high abundance. Furthermore, positive population-level effects of large predators with low abundance are driven by their strong *per capita* effects. This example shows that net interaction strengths emerging from

allometric constraints on abundance, diet breadth and feeding strength can be positive, neutral or negative depending on the body masses of the involved species. These implications of allometric theory yield the following hypotheses on the effects of predator removal, which were tested in a microcosm experiment with differently-sized generalist predators. (1) Small predators exert a negative effect on the basal prey; whereas their *per capita* effect is weak, their high abundance leads to a strong population-level effect. (2) Large predators exert a positive effect on the basal prey, with similar strength at the *per capita* and population levels.

To attribute the effects of losing a predator species to its body mass, we employed an empirically well-founded allometric model to predict the outcome of the experiment. These quantitative analyses were based on a simulation of population dynamics discriminating the predator species only by their average body mass. The qualitative and quantitative consistency of experiment and simulation corroborated the proposed allometric mechanisms. Thus, we anticipate that the apparently idiosyncratic effects of specific predator loss may become comprehensible in the light of allometry.

Material and methods

Experiment

We performed a microcosm experiment manipulating the composition of a terrestrial arthropod community to test the implications of allometry in a simplified food web context. It included three generalist predator species of different body masses: the large centipede *Lithobius forficatus* (Linnaeus, 1758), the intermediately-sized spider *Pardosa lugubris* (Walckenaer, 1802), and the small mite *Hypoaspis miles* (Berlese, 1892). The population density of the basal resource to all predators, the detritivorous springtails *Heteromurus nitidus* (Templeton, 1835), was evaluated as the response variable. We adopted an 'allometric design' for predator experiments with initial predator abundances following a negative three-quarter power law with their body masses (Fig. 4.2; see below).

The experiment was set up in 30 × 30 × 15 cm acrylic glass microcosms. The bottom was filled with dental cast containing activated charcoal for moisture control. Herein, a layer of 1000 g defaunated soil (deep frozen at – 80 °C for 3 days and dried at + 60 °C for 7 days) was added and moistened with 1 L of deionized water. As a litter layer, 12.0 g of cut and defaunated grassland litter (deep frozen at – 80 °C for 3 days and dried at + 60 °C for 3 days, cut to a maximum length of 10 cm) were placed homogeneously on top of the soil. The microcosms were covered with gauze of 100 μm mesh size. Approximately 40 mL of water were sprayed through the gauze every second day. The microcosms were placed in a controlled greenhouse climate chamber, with temperature varying between 15 °C at night and up to 22 °C during the day (mean 16.2 °C). Humidity was automatically regulated to approximately 70%. Fifty springtail individuals were

added to each microcosm twice: 6 weeks (t_{-2}) and 4 weeks (t_{-1}) before the experiment started. To foster establishment of stable populations of springtails, 70 mg of yeast were added at t_{-1} as a directly available resource to each of the microcosms. The mean individual body mass of the springtails was 0.10 mg (± 0.02SD).

The centipede *L. forficatus* inhabits the litter layer of deciduous forests and acts as a sit and wait predator. The mean body mass of adult centipedes used in the experiment was 125.3 mg (± 41.4SD). The wolf spider *P. lugubris* is a non-web building sit and pursue predator preying on smaller arthropods in litter systems of deciduous forests. The mean body mass of spiders used in the experiment was 25.7 mg (± 6.2SD). Females (and some subadults of undetermined sex) were used for the experiment to reduce the risk of cannibalism on males. Egg sacs were removed before the experiment. Spiders and centipedes were caught by hand in the field. The mite *H. miles* is a generalist predator which is used as a biocontrol agent against springtails and other insect pest species. The mean individual body mass of mites used in the experiment was 0.16 mg (± 0.02SD). The mites were purchased from Katz Biotech AG (Baruth, Germany).

Preliminary studies indicated that all predator species potentially feed on the smaller species used in the experiment. Spider and centipede individuals were weighed before and after the experiment.

The experiment started with the addition of predators (t_0). The full three-predator treatment and the three knock-out treatments, each lacking one of the three predator species, were replicated five times (for initial densities see next section). The replicates were set up in a blocked design to accommodate for sun patch and ventilation effects. At the same time, five replicates were terminated and the springtails were isolated by heat extraction after Macfadyen (1961). The average springtail density at t_0 was 912(± 528SD, $n = 5$). The experiment was terminated after 48 days (t_1). The spiders and centipedes were collected by hand. Heat extraction was applied to a quarter of the microcosm content, transferring the springtails and mites into saturated saline solution. Again, five control replicates without predators were evaluated, yielding an average springtail density at t_1 of 7401(± 2678SD, $n = 5$). Biomasses of springtails and mites in the microcosms were calculated from their abundance and their average *per capita* fresh weight. One three-predator replicate was discarded from data analysis, because the springtail and predator populations were profoundly affected by very low water content.

Allometric design

Two substantial problems hinder the experimental detection of the effects of predator loss: First, the ontogenetic mass distribution within a taxonomic species causes a wide range of ecological behaviour, expressed as noise in the observations of effects within diversity experiments. In our experiment, we tackled this problem by keeping the mass range for each species narrow and without overlap to the other species.

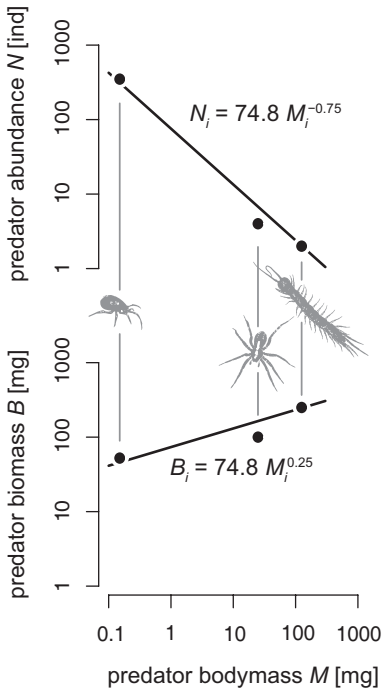

Figure 4.2 – Allometric design for predator-diversity experiments. The initial abundances and biomasses of the three predators depended on their body mass according to an allometric power-law relationship. Predators from left to right: the predatory mite *Hypoaspis miles*, the spider *Pardosa lugubris*, the centipede *Lithobius forficatus*.

Secondly, predator abundance is usually considered as an independent parameter that needs to be standardized in an additive or substitutive design (Byrnes and Stachowicz, 2009). Hence, the response to species identity is corrected for abundance effects. This may be appropriate for experiments in which body mass is of minor relevance for species interaction effects (e.g. plant or parasitoid systems). In most consumer diversity experiments, however, standardized abundances multiplied by specific body masses result in severe differences in total predator biomasses across treatments. The conclusions that can be drawn from either design confound identity effects with biomass effects (O'Connor *et al.*, 2008). Similarly, experiments with standardized biomass result in a bias by severely different predator densities across treatments. We anticipate that experimental systems where species effects predominantly depend on species' body masses have a high risk of misinterpretation when employing traditional additive or substitutive designs. Therefore, we refrain from keeping abundances or biomasses constant across treatments. Alternatively, species abundances can vary according to natural abundance-mass relationships based on field densities (O'Connor *et al.*, 2008) or allometric power-law relationships (Griffiths *et al.*, 2008).

In our experiment, we chose the initial abundances of the predators to follow a negative three-quarter power law with their body masses (Fig. 4.2). For this prototype of an allometric design we chose a relatively steep scaling exponent to ensure both a strong contrast between the predator treatments and consistency with allometric theory (Brown *et al.*, 2004). Empirically, the scaling exponents of mass-abundance relationships vary from local ($-1/4$) to global ($-3/4$) scales (White *et al.*, 2007). To avoid effects of species extinctions caused by random events,

at least two individuals of each species were introduced into the microcosm. Therefore, the power law was calibrated based on two individuals per microcosm of the largest predator, the centipede ($N_i = 74.8 \cdot m_i^{-0.75}$; Fig. 4.2). This yielded projected abundances of 300 mites and 6.6 spiders per microcosm. The abundance of spiders was decreased to four individuals to reduce the likelihood of cannibalism. Due to delayed availability of mites at t_0 and during the first week of the experiment, only 250 mites were introduced initially. Another 100 individuals were added after one week to recover the desired mass–abundance relationship yielding around 350 mites per microcosm. The biomasses during the experiment (springtails: 0.43–13.15 g m^{-2}; mites: 0.03–5.46 g m^{-2}; spiders: 0.15–1.19 g m^{-2}; centipedes: 1.06–2.85 g m^{-2}) corresponded to field data (springtails: 0.61 g m^{-2}; predatory mites: 0.18 g m^{-2}; spiders: 0.19 g m^{-2}; centipedes: 1.06 g m^{-2}; dry-weight; from Schaefer, 1990; multiplied by dry-to-fresh-weight conversion factor of 4 from Peters, 1983).

Defining the allometric model

We estimate allometric trophic effects in the context of a food web with a mechanistic model for dynamical feeding strength. The backbone of this model is a type II functional response (Holling, 1959*b*) with predator interference (Skalski and Gilliam, 2001).

$$F_{ij} = \frac{aN_i}{1 + c\left(N_j - 1\right) + ahN_i}, \tag{4.1}$$

describes the feeding rate [$\text{ind}_i\ h^{-1}$] of a predator j, depending on its own abundance N_j [ind_j microcosm^{-1}] and the abundance N_i of a prey i [ind_i microcosm^{-1}]. The realized attack rate a [microcosm h^{-1}] (the unit 'microcosm' includes the area of the experimental microcosms, 0.09 m^2, and effects of habitat structure) represents the encounters leading to captures. The handling time h [h ind_i^{-1}] is the time required for processing and digesting one prey item (see Jeschke *et al.*, 2002 for details). The predator interference c [microcosm ind_j^{-1}] is the time that is lost due to encounters of a con-specific ("Beddington-DeAngelis model" from Skalski and Gilliam, 2001). To model allometric dependencies, we define a_{ij}, h_{ij} and c_j as functions of prey body mass m_i [mg ind_i^{-1}] and predator body mass m_j [mg ind_j^{-1}] as suggested by former studies on terrestrial arthropods (Brose *et al.*, 2008; Vucic-Pestic *et al.*, 2010; Rall *et al.*, 2011). For the attack rate, we differentiate into a mechanistic encounter rate and the likelihood that an encounter is successful for the predator:

$$a_{ij} = \underbrace{a_0 m_i^{0.25} m_j^{0.25}}_{\text{encounter}} \cdot \underbrace{\left(\frac{R}{R_{\text{opt}}} \mathrm{e}^{1 - \frac{R}{R_{\text{opt}}}} \right)}_{\text{success}}. \tag{4.2}$$

The encounter rate depends on predator and prey speed, which scale positively with body mass to the power of 1/4 (Peters, 1983), and the normalization constant a_0. The likelihood of success is a phenomenological description of the predator's inability to subdue relatively small or large prey. Here, we used a generalized Ricker function that is maximized to one if the body-mass ratio between predator and prey, R (m_j/m_i), reaches the optimal body-mass ratio R_{opt} (Persson *et al.*, 1998). The width of the curve is determined by γ. The time needed by one predator to handle one prey item,

$$h_{ij} = h_0 R^{-0.25} = h_0 m_i^{0.25} m_j^{-0.25}, \tag{4.3}$$

depends on R to the power of $-1/4$ and the normalization constant h_0. In absolute terms, h_{ij} increases with prey body mass to the power of 1/4 and decreases with predator body mass to the power of $-1/4$. Predator interference is assumed to depend on the intra-specific encounter rate [microcosm h^{-1}] and a fixed amount of time spent during each encounter event [h ind_j^{-1}] (Skalski and Gilliam, 2001). Therefore, the interference factor,

$$c_j = c_0 m_j^{0.25} m_j^{0.25} = c_0 m_j^{0.5}, \tag{4.4}$$

scales positively with the movement speeds of both encountering individuals, each defined by predator body mass m_j to the power of 1/4 (Peters 1983), resulting in an exponent of 0.5, and a normalization constant c_0.

Simulation of population dynamics

For a dynamic prediction of the predators' net effects over the experimental time we simulated bioenergetic population dynamics following allometric constraints (Yodzis and Innes, 1992; Otto *et al.*, 2007; Berlow *et al.*, 2009) using R 2.14.0 (R Development Core Team, 2011) with the package 'deSolve' (Soetaert *et al.*, 2010) and the solver 'rk45dp7' (Runge-Kutta family: Dormand-Prince 4(5), local order 7). The population density of the basal species i is defined as

$$\frac{dN_i}{dt} = N_i r \left(1 - \frac{N_i}{K}\right) - \sum_j \frac{N_j a_{ij} N_i}{1 + c_j \left(N_j - 1\right) + \sum_k \left(a_{kj} h_{kj} N_k\right)} \tag{4.5}$$

The growth model, with the intrinsic growth rate $r = 0.00461$ [h^{-1}] and the carrying capacity $K = 7671$ [ind microcosm^{-1}] was parameterized by fitting the logistic growth model to a dataset of springtail densities at t_{-1} (initial density = 100 ind microcosm^{-1}), t_0 and t_1 (control treatment without predators). The demands of population i are determined by the sum of feeding rates of its predators j. In this multi-prey functional response, each predator j feeds on multiple prey

species k (Kalinkat *et al.*, 2011). The population density of each consumer species j is defined as

$$\frac{dN_j}{dt} = \frac{N_j \sum_i \left(a_{ij} N_i e_{ij}\right)}{1 + c_j \left(N_j - 1\right) + \sum_i \left(a_{ij} h_{ij} N_i\right)} - \sum_l \frac{N_l a_{jl} N_j}{1 + c_l \left(N_l - 1\right) + \sum_k \left(a_{kl} h_{kl} N_l\right)} - x_j N_j, \tag{4.6}$$

where the increase per time step is the sum of the feeding on all its prey species i, multiplied by the conversion efficiency (i.e., the number of predator individuals that can grow from one prey individual),

$$e_{ij} = e\frac{m_i}{m_j}, \tag{4.7}$$

using the assimilation efficiency $e = 0.85$ for carnivores (Peters, 1983; Yodzis and Innes, 1992). The density of predator j declines due to predation from its own predators l. The metabolic demands of the predator j follow an allometric model with empirically fitted parameters after Ehnes *et al.* (2011),

$$x_j = x_o m_j^{0.695} \mathrm{e}^{\frac{-E}{kT}} \frac{3}{7 m_j}, \tag{4.8}$$

where $E = 0.686$ [eV] is the activation energy and $x_0 = \mathrm{e}^{23.05}$ the normalisation constant, k the Boltzmann's constant ($8.617 \cdot 10^{-5}$ [eV K^{-1}]) and $T = 289.35$ [K] (16.2 °C) the average temperature during the experiment. We derived a field metabolic rate by converting the parameters provided by Ehnes *et al.* (2011) from resting metabolism to activity metabolism (factor 3; Peters, 1983), from Joule to mg (1 mg of biomass contains 7 Joule; Peters, 1983) and from biomass to density (divided by m_j). Simulations of the three-predator community and three knock-out communities, each lacking one of the three predators, were run over 1152 hours (48 days), which is equivalent to the experimental time. The same initial predator and prey densities (densities at t_0) and average body masses as in the experiment were used. Species density was set to zero if it fell below one during the simulation (i.e., a species with less than one individual is assumed to be extinct). The final predator and prey densities were converted to gram biomass before calculating interaction strengths.

Interaction strengths

The final population biomasses of the experiment and of the simulation were used to calculate population level and *per capita* interaction strengths (*IS*). We define the population level IS_{ij} of species j (predator) on species i (prey) according to the $\log_{10}$ ratio of the biomass of i in the presence and absence of j (Otto *et al.*, 2008),

$$IS_{ij} = \log_{10}\left(\frac{B_i^{+j} + 1}{B_i^{-j} + 1}\right), \tag{4.9}$$

where B_i^{-j} is the biomass of i in the absence of j [g] and B_i^{+j} is the biomass of i in the presence of j [g]. A constant value of one was added to the enumerator and the denominator to prevent division by zero. To calculate IS_{ij} of each predator j within the experimental food web on the springtail population, we applied equation 4.9 with B_i^{+j}, the final springtail biomass from one three-predator replicate (n = 4), and B_i^{-j}, the springtail biomass from one knock-out replicate lacking species j (n = 5). Recombination of replicates yielded twenty IS_{ij} values for each interaction with the arithmetic mean $\overline{IS_{ij}}$. The probability of $\overline{IS_{ij}}$ being equal to zero was determined by comparing the means of all replicates' B_i^{+j} and B_i^{-j} with a two-tailed Student's t-test. The respective *per capita* IS_{ij} (i.e., the effect per predator individual) were calculated by dividing IS_{ij} by $\hat{n}_j$, the mean of the initial and final abundance of species j in the three-predator replicate. The interaction strengths of centipedes, spiders, and mites on each other were calculated in the same manner.

For the simulation data, we combined B_i^{+j}, the biomass of i at the end of the simulation in the three-predator module against B_i^{-j}, the final biomass of i in the knock-out module lacking species j.

Parameter Selection

The allometric model includes 18 parameters: 13 empirically-derived and five free parameters (a_0, c_0, R_{opt}, γ, h_0). The latter five parameters were chosen manually to maximise the correlation (Pearson's r) between simulated and experimental IS_{ij}. The normalisation constants $a_0 = 0.1$ and $c_0 = 1.0$ incorporate effects of habitat structure and area of the microcosms on encounter rates, which were not quantified for this experiment. The success likelihood parameters, $R_{opt} = 100$ and $\gamma = 0.5$ (Brose *et al.*, 2008) and the constant of handling time $h_0 = 7.5$ (Rall *et al.*, 2011) were chosen within the range of empirically reported values. They are specific to predator-prey interactions and independent from structure and area of the microcosm. We also tested whether a model omitting predator interference (by setting $c_0 = 0$; Skalski and Gilliam, 2001) would perform equally well. This model overestimated the effects of the smallest predators, the mites, compared to the results of the experiment. In general, interference models fit empirical data better than classic Holling-type functional responses (Skalski and Gilliam, 2001; Lang *et al.*, 2011). The final parameters were used to calculate static estimates of feeding rates of all predator-prey pairs from equations 4.1–4.4, by inserting the predators' initial densities N_j and assuming $N_i = 74.8 \cdot m_i^{-0.75}$ with the mean body masses given above.

Results

Static Estimates of Allometric Feeding Rates

Static estimates of feeding rates (not accounting for population dynamics) of all predator-prey pairs were calculated from equation 4.1 (Materials and Methods; Fig. 4.3): The small mites prey on the springtails with very low *per capita* feeding rates ($F_{ij}/n_j = 0.0184$ ind$_i$ h^{-1} ind$_j^{-1}$; Fig. 4.3a). However, they impose a strong population feeding rate on the basal springtails due to their high abundance ($F_{ij} = 6.456$ ind$_i$ h^{-1}; Fig. 4.3b). Their high abundance also causes strong intra-specific interference, which depresses the maximum of the *per capita* feeding curve more than for the larger predators with lower densities and less intra-specific interference. The intermediately-sized spiders feed on the springtails ($F_{ij}/n_j = 0.434$; $F_{ij} = 1.736$) and the mites ($F_{ij}/n_j = 0.399$; $F_{ij} = 1.595$) with similar intensity. Centipedes as the largest predators impose strong intraguild predation on mites ($F_{ij}/n_j = 0.274$; $F_{ij} = 0.548$) whereas exhibiting similarly weak predation on spiders ($F_{ij}/n_j = 0.083$; $F_{ij} = 0.167$) and on the basal springtails ($F_{ij}/n_j = 0.079$; $F_{ij} = 0.158$).

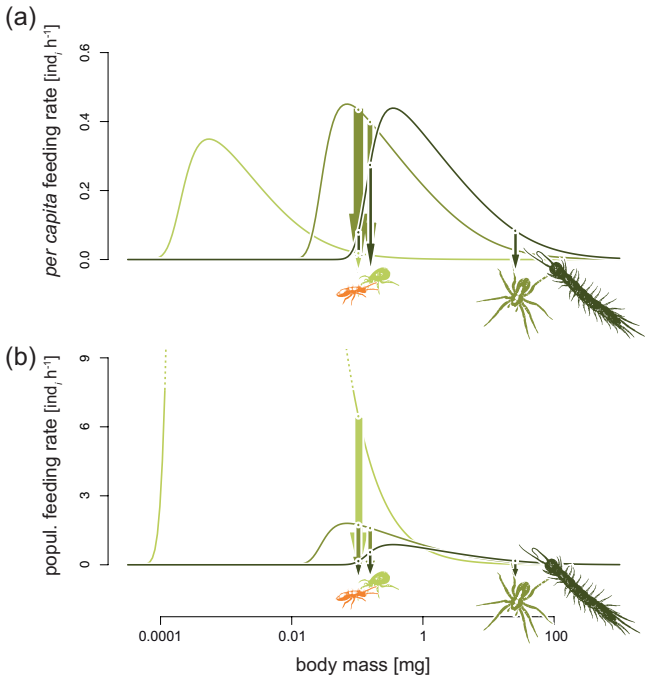

Figure 4.3 – Analogous to Fig. 4.1a: (a) *per capita* feeding rates [ind$_i$ h^{-1}] (indicated by arrow length) expected from the allometric model: the smallest predator (mite) will feed only on springtails; the largest predator (centipede) will prefer the small intraguild prey (mites) over spiders and springtails; the intermediately-sized predator (spider) should have similar preference for springtails and mites. (b) Multiplication of *per capita* effects with population densities yields population-level feeding rates: The strongest feeding rates of the mites should be on the basal springtails; the large centipedes should act predominantly as intraguild predator on the mites; spiders should feed on both, mites and springtails indifferently. Predator assumptions: initial densities and average body masses from experiment. Prey densities: $N_i = 74.8 \cdot m_i^{-0.75}$.

Table 4.1 – Average interaction strengths $\overline{IS_{ij}}$ measured in the experiment and IS_{ij} predicted in the simulation using an allometric model. Population level IS_{ij} are the $\log_{10}$-ratios between the biomass of the affected species i in presence and absence of j. For the experiment, the probability for a true difference of i's biomass in the presence and absence of j was calculated by Student's t-test. For *per capita* IS_{ij} the population IS_{ij} was divided by $\hat{n}_j$, the mean of initial and final abundance of j. The predators were the mite *Hypoaspis miles*, the spider *Pardosa lugubris*, and the centipede *Lithobius forficatus*. The detritivore springtail *Heteromurus nitidus* was evaluated as the lowest trophic level.

	Experiment			Simulation	
	population		*per capita*	population	*per capita*
$j > i$	$\overline{IS_{ij}}$ ±SD	$P(>t)$	$\overline{IS_{ij}}$ ±SD	IS_{ij}	IS_{ij}
L. forficatus > *P. lugubris*	−0.0050±0.0047	0.098	−0.0031±0.0030	−0.0259	−0.0119
L. forficatus > *H. miles*	−0.0206±0.0600	0.519	−0.0126±0.0381	0.0144	0.0066
L. forficatus > *H. nitidus*	0.0398±0.0453	0.180	0.0227±0.0256	0.0484	0.0222
P. lugubris > *L. forficatus*	0.0237±0.0264	0.124	0.0118±0.0132	0.1120	0.0430
P. lugubris > *H. miles*	0.0375±0.0462	0.156	0.0188±0.0231	0.0317	0.0121
P. lugubris > *H. nitidus*	0.0069±0.0441	0.789	0.0035±0.0220	0.0877	0.0336
H. miles > *L. forficatus*	−0.0106±0.0235	0.413	0.0000±0.0000	−0.0237	−0.0001
H. miles > *P. lugubris*	−0.0018±0.0037	0.374	0.0000±0.0000	−0.3367	−0.0009
H. miles > *H. nitidus*	−0.1490±0.0989	0.024*	−0.0002±0.0001	−0.1471	−0.0003

* $P < 0.05$; Pearson correlation coefficient of simulation and experiment for population effects $r = 0.85$, one-tailed $P = 0.002$; for *per capita* effects $r = 0.52$, one-tailed $P = 0.076$.

Dynamic Interaction Strengths

The experiment and the simulation of population dynamics yielded *per capita* and population level interaction strengths of each predator on all other species in the system (Table 4.1). We focus on the net effects on the lower trophic level, the springtails. In the simulation (Fig. 4.4a, inner bar-plots), net population interaction strength of the mites was negative and resulted from high population density. The net population effects of the spiders and centipedes on the springtails were positive and caused by their strong *per capita* interaction strengths. In the experiment (Fig. 4.4a, outer bar-plots), the smallest predator, the mites, had very weak negative *per capita* effects, but they imposed strongly negative population-level effects on springtails due to high population densities (two-tailed Student's t-test $P = 0.024$; Table 4.1). The intermediately-sized predator, the spider, had no effect on the springtails ($P = 0.789$; Table 4.1). The largest predator, the centipede, had a marginally significant positive net effect on springtails ($P = 0.098$; Table 4.1). The centipede's positive *per capita* and population interaction strengths were of similar intensity. The experimental and simulated IS_{ij} were positively correlated at the population level ($r = 0.85$; $P = 0.002$; Fig. 4.4b), whereas the positive correlation at the *per capita* level was only marginally significant ($r = 0.52$; $P = 0.076$). The IS_{ij} from centipedes on mites was negative in the experiment but positive in the simulation. The IS_{ij} from spiders on centipedes and springtails were overestimated by the simulation (Fig. 4.4b).

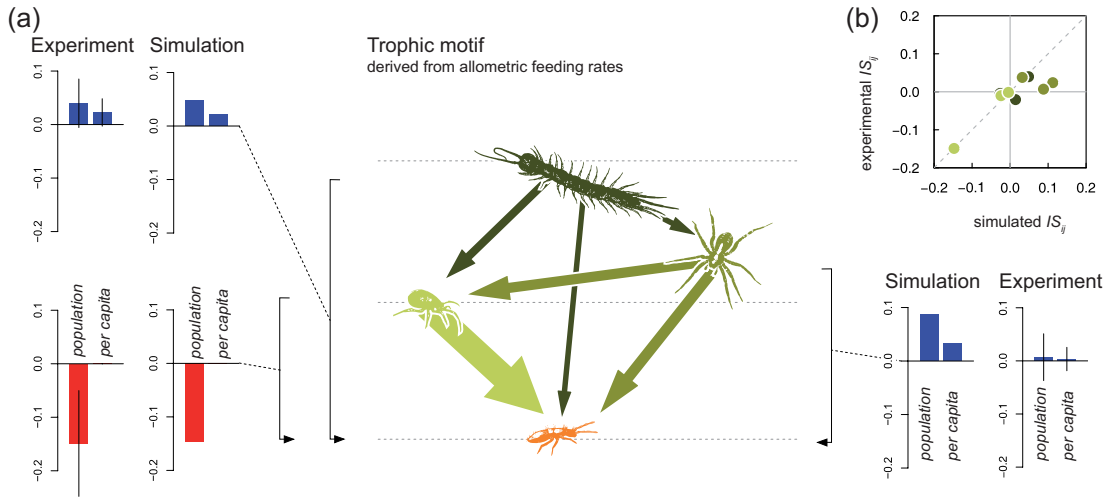

Figure 4.4 – (a) The simulation of population dynamics yields cumulative net interaction strengths of the predators over time. The effective trophic level (grey dotted lines) of the predators can be estimated from the relative feeding rates (center diagram; arrow width represents relative feeding rate from Fig. 4.3a). The inner bar-plots show the interaction strength IS_{ij} of the predators j on the springtails i derived from the simulation. The outer bar-plots show the congruent experimental population and *per capita* IS_{ij} (averaged; vertical lines represent one standard deviation). (b) All population IS_{ij} of simulation vs. experiment; color coding complies with the species in (a), center diagram.

Discussion

In this study, we employed an allometric model to understand interaction strengths in an experimental invertebrate community from the litter layer. The empirically derived body mass constraints on feeding rates and abundances in the model predicted the consequences of losing a predator from the food web. Hence, in the experiment and the simulation the net effect of a predator on lower trophic levels emerged out of the food web context and characteristic species traits, which were both constrained by body masses. Both the simulation and the experiment showed the same apparently idiosyncratic effects: (1) The small predators had a strong negative population effect on the basal prey as a result of their high population density. (2) The large predators had a positive population effect on the basal species due to predominant intraguild feeding. The estimation of static feeding rates based on the initial densities in combination with a dynamic simulation provide a mechanistic understanding of negative, neutral or positive predator effects on lower trophic levels. Our approach therefore offers a novel and critically important integration of predator-prey theory and biodiversity-ecosystem functioning experiments (Ives *et al.*, 2005).

The interaction strengths observed in the experiment illustrate how strong effects of small predators emerge from their sheer abundance, whereas effects of large predators are mainly determined by their high *per capita* feeding rates. Moreover, the positive net effect of large centipedes caused by frequent intraguild feeding and the negative net effects of small mites are

qualitatively and quantitatively consistent with the allometric simulations. However, the net interaction strengths of the intermediately-sized spiders were overestimated by the allometric model. Biological traits not covered by the allometric model may be responsible for the weak effects of the spiders in the experiment. Cannibalism diminished their population density, even in the treatments where spiders did not suffer top-down predation by centipedes. Furthermore, spiders roamed on top of the litter layer, whereas springtails, centipedes and mites predominantly dwelled in the interspace between soil and litter. Thus, despite the successful predictions achieved in the present study, we caution that allometry is no panacea for solving complexity issues. In less reductionist multi-trophic experiments, predator effects may also depend on other species traits of predators or prey including differences in hunting mode and habitat domain (Schmitz, 2007), species phenology (Otto *et al.*, 2008) or stoichiometry (Fagan and Denno, 2004). The predictions of the allometric concept applied here are based only on species body masses. The scaling relationships chosen for attack rate, handling time and predator interference are parsimonious with assumptions and parameters. However, the modelling framework is flexible to account for more complex allometric relationships or species traits that are independent of body masses (Jeschke *et al.*, 2002). For instance, it may be supplemented by dependencies of the hill-exponent of the functional response on body mass (Vucic-Pestic *et al.*, 2011) or of handling time and attack rate on temperature (Brown *et al.*, 2004; Vucic-Pestic *et al.*, 2011). Furthermore, the unimodal hump-shaped feeding curves (equation 4.2; Fig. 4.1a) used in our model are phenomenological (Persson *et al.*, 1998) and may be substituted by alternative asymmetric or multi-modal feeding curves. The latter can arise mechanistically from skewed predator size preferences coinciding with prey defense traits and non-interval feeding ranges (Zook *et al.*, 2010; Stouffer *et al.*, 2011). In addition, this allometric modelling framework can easily be extended by making any parameter dependent on body-mass independent traits such as phylogenetic constraints of metabolism (Ehnes *et al.*, 2011). In this vein, allometric feeding rate models can be flexibly merged with phylogenetic characteristics (Rall *et al.*, 2011). Although the present study focuses on trophic interactions, non-trophic traits of predator and prey species, such as facilitation or ecosystem engineering, also determine species effects in the ecosystem. To date, theoretical modelling frameworks integrating non-trophic as well as trophic interactions are in their beginnings (Fontaine *et al.*, 2011; Kéfi *et al.*, 2012). Overall, the concept of allometric feeding rates can serve as a new baseline for the integration of different theoretical concepts of species interactions.

We have shown how an allometric modeling approach can be used to understand net interaction strengths within a predator removal experiment. We advocate that this approach allows interpretation of results from experiments using classical additive or substitutive designs focusing on consumer identity and diversity effects. Many of those multiple-predator experiments could be interpreted mechanistically when compared to theoretical predictions of a reductionist allometric model (Ives *et al.*, 2005; Byrnes and Stachowicz, 2009).

One centrally important question remaining is whether the allometric assumptions and subsequent conclusions hold for more diverse, natural ecosystems. For the food web of the litter layer, our finding of a cascading effect suggests that body-mass driven intraguild predation reduces top-down control on decomposers. This is consistent with experimental data from litter food webs (Oelbermann *et al.*, 2008) and the general observation of trickling cascades in terrestrial ecosystems (Halaj and Wise, 2001; Letourneau *et al.*, 2009). On a wider scope, several studies on complex food webs support the proposed structure. First, species body masses successfully predict the number of links to predators and prey (Otto *et al.*, 2007; Digel *et al.*, 2011), predator trophic levels (Riede *et al.*, 2011) and food web structure (Petchey *et al.*, 2008*a*). Second, analyses of interaction strengths in complex food webs have documented similar body-mass constraints (Berlow *et al.*, 2009). Together, these findings suggest that allometry is centrally important in structuring complex food webs and its constraints contribute significantly to the net effect of multiple predators.

Conclusion

We used the easy-to-assess parameter 'body mass' to mechanistically explain the observation of idiosyncratic predator effects on lower trophic levels. These effects were mediated by intraguild predation as the transition state between exploitative competition and trophic cascades. Depending on the body-mass structure of the predator community, the basal prey population either benefits (if a large intraguild predator predominantly feeds within the predator guild) or suffers (if a small intraguild predator predominantly feeds on the shared prey). While the reductionist approach of allometric modeling reduces the complexity of predator effects to a single body-mass dimension, it can easily be extended by additional body-mass independent dimensions such as phylogenetic characteristics. Accounting for predator body masses in experiments and theory promises a fruitful avenue for predicting and understanding apparently idiosyncratic effects within those tightly-woven natural food webs comprising frequent intraguild interactions.

Acknowledgements

We thank E. O'Gorman, A. Binzer, B.C. Rall and two anonymous referees for very helpful comments on the manuscript; B.C. Rall and C. Guill for contributions to the modelling framework; R.B. Ehnes and G. Kalinkat, M. Kandziora, A. König, F. Grischkat, S. Mohr and all the other helpers for assistance with experimental work. F.D.S. is funded by Deutsche Bundesstiftung Umwelt (DBU, http://www.dbu.de) and partly funded by the DFG Priority Program 1374 "Infrastructure-Biodiversity-Exploratories" (BR 2315/7). U.B. is funded by the German Research Foundation (BR 2315/13).

Chapter 5.

Size-structured intraguild predation simplifies the prediction of interaction strengths in complex food webs

Florian D. Schneider and Ulrich Brose

Summary

1. The strengths of interactions among species in multi-trophic communities are difficult to predict. Especially the interaction strengths depend on traits of predator and prey species as well as on the food-web context.

2. In a microcosm experiment, we measured the net effects of five predators on the decomposer community while comparing simple monocultures with single predators to complex communities in which all predators co-occurred. The interaction strengths in simple communities were almost exclusively negative and reflect direct feeding effects of predators on their prey. Embedded in a complex community, the predators' net effects were determined by their ability for intraguild predation, which leads to positive net effects of large predators on small basal target species.

3. We find that the quantity of the per capita interaction strengths (absolute values, weak *vs.* strong) is predicted well by a multiple linear model using the population level parameters predator species body mass, m_i, and target species population density, N_j. A more informative model uses the same parameters to predict qualitatively differentiated interaction strengths (negative *vs.* positive). This qualitative model predicts negative effects in simple communities and positive effects of large predators on abundant prey in complex communities. This corresponds to expectations from allometrically constraint intraguild feeding.

4. Surprisingly, we found that predictions of interaction strengths were more consolidated and accurate in complex communities than in the simple food webs.

5. We conclude that the increased occurrence of intraguild predation in complex communities enabled positive effects of large predators and dampens effects of small predators. In total this consolidates the distribution of interaction strengths within complex communities and improves their predictability.

Keywords | Biodiversity–ecosystem functioning, body size, multi-trophic, trophic cascade, species richness

Introduction

Predator species interact in complex ways. Changes in a particular predator species population may affect other species populations positively or negatively in a way that is unpredictable in advance (Yodzis, 2001, Chapter 3 in this thesis). The response of a focal species to a specific predator species loss, the interaction strength, was thus described as 'idiosyncratic' (Lawton, 1994; Emmerson *et al.*, 2001), which often is used as synonym for unpredictable. Indeed, numerous experiments on predator removal from intact systems ambigously result in positive, neutral and negative effects on the trophic level below (Schmitz *et al.*, 2000; Halaj and Wise, 2001; Letourneau *et al.*, 2009).

The net interaction strengths of a particular predator onto a target species may be understood, however, if the rates of all involved feeding interactions are taken into account. This calls for a detailed investigation of trophic motifs and food webs, including the topologies, population densities and a quantitative resolution of feeding rates (Williams and Martinez, 2000; Dunne, 2006; Berlow *et al.*, 2009). Indeed, the relative distribution of feeding rates in a three species motif determines the net interaction strengths of the top predator on the basal prey. It may have negative net effects if the top predator predominantly feeds on the basal prey, or positive net effects, if it prefers the intermediate prey, which releases the basal prey from a feeding pressure (Holt and Polis, 1997; Finke and Denno, 2004). This pattern of intraguild predation is very common in natural food webs (Bascompte and Melian, 2005; Stouffer *et al.*, 2007) and was found to promote species coexistence (Kondoh, 2008; Gellner and McCann, 2012). Thus, knowing the feeding rates enables us to estimate the net interaction strengths of a predator on a target species.

A realistic distribution of feeding rates in a multi-trophic context can be reproduced by the assumption of allometric constraints on diet breadth (Petchey *et al.*, 2008*a*; Digel *et al.*, 2011) and consumption rates (Brose *et al.*, 2008; Rall *et al.*, 2011). For instance, the hump-shaped body-mass dependency of consumption rates was successfully used to predict the quality (negative *vs.* positive) and quantity (strong *vs.* weak) of interaction strengths in a microcosm experiment with co-occurring predator species (Schneider *et al.*, 2012; Chapter 4). Thereafter, in a community of differently sized predators, we would expect weak per capita interaction strengths for small species and strong effects for large species. The net interaction strength between a predator and a basal prey should be negative, where a small predator predominantly feeds on the basal prey and is not capable of intraguild predation. Positive net effects are expected, however, where a large predator prefers the intraguild prey over the basal prey ((Schneider *et al.*, 2012); Chapter 4). Thus, interaction strengths within multi-trophic predator communities become resolvable in quality and quantity if the body masses of predator and prey are taken into account.

Subsequently, we want to test the expectations described above as hypotheses in the present study where we report the results of a microcosm experiment measuring the response of seven

basal feeding detritivore species after removal of particular predator species. We compare the effects of five predators in monoculture against the effects of the same predators if co-occurring in a multi-predator community. Thus, we compare the interaction strengths in simple against complex systems. Here, complexity refers to the increased number of feeding interactions. Most importantly, in the experimental community of differently sized, generalist predators, the opportunities for intraguild predation are enhanced. This potentially triggers positive effects of top predators on the basal prey, by reducing the feeding pressure by the other predator (Finke and Denno, 2004). We expect complexity to alter the general pattern of interaction strengths observed in the experimental communities.

Surprisingly, it was found in theory that with increasing food-web complexity the prediction of interaction strengths will not become more complicated (Brose *et al.*, 2005). Instead, the prediction of the quantity of interaction strengths using population-level parameters such as biomass density and average body mass becomes more consolidated in more diverse systems, as was shown in simulations of niche-model food webs with varying species number (Berlow *et al.*, 2009). Those findings fuel the hypothesis that the processes in complex systems may not be more difficult but easier to predict (McGrady-Steed *et al.*, 1997). We investigate, whether this consolidation is reproduced in our microcosm experiment comparing simple and complex communities and whether the increased occurrence of intraguild predation may form the mechanism behind that phenomenon.

The central questions of this study are: How do the interaction strengths differ between simple monocultures and a complex, interconnected predator community? Is there a way to predict the quantity and quality of these interaction strengths by population-level parameters such as species body masses and densities? How does increased complexity alter the predictive power of these parameters?

Materials and methods

We conducted a microcosm experiment simulating a litter system of deciduous forests with a standardized detritivore community. We manipulated the composition of predator communities from a pool of five predator species of different body mass.

Microcosm set up and maintenance

The microcosms consisted of a plastic tube with a diameter of 22 cm. The ground plate was drilled with 37 drainage holes of 1 cm diameter and mold with Plaster of Paris (150 g plaster, 3 g activated charcoal, 150 ml water) to maintain a constant humidity within the microcosms. A cutout of 15 cm diameter in the lid of the microcosms was covered with gauze with a mesh size of 100 μm. The plaster was watered with 90 ml of distilled H_2O, which is close to the saturation

point, and covered with a layer of 250 g soil (pH = 3.3; max. field capacity: 64 %; dried at 80°C; sieved through 2 mm grid). The soil was watered with 125 ml of distilled H_2O, which is 78.5 % of the maximum field capacity. For each microcosm, 6.0 g of beech (*Fagus sylvatica*) and 1.5 g of maple (*Acer pseudoplatanus*) leaves were weighed and placed as a mixture inside the microcosms. The litter was watered initially with 25 ml of distilled water.

The experiment was conducted in five blocks which were set up in one week intervals. The microcosms were set up in a controlled climate chamber and were rotated block-wise every week to account for heterogeneous ventilation and temperature. Twice a week, 25 ml of distilled water were sprayed into each microcosm. Additionally, once a week the microcosms were adjusted to the initial total weight by adding additional water. The average evaporation was 9.9 ml (±1.0 std. dev.) per day, which was around 4% of the total water content. Temperature and humidity within the microcosms was logged (15.3°C±0.3 std. dev.; 91.1 % relative humidity ±4.8 std. dev.).

Organisms and treatments

After twelve days, a standardized community of detritivores was added to all microcosms. One day later, communities of up to five predatory species (Figure 5.1a) were initiated in twelve different treatments: A control containing only the detritivore community (n = 10; densities given in Table 5.1 in supplementary material on page 100); Five different single predator treatments each containing one of the five predator species (n = 5 each); A full treatment containing all five predator species (n = 10); Five knockout treatments each lacking one of the five predator species (n = 5 each). The initial abundances (Table 5.1, Fig. 5.5 in supplementary material) were combined additively in the treatments with multiple predator species.

These detritivore and predator species for the experimental community were selected to yield a maximal size spectrum and functional variability, and for reasons of seasonal and logistical availability (practical rearing and sampling methods): The detritivore community comprised a small (*Folsomia candida*) and a large (*Heteromurus nitidus*) species of springtails, adult isopods of two species (*Oniscus asellus*, *Porcellio scaber*), juvenile isopods (*Oniscus asellus*, *Porcellio scaber*, *Armadillidium vulgare*), millipedes (*Cylindroiulus punctatus*, *Tachipodoiulus niger*, *Ommatoiulus sabulosus*) and earthworms (*Dendrobaena octaedra*, *Dendrodilus rubidus*). Juvenile isopods, millipedes and earthworms were not differentiated to taxonomic species level (Table 5.1; Figure 5.1a) but are in the following each grouped to one experimental 'species'.

The treatments represented different combinations of five experimental predator 'species' (Table 5.1; Figure 5.1a): large centipedes (*Lithobius forficatus*, *Lithobius variegatus*), lycosid spiders (*Pardosa lugubris*), linyphiid spiders (*Helophora insignis*), small centipedes (*Lithobius piceus*, *Lithobius melanops*) and gamasid mites (*Pergamasus crassipes*). The potential feeding links between the species (Fig. 5.1a) were determined in qualitative feeding experiments, ob-

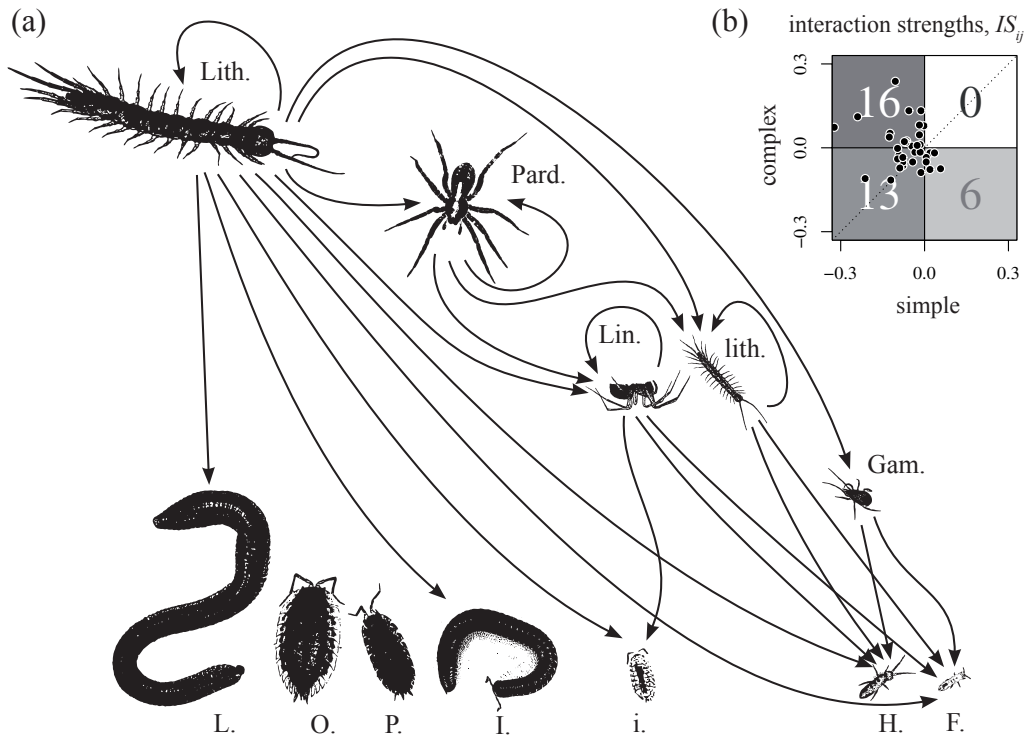

Figure 5.1 – (a) Potential direct feeding links within the complex community. The standardized detritivore community (**L**umbricidae, ***O****niscus asellus*, ***P****orcellio scaber*, **I**ulidae, juvenile **i**sopods, ***H****eteromurus nitidus*, ***F****olsomia candida*) are preyed upon by different sets of predators (***Lith****obius* sp., ***Pard****osa lugubris*, **Lin**yphiidae, small **lith**obiidae, **Gam**asinae). (b) Interaction strengths observed in simple communities with only one predator present *vs.* complex communities with all predators co-occurring. Both observations are totally uncorrelated in their quantity (ANCOVA: $R^2 = 0.034$; $p = 0.286$) and quality (only 13 out of 35 interactions show the same sign in simple and complex communities).

serving the feeding events in repeated direct confrontations between two individuals of different species in small vessels (4 cm diameter with plaster ground).

Spiders, large centipedes, earthworms, isopods, and millipedes were collected by hand, by litter sieving and by suction sampling in the litter layer and under decaying wood. Smaller individuals of centipedes, isopods, millipedes and mites were isolated from forest floor by Berlese heat extraction. The initial densities represent natural levels, which can be assumed to be energetically balanced by the species' foraging. This opposes classical additive designs of predator diversity studies, where all species are introduced with the same population or biomass density. In this case, the difference in species body mass would cause quite arbitrary levels in species biomasses or population densities, respectively (Schneider *et al.*, 2012; Jochum *et al.*, 2012; Chapters 4 and 6). This 'allometric design' for predator experiments assumes population density, N, to depend on body mass, m, following a power-law scaling (predators: $N_i = 0.82 m_i^{-0.46}$; detritivores: $N_j = 1.41 m_j^{-0.70}$; see supplementary material , Table 5.1, Fig. 5.5).

Data collection and processing

After 52 days, the larger animals were collected by hand and weighed alive. The individual weights of each species were summed and transformed to population biomass densities, B (g / m^2). The smaller animals were transferred by heat extraction into saturated saline solution. Springtails and mites were counted and species biomass densities (g / m^2) were estimated by multiplying population densities with average body masses. Interaction strengths of predator i on species j, IS_{ij} , were calculated as the log-ratio between the change in j's biomass in presence of i and the change in j's biomass in absence of i (Berlow *et al.*, 1999).

$$IS_{ij} = \ln \frac{\Delta B_j^{+i} + 1}{\Delta B_j^{-i} + 1} \tag{5.1}$$

The proportional change in j's biomass, ΔB_j, was defined as the ratio between its initial and final biomass density in one replicate, to remove effects of initial variation in the replicates. Combining all replicates of the presence treatment (i.e., single predator treatment, $n = 5$, or full community treatment, $n = 10$) with all replicates of the absence treatment (i.e., detritivore control, $n = 10$, or knockout-treatment, $n = 5$) yielded the average IS_{ij} . Per capita interaction strengths were calculated by dividing IS_{ij} by the average number of individuals of N_i throughout the experiment (average of initial and final density). The significant deviation of IS_{ij} from zero was determined via linear mixed effect models, including experimental block as a random effect.

Descriptive linear modeling

We investigated the predictability of interaction strengths between predators and the detritivore community. As predictive parameters we used averaged species level parameters determined from the microcosms containing the influencing species at the final state of the experiment. This is analogue to the parameters that could be assessed in studies without *a priori* knowledge about the populations. The parameters were predator body mass, m_i, prey body mass, m_j, and the predator-prey body mass ratio, R_{ij}, predator and prey population densities, N_i and N_j, and biomass densities, B_i and B_j (all $\log_{10}$-transformed, densities per m^2). We composed all single-parameter models with and without quadratic terms (to test for curvature; $7 \times 2 = 14$ models), and all additive two-parameter models with one parameter describing i and one describing j, with and without interaction term, and with and without one or both quadratic terms ($14 \times 2 \times 4 = 112$ models; the parameter pair R_{ij} and N_j was eliminated due to strong autocorrelation). To test for a difference between simple and complex communities, we alternatively nested all models into the factorial parameter 'complexity' (doubling the number of models). All 252 models were applied to explain population level and per capita IS_{ij} and alternatively

the absolute values thereof. The prediction of absolute values enables a log-transformation to account for the non-normal distribution of the IS_{ij} values. The models on qualitative IS_{ij} cannot account for that fact. Thus, strong absolute values have more influence on the least squares fit than weak absolute values. The most parsimonious models for each target metric were identified via Akaike's Information Criterion, AIC.

Results

Interaction strengths in simple *vs.* complex communities

Due to the allometric initialization of the experiment, we assume that the interaction strengths we measured correspond to those in energetically balanced, dynamic ecosystems. Some predator–prey interaction strengths can clearly be differentiated from zero (mixed effect models, $n = 50$; see supplementary material Table 5.2). In the simple community (Fig. 5.2a), the mites of the order Gamasinae imposed significant negative effects on both of the springtail species (j = *H. nitidus*: $IS_{ij} = -0.127$, $p < 0.05$; j = *F. candida*, $IS_{ij} = -0.323$; $p < 0.01$) and the isopod *P. scaber* ($IS_{ij} = -0.096$; $p < 0.05$). The small centipedes affected the smaller springtails *F. can-*

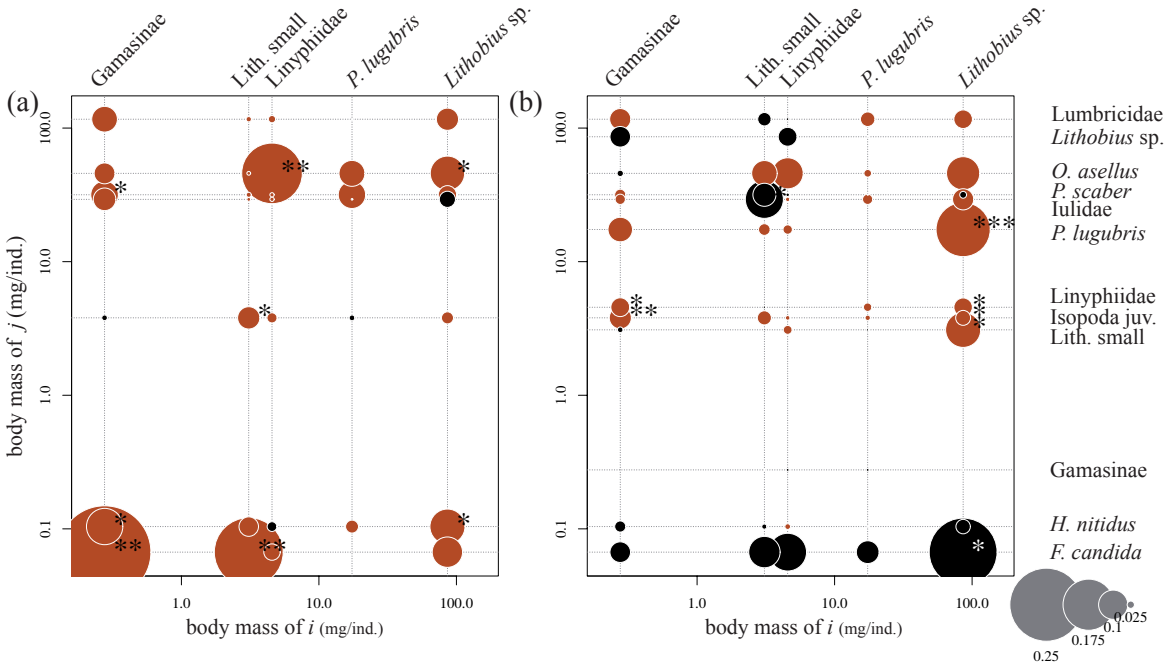

Figure 5.2 – Species level illustration of interaction strength of a predator i (columns) and a target species j (rows), sorted by their body mass. (a) Simple communities with each predator in monoculture. (b) Complex communities with all predator co-occurring. The size of symbols indicates absolute interaction strengths. Red symbols are negative effects, black symbols are positive effects. Asterisks indicate significant deviation from zero (mixed effect model including 'block' as a random factor, see materials and methods): * $p < 0.05$, ** $p < 0.01$, *** $p < 0.001$.

dida (IS_{ij} = −0.240, $p < 0.01$) and juvenile isopods (IS_{ij} = −0.078, $p < 0.05$). The small linyphiid spiders negatively affected the larger isopod *O. asellus* (IS_{ij} = −0.2115, $p < 0.01$), which was also affected by the large centipedes of the genus *Lithobius* (IS_{ij} = −0.120, $p < 0.05$). Those also reduced the population of the springtail *H. nitidus* (IS_{ij} = −0.122, $p < 0.05$).

In the complex community (Fig. 5.2b), the mites negatively affected the linyphiid spiders (IS_{ij} = −0.066, $p < 0.05$) and the juvenile isopods (IS_{ij} = −0.077, $p < 0.01$). The presence of small centipedes enhanced the density of millipedes (IS_{ij} = 0.133, $p < 0.05$). The large centipedes affected juvenile isopods (IS_{ij} = −0.052, $p < 0.05$) and the intermediately sized predators negatively (j = small Lithobiida, IS_{ij} = −0.122, $p < 0.05$; j = Linyphiidae, IS_{ij} = −0.064, $p < 0.05$; j = *P. lugubris*, IS_{ij} = −0.189, $p < 0.001$), while it enhanced the population of the springtail *F. candida* (IS_{ij} = 0.237, $p < 0.05$). The effects on Gamasinae equal zero in all cases, because they became extinct in all replicates, including the knock-out treatments. However, they persisted at least long enough to cause significant effects.

Quantitative and qualitative prediction of interaction strengths

The interaction strengths in the complex community are entirely unrelated to those in the simple communities including only one predator (ANCOVA: R^2 = 0.034; p = 0.286). The quality of the interaction strength (i.e. the algebraic sign) accords in only 13 out of 35 observations (37%) between simple and complex communities (Fig. 5.1b). The per capita IS_{ij} result in better predictions than population IS_{ij} , while for both the same parameter combinations are identified as most efficient predictors (supplementary material Tables 5.3–5.6). In the following, we focus on the per capita effects, because they also represent a more general quantity that can be scaled to populations of different size by multiplying with population density.

At first we compared models to describe the quantity of interaction strengths without regard to the algebraic sign. Those absolute per capita interactions strengths were best described by a model incorporating predator body mass, m_i, and prey population density, N_j (R^2 = 0.382;

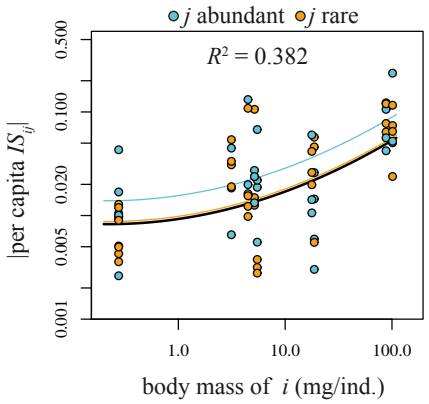

Figure 5.3 – Quantitative model describes $\log_{10}$-transformed absolute per capita interaction strengths with predator body mass, m_i, and target species population density, N_j. Black line is the prediction for median N_j. Coloured lines and symbols represent predictions and observed values (blue: upper 50%-quantile, i.e. abundant N_j; yellow: lower 50%-quantile, i.e. rare N_j).

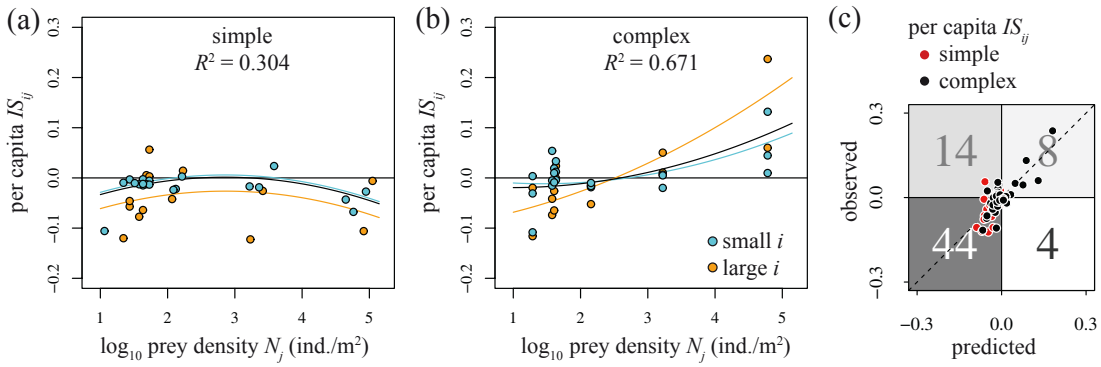

Figure 5.4 – Qualitative model for per capita interaction strengths. The most parsimonious model includes predator body mass, m_i, and target species population density, N_j, nested into complexity. (a) in simple communities (b) in complex communities. Black line is the prediction for median m_i. Coloured lines and symbols represent predictions and observed values for small (blue: lower 50%-quantile) and large (yellow: upper 50%-quantile) predators. (c) Quality of model prediction. Large numbers show density of qualitative matches (lower left + upper right) and mismatch (upper left + lower right) between prediction and observation.

see supplementary material Tables 5.3 and 5.4). The per capita effect increased quadratically with predator body mass. Thus, small predator individuals are predicted to have small effects, whereas large predator individuals should have strong effects on other species (Fig. 5.3). The population density, N_j, of the target species contributes additively to per capita IS_{ij} , with weakest effects on species with intermediate N_j and quadratically increasing effects on species with high N_j (Fig 5.3, coloured symbols and lines for upper and lower 50%-quantiles: blue = high population densities of target species j; yellow = low population densities). The comparison of AIC detected no significant difference in the distribution of absolute per capita IS_{ij} between the simple and the complex community. The models that described untransformed, real IS_{ij} scored best when incorporating complexity as an explanatory parameter together with m_i and N_j ($R^2 =$ 0.595; see supplementary material Tables 5.5 and 5.6). In the simple community (Fig. 5.4a), the model predicted predominantly negative interaction strengths with slightly stronger negative effects on both extremely rare and abundant populations. Strong negative per capita IS_{ij} are correlated with very small and very large predator body mass (Fig. 5.4a, upper and lower 50%-quantiles: blue = small body mass of removed species i, yellow = large body mass of i). These effects do only weakly interact in simple communities. The complex community (Fig. 5.4b) produced positive interaction strengths of large predators on abundant target populations, while on species with low population densities the effect of large predators was negative. The predicted IS_{ij} approximates zero for the effects of predator species of small body mass (Fig. 5.4b, upper and lower 50%-quantiles: blue = small i, yellow = large i).

The qualitative model predicted 59.5 % of the total variation in IS_{ij} and matched the sign of the per capita effects in 52 out of 70 cases (74.3%, Fig. 5.4c, count of symbols in lower left plus upper right field). Interestingly, in complex systems the models explained twice as much of the

variation in the observed per capita interaction strengths than in simple communities (simple: $R^2 = 0.304$, complex: $R^2 = 0.671$; Fig. 5.4a, b).

Discussion

The aim of the study was the prediction of interaction strengths in multi-predator assemblages. Interaction strengths of predators on a target detritivore species differed strongly between a simple predator monoculture and the complex predator communities. Given the evident lack of correlation, the prediction of interaction strengths in complex communities from the observation in simple communities must be considered futile. The increased occurrence of intraguild predation fundamentally changes the net effects on basal species within the complex community. We found, however, that quantity and quality of interaction strengths are predictable by the body mass of the predator and the population density of the target species. This provides new perspectives for an estimation of the net effects of the predator community on the process rates on lower trophic levels from accessible population parameters. This prediction becomes even more precise when the complexity of the community increases. These counterintuitive results indicate the existence of an undescribed mechanism that consolidates the net effects within the predator community for systems of higher diversity. We propose that this consolidation originates from the increased occurrence of intraguild predation motifs with increasing predator diversity.

Interaction strengths in simple *vs.* complex communities

Before discussing the interaction strengths observed in our experiment, we want to emphasize the importance of the allometric design. Estimates of per capita effects always are biased by the *a priori* definitions of experimental species density. The standardization of each species to equal individual density, which is common in consumer diversity experiments (Byrnes and Stachowicz, 2009), would cause a strong bias by biomass density, because species differ in individual body mass. Instead, the densities need to be balanced by allometric mass-abundance relationships (Schneider *et al.*, 2012) or empirically derived densities (Finke and Denno, 2004) to achieve realistic effects of species removal. Therefore, this experiment was initiated with predator individual densities that reflect the predator populations in nature, scaling negatively with body mass. Thus, the interaction strengths measured in the experiment reflect natural conditions (see supplementary material, Table 5.1, Fig. 5.5).

Our knowledge about potential feeding links between the species in our experimental community (Fig. 5.1a) and the observed net interaction strengths (Fig. 5.2) allow a deduction of the feeding relationships within the community. In the simple communities each containing only one predator in monoculture, the detected negative interaction strengths on the species

level reveal direct feeding on the detritivores. The most prominent effects are observed on the smallest detritivore species, the springtails. These effects were significantly negative for predators of all sizes (Gamasinae, small & large centipedes) and indicate the consequences of direct feeding. The strongest feeding, however, was observed by the smallest predators, the mites. The largest predators caused weaker population effects. These observations match the quantitative expectations from allometric constraints on predator feeding, predicting strong absolute population effects of small predators due to their high population densities, and weak absolute population effects for large predators (Schneider *et al.*, 2012).

Further, these effects were neutralized or turned into positive effects in complex communities with other predators present. This is due to the occurrence of intraguild predation among the predators (Fig. 5.1a). In the complex community, several negative effects of large centipedes on other predators indicate direct feeding which in turn reduces the feeding effect of the intraguild prey on the basal resource. Thus, the springtail prey is released from top down pressure and benefits from the increased complexity. Such trophic cascades due to intraguild predation which cause a qualitative shift from negative to positive interaction strengths on the basal species are common phenomena with increasing species richness (Finke and Denno, 2004, 2005). Moreover, the body mass structure of the community provides a mechanism for the increasing opportunities for intraguild predation, since large generalist predators likely include smaller predators, which feed on a shared basal prey, into their prey range (Schneider *et al.*, 2012). In simple communities, body mass might only induce quantitative changes by enhancing direct per capita feeding rates for large predators. In complex communities body mass determines the quality of the interaction by inducing positive net effects for large predators and diminishing population effects of small predators. Acknowledging body mass as a determinant of intraguild predation explains the improved predictability of interaction strengths.

Thus, the knowledge about the species-specific feeding enables us to disentangle the trophic relationships within the community. Note that we focused on the discussion of trophic effects although we have to acknowledge that several non-trophic effects took action within the community. Some negative interaction strengths do not correspond to an observation of direct feeding (e.g. Linyphiidae on *O. asellus*, Gamasinae on *P. scaber*). The nature of these interaction effects was not investigated in this study and is subject to speculations only. A reason could be facilitative effects (Kéfi *et al.*, 2012) between springtails and isopods via a microbial loop (Scheu and Setälä, 2002) which would reduce the fitness of isopods when springtail populations are diminished.

Quantitative and qualitative prediction of interaction strengths

In natural communities with far more predator species than commonly used in microcosm experiments, a measurement of all species-specific interaction strengths are rendered impossi-

ble. The allometric constraints on predator feeding and abundance may provide mechanistic explanations for the observed net effects in dependence on body mass (Schneider *et al.*, 2012), but it is still unclear if these predictions hold in more speciose communities. Consequently, we addressed the question whether interaction strengths of predators on the basal species are quantitatively and qualitatively predictable from accessible population parameters of removed species and target species like density and average body mass. In absolute terms, the predator's per capita effect on the basal species is most efficiently explained by its own body mass, m_i, and the population density of the target species, N_j. The model predicts weak effects for predators of small body mass and strong effects for large predators, as expected from allometrically constrained predators (Schneider *et al.*, 2012). This pattern also accords to simulations of species loss from model food webs, where per capita IS_{ij} increased exponentially with predator body mass (Berlow *et al.*, 2009). From allometric mass-abundance scaling (White *et al.*, 2007; Ehnes et al., in preparation) we would expect that the weak per capita effects of small predators are naturally amplified by their high population densities (Schneider *et al.*, 2012). The quantitative model, however, was not able to predict whether a species affects another species positively or negatively.

Therefore, we also discuss a model that succeeds best in a qualitative prediction of per capita interaction strengths. The parameters included in this model were the same as in the quantitative model: predator body mass, m_i, and target species population density, N_j. The coefficients for simple and complex communities, however, differed significantly. In the simple communities with only one predator, almost exclusively negative interaction strengths were observed. The model fit therefore was predicting negative values, except for the effects of intermediately-sized predators on prey of intermediate density which are rather expected to be neutral. For complex communities, the pattern is different especially for large predators whose effects strongly depend on prey population densities. For abundant populations, the effects are expected to be positive. In contrast, the per capita effect of small predators is expected to be neutral. Thus, increasing complexity allows large predators to switch their net effect on abundant basal prey from negative to positive effects. This can be explained by the occurrence of intraguild predation of large predators in the complex communities. Coincidently, the intraguild feeding eliminates any negative net effect of small predators on detritivores, which was observed in the simple systems. Qualitatively, however, the sign of an interaction is explained very successfully by our model in 74 % of the cases.

Due to the balanced experimental design which mimics natural mass-abundance relationships, the population density of the target species is strongly correlated with its body mass. High population density of the target species must in any case be considered as coupled to small average body masses. The best model predicting per capita IS_{ij} just from the body masses of predator and target species is found on rank 8 and scores only 3.2 ΔAIC worse than the discussed model because it explains less variation in the response parameter (33 %; Table 5.4).

Nonetheless, average body mass of the target species may be considered as prior to population density because it is easier to estimate in the field. All these findings are in perfect accordance to the expectations from allometrically constraint predator behavior, which predict positive net effects of large predators on small, or abundant, basal resources due to intraguild predation (Schneider *et al.*, 2012).

Predictability improves with complexity

We found that the variation in interaction strengths in complex predator communities is predicted more accurately by the population level parameters than in simple communities. The increase in coefficient of determination was described before for interaction strengths in simulated food webs of variable diversity (Berlow *et al.*, 2009). We argue that an important mechanism for this consolidation should be the increasing occurrence of intraguild predation motifs in complex communities. The motif acts as a stabilizing buffer mechanism if the feeding rates of the top predator are distributed asymmetrically with strong feeding on the intraguild prey and weak feeding on the basal prey (Emmerson and Yearsley, 2004; Vandermeer, 2006; Kondoh, 2008; Gellner and McCann, 2012). In our experiment, this asymmetry arises from differences in species body mass and turns the net effect of a large top predator on the basal prey to a positive one. At the same time, the negative effect of small predators is diminished due to their exposition to intraguild feeding. Alltogether, intraguild predation and the distribution of weak and strong, positive and negative interaction strengths must be regarded a consequence of the general body mass dependency of feeding rates (Kondoh, 2008; Schneider *et al.*, 2012; Rall et al. in preparation). As a consequence, the variation of interaction strengths becomes more consolidated by the occurrence of intraguild predation. This corroborates the hypothesis that the net effects within diverse and complex predator communities are predictable by population level parameters.

Conclusion

We found that both quantity and quality of interaction strengths in multi-predator communities are well predictable by population properties of predator and target species. Furthermore, our study corroborates the astounding conclusion of Berlow *et al.* (2009) that increasingly complex systems are simpler to predict. In this study, we connected the improved predictability with the increasing occurrence of intraguild predation. Thus, we conclude that body mass driven intraguild predation must be considered a major mechanism in distributing the weak and strong interactions within complex trophic communities. The integration of body masses as an explanatory parameter is vital to understand how intraguild predation consolidates the effects on the trophic level below and shapes the functioning of diverse communities.

Acknowledgements

Special thanks to Petra Hosumbek for collecting, rearing and maintaining the organisms and assisting in experimental work. We thank Katarina Fußmann, Marius Reinhardt, Thomas Schimmer, Katrin Spindler, Chris K. Sprengel, and Theodora Volovei for assistance in the experimental work. F.D.S. has been funded by a fellowship of Deutsche Bundesstiftung Umwelt (www.dbu.de).

Supplementary material to Chapter 5

Florian D. Schneider and Ulrich Brose

Allometric design of the experiment

Table 5.1 – Initial densities of species. Average body masses, m, initial number of individuals per microcosm, N, and total population biomass per microcosm, B.

	body mass		experimental density	
	m (± std. dev.) (mg / ind.)		N (ind./microcosm)	B (mg/microcosm)
detritivores:				
Folsomia candida	0.067	$n = 300$	250	15.8
Heteromurus nitidus	0.104(±0.027)	$n = 553$	100	10.4
juvenile Isopoda*	3.798(±3.215)	$n = 132$	10	33.4
Iulidae*	29.277(±6.759)	$n = 140$	2	58.6
Porcellio scaber	32.053(±6.346)	$n = 147$	2	64.1
Oniscus asellus	46.406(±8.846)	$n = 87$	1	46.4
Lumbricidae*	116.549(±22.849)	$n = 140$	2	233.1
predators:				
Gamasinae*	0.276	$n = 34$	15	4.2
Linyphiidae*	4.559(±0.939)	$n = 70$	2	9.1
small Lithobiida*	3.088(±1.082)	$n = 140$	4	12.0
Pardosa lugubris	17.524(±4.228)	$n = 70$	2	35.0
Lithobius sp.*	86.093(±22.195)	$n = 38$	1	86.1

*not differentiated to species level; std. dev. shows variation of individual body masses within the sample of size n.

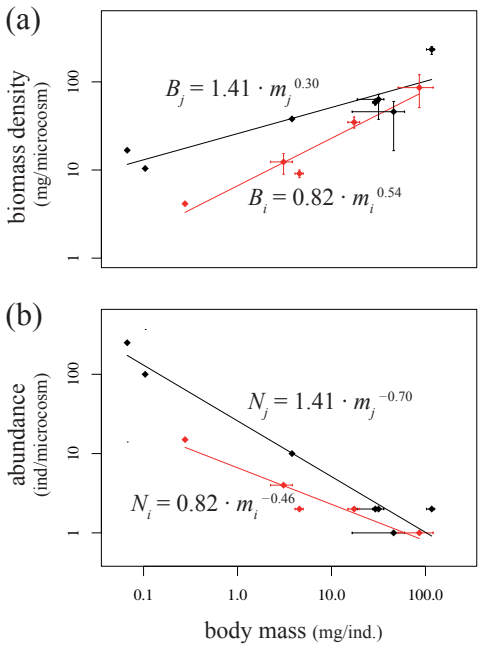

Figure 5.5 – Allometric design of the experiment. Initial predator (i) and detritivore (j) densities were introduced to reflect the natural scaling of (a) population biomass density and (b) abundance with body mass. The different scalings for predators (red diamonds ± std. dev., red regression line) and detritivores (black diamonds ± std. dev., black regression line) follow field densities.

Per capita and population level IS_{ij}

Table 5.2 – Population level and per capita (p.c.) Interaction strengths of all predators i on all target species j within the simple and complex communities. Explanatory parameters that were used in multiple-linear models are body masses, m, population densities, N, and biomasses, B, of i and j as well as the body mass ratio, R_{ij}.

i	j	$IS_{ij} \pm std.dev.$	p	$p.c.IS_{ij}$	m_i (g/ind)	m_j (g/ind)	B_i (g/m^2)	B_j (g/m^2)	N_i (ind/m^2)	N_j (ind/m^2)	$\log_{10} R_{ij}$
simple											
Lithobius sp.	*H.nitidus*	−0.1224±0.1084	0.039*	−0.1224	88.04	0.10	2329.2	177.5	27	1698	2.9
Lithobius sp.	*F. candida*	−0.1061±0.2489	0.241	−0.1061	88.04	0.07	2329.2	5518.8	27	82393	3.1
Lithobius sp.	juv. Isopoda	−0.0422±0.1101	0.316	−0.0422	88.04	3.83	2329.2	465.9	27	117	1.4
Lithobius sp.	*O. asellus*	−0.1201±0.1369	0.016*	−0.1201	88.04	48.90	2329.2	898.5	27	22	0.3
Lithobius sp.	*P. scaber*	−0.0640±0.1579	0.334	−0.0640	88.04	34.97	2329.2	1624.1	27	43	0.5
Lithobius sp.	Iulidae	0.0564±0.1010	0.102	0.0564	88.04	29.77	2329.2	1719.6	27	54	0.5
Lithobius sp.	Lumbricidae	−0.0774±0.1783	0.349	−0.0774	88.04	131.48	2329.2	5267.3	27	38	−0.2
P. lugubris	*H.nitidus*	−0.0452±0.1273	0.438	−0.0259	18.74	0.10	777.7	271.9	43	2605	2.3
P. lugubris	*F. candida*	−0.0014±0.2599	0.750	−0.0059	18.74	0.07	777.7	7483.6	43	111732	2.4
P. lugubris	juv. Isopoda	0.0200±0.1023	0.606	0.0145	18.74	4.19	777.7	685.2	43	169	0.7
P. lugubris	*O. asellus*	−0.0904±0.1361	0.059	−0.0571	18.74	55.85	777.7	1236.9	43	27	−0.5
P. lugubris	*P. scaber*	−0.0956±0.1444	0.104	−0.0460	18.74	38.13	777.7	1304.6	43	27	−0.3
P. lugubris	Iulidae	0.0059±0.1256	0.962	0.0055	18.74	28.08	777.7	1434.7	43	48	−0.2
P. lugubris	Lumbricidae	0.0050±0.1078	0.921	0.0030	18.74	121.89	777.7	7134.1	43	54	−0.8
small Lithobiida	*H.nitidus*	−0.0680±0.1148	0.193	−0.0187	5.48	0.10	453.2	239.0	90	2290	1.7
small Lithobiida	*F. candida*	−0.2404±0.2338	0.006**	−0.0677	5.48	0.07	453.2	3877.7	90	57889	1.9
small Lithobiida	juv. Isopoda	−0.0779±0.1155	0.030*	−0.0220	5.48	2.52	453.2	354.8	90	133	0.7
small Lithobiida	*O. asellus*	−0.0132±0.0364	0.242	−0.0032	5.48	55.00	453.2	1447.8	90	27	−1.0
small Lithobiida	*P. scaber*	−0.0175±0.0768	0.512	−0.0038	5.48	41.90	453.2	1751.8	90	43	−0.9
small Lithobiida	Iulidae	−0.0135±0.1113	0.596	−0.0028	5.48	30.81	453.2	1271.5	90	43	−0.7
small Lithobiida	Lumbricidae	−0.0185±0.1072	0.598	−0.0055	5.48	122.25	453.2	6433.1	90	54	−1.3
Linyphiidae	*H.nitidus*	0.0340±0.1680	0.470	0.0237	5.16	0.10	259.5	399.1	43	3829	1.7
Linyphiidae	*F. candida*	−0.0571±0.2113	0.339	−0.0273	5.16	0.07	259.5	5960.1	43	88983	1.9
Linyphiidae	juv. Isopoda	−0.0354±0.0944	0.197	−0.0238	5.16	4.33	259.5	476.7	43	122	0.2
Linyphiidae	*O. asellus*	−0.2115±0.1761	0.007**	−0.1058	5.16	42.79	259.5	447.3	43	12	−0.9
Linyphiidae	*P. scaber*	−0.0149±0.0850	0.631	−0.0126	5.16	34.27	259.5	1883.2	43	48	−0.8
Linyphiidae	Iulidae	−0.0151±0.1276	0.695	−0.0149	5.16	28.11	259.5	1289.3	43	43	−0.7
Linyphiidae	Lumbricidae	−0.0254±0.1213	0.584	−0.0133	5.16	117.98	259.5	6130.1	43	54	−1.4
Gamasinae	*H.nitidus*	−0.1268±0.1097	0.036*	−0.0169	0.28	0.10	1.0	173.4	1	1658	0.4
Gamasinae	*F. candida*	−0.3234±0.1989	0.003**	−0.0431	0.28	0.07	1.0	2981.9	1	44512	0.6
Gamasinae	juv. Isopoda	0.0196±0.0891	0.657	0.0026	0.28	4.15	1.0	671.7	1	164	−1.2
Gamasinae	*O. asellus*	−0.0728±0.1446	0.147	−0.0097	0.28	36.95	1.0	953.1	1	22	−2.1
Gamasinae	*P. scaber*	−0.0962±0.0756	0.014*	−0.0128	0.28	33.10	1.0	1284.8	1	38	−2.1
Gamasinae	Iulidae	−0.0789±0.1543	0.198	−0.0105	0.28	29.86	1.0	967.2	1	33	−2.0
Gamasinae	Lumbricidae	−0.0897±0.1588	0.204	−0.0120	0.28	116.73	1.0	4858.9	1	43	−2.6
complex											
Lithobius sp.	*H.nitidus*	0.0504±0.1210	0.266	0.0504	101.32	0.10	2838.5	174.4	27	1668	3.0
Lithobius sp.	*F. candida*	0.2369±0.2000	0.034*	0.2369	101.32	0.07	2838.5	4056.1	27	60552	3.2
Lithobius sp.	juv. Isopoda	−0.0522±0.0574	0.021*	−0.0522	101.32	2.43	2838.5	346.9	27	143	1.7
Lithobius sp.	*O. asellus*	−0.1160±0.1628	0.155	−0.1160	101.32	46.80	2838.5	1005.8	27	19	0.3
Lithobius sp.	*P. scaber*	0.0238±0.1383	0.484	0.0238	101.32	31.07	2838.5	1646.3	27	43	0.5

i	j	IS_{ij} ±*std.dev.*	p	$p.c.IS_{ij}$	m_i	m_j	B_i	B_j	N_i	N_j	$\log_{10} R_{ij}$
complex (continued)											
Lithobius sp.	Iulidae	−0.0739±0.1116	0.166	−0.0739	101.32	29.44	2838.5	1411.2	27	38	0.5
Lithobius sp.	Lumbricidae	−0.0648±0.1379	0.351	−0.0648	101.32	116.45	2838.5	4963.2	27	40	−0.1
Lithobius sp.	Gamasinae	0.0047±0.0331	0.743	0.0047	101.32	0.28	2838.5	3.9	27	12	2.6
Lithobius sp.	Linyphiidae	−0.0645±0.0810	0.040*	−0.0645	101.32	4.49	2838.5	1.0	27	1	1.4
Lithobius sp.	small Lithobiida	−0.1225±0.1505	0.033*	−0.1225	101.32	3.14	2838.5	100.5	27	33	1.5
Lithobius sp.	*P. lugubris*	−0.1891±0.0976	< 0.001***	−0.1891	101.32	17.73	2838.5	291.1	27	17	0.8
P. lugubris	*H.nitidus*	0.0049±0.1202	0.982	0.0106	17.73	0.10	291.1	174.4	17	1668	2.2
P. lugubris	*F. candida*	0.0794±0.2139	0.474	0.0601	17.73	0.07	291.1	4056.1	17	60552	2.4
P. lugubris	juv. Isopoda	−0.0186±0.0923	0.560	−0.0142	17.73	2.43	291.1	346.9	17	143	0.9
P. lugubris	*O. asellus*	−0.0267±0.2125	0.805	−0.0198	17.73	46.80	291.1	1005.8	17	19	−0.4
P. lugubris	*P. scaber*	−0.0038±0.1426	0.939	−0.0007	17.73	31.07	291.1	1646.3	17	43	−0.2
P. lugubris	Iulidae	−0.0357±0.1148	0.576	−0.0416	17.73	29.44	291.1	1411.2	17	38	−0.2
P. lugubris	Lumbricidae	−0.0507±0.1605	0.512	−0.0261	17.73	116.45	291.1	4963.2	17	40	−0.8
P. lugubris	Gamasinae	0.0103±0.0311	0.505	0.0068	17.73	0.28	291.1	3.9	17	12	1.8
P. lugubris	Linyphiidae	−0.0295±0.0596	0.168	−0.0236	17.73	4.49	291.1	1.0	17	1	0.6
P. lugubris	small Lithobiida	0.0086±0.0959	0.803	0.0072	17.73	3.14	291.1	100.5	17	33	0.8
P. lugubris	*Lithobius* sp.	0.0041±0.0190	0.610	0.0035	17.73	101.32	291.1	2838.5	17	27	−0.7
small Lithobiida	*H.nitidus*	0.0180±0.1425	0.910	0.0065	3.14	0.10	100.5	174.4	33	1668	1.5
small Lithobiida	*F. candida*	0.1095±0.2421	0.408	0.0448	3.14	0.07	100.5	4056.1	33	60552	1.7
small Lithobiida	juv. Isopoda	−0.0492±0.1174	0.253	−0.0184	3.14	2.43	100.5	346.9	33	143	0.1
small Lithobiida	*O. asellus*	−0.0890±0.1746	0.315	−0.0309	3.14	46.80	100.5	1005.8	33	19	−1.2
small Lithobiida	*P. scaber*	0.0804±0.2122	0.393	0.0334	3.14	31.07	100.5	1646.3	33	43	−1.0
small Lithobiida	Iulidae	0.1329±0.1323	0.018*	0.0539	3.14	29.44	100.5	1411.2	33	38	−1.0
small Lithobiida	Lumbricidae	0.0469±0.1828	0.515	0.0190	3.14	116.45	100.5	4963.2	33	40	−1.6
small Lithobiida	Gamasinae	0.0047±0.0331	0.716	0.0019	3.14	0.28	100.5	3.9	33	12	1.1
small Lithobiida	*P. lugubris*	−0.0407±0.1693	0.446	−0.0166	3.14	17.73	100.5	291.1	33	17	−0.7
small Lithobiida	*Lithobius* sp.	0.0060±0.0206	0.479	0.0025	3.14	101.32	100.5	2838.5	33	27	−1.5
Linyphiidae	*H.nitidus*	−0.0199±0.1087	0.542	−0.0199	4.49	0.10	1.0	174.4	1	1668	1.6
Linyphiidae	*F. candida*	0.1318±0.2037	0.206	0.1318	4.49	0.07	1.0	4056.1	1	60552	1.8
Linyphiidae	juv. Isopoda	−0.0163±0.0808	0.405	−0.0163	4.49	2.43	1.0	346.9	1	143	0.3
Linyphiidae	*O. asellus*	−0.1084±0.1646	0.194	−0.1084	4.49	46.80	1.0	1005.8	1	19	−1.0
Linyphiidae	*P. scaber*	0.0123±0.1548	0.770	0.0123	4.49	31.07	1.0	1646.3	1	43	−0.8
Linyphiidae	Iulidae	−0.0155±0.1212	0.888	−0.0155	4.49	29.44	1.0	1411.2	1	38	−0.8
Linyphiidae	Lumbricidae	0.0098±0.1951	0.929	0.0098	4.49	116.45	1.0	4963.2	1	40	−1.4
Linyphiidae	Gamasinae	0.0103±0.0311	0.505	0.0103	4.49	0.28	1.0	3.9	1	12	1.2
Linyphiidae	small Lithobiida	−0.0309±0.1582	0.445	−0.0309	4.49	3.14	1.0	100.5	1	33	0.2
Linyphiidae	*P. lugubris*	−0.0328±0.1572	0.475	−0.0328	4.49	17.73	1.0	291.1	1	17	−0.6
Linyphiidae	*Lithobius* sp.	0.0657±0.1265	0.147	0.0657	4.49	101.32	1.0	2838.5	1	27	−1.3
Gamasinae	*H.nitidus*	0.0389±0.0785	0.312	0.0051	0.28	0.10	3.9	174.4	12	1668	0.4
Gamasinae	*F. candida*	0.0720±0.1845	0.413	0.0096	0.28	0.07	3.9	4056.1	12	60552	0.6
Gamasinae	juv. Isopoda	−0.0771±0.0753	0.003**	−0.0101	0.28	2.43	3.9	346.9	12	143	−0.9
Gamasinae	*O. asellus*	0.0222±0.2474	0.895	0.0036	0.28	46.80	3.9	1005.8	12	19	−2.2
Gamasinae	*P. scaber*	−0.0391±0.1283	0.562	−0.0043	0.28	31.07	3.9	1646.3	12	43	−2.0
Gamasinae	Iulidae	−0.0358±0.1166	0.580	−0.0050	0.28	29.44	3.9	1411.2	12	38	−2.0
Gamasinae	Lumbricidae	−0.0739±0.1379	0.314	−0.0090	0.28	116.45	3.9	4963.2	12	40	−2.6
Gamasinae	Linyphiidae	−0.0657±0.0843	0.045*	−0.0086	0.28	4.49	3.9	1.0	12	1	−1.2
Gamasinae	small Lithobiida	0.0197±0.1315	0.838	0.0026	0.28	3.14	3.9	100.5	12	33	−1.0
Gamasinae	*P. lugubris*	−0.0855±0.1499	0.150	−0.0112	0.28	17.73	3.9	291.1	12	17	−1.8
Gamasinae	*Lithobius* sp.	0.0718±0.1236	0.098	0.0093	0.28	101.32	3.9	2838.5	12	27	−2.6

Results of model comparison

Table 5.3 – Comparison of models predicting $\log_{10}|\text{per capita } IS_{ij}|$. Top 25 models out of 252, sorted by increasing AIC. Parameters as in Table 5.2. $a-f$ are the coefficients of the model which are fitted by least squares. Coefficients indexed with C take different values for simple and complex communities. ε is the unexplained residual variation (gaussian).

$\log_{10}\lvert pcIS_{ij}\rvert =$	*d.f.*	AIC	ΔAIC	R^2
$a+b\log_{10}m_i+c\log_{10}N_j+d(\log_{10}m_i)^2+e(\log_{10}N_j)^2+\varepsilon$	5	81.587	0.000	0.382
$a+b\log_{10}m_i+c\log_{10}N_j+d(\log_{10}N_j)^2+\varepsilon$	4	82.674	1.087	0.354
$a+b\log_{10}m_i+c\log_{10}N_j+d\log_{10}m_i\cdot\log_{10}N_j+e(\log_{10}m_i)^2+f(\log_{10}N_j)^2+\varepsilon$	6	83.294	1.707	0.384
$a+b\log_{10}m_i+c\log_{10}N_j+d(\log_{10}m_i)^2+\varepsilon$	4	84.119	2.531	0.341
$a+b\log_{10}m_i+c\log_{10}N_j+d\log_{10}m_i\cdot\log_{10}N_j+e(\log_{10}N_j)^2+\varepsilon$	5	84.406	2.819	0.356
$a_C+b_C\log_{10}N_i+c_C\log_{10}R_{ij}+d_C(\log_{10}N_i)^2+\varepsilon$	8	84.466	2.879	0.409
$a_C+b_C\log_{10}m_i+c_C\log_{10}N_j+d_C(\log_{10}m_i)^2+e_C(\log_{10}N_j)^2+\varepsilon$	10	84.747	3.159	0.439
$a+b\log_{10}m_i+c\log_{10}R_{ij}+d(\log_{10}m_i)^2$	4	84.773	3.185	0.334
$a+b\log_{10}B_i+c\log_{10}N_j+d(\log_{10}B_i)^2+e(\log_{10}N_j)^2+\varepsilon$	5	84.782	3.195	0.353
$a+b\log_{10}m_i+c\log_{10}m_j+d(\log_{10}m_i)^2+\varepsilon$	4	84.783	3.196	0.334
$a+b\log_{10}m_i+c\log_{10}N_j+\varepsilon$	3	84.939	3.351	0.313
$a+b\log_{10}B_i+c\log_{10}R_{ij}+d(\log_{10}B_i)^2+\varepsilon$	4	85.240	3.653	0.330
$a+b\log_{10}m_i+c\log_{10}m_j+\varepsilon$	3	85.475	3.888	0.308
$a+b\log_{10}m_i+c\log_{10}R_{ij}+\varepsilon$	3	85.488	3.900	0.308
$a+b\log_{10}R_{ij}+c\log_{10}m_j+\varepsilon$	3	85.585	3.997	0.307
$a+b\log_{10}m_i+c\log_{10}m_j+d(\log_{10}m_i)^2+e(\log_{10}m_j)^2+\varepsilon$	5	85.638	4.050	0.345
$a+b\log_{10}m_i+c\log_{10}N_j+d\log_{10}m_i\log_{10}N_j+e(\log_{10}m_i)^2+\varepsilon$	5	85.983	4.395	0.342
$a+b\log_{10}B_i+c\log_{10}N_j+d\log_{10}B_i\log_{10}N_j+e(\log_{10}B_i)^2+f(\log_{10}N_j)^2+\varepsilon$	6	86.060	4.472	0.360
$a+b\log_{10}R_{ij}+c\log_{10}m_j+d(\log_{10}m_j)^2+\varepsilon$	4	86.202	4.614	0.321
$a+b\log_{10}m_i+c\log_{10}m_j+d(\log_{10}m_j)^2+\varepsilon$	4	86.404	4.816	0.319
$a+b\log_{10}m_i+c\log_{10}N_j+d\log_{10}m_i\log_{10}N_j+e(\log_{10}m_i)^2+f(\log_{10}N_j)^2+\varepsilon$	12	86.568	4.981	0.457
$a+b\log_{10}m_i+c\log_{10}R_{ij}+d(\log_{10}m_i)^2+e(\log_{10}R_{ij})^2+\varepsilon$	5	86.686	5.099	0.335
$a+b\log_{10}m_i+c\log_{10}R_{ij}+d\log_{10}m_i\log_{10}R_{ij}+e(\log_{10}m_i)^2+\varepsilon$	5	86.751	5.164	0.335
$a+b\log_{10}m_i+c\log_{10}m_j+d\log_{10}m_i\log_{10}m_j+e(\log_{10}m_i)^2+\varepsilon$	5	86.761	5.174	0.334
$a+b\log_{10}m_i+c\log_{10}R_{ij}+d\log_{10}m_i\log_{10}R_{ij}+\varepsilon$	4	86.776	5.189	0.315

Table 5.4 – The most parsimonious model from Table 5.3 predicts $\log_{10}|\text{per capita } IS_{ij}|$ by the predator body mass, m_i, and by the target species population density, N_j.

	Estimate	Std. Error	t-value	p
intercept	−1.472	0.366	−4.018	< 0.001***
$\log_{10}m_i$	0.151	0.109	1.383	0.172
$\log_{10}N_j$	−0.497	0.287	−1.730	0.088.
$(\log_{10}m_i)^2$	0.114	0.067	1.712	0.092.
$(\log_{10}N_j)^2$	0.097	0.047	2.085	0.041*

Table 5.5 – Comparison of models predicting per capita IS_{ij} . Parameters and coefficients as in Table 5.3.

$pcIS_{ij}$ =	*d.f.*	AIC	ΔAIC	R^2
$a_C + b_C \log_{10} m_i + c_C \log_{10} N_j + d_C \log_{10} m_i \log_{10} N_j + e_C (\log_{10} m_i)^2 + f_C \log_{10} N_j)^2 + \varepsilon$	12	−248.113	0.000	0.595
$a_C + b_C \log_{10} m_i + c_C \log_{10} N_j + d_C \log_{10} m_i \log_{10} N_j + e_C (\log_{10} N_j)^2 + \varepsilon$	10	−247.915	0.198	0.570
$a_C + b_C \log_{10} m_i + \log_{10} N_j + \log_{10} m_i \log_{10} N_j + \varepsilon$	8	−247.277	0.835	0.541
$a_C + b_C \log_{10} m_i + c \log_{10} N_j + d_C \log_{10} m_i \log_{10} N_j + e_C (\log_{10} m_i)^2 + \varepsilon$	10	−247.049	1.063	0.565
$a_C + b_C \log_{10} R_{ij} + c_C \log_{10} B_j + d_C \log_{10} R_{ij} \log_{10} B_j + e_C (\log_{10} R_{ij})^2 + \varepsilon$	10	−235.750	12.362	0.489
$a_C + b_C \log_{10} R_{ij} + c_C \log_{10} m_j + d_C \log_{10} R_{ij} \log_{10} m_j + \varepsilon$	8	−234.505	13.608	0.449
$a_C + b_C \log_{10} R_{ij} + c_C \log_{10} B_j + d_C \log_{10} R_{ij} \log_{10} B_j + e_C (\log_{10} R_{ij})^2 + f_C (\log_{10} B_j)^2 + \varepsilon$	12	−234.278	13.835	0.507
$a_C + b_C \log_{10} R_{ij} + c_C \log_{10} B_j + d_C (\log_{10} R_{ij})^2 + \varepsilon$	8	−233.710	14.402	0.443
$a_C + b_C \log_{10} m_i + c_C \log_{10} R_{ij} + d_C (\log_{10} m_i)^2 + e_C (\log_{10} R_{ij})^2 + \varepsilon$	10	−233.040	15.073	0.469
$a_C + b_C \log_{10} B_i + c_C \log_{10} N_j + d_C \log_{10} B_i \log_{10} N_j + e_C (\log_{10} B_i)^2 + f_C (\log_{10} N_j)^2 + \varepsilon$	12	−232.440	15.673	0.494
$a_C + b_C \log_{10} R_{ij} + c_C \log_{10} m_j + d_C (\log_{10} R_{ij})^2 + \varepsilon$	8	−232.349	15.764	0.432
$a_C + b_C \log_{10} m_i + c_C \log_{10} R_{ij} + d_C (\log_{10} R_{ij})^2 + \varepsilon$	8	−232.233	15.880	0.431
$a_C + b_C \log_{10} B_i + c_C \log_{10} N_j + d_C \log_{10} B_i \log_{10} N_j + e_C (\log_{10} B_i)^2 + \varepsilon$	10	−232.149	15.964	0.462
$a_C + b_C \log_{10} B_i + c_C \log_{10} N_j + d_C \log_{10} B_i \log_{10} N_j + \varepsilon$	8	−231.715	16.398	0.427
$a_C + b_C \log_{10} B_i + c_C \log_{10} N_j + d_C \log_{10} B_i \log_{10} N_j + e_C (\log_{10} N_j)^2 + \varepsilon$	10	−231.562	16.550	0.457
$a_C + b_C \log_{10} B_i + c_C \log_{10} R_{ij} + d_C (\log_{10} B_i)^2 + e_C (\log_{10} R_{ij})^2 + \varepsilon$	10	−231.505	16.607	0.457
$a_C + b_C \log_{10} R_{ij} + c_C \log_{10} m_j + d_C \log_{10} R_{ij} \log_{10} m_j + e_C (\log_{10} m_j)^2 + \varepsilon$	10	−231.382	16.730	0.456
$a_C + b_C \log_{10} R_{ij} + c_C \log_{10} m_j + d_C \log_{10} R_{ij} \log_{10} m_j + e_C (\log_{10} R_{ij})^2 + \varepsilon$	10	−231.301	16.811	0.455
$a_C + b_C \log_{10} m_i + c_C \log_{10} m_j + d_C \log_{10} m_i \log_{10} m_j + e_C (\log_{10} m_j)^2 + \varepsilon$	10	−231.273	16.840	0.455
$a_C + b_C \log_{10} m_i + c_C \log_{10} R_{ij} + d_C \log_{10} m_i \log_{10} R_{ij} + e_C (\log_{10} R_{ij})^2 + \varepsilon$	10	−231.216	16.896	0.455
$a_C + b_C \log_{10} N_j + \varepsilon$	4	−231.109	17.004	0.352
$a_C + b_C \log_{10} m_i + c_C \log_{10} N_j + \varepsilon$	6	−231.042	17.070	0.387
$a_C + b_C \log_{10} R_{ij} + c_C (\log_{10} R_{ij})^2 + \varepsilon$	6	−230.817	17.296	0.385
$a_C + b_C \log_{10} R_{ij} + c_C \log_{10} m_j + d_C \log_{10} R_{ij} \log_{10} m_j + e_C (\log_{10} R_{ij})^2 + f_C (\log_{10} m_j)^2 + \varepsilon$	12	−230.785	17.327	0.482
$a_C + b_C \log_{10} N_j + c_C (\log_{10} N_j)^2 + \varepsilon$	6	−230.578	17.535	0.383

Table 5.6 – The most parsimonious model from Table 5.5 predicts per capita IS_{ij} by complexity C, body mass m_i and popul. density N_j.

	Estimate	Std. Error	*t*-value	*p*
C = simple				
intercept	−0.107	0.068	−1.576	0.121
$\log_{10} m_i$	0.004	0.021	0.205	0.838
$\log_{10} N_j$	0.057	0.036	1.577	0.120
$(\log_{10} m_i)^2$	−0.016	0.009	−1.860	0.068.
$(\log_{10} N_j)^2$	−0.010	0.006	−1.706	0.093.
$\log_{10} m_i \log_{10} N_j$	0.000	0.007	0.018	0.986
C = complex				
intercept	0.032	0.049	0.664	0.509
$\log_{10} m_i$	−0.067	0.021	−3.237	0.002**
$\log_{10} N_j$	−0.034	0.038	−0.897	0.373
$(\log_{10} m_i)^2$	−0.003	0.008	−0.356	0.723
$(\log_{10} N_j)^2$	0.007	0.006	1.201	0.235
$\log_{10} m_i \log_{10} N_j$	0.030	0.006	4.690	< 0.001***

Chapter 6.

Climate-induced changes in bottom-up and top-down processes independently alter a marine ecosystem

Malte Jochum, Florian D. Schneider, Tasman P. Crowe, Ulrich Brose, Eoin J. O'Gorman

Abstract

Climate change has complex structural impacts on coastal ecosystems. Global warming is linked to a widespread decline in body size, while increased flood frequency can amplify nutrient enrichment through enhanced run-off. Altered population body-size structure represents a disruption in top-down control, while eutrophication embodies a change in bottom-up forcing. These processes are typically studied in isolation and little is known about their potential interactive effects. Here, we present the results of an in situ experiment examining the combined effects of top-down and bottom-up forces on the structure of a coastal marine community. Reduced average body mass of the top predator (the shore crab, *Carcinus maenas*) and nutrient enrichment combined additively to alter mean community body mass. Nutrient enrichment increased species richness and overall density of organisms. Reduced top-predator body mass increased community biomass. Additionally, we found evidence for an allometrically-induced trophic cascade. Here, the reduction in top-predator body mass enabled greater biomass of intermediate fish predators within the mesocosms. This in turn suppressed key micrograzers, which led to an overall increase in microalgal biomass. This response highlights the possibility for climate-induced trophic cascades, driven by altered size structure of populations, rather than species extinction.

Keywords | multiple stressors, trait-mediated, functional trait, European green crab, Lough Hyne, biodiversity.

Introduction

Ecosystems are being affected by climate change in many ways. The physical environment is being altered by changes in means and variation in temperature, UV radiation and precipitation (IPCC Core Writing Team *et al.*, 2007), with increased frequency of extreme events likely to have some of the greatest effects (Gaines and Denny, 1993). The fact that organisms are responding with changes in distribution and phenology has now been well documented (Parmesan *et al.*, 2003). More recently, it has emerged that there is also a trend for reduced body size in response to climate change (Daufresne *et al.*, 2009; Gardner *et al.*, 2011; Sheridan and Bickford, 2011). Community interactions, food webs and ecosystem processes are very likely to be disrupted by these changes, but relevant experimental evidence is limited. Although there has been considerable research on responses to aspects of climate change by individual species, much less work has been carried out on the combined effects of multiple aspects of climate change at higher levels of biological organisation, capturing the complex changes in abiotic and biotic variables that will arise (Harley *et al.*, 2006; Montoya and Raffaelli, 2010).

In freshwater, estuarine and coastal marine ecosystems, another key impact of climate change will be the increased frequency of extreme precipitation events (Van De Pol *et al.*, 2010). Resultant flooding can bring about an intensified input of terrestrially derived contaminants such as biocides and nutrients, which imposes stress on aquatic ecosystems. This can lead to marked changes in productivity, modifying ecosystems via impacts on diversity, community structure and stability (Bonsdorff *et al.*, 1997; Smith *et al.*, 1999; Petchey *et al.*, 1999). Eutrophication has even been linked to decreasing mean body size in marine communities (Beukema, 1991), which should decrease community stability (Brose *et al.*, 2006*a*; Otto *et al.*, 2007) and severely modify the strength of species interactions (Berlow *et al.*, 2009). In a theoretical study in this theme issue, Binzer et al. show that an increase in consumer body mass and warming synergistically buffer the consequences of nutrient enrichment (Binzer *et al.*, 2012). Thus, not only is climate change itself multi-faceted, but it influences systems that are also being affected by a wide range of local stressors (Halpern *et al.*, 2008). In developing strategies to minimise and offset the impacts of climate change, it is vital that we improve understanding of how multiple global and local stressors combine to influence ecosystems (Crain *et al.*, 2008). In this way, management interventions can be targeted to localised pressures which, when magnified by climate change, would have greatest impact and whose reduction would therefore be most beneficial. Given the degree of complexity involved, it is vital that generalities are identified that can guide decisions where specific data are not available.

Ecosystems can be bottom-up controlled through nutrient availability or top-down controlled through predation and consumer effects (Power, 1992). The impacts of individual species loss can therefore cascade through food webs, secondarily affecting species further up or down the food chain (Estes *et al.*, 1998; Byrnes *et al.*, 2006; Berlow *et al.*, 2009) and sometimes inducing

major regime shifts (Daskalov *et al.*, 2007). Such cascades have been found in a variety of ecosystems (Borer *et al.*, 2005) and tend to be stronger if larger species from higher trophic levels are lost (Estes *et al.*, 1998; Berlow *et al.*, 2009). Thus, the interaction of altered top-down forcing, driven by the loss of large top predators, and bottom-up processes, driven by energy supplements to the basal resources, may play an important role in determining community structure and dynamics (Borer *et al.*, 2006).

Climatic stressors do not lead to instantaneous species extinctions but take effect gradually and indirectly, as reviewed by Brose et al. (2012). Metabolic rates are very sensitive to increased temperature (Ehnes *et al.*, 2011) and as a consequence warming also modifies feeding and interaction strengths (Rall *et al.*, 2010; Vucic-Pestic *et al.*, 2011; Rall *et al.*, 2012; Twomey *et al.*, 2012), imposes demographic changes (Parmesan *et al.*, 2003), and alters population size structure (Daufresne *et al.*, 2009; Gardner *et al.*, 2011; Sheridan and Bickford, 2011; Yvon-Durocher *et al.*, 2011) and linkages to other populations (Petchey, 2010). Investigating the effects of gradual changes in predator population size structure, in contrast to their complete removal, is therefore needed to provide a higher resolution of insight into top-down mechanisms.

Bottom-up and top-down forces have typically only been studied in isolation, but there have been attempts to disentangle their effects (e.g. Hunter and Price, 1992; Rall *et al.*, 2012; Greig *et al.*, 2012) and some interactions between them have been shown (Worm *et al.*, 2002; Shurin *et al.*, 2012). An improved understanding of interactions between bottom-up and top-down processes could provide a basis for generalisations in assessing impacts of different elements of climate change combined with local stressors. Thus, in the current study, we aim to disentangle the individual and combined (additive, synergistic or antagonistic) effects of nutrient availability (bottom-up) and the size structure of predatory crab populations (top-down) in a marine ecosystem on mean community body mass, abundance and biomass (all three parameters averaged across all species except the manipulated crabs), species richness and the biomass and abundance of individual taxa from all trophic levels in the community.

Methods

The study was conducted at Lough Hyne, a highly sheltered marine nature reserve in southwest Ireland (`N 51°29'52' W 9°17'46'`), from July 29th to September 16th, 2011. Due to its biological and physical conditions, Lough Hyne is well suited to experimental work and is broadly representative of temperate, shallow-water Atlantic communities (see O'Gorman *et al.*, 2010 and references therein). An experiment was established, with cages measuring 42 × 41 × 10 cm and a mesh width of approximately 7 mm. The cages were loaded with 5 kg of 1–2 cm gravel at the outset and situated in the shallow subtidal of a bay with weak current on the south shoreline of Lough Hyne. Two blocks were set up at a depth of 1 m and two blocks at a depth of 1.5 m at low tide (tidal range being approximately 1 m). The distance between any two cages was

at least 2.5 m to reduce the likelihood of confounding factors. Two experimental factors were manipulated in a full-factorial design: (1) "bottom-up treatments" in which fertiliser pellets were added to cages to yield an enriched nutrient level compared to cages with ambient levels; (2) "top-down treatments" in which the body mass of the top predator was altered by placing populations with small, medium and large average body mass into the cages, plus a control without predators. Each treatment was replicated four times in randomised blocks, yielding a total of 32 cages.

Bottom-up treatments

Nutrient enrichment was achieved by placing a mesh bag filled with 500 g of plant fertiliser pellets (Scotts Miracle-Gro® Osmocote slow release all purpose plant food: NPK(Mg), 17:9:11(:2) %) in each cage. This quantity was chosen based on the successful application of nutrient enrichment in previous marine research (Atalah and Crowe, 2010). Identical mesh bags containing 500 g of gravel, were placed in the cages with ambient nutrient levels to avoid procedural confounding. The nutrient enrichment was validated by water samples taken two weeks after the start of the experiment. Herein, the total nitrogen content of ambient (n = 16) and enriched (n = 16) cages differed significantly (two tailed t-test: $t = 3.632$, $df = 15.4$, $p = 0.002$). The ambient cages also did not differ from background samples (n = 4), taken from several locations further along the shore (two tailed t-test, $t = -0.456$, $df = 4.4$, $p = 0.671$).

Top-down treatments

The European green crab or shore crab, *Carcinus maenas*, which is native to Lough Hyne, was chosen as the top predator in the experiment. *C. maenas* expresses very high abundance and covers a wide range of individual body sizes. It is an aggressively competing omnivore with a wide tolerance for many environmental factors (Klassen and Locke, 2007). This flexibility may reflect a special aptitude in adjusting individual growth, reproduction rate and population size structure gradually to temperature and other external stressors, as demonstrated for the similarly dominant Portunid blue crab, *Callinectes sapidus* (Fisher, 1999). Originating from Europe and North Africa, *C. maenas* has invaded rocky shores all over the world and threatens to outcompete many native species (Klassen and Locke, 2007). Hence, its ecological impacts on other species are of the utmost interest. Thus, *C. maenas* is a suitable experimental organism to simulate changes in population size structure as caused by warming.

Individual body mass of *C. maenas* was calculated using a carapace-width to fresh-weight relationship from the study site (O'Gorman and Emmerson, 2010). Both male and female individuals were used in the experiment, although crabs parasitised by the rhizocephalan *Sacculina carcini* were excluded. The top-down manipulation comprised four levels, one control without crabs and three body size classes: small (S), medium (M) and large (L), initiated

with average body masses, M_C, of M_{CS} = 6.00 g (range from 1.86 to 16.68 g), M_{CM} = 12.93 g (3.60 – 39.01 g), M_{CL} = 24.48 g (8.18 – 72.29 g). These were achieved by employing an allometric design (see Schneider *et al.*, 2012 and supplementary material on page 120). The established densities of *C. maenas*, N_C, were assumed to depend on the average population body mass following an allometric power law (figure 6.3 in supplementary material). This yielded differing densities in the three treatments (N_{CS} = 10, N_{CM} = 7 and N_{CL} = 6) which represent a trade-off between fixing the biomass or abundance of the crabs over all treatments. The average top-predator body mass increased slightly during the experiment due to individual growth and higher crab mortality of smaller crabs. The latter was most likely caused by cannibalism. Out of 184 crabs introduced to the experiment, 112 crabs survived until the end. The final body size distribution of crabs for each cage still largely reflected the initial distribution (figure 6.3 in supplementary material).

Note that while the body size classes of *C. maenas* used in this experiment probably represent different ontogenetic stages in their growth, gut content analysis carried out on the crabs at the end of the experiment suggests that the taxonomic composition of the diet was largely similar across the size classes (see table 6.2 in supplementary material). Instead, the variation in *C. maenas* body size determines the optimal foraging niche, with different taxonomic groups representing a greater proportion of the diet for different size classes of crabs (most likely related to strength of the chelae, mobility and intimidating presence).

Measuring response variables

To sample small invertebrate species, each cage was supplied with a settlement pad attached to its ground mesh (red plastic pot scourer, polyamide, approximately 7.5 × 6 × 3.5 cm). Pot scourers are commonly used to sample mobile benthic invertebrates (see O'Gorman *et al.*, 2008 and references therein). At the end of the experiment, contents of the settlement pads were flushed through a fine laboratory test sieve (250 μm). Larger animals were collected from each cage by hand and stored in ethanol. All animals were identified and counted. Sessile species were counted within an area of 10 × 10 cm on the inside roof of the cages (*Janua pagenstecheri* and *Pomatoceros triqueter*) or on the entire inside roof (*Ascidiella aspersa*). In total, 33,843 individuals from 119 taxa were extracted from the cages. 93 taxa were identified to species level (see table 6.3 in supplementary material for details). Up to 25 individuals per species and cage were measured for body-mass estimates using vernier callipers or a glass micrometer (50 mm in 0.1 mm divisions). Individual lengths were converted to body masses using length to dry-weight relationships (O'Gorman and Emmerson, 2010). Where species-specific length-weight relationships were not available, relationships of the closest relative species or a similarly shaped species were assumed. Dry weights were transformed to fresh weights by multiplying by a factor of four (Peters, 1983). For *C. maenas*, *Gobiusculus flavescens*, *Marthasterias glacialis*,

Palaemon serratus and *Pomatoschistus pictus*, lengths were directly calculated to fresh weight due to available length-fresh weight relationships. To unify the different methods of sampling (pot scourers, direct sampling and counting), population densities were scaled to number of individuals per square meter. Population biomass (g m^{-2}) was calculated by multiplying the average species body mass by population density. The chlorophyll content of microalgae was quantified on glass microscope slides (5.5 × 2.6 cm) hanging from the lid of the cage. Here, standardized acetone extraction was applied (Parsons *et al.*, 1984) and the concentration of chlorophyll in the extract was measured.

Statistical analyses

Statistical data processing was performed with R 2.14.0 (R Development Core Team, 2011). The effect of the top-predator body mass and fertilisation was tested on the following response parameters: number of species, S, within each cage (subsequently termed species richness); total community biomass density, B (g m^{-2}); total community individual density, N (ind. m^{-2}), and average community body mass, M (g $ind.^{-1}$) of all individuals in the cage. Furthermore, we examined the change in biomass and abundance of every functional species (i.e. taxonomic species or grouping of species that carry out similar functional roles in the system) in the experiment in response to the bottom-up and top-down treatments. Finally, microalgal chlorophyll was tested as a proxy for primary production. The aim here was to determine whether a trophic cascade permeated through the animal community to alter the standing stock of microalgae in the system. Linear mixed effects models (Pinheiro *et al.*, 2011; Zuur *et al.*, 2009) were employed to describe this set of response parameters, accounting for experimental block as a random factor. The average body mass of the predator population, $M_C^{'}$, the presence or absence of fertiliser in the cage, *Nut* , and the interaction of both were used as explanatory parameters (fixed effects). For the continuous parameter $M_C^{'}$, the mean of the top-predator body mass at the beginning and at the end of the experiment were averaged for each replicate. The binary parameter *Nut* was given a value of 0 for ambient nutrient level and 1 for enriched nutrient level. For species densities and biomasses with zeros in some replicates, a value of one was added to all replicates. All response parameters were $\log_{10}$-transformed to meet the assumptions of normality and homogeneity of variance.

Results

The linear models did not indicate any significant interaction between nutrient enrichment and average top-predator body mass in affecting the response parameters (table 6.1, $Nut : M_C^{'}$; $p > 0.05$, Wald F-test). The average community body mass, M, was additively affected by top-down and bottom-up treatments. It responded positively to decreasing top-predator body mass

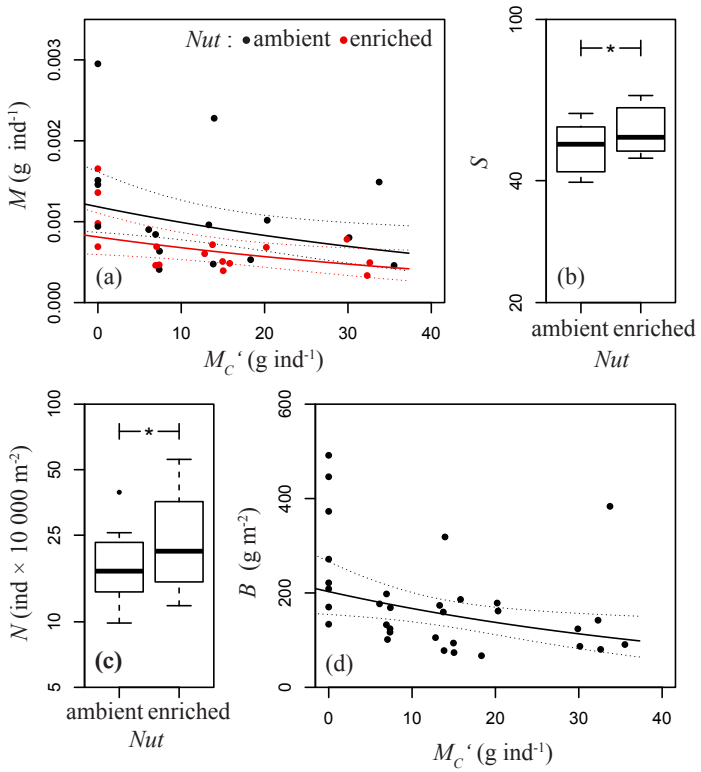

Figure 6.1 – The average body mass of the top predator (*C. maenas*), $M_C^{'}$, and nutrient addition, *Nut* (highlighted in red), had (a) additive effects on average individual body mass M of all other species; $\log_{10} M = -2.927(\pm 0.066 SE) - 0.008(\pm 0.003) \cdot M_C^{'} - 0.165(\pm 0.072) \cdot Nut$. Addition of nutrients had a significant effect on (b) species richness S, $\log_{10} S = 1.683(\pm 0.016) + 0.041(\pm 0.017) \cdot Nut$, and (c) total individual density N, $\log_{10} N = 5.251(\pm 0.054) + 0.112(\pm 0.043) \cdot Nut$; * $p < 0.05$ (F-test on simplified mixed effect model with only Nut as explanatory variable). Predator body mass affected (d) total biomass B, $\log_{10} B = 2.307(\pm 0.058) - 0.008(\pm 0.003) \cdot M_C^{'}$. (a) and (d) linear models on $\log_{10}$-transformed response variables with 95% confidence bands. Response variables were corrected for the random effect of experimental block.

(table 6.1, x-axis in figure 6.1*a*, $p = 0.026$) and negatively to nutrient enrichment (table 6.1, black *vs* red points in figure 6.1*a*, $p = 0.033$). Nutrient enrichment caused a significant increase in species richness, S, (table 6.1, figure 6.1*b*, $p = 0.023$) and the overall density of individuals, N, (table 6.1, figure 6.1*c*, $p = 0.019$). There was no significant effect of top-predator body mass on either species richness or density. The reduction in top predator body mass caused a significant increase in the overall biomass density of the community, B, (table 6.1, figure 6.1*d*, $p = 0.023$). There was no significant effect of nutrient enrichment on overall biomass.

A number of key functional species were significantly affected by decreasing top-predator body mass, which is strictly coupled to a decrease in biomass (figure 6.2*a*). The biomass density of the order Perciformes increased significantly with decreasing top-predator body mass (table 6.1, figure 6.2*b*, $p = 0.005$). Here, the Perciformes comprise the painted goby, *P. pictus* and two-spot goby, *G. flavescens*. The two most prominent meiofaunal micrograzers in the system,

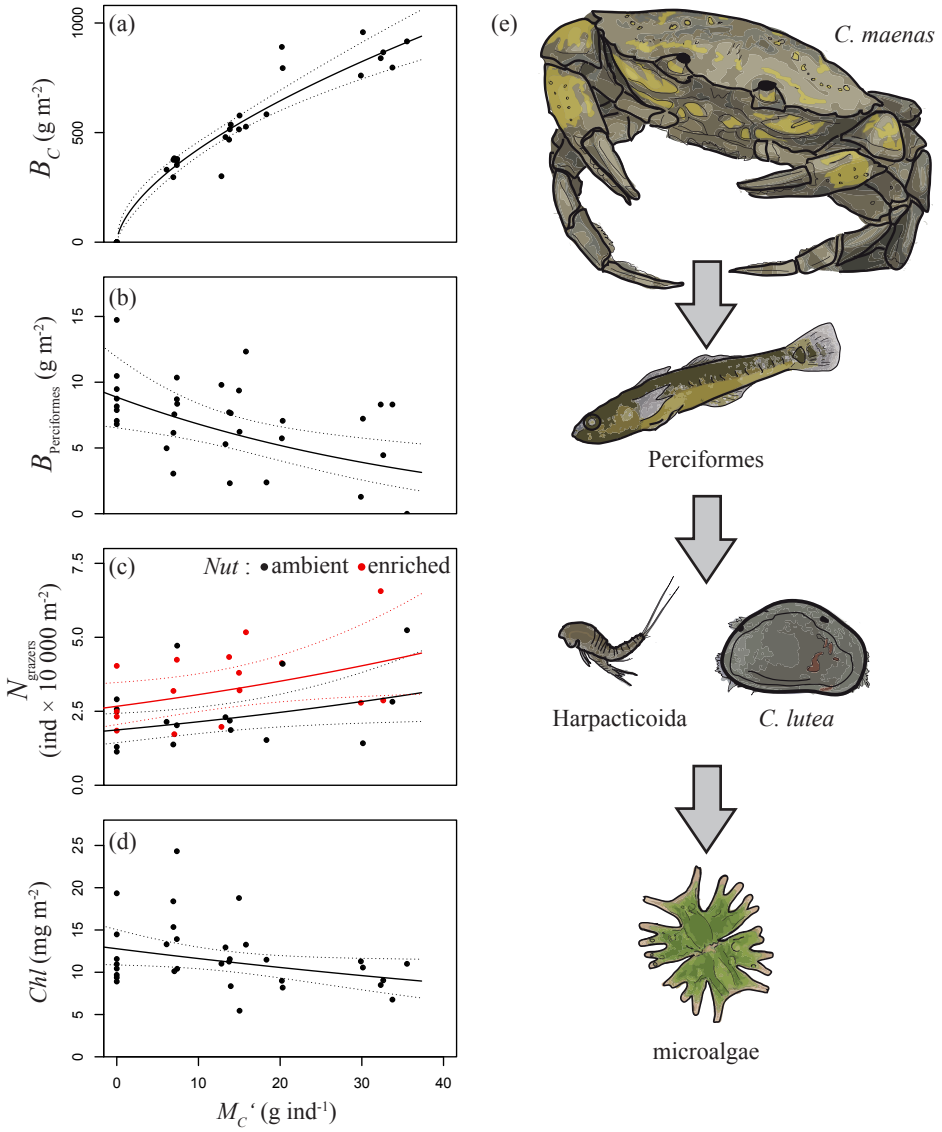

Figure 6.2 – Allometric trophic cascade. With an increase in average body mass of the top predator (*C. maenas*), $M_C^{'}$, (a) its biomass, B_C, increased following an allometric power law, $B_C = 2.02 \cdot M_C^{'0.60}$. In consequence, (b) the group of Perciformes decreased in biomass, $\log_{10}(B_{Perciformes}+1) = 0.994(\pm 0.057 SE) - 0.01(\pm 0.003) \cdot M_C^{'}$, (c) the predominant mobile grazers, *C. lutea* and the crustacean order of Harpacticoida, increased in population density (and also as a consequence of nutrient addition) $\log_{10} N_{grazers} = 4.269(\pm 0.056) + 0.006(\pm 0.003) \cdot M_C^{'} + 0.155(\pm 0.058) \cdot Nut$, and (d) the chlorophyll concentration of microalgal biofilm on glass slides decreased, $\log_{10} Chl = 1.107(\pm 0.035) - 0.004(\pm 0.002) \cdot M_C^{'}$. Response variables were corrected for the random effect of experimental block. Lines show back-transformed, log-linear models with 95% confidence bands. (e) Hypothesized trophic cascade.

Table 6.1 – Wald F-tests for linear mixed effect models to describe response parameters. Top-predator body mass, $M_C^{'}$, as continuous and nitrogen fertiliser, *Nut* , as binary fixed effects (inserted sequentially). Treatment block is taken into account as a random effect. The community response variables are: average community body mass, M, species richness, S, overall density of individuals, N, and overall biomass density, B. Population response variables are: the biomass density of Perciformes, the individual density of meiofaunal micrograzers, and the chlorophyll concentration on glass slides. p-values are the likelihood for a parameter to equal zero. $Nut : M_C^{'}$ is the test for an interactive effect of both explanatory parameters.

	$\log_{10} M$(g m^{-2})		$\log_{10} S$		$\log_{10} N$ (ind. m^{-2})		$\log_{10} B$ (g m^{-2})	
	F-value	p-value	F-value	p-value	F-value	p-value	F-value	p-value
(Intercept)	7217.654	<0.001 ***	17013.970	<0.001 ***	11541.500	<0.001 ***	3201.263	<0.001 ***
Nut	5.112	0.033 *	5.880	0.023 *	6.256	0.019 *	0.479	0.495
$M_C^{'}$	5.593	0.026 *	0.089	0.768	0.162	0.690	5.903	0.023 *
Nut:$M_C^{'}$	0.251	0.621	0.438	0.514	0.043	0.837	0.122	0.730

	$\log_{10} B_{\text{Perciformes}} + 1$ (g m^{-2})		$\log_{10} N_{\text{grazer}}$ (ind. m^{-2})		$\log_{10}$ chlorophyll (mg m^{-2})	
	F-value	p-value	F-value	p-value	F-value	p-value
(Intercept)	543.221	<0.001 ***	17061.320	<0.001 ***	2194.009	<0.001 ***
Nut	2.661	0.115	6.939	0.014 *	1.246	0.275
$M_C^{'}$	9.433	0.005 **	5.493	0.027 *	4.286	0.049 *
Nut:$M_C^{'}$	0.030	0.864	0.001	0.975	0.987	0.330

Numerator degrees of freedom, *d.f.* = 1; denominator *d.f.* = 25; F- and p-values for Wald tests; * $p < 0.05$; ** $p < 0.01$; *** $p < 0.001$

harpacticoid copepods and the dominant ostracod, *C. lutea*, showed a reduction in individual density with decreasing top-predator body mass (table 6.1, x-axis in figure 6.2*c*, $p = 0.027$), while being additively increased by nutrient enrichment (table 6.1, black *vs* red points in figure 6.2*c*, $p = 0.014$). Chlorophyll concentration also increased significantly with decreasing top-predator body mass (table 6.1, figure 6.2*d*, $p = 0.049$). These three organism groups represent a trophic cascade following altered top-predator body mass (figure 6.2*e*). The decreasing biomass of the apex predator, *C. maenas*, released the intermediate predator order, Perciformes, which increased in biomass. These fish predators then fed down on the harpacticoid copepods and the ostracod *C. lutea*, suppressing their population density. Finally, the decline of these micrograzers resulted in the increased standing stock of microalgae (represented by an increased concentration of chlorophyll) at the bottom of the food web.

Discussion

We employed a field experiment investigating the effects of nutrient enrichment and altered top-predator population size structure, two major stressors resulting from a combination of climatic and anthropogenic impacts. We found evidence for bottom-up and top-down forces driving different parts of the benthic community. The species richness and overall density of individual organisms increased, while mean community body mass decreased with nutrient enrichment. Community biomass and mean community body mass increased with decreasing

top-predator body mass. The data do not support an interaction of bottom-up and top-down forces for any response parameter. Mean community body mass and micrograzer abundance responded to both nutrient enrichment and altered top-predator body mass, revealing the additive nature of both stressors. Interestingly, a four-level trophic cascade driven by altered top-predator body mass suggests that shifts in population size structure, as induced by climate change, can have severe consequences across trophic levels. Our study documents a gradual effect of altered population size structure on community structure, which takes effect prior to rigorous extinction. We anticipate that this simulates the indirect effects on communities after gradual warming and echoes the effects of warming described by Brose *et al.* (2012) and Shurin *et al.* (2012).

Previous research on trophic cascades has focused on the potential for extinction or changes in the population abundance of top predators to alter the subsequent trophic levels (reviewed by Heithaus *et al.*, 2008). Here, we demonstrate that changes in the body size structure of an apex predator population have the capacity to bring about a cascade of alterations in the biomass or abundance of other key groups (see figure 6.2). A reduction in the mean body mass of *C. maenas* increased the biomass of the next lower trophic level, the intermediate predators comprised by two small gobies of the order Perciformes in this experiment (O'Gorman *et al.*, 2010). Given that Perciformes do not form a large part of the diet of the crabs in this experiment (see table 6.2), this effect is most likely mediated by behavioural interactions. For example, competition and fear of predation often lead to effects that are even stronger than direct consumption (Werner and Peacor, 2003). Additionally, the Perciformes have previously been shown to avoid predators and aggregate in areas where risk of predation is reduced (O'Gorman *et al.*, 2008). As the biomass of the Perciformes increased, they suppressed the abundance of key meiofaunal micrograzers. Harpacticoid copepods and phytal ostracods like *C. lutea* are recognised as the most important consumers of microalgae in marine systems (Montagna *et al.*, 1995; Carman *et al.*, 1997; Ólafsson *et al.*, 1999). They often feed above the benthos through filter feeding (De Troch *et al.*, 2005) and grazing of epiphytic biofilms (Buffan-Dubau and Carman, 2000; De Troch *et al.*, 2008). Both taxa are also observed prey of Perciformes in the Lough Hyne system (O'Gorman *et al.*, 2010). Finally, as micrograzer abundance was suppressed, the standing stock of microalgal biomass increased, as observed through the higher concentration of chlorophyll. Crucially, this allometrically-induced trophic cascade simulates the expected response of natural predator communities to the effects of global warming (Daufresne *et al.*, 2009; Gardner *et al.*, 2011; Sheridan and Bickford, 2011; Brose *et al.*, 2012; Shurin *et al.*, 2012). We caution that, as in most studies on trophic cascades, the described cascading effect on biomass densities is phenomenological only and not corroborated by observations of direct feeding or indirect interactions. However, direct feeding data of the top predator obtained by stomach content analyses (see table 6.2) support our interpretation. Overall, our results suggest that warming-induced reductions in top predator body mass may cascade to lower trophic levels, profoundly affecting ecosystem functions.

Average community body mass scaled negatively with nutrient enrichment and positively with decreasing top-predator body mass, exhibiting a cumulative effect of bottom-up and top-down forces (see figure 1*a*). The top-down effect on average community body mass is most likely driven by the ability of the apex predator to suppress the next trophic level below, either through direct consumption or trait-mediated indirect interactions (O'Gorman *et al.*, 2008; Werner and Peacor, 2003). Given that body size is correlated with trophic height (Brose *et al.*, 2012; Digel *et al.*, 2011; Riede *et al.*, 2011), this next trophic level should consist of predators intermediate in size to the apex crabs and the primary consumers in the system. As the size structure of the apex predator shrinks, it exerts increasingly less control over the intermediate predators, thus promoting a community dominated by larger intermediate predators, as observed by the trophic cascade in the system (see figure 6.2*b*). Allometric diet-breadth theory (Petchey *et al.*, 2008*a*) suggests that the intermediate predators may in turn shift the size distribution of the primary consumers towards smaller body mass. But given the large disparity in size between intermediate predators such as the fish in this study and the invertebrate primary consumers (e.g. copepods, ostracods, snails and bivalves), the cumulative effect is an overall increase in mean community body mass with decreasing top-predator body mass (see figure 6.1*a*) and a coincident increase in total community biomass (see figure 6.1*d*), which is consistent with prior studies (Daufresne *et al.*, 2009; Shurin *et al.*, 2012). Further experimentation would be required, however, to determine if this is just a short-term effect that may be ameliorated over time or change during seasons (Shurin *et al.*, 2012).

The negative bottom-up effect of nutrient enrichment on mean community body mass is less intuitive. The key to understanding the underlying mechanism centres on the increased species richness and density of organisms in the system (figure 6.1*b*-*c*). Consistent with meta-analyses (Borer *et al.*, 2006), bottom-up supply caused the arrival of more grazer species and an increase in the abundance of micrograzers (figure 6.2*c*). It is likely that the influx of nutrients to the system promoted increased primary production (similar to Harding and Perry, 1997). Although the standing stock of chlorophyll in the cages remained constant in response to nutrient enrichment, the increased diversity and abundance of grazers most likely channelled the additional energy rapidly through the system via intense grazing pressure (Alpine and Cloern, 1992). Indeed, harpacticoid copepods and ostracods have been shown to exponentially increase grazing rates in response to increased microalgal availability (Montagna *et al.*, 1995). The increased number and abundance of these small primary consumers in response to nutrient addition thus lowered the mean body size of the community. This prevented an overall increase in community biomass with nutrient enrichment, as might be expected from previous research (Beukema, 1991). Perhaps with a longer duration of study or a system unconstrained by cage structures, the energy supplement from the grazer community would sustain more higher trophic-level (i.e. larger) animals, thus increasing mean community body size and total biomass.

Conclusion

Our data highlight how global change might alter community dynamics in marine ecosystems by providing new insight into mechanisms of bottom-up and top-down control and their relationship and relative importance under climate-change scenarios. Nutrient enrichment seems to control the food web via a diversity-abundance channel, while top-predator body mass affects overall biomass and community structure. The allometrically-induced trophic cascade described here highlights how changes to the body-size structure of top predators can lead to severe consequences for the whole food web below, thus illustrating the concept of thermal top-down cascades. In a similar way, changes in prey population size structure are likely to trigger bottom-up cascading effects on the predators of the focal species. Alterations of this kind are highly likely to be mediated by climatic changes in the coming years. It is therefore of great interest to look beyond removal experiments and further investigate the impacts of altered population size structure. This will lead to a new quality of predictions about the gradual consequences of growing numbers of climate- and human-induced stressors to ecosystems. The interrelation of bottom-up and top-down forces is further influenced and complicated by additional stressors. Therefore, it is of major importance to investigate ecosystem responses to multiple stressors, including natural and anthropogenic sources of disturbance. Recent findings suggest that research into multiple stressors must take account of global change (O'Gorman *et al.*, 2012). We therefore have to integrate our knowledge and efforts derived from multiple fields of research to counter the impacts of the growing human population and its pressure on ecosystems worldwide.

Acknowledgements

M.J. was funded by the Evangelisches Studienwerk Villigst e.V.; F.D.S. was funded by the Deutsche Bundesstiftung Umwelt (www.dbu.de); T.P.C. was supported by Science Foundation Ireland's Research Frontiers Programme (08/RFP/EOB1057); U.B. is funded by the German Research Foundation (BR 2315/13); E.J.O'G. was funded by IRCSET during the study and is currently funded by NERC grant NE/I009280/1. Thanks to Tânia Salvaterra for help with the setup of the experiment and to Jennifer Coughlan for assistance in the lab.

Supplementary material to Chapter 6

Malte Jochum, Florian D. Schneider, Tasman P. Crowe, Ulrich Brose, Eoin J. O'Gorman

Allometric design

With our top-down treatment, we intended to alter average top-predator (*Carcinus maenas*) body mass, M_C, over three levels: small (S), medium (M) and large (L). Controlling either biomass or abundance at a fixed level, while varying average body mass, would yield contrasting effects of abundance and biomass, respectively. We addressed this problem, by applying an allometric design (Schneider *et al.*, 2012). Here, biomass and population density are not assumed to be independent, but rather do depend on the average population body mass following an allometric power law. The densities consequently established in the different treatments then reflect a more natural population structure on an objective basis. Therefore, the initial densities, N_C, per cage were defined as

$$N_C = 14.5 \cdot M_C^{-0.25}. \tag{6.1}$$

Aiming to achieve initial average body masses of M_{CS} = 5 g, M_{CM} = 15 g, M_{CL} = 25 g, this yielded N_{CS} = 10, N_{CM} = 7 and N_{CL} = 6 (figure 6.3). This relationship mimicked empirical data from mesocosm communities at the study site (O'Gorman and Emmerson, 2011). To achieve log-normally distributed individual body masses around the intended average body masses, individuals were chosen after the following scheme: (1) 9 small and 1 medium crab for treatment S; (2) 5 small and 2 medium crabs for treatment M; (3) 3 small, 2 medium, and 1 large crab for treatment L. The treatment scheme was chosen manually to produce the

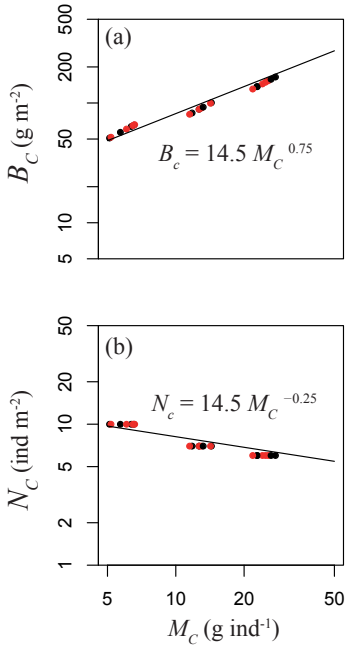

Figure 6.3 – Initial biomass density, B_C, and population density, N_C, of the top-predator species *C. maenas* are determined by its average body mass M_C. Black points signify ambient nutrient level; red points signify enriched nutrient level.

intended means out of the average body masses of each size class. This procedure succeeded in producing populations with log-normally distributed individual body masses (standard deviations σS = 0.60, σM = 1.01, σL = 1.94; figure 6.1) and significantly different average body masses for each treatment level (M_{CS} = 6.00 g, M_{CM} = 12.93 g, M_{CL} = 24.48 g; one-way ANOVA: Sums of Squares = 1393.8, residual $d.f.$ = 21, F = 405.62, $p < 0.001$; figure 6.1).

	Carcinus maenas		
Taxon consumed	Small	Medium	Large
Algae	2.8	6.1	1.4
Amphipoda	8.5	4.1	1.4
Bivalvia	7.1	12.2	55.1
Cyclopoida	1.4	2.0	2.9
Decapoda	15.5	18.4	7.2
Foraminifera	36.7	28.6	2.9
Gastropoda	2.8	2.0	2.9
Harpacticoida	7.1	8.2	13.0
Nematoda	1.4	10.2	5.8
Ostracoda	1.4	2.0	2.9
Perciformes	4.2	0.0	0.0
Sabellida	11.0	6.1	4.3
Sum	100.0	100.0	100.0

Table 6.2 – Proportion (%) of different animal groups found in the stomach contents of *C. maenas* individuals from the mesocosm experiment, averaged by size class: small (n = 27), medium (n = 22) and large (n = 9). Note that *C. maenas* with empty stomach contents were excluded from the analysis. The composition of the diet was largely similar for each of the three size classes (although Perciformes were only found to be consumed by small crabs). The diet of the small and medium crabs was dominated by Foraminfera and Decapoda, however, while the diet of the large crabs was dominated by Bivalvia and Harpacticoida. Note that the number of large crabs with stomach contents was very small (four out of eight crabs), so these data were supplemented with five large crabs from an experiment carried out three years previously (similar time of year, duration and cages).

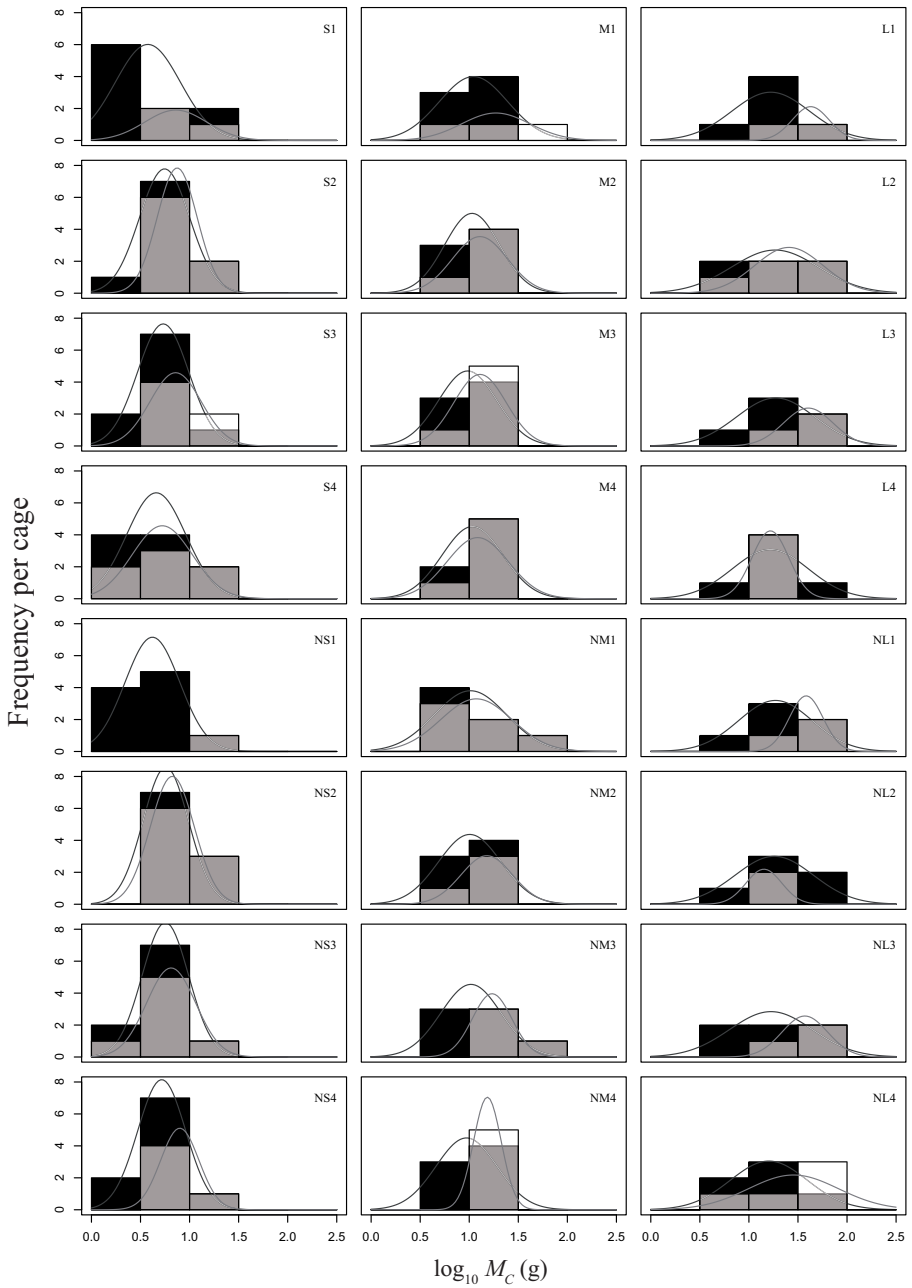

Figure 6.4 – Body-mass structure of the initial (black) and final (transparent) populations within each replicate. Colour scheme appears grey where distributions overlap. The intended body-mass treatment levels are labeled S, M, and L; the nutrient-enrichment treatments are labeled N. Numbers are replicates of each treatment.

Table 6.3 – Species found in the cages in alphabetical order. Body masses are given in grams of fresh weight. See footnote for other definitions.

Taxon name	order	mean body mass	A)	B)
Abludomelita obtusata	Amphipoda	$0.238(0.126-0.350)\times10^{-2}$	1	5
Alentia gelatinosa	Phyllodocida	$0.113(0.113-0.113)\times10^{0}$	1	5
Alvania beani	Neotaenioglossa	$0.440(0.009-1.790)\times10^{-2}$	1	5
Aora gracilis	Amphipoda	$0.491(0.013-1.556)\times10^{-3}$	1	5
Arabella iricolor	Eunicida	$0.656(0.001-3.354)\times10^{-1}$	1	5
Arenicola defodiens	Capitellida	$1.796(0.046-3.501)\times10^{0}$	2	5
Ascidiella aspersa	Phlebobranchia	$0.100(0.002-1.596)\times10^{0}$	3	5
Asterina phylactica	Valvatida	$0.480(0.001-1.436)\times10^{-2}$	1	5
Athanas nitescens	Decapoda	$0.141(0.000-0.216)\times10^{-1}$	2	5
Bittium reticulatum	Neotaenioglossa	$0.462(0.003-2.213)\times10^{-2}$	1	5
Buccinum undatum	Neogastropoda	$0.702(0.008-1.347)\times10^{-2}$	1	5
Caprella acanthifera	Amphipoda	$0.205(0.009-1.009)\times10^{-3}$	1	5
Caprella linearis	Amphipoda	$0.122(0.077-0.168)\times10^{-3}$	1	5
Carcinus maenas juv.	Decapoda	$0.181(0.023-0.658)\times10^{-1}$	1	6
Chironomidae spp.	Diptera	$0.118(0.004-0.771)\times10^{-3}$	1	5
Cingula trifasciata	Littorinimorpha	$0.471(0.219-0.925)\times10^{-2}$	1	5
Circomphalus casina	Veneroida	$0.775(0.775-0.775)\times10^{-2}$	1	5
Coriandria fulgida	Littorinimorpha	$0.360(0.034-0.613)\times10^{-3}$	1	5
Crassicorophium bonnellii	Amphipoda	$0.104(0.044-0.155)\times10^{-2}$	1	5
Crassicorophium crassicorne	Amphipoda	$0.384(0.009-2.592)\times10^{-3}$	1	5
Cyclopoida	Cyclopoida	$0.331(0.054-1.260)\times10^{-4}$	1	5
Cyprid larvae	Cirripedia	$0.124(0.027-0.213)\times10^{-2}$	1	5
Cythere lutea	Podocopida	$0.212(0.014-1.044)\times10^{-3}$	1	5
Cytherois fischeri	Podocopida	$0.179(0.014-0.443)\times10^{-3}$	1	5
Cytherura gibba	Podocopida	$0.268(0.268-0.268)\times10^{-3}$	1	5
Dexamine spinosa	Amphipoda	$0.254(0.008-4.097)\times10^{-3}$	1	5
Ephyra larva of jellyfish	Cnidaria	$0.471(0.270-0.901)\times10^{-4}$	1	5
Epilepton clarkiae	Veneroida	$0.977(0.088-2.432)\times10^{-3}$	1	5
Epilepton clarkiae (juv.)	Veneroida	$0.438(0.120-3.836)\times10^{-4}$	1	5
Ericthonius punctatus	Amphipoda	$0.276(0.002-0.661)\times10^{-2}$	1	5
Eteone picta	Phyllodocida	$0.294(0.012-0.572)\times10^{-1}$	1	5
Foraminifera A	Foraminifera	$0.721(0.013-2.924)\times10^{-3}$	1	5
Foraminifera B	Foraminifera	$0.377(0.035-2.016)\times10^{-4}$	1	5
Foraminifera C	Foraminifera	$0.210(0.130-0.330)\times10^{-4}$	1	5
Foraminifera D	Foraminifera	$0.868(0.035-6.392)\times10^{-4}$	1	5
Foraminifera F	Foraminifera	$0.337(0.035-1.225)\times10^{-4}$	1	5
Galathea squamifera	Decapoda	$0.338(0.117-2.079)\times10^{1}$	2	5
Gammarella fucicola	Amphipoda	$0.603(0.039-2.316)\times10^{-2}$	1	5
Gammaridea A	Amphipoda	$0.252(0.028-1.682)\times10^{-3}$	1	5
Gammaridea spp.	Amphipoda	$0.135(0.002-5.503)\times10^{-3}$	1	5
Gammaropsis maculata	Amphipoda	$0.216(0.009-1.345)\times10^{-3}$	1	5
Gammarus locusta	Amphipoda	$0.390(0.008-2.478)\times10^{-3}$	1	5

Taxon name	order	mean body mass	A)	B)
Gammarus zaddachi	Amphipoda	$0.329(0.014-1.204)\times10^{-2}$	1	5
Gibbula umbilicalis	Vetigastropoda	$0.259(0.000-1.825)\times10^{-1}$	1	5
Gobiusculus flavescens	Perciformes	$0.216(0.069-0.447)\times10^{0}$	2	6
Halacarellus basteri	Acarina	$0.549(0.126-1.744)\times10^{-5}$	1	5
Harpacticoida	Harpacticoida	$0.255(0.054-0.985)\times10^{-4}$	1	5
Hiatella arctica	Euheterodonta	$0.123(0.015-2.405)\times10^{-3}$	1	5
Insect larva A	insecta	$0.342(0.342-0.342)\times10^{-3}$	1	5
Insect larva B	insecta	$0.231(0.231-0.231)\times10^{-4}$	1	5
Isopod A	Isopoda	$0.231(0.231-0.231)\times10^{-4}$	1	5
Isopod B	Isopoda	$0.277(0.174-0.368)\times10^{-4}$	1	5
Janua pagenstecheri	Sabellida	$0.105(0.000-0.018)\times10^{-1}$	4	5
Kefersteinia cirrata	Phyllodocida	$0.193(0.001-2.683)\times10^{-2}$	1	5
Lembos websteri	Amphipoda	$0.468(0.038-2.104)\times10^{-4}$	1	5
Lepadogaster lepadogaster	Gobiesociformes	$0.493(0.493-0.493)\times10^{0}$	2	5
Leptocheirus tricristatus	Amphipoda	$0.103(0.089-0.117)\times10^{-3}$	1	5
Leptochelia savignyi	Tanaidacea	$0.595(0.231-4.774)\times10^{-4}$	1	5
Leptocythere pellucida	Podocopida	$0.117(0.014-0.268)\times10^{-3}$	1	5
Leptomysis lingvura	Mysida	$0.434(0.434-0.434)\times10^{-5}$	1	5
Littorina mariae	Littorinimorpha	$0.577(0.023-1.325)\times10^{-3}$	1	5
Loxoconcha rhomboidea	Podocopida	$0.112(0.014-0.443)\times10^{-3}$	1	5
Macrochaeta clavicornis	Terebellida	$0.111(0.002-3.559)\times10^{-3}$	1	5
Macropodia rostrata	Decapoda	$2.471(0.701-4.240)\times10^{0}$	2	5
Maera grossimana	Amphipoda	$0.321(0.233-0.410)\times10^{-2}$	1	5
Malacoceros fuliginosus	Spionida	$0.062(0.003-1.299)\times10^{-2}$	1	5
Marthasterias glacialis	Forcipulatida	$5.015(5.015-5.015)\times10^{0}$	2	6
Melita palmata	Amphipoda	$0.102(0.036-0.184)\times10^{-3}$	1	5
Microdeutopus anomalus	Amphipoda	$0.775(0.775-0.775)\times10^{-4}$	1	5
Microprotopus maculatus	Amphipoda	$0.110(0.032-0.437)\times10^{-3}$	1	5
Modiolula phaseolina (juv.)	Mytiloida	$0.133(0.095-0.145)\times10^{-3}$	1	5
Munna kroyeri	Isopoda	$0.243(0.054-1.118)\times10^{-4}$	1	5
Mytilus edulis	Mytiloida	$0.365(0.004-0.726)\times10^{0}$	1	5
Mytilus edulis (juv.)	Mytiloida	$0.185(0.014-2.374)\times10^{-3}$	1	5
Nannastacus unguiculatus	Cumacea	$0.327(0.067-0.577)\times10^{-4}$	1	5
Nebalia bipes	Nebaliacea	$0.121(0.049-1.570)\times10^{-3}$	1	5
Nematoda spp.	Nematoda	$0.136(0.000-0.743)\times10^{-2}$	1	5
Nereis sp.	Phyllodocida	$0.021(0.001-4.669)\times10^{-3}$	1	5
Omalogyra atomus	Heterostropha	$0.771(0.130-4.546)\times10^{-4}$	1	5
Onoba semicostata	Littorinimorpha	$0.400(0.012-0.998)\times10^{-2}$	1	5
Ophiothrix fragilis	Ophiurida	$0.185(0.111-0.298)\times10^{0}$	2	5
Ophiura ophiura	Ophiurida	$0.187(0.006-1.454)\times10^{-2}$	1	5
Ophiuroidea spec.	Ophiurida	$0.863(0.090-4.187)\times10^{-2}$	1	5
Ostracod A	Ostracoda	$0.201(0.041-0.361)\times10^{-4}$	1	5
Ostracod B	Ostracoda	$0.361(0.361-0.361)\times10^{-4}$	1	5
Palaemon serratus	Decapoda	$0.694(0.016-1.694)\times10^{-1}$	2	6
Paradoxostoma variabile	Podocopida	$0.331(0.014-1.044)\times10^{-3}$	1	5

Taxon name	order	mean body mass	A)	B)
Parvicardium exiguum	Veneroida	$0.118(0.001-6.025)\times10^{-2}$	1	5
Parvicardium ovale	Veneroida	$0.756(0.057-2.161)\times10^{-1}$	1	5
Phyllodoce lamelligera	Phyllodocida	$0.336(0.011-0.979)\times10^{0}$	1	5
Phyllodoce maculata	Phyllodocida	$0.756(0.756-0.756)\times10^{-1}$	1	5
Phyllodocidae spp.	Phyllodocida	$0.094(0.004-9.703)\times10^{-3}$	1	5
Pisidia longicornis	Decapoda	$0.867(0.012-2.365)\times10^{-1}$	2	5
Platynereis dumerili	Phyllodocida	$0.240(0.017-1.065)\times10^{-2}$	1	5
Polychaete A	Polychaeta	$0.477(0.477-0.477)\times10^{-3}$	1	5
Pomatoceros triqueter	Sabellida	$0.116(0.000-0.172)\times10^{-1}$	4	5
Pomatoschistus pictus	Perciformes	$1.216(0.400-2.124)\times10^{0}$	2	6
Pontocrates altamarinus	Amphipoda	$0.205(0.137-0.273)\times10^{-3}$	1	5
Protodorvillea kefersteini	Eunicida	$0.151(0.002-0.979)\times10^{-2}$	1	5
Retusa obtusa	Cephalaspidea	$0.476(0.476-0.476)\times10^{-3}$	1	5
Retusa truncatula	Cephalaspidea	$0.150(0.026-0.363)\times10^{-2}$	1	5
Rissoa parva	Littorinimorpha	$0.286(0.036-1.155)\times10^{-2}$	1	5
Rissoa sarsi	Littorinimorpha	$0.150(0.018-0.664)\times10^{-2}$	1	5
Rissoella diaphana	Gigartinales	$0.112(0.018-0.323)\times10^{-2}$	1	5
Rissoella opalina	Gigartinales	$0.233(0.034-0.949)\times10^{-3}$	1	5
Sabella pavonina	Sabellida	$0.148(0.005-0.743)\times10^{-3}$	1	5
Sagartia elegans	Actiniaria	$0.129(0.004-0.726)\times10^{0}$	2	5
Sagitta elegans	Aphragmophora	$0.116(0.005-0.498)\times10^{-3}$	1	5
Semicytherura nigrescens	Podocopida	$0.387(0.139-0.786)\times10^{-4}$	1	5
Siriella armata	Mysida	$0.206(0.011-0.451)\times10^{-3}$	1	5
Skenea serpuloides	Vetigastropoda	$0.466(0.033-1.494)\times10^{-3}$	1	5
Stenothoe marina	Amphipoda	$0.155(0.017-0.890)\times10^{-4}$	1	5
Syllidae A	Phyllodocida	$0.199(0.009-2.055)\times10^{-4}$	1	5
Tapes aureus	Veneroida	$0.104(0.104-0.104)\times10^{0}$	2	5
Trivia monacha	Littorinimorpha	$0.937(0.937-0.937)\times10^{0}$	2	5
Velutina velutina	Littorinimorpha	$0.129(0.129-0.129)\times10^{-3}$	1	5
Worm A	Annelida	$0.104(0.002-0.517)\times10^{-1}$	1	5
Worm B	Annelida	$0.905(0.055-1.559)\times10^{-2}$	2	5
Xestoleberis aurantia	Podocopida	$0.443(0.041-2.682)\times10^{-4}$	1	5

A)	sampling method:	area	cm^2	factor to m^2
1	pot scourer	7.5 × 6 cm	45	222.2
2	whole cage	41 × 42 cm	1722	5.807
3	cage lid	41 × 42 cm	1722	5.807
4	cage lid	10 × 10 cm	100	100.0

B) length-weight calculation:

5 length to dry-weight; multiplied with dry-weight to fresh-weight conversion factor 4 after Peters (1983).

6 length to fresh-weight

Chapter 7.

How predator diversity drives ecosystem functioning in complex food webs

Florian D. Schneider, Ulrich Brose, Björn C. Rall and Christian Guill

Abstract

Species diversity is under pressure on global and local scales, but the consequences of that decline for ecosystem functioning are poorly understood. Especially the effects of predator species loss on system stability, biomass stocks, and process rates remain unpredictable and hard to generalize across ecosystems. To fill this void, we propose a dynamic modeling approach based on predator-prey and food-web theory to obtain a theory that provides a generic understanding how predator loss affects these ecosystem-level properties. In this model, predator species are differentiated by simple rules for the body-mass scaling of diet breadth and feeding rates. We generate communities of varying predator diversity and random species body masses but with allometric constraints in respect of diets and feeding strengths. On these communities, we investigate the correlation between diversity and ecosystem functioning. We show that the proportion of species that persists over time saturates to a maximum with increasing initial predator diversity. The trait-based metric of functional diversity also saturates, but at lower levels than expected after random species loss. Thus, a predator which adds unique traits to functional diversity bears a higher risk of extinction. Surprisingly, high functional diversity constrains total predator and basal biomass to lower levels. With increasing diversity, we observed an increasing leakage of the predator community due to higher rates of respiration and intraguild predation, while – against all expectations – the total feeding of predators on basal species was also increased. The basal community was not released from top-down pressure with increasing diversity because the predator community became dominated by smaller species, which increased the total energy throughput. Allometric food-web theory enables a mechanistic understanding and provides a null-expectancy for the biodiversity–ecosystem functioning relationships, showing that enriched diversity does not necessarily correlate with increasing basal productivity.

Keywords | Biodiversity–ecosystem functioning, food web, allometric theory, population dynamics, predator–prey, trophic cascade, omnivory

Introduction

The interdependent relationship between species diversity and ecosystem functioning is both obvious and enigmatic. On the one hand, it is plain clear that ecosystem functioning is a product of the activity of organisms (Hooper *et al.*, 2005). Motivated by the recent rates of species extinction in all global ecosystems, the search for a correlation between biodiversity and the magnitude and stability of ecosystem functioning is one of the driving forces in ecological research of the past two decades (the biodiversity–ecosystem functioning, 'BEF', debate; Naeem *et al.*, 2002; Hooper *et al.*, 2005; Loreau, 2010*b*). On the other hand, the description of this correlation is very complicated: Apparently idiosyncratic, positive as well as negative consequences of predator species loss from multi-trophic communities were observed (Halaj and Wise, 2001; Shurin *et al.*, 2002; Bruno *et al.*, 2008; Letourneau *et al.*, 2009; Reiss *et al.*, 2009), which cannot be explained by species number alone. Indirect trophic-cascading effects due to feeding on other predators (subsequently termed 'intraguild predation') are widespread and important in shaping the variable net effects of predator communities (Sih *et al.*, 1998; Finke and Denno, 2005; Ives *et al.*, 2005; Bruno *et al.*, 2008). This led researchers to doubt the notion that distinct trophic levels of predators determine the total effects of predator communities on the functions of an ecosystem (Pace *et al.*, 1999; Polis *et al.*, 2000). Instead, communities were increasingly perceived as diverse and highly inter-connected food webs (Pace *et al.*, 1999; Duffy, 2002). The hypothesis, that the total trophic effect on the basal community generally must be dampened with increasing diversity, mediated by increased intraguild feeding (Strong, 1992; Pace *et al.*, 1999; Duffy *et al.*, 2007), eludes clear acceptance or rejection. Indeed, real multi-trophic communities feature many generalist predators that feed on more than one trophic level with differentiated and dynamic interaction strengths, which blurs any distinction between trophic levels and hinders prediction of consequences of a specific predator species loss. Empirical manipulation on trophic cascades, however, is limited to low-diversity micro- and mesocosm communities with inconsistent measured effects (Schmitz *et al.*, 2000; Halaj and Wise, 2001; Bruno *et al.*, 2008; Cardinale *et al.*, 2009).

To simplify the subject, 'functional diversity' was defined as a new metric for the coverage of trait space by species in a local ecosystem (Petchey and Gaston, 2006; Petchey *et al.*, 2008*b*, 2009; Reiss *et al.*, 2009). This usually also includes the trophic position of a predator species. In this framework, two species are termed redundant if they add similar traits to functional diversity of a community, or complementary if they contribute different traits. Therefore, functional diversity is supposed to be a better predictor of ecosystem functioning than taxonomic species richness (Hooper *et al.*, 2002; Reiss *et al.*, 2009). A species that is complementary to all other species is contributing unique traits to the community (Petchey *et al.*, 2008*b*). Surprisingly, although they are expected to profit from having no direct niche competitor, those species were found to be disproportionately at risk of extinction after perturbations (Petchey *et al.*, 2008*b*; O'Gorman

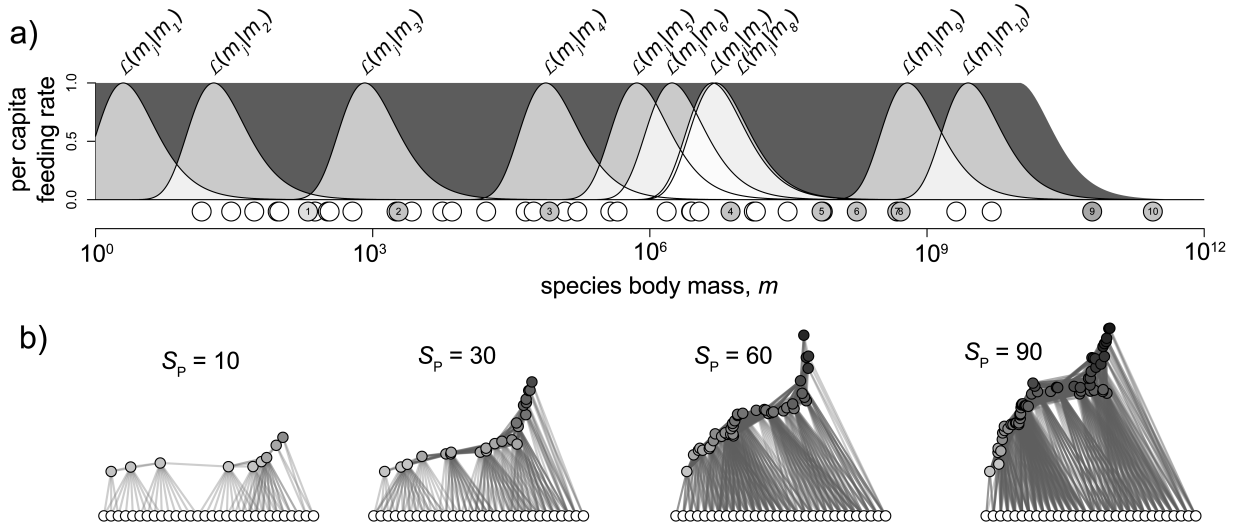

Figure 7.1 – Allometrically constraints determine food web structure and feeding rates. Each simulated food web is initiated with S_P predators (numbered grey circles) on 30 basal species (white circles). All body masses are assigned randomly. Predator i feeds on prey j if feeding rates are above a relative threshold (see methods). In a) the normalized feeding rates, i.e. the feeding likelihoods $\mathcal{L}$, of all predators within an exemplary community with $S_p = 10$ are depicted (curves above white areas), yielding the first food web depicted in b). b) basal species are ordered by body mass, predators are ordered by the average position of their direct prey species (x-axis) and by their average trophic level (y-axis).

and Emmerson, 2010). This illustrates that extinction of a species does not happen by chance, but as a consequence of the species' trophic position, its uniqueness or redundancy, and the strength of the interactions with all other neighboring or remote species in the ecosystem (Duffy *et al.*, 2007). Most importantly, a population's persistence is a consequence of all energetic processes within the entire community. Thus, species richness may not be perceived as the cause of ecosystem functioning but as its consequence.

We anticipate that the concepts outlined above can be cast into a unifying ecological framework by applying a network-theoretic approach, assuming that the species (nodes), connected by trophic relations (edges), interact in concert to compose the higher level characteristics of ecosystems (Ives *et al.*, 2005; Loreau, 2010*b*; Reiss *et al.*, 2009; Cardinale *et al.*, 2009). The integration of food web theory and dynamic predator–prey theory into biodiversity–ecosystem functioning research was demanded before to scale the findings from the experimental systems, which usually are restricted to low levels of species richness, to natural diversity levels (Ives *et al.*, 2005; Loreau, 2010*a*). To date, food web theory has proven to be a useful tool in biodiversity–ecosystem functioning research to investigate how feeding relationships and community structure must be organized to warrant long term persistence (May, 1973*b*; McCann, 2000; Williams and Martinez, 2000; Dunne, 2006). Furthermore, it can scale identified mechanisms to species rich and complex communities (Ives *et al.*, 2005) and make predictions about the consequences of altered diversity across trophic levels (Thébault and Loreau, 2003, 2005; Holt, 2002). With few exceptions, however, either species richness within a trophic level

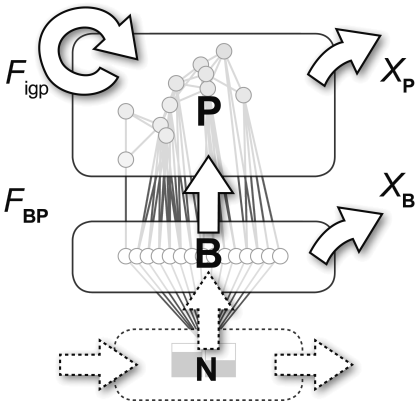

Figure 7.2 – Schematic diagram of the food web model. A basal community, **B**, feeds on two nutrient ressources, **N**, competitively. The community of generalist predators, **P**, feeds on the basal community with rate F_{BP}, but also on members of the own guild with rate F_{igp}. Both, basal and predator community, lose energy due to metabolic demands, X_B & X_P. The nutrients are controlled by a constant global turnover.

('horizontal' diversity) or the number of trophic levels ('vertical' diversity) were investigated separately (Duffy *et al.*, 2007; Loreau, 2010*b*). None of the models reflect the infinite variability of natural food webs, that differ strongly in species richness and composition, population densities and abiotic conditions.

The allometric theory of ecology, which always progressed alongside the biodiversity–ecosystem functioning debate, identified body mass as an important determinant of multiple species traits, such as feeding rates (Vucic-Pestic *et al.*, 2010; Brose *et al.*, 2008), niche differentiation (Digel *et al.*, 2011; Petchey *et al.*, 2008*a*; Stouffer *et al.*, 2011; Schneider *et al.*, 2012), and food web structure (Otto *et al.*, 2007; Petchey *et al.*, 2008*a*; Riede *et al.*, 2011). Thus, allometric theory provides a framework that can be used to study how mechanisms on population level emerge systemic behavior and ecosystem functioning with a wide parametric variety (Woodward *et al.*, 2005). Therefore, in this study we propose an integrative allometric model that defines the predator species' prey ranges as a function of their body mass. More specific, feeding rates are a function of predator and prey body masses and of their biomass densities (Vucic-Pestic *et al.*, 2010; Brose *et al.*, 2008) that are simulated dynamically over time (Yodzis and Innes, 1992; Schneider *et al.*, 2012). A predator's prey range includes all species present in the local food web, including other predators, that are within a certain body-mass range (Fig. 7.1*a*; Petchey *et al.*, 2008*a*). By this definition, similarly sized species are redundant (as species 7 and 8 in Fig. 7.1*a*), while differently sized species are complementary (as species 3 and 4 in Fig. 7.1*a*). A species that is complementary to all other species (species 3) is subsequently characterized as 'unique' species (Petchey *et al.*, 2008*b*). Building upon this allometric food-web model, we defined a trait-based metric for functional diversity, *FD*, as the proportion of niche space that is covered by the possible feeding range of all predators (Fig. 7.1*a*, union of pale areas divided by grey background area).

We apply this model to simulate population dynamics in 40 000 communities over a large gradient of predator species richness. We assembled 1 to 100 predator species of random body mass to build plausible communities of variable vertical and horizontal diversity. Thus, the total

effect of the entire predator community (**P** in Fig. 7.2) on the basal community (**B** in Fig. 7.2) emerges explicitly from the allometric constraints on the population level. We first investigate how an increasing diversity of generalist predators affects the species persistence and preserves functional diversity of food webs. Further, we address whether redundancy or uniqueness of the species on the niche axis sustains functional diversity over time. Finally, we consider how ecosystem functioning, defined as stocks of total biomass of basal species and predator species (Fig. 7.2, **B** & **P**), rates of total biomass flow (Fig. 7.2, F_{BP} & F_{igp}) and total respiration (Fig. 7.2, X_{P} & X_{B}), changes with predator functional diversity. This aims at the understanding whether trophic cascades are dampened in diverse communities thus testing a long-established hypothesis (Strong, 1992; Pace *et al.*, 1999; Cardinale *et al.*, 2009): High diversity should lead to a lower total predator biomass due to increased intraguild feeding which – as a direct consequence – releases the basal community to grow to larger total biomass.

Results

Species persistence and functional diversity

The initial number of predators affected the stability of the food webs in terms of species survival over time (i.e. persistence, Fig. 7.3*a*) and provided a higher functional diversity of the community (Fig. 7.3*b*). In a food web with two resources (nutrients) and only competitive basal feeders no more than two species can coexist. By adding an increasing number of predator species on top of the basal community, coexistence is increasingly enabled (Fig. 7.3*a*) until the expected species persistence saturates at 0.846 ± 0.003 (Std. error; nonlinear logistic model, see material and methods). This can be interpreted as an expected long-term survival of 85% of the initialized species in a diverse community. For those diverse communities of more than approximately 20 predator species, the gain in persistence per additional species is low. In contrast, food webs of low predator diversity have a higher risk of further extinctions, which also means that species poor communities benefit most from the addition of species.

High predator diversity also yields higher functional diversity. Parallel to species persistence, the expected functional diversity saturates with increasing initial predator species richness at a value of 0.774 ± 0.005 (Fig. 7.3*b*). This general pattern of saturation already existed in the initial food webs due to the increasing redundancy of the predators (i.e. an overlap of species' niche ranges) and is preserved throughout the dynamic simulations. We therefore investigated how the loss of species over the population dynamics affects functional diversity of the community. We found that the functional diversity after dynamic extinction, FD_{sim}, is on average $8.5(\pm 0.005)\%$ lower than in case of random loss of an equal number of species , FD_{rd} (see materials and methods). This means, that an initially high functional diversity is diminished disproportionately by selective extinction. There are two possible reasons: Populations of species within a certain size

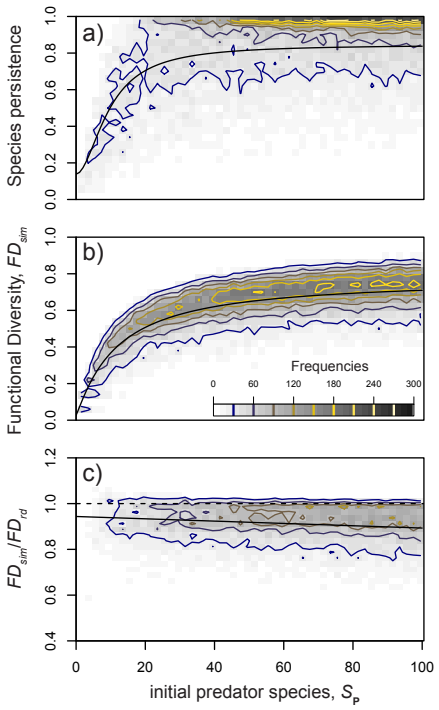

Figure 7.3 – Inital predator species richness, S_P, leads to stabilized food webs in terms of (a) improved species persistence and (b) higher functional diversity. Both functions saturate with increasing species richness. Black lines represent 4-parameter logistic models. (c) The functional diversity after dynamic extinctions is systematically lower than after random extinctions, resulting in a FD_{sim}/FD_{rd} below one. FD_{sim}/FD_{rd} decreases with initial species richness. Black line represents a linear model with gamma error.

range, which are not feasible due to the lack of a suitable resource, may become systematically extinct. This would be comparable to the loss of a whole functional group after a perturbation event. The loss of whole functional groups should have a higher impact on the ratio FD_{sim}/FD_{rd} in species poor communities where a smaller proportion of niche space is covered initially. This is, however, not corroborated by the pattern in FD_{sim}/FD_{rd} which actually decreases with initial predator species number (Fig. 7.3*c*; $FD_{sim}/FD_{rd} = 0.944(\pm 0.001) - 0.0005(\pm 0.00002) \cdot S_p$; linear least squares, see material and methods; Fig. 7.3*c*). Alternatively, the systematic loss of functional diversity could be due to the selective loss of functionally unique species without a similarly sized counterpart. They add more to the functional diversity than redundant species. The likelihood for unique species in the initial species pool increases with species richness because of the log-normal assignment of body masses.

Effects on stocks and rates

The species that comprise the final community after dynamic simulations were 'selected' by energetic processes among the allometrically defined species. Analogue with field applications of functional diversity, we can perceive the trait-based metric as a consequence of dynamic processes and use it as a predictor of ecosystem functioning. In this section, we therefore present the total biomass stocks and process rates as a consequence of these dynamic processes within the community. Increasing functional diversity decreased total biomass of the basal

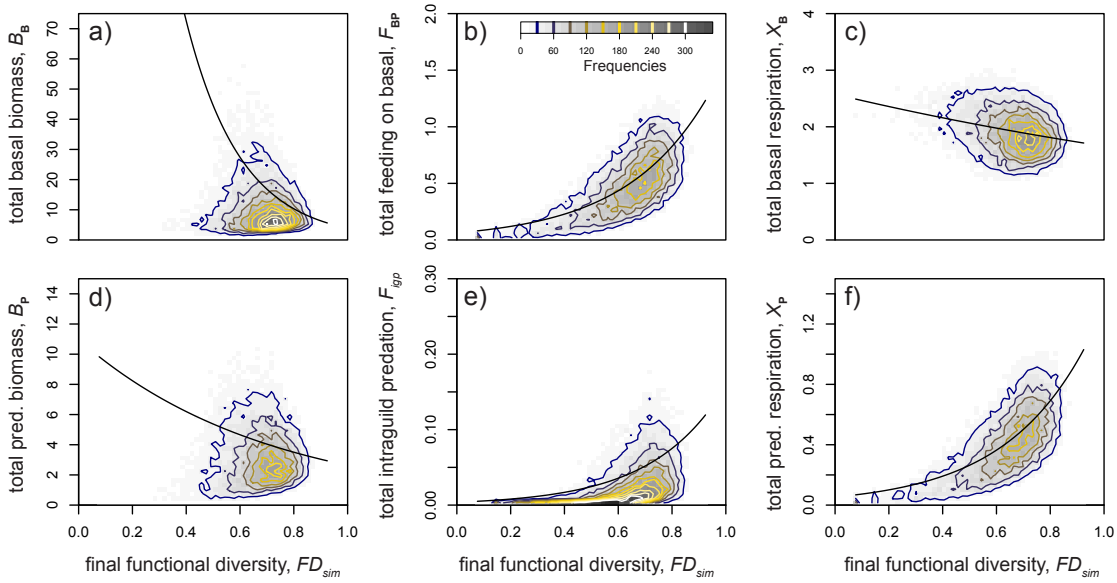

Figure 7.4 – Predator functional diversity affects ecosystem functioning. With increasing functional diversity (a) total basal biomass decreased and the total feeding on basal species (b) increased. (c) Total basal respiration decreased. (d) Total predator biomass also decreased with functional diversity due to (e) increasing rates of intraguild feeding and (f) predator respiration.

community ($\log B_B = 6.23(\pm 0.02) - 4.87(\pm 0.04) \cdot FD_{sim}$; Fig. 7.4*a*) while the flow of biomass into the predator community increased ($\log F_{BP} = -2.76(\pm 0.01) + 3.22(\pm 0.02) \cdot FD_{sim}$; Fig. 7.4*b*). Moreover, with increasing functional diversity total respiration of basal species decreased ($\log X_B = 0.95(\pm 0.00) - 0.44(\pm 0.01) \cdot FD_{sim}$; Fig. 7.4*c*). The total predator biomass, however, also decreased with higher functional diversity ($\log B_b = 2.39(\pm 0.02) - 1.43(\pm 0.03) \cdot FD_{sim}$; Fig. 7.4*d*). This was due to increasing intraguild predation ($\log F_{igp} = -5.57(\pm 0.03) + 3.73(\pm 0.05) \cdot FD_{sim}$; Fig. 7.4*e*) and total predator respiration ($\log X_P = -2.94(\pm 0.01) + 3.21(\pm 0.02) \cdot FD_{sim}$; Fig. 7.4*f*). Thus, with increasing functional diversity the total biomass of the predator community was constrained to lower levels due to enhanced predator feeding rates. At the same time, increased leakage due to respiration and intraguild predation made the predator community less efficient in maintaining biomass.

Discussion

In this study, we applied a simulation approach to scale the diversity of allometrically constrained predators. We investigated the consequences of increased predator species richness for ecosystem functioning in terms of species persistence and functional stability and, on the community level, on standing stocks and process rates. We found that an increase in initial predator species richness provides a higher species persistence and higher functional diversity, both saturating against a maximum with increasing species richness. Interestingly, functionally

unique species appear to have a higher extinction risk than redundant species, resulting in a preserved functional diversity that is lower than expected by chance. Furthermore, with an increase in functional diversity total biomass of both the basal and the predator community decreases. The efficiency of the predator community in maintaining biomass declines due to predator metabolism and intraguild predation. In common hypothesis of community trophic cascades, speciose predator communities are expected to promote intraguild predation which in turn is supposed to dampen the net effect on the basal community (Strong, 1992; Pace *et al.*, 1999). We could show, that indeed increased intraguild predation leads to reduced total predator biomass. We reject, however, the second part of this logic chain and show that basal community suppression not necessarily must originate in high predator biomass.

Species persistence and functional diversity

We varied the initial number of predator species with randomly drawn body masses and simulated the population dynamics of these food webs, forcing the population densities to approximate an attractor in phase space. The allometric model is characterized by sigmoid functional responses, frequently leading into stable equilibrium dynamics (Rall *et al.*, 2008). This caused non-random extinctions for some species from both the basal and predator guild. Thus, in this study, stability is investigated in terms of persistence of species richness after a perturbation dependent on initial predator species number, S_P. An increasing number of predators reduces the chance for a basal species to be excelled by a competitor, because more basal species are put under top-down control. With the loss of species, functional diversity is reduced as well. Furthermore, we found that the decline of functional diversity is greater than expected based on random extinction models. Our results suggest that functionally unique species are more vulnerable to extinction than redundant species. This is counterintuitive but corroborates the findings of higher extinction likelihoods for functionally unique species from complex communities in empirical data (O'Gorman and Emmerson, 2010; Petchey *et al.*, 2008*b*) and simulations (Petchey *et al.*, 2008*b*).

Effects on stocks and rates

The total biomass stock of the basal community shows a negative correlation with functional diversity while the summed rates of energy flow between basal species and predators increase with diversity. Surprisingly, the total biomass of the predator community also decreases as functional diversity increases. Thus, although more energy is available for the predators, their total biomass is constrained to lower levels. This indicates an enhanced throughput of energy through the predator community with increasing functional diversity. The increase in total intraguild predation rate and in total respiration rate of the predator community caused the

predator community in diverse systems to be less efficient in maintaining biomass. The increase in total intraguild predation is the consequence of the wider niche coverage since this enhances the likelihood to be controlled by another predator, not only for basal species but also for smaller and intermediately sized predators.

In the framework of the allometric model, the increase in metabolic demands at decreasing total biomass of the predator community means that the average individual body size decreases with increasing functional diversity. Why are the energetics of the simulation beneficial to small species and hindering for large predators? The diet of a predator is composed of prey of different trophic levels. For large predators, this prey has on average a high trophic position which means that their energetic supply must undergo more steps of biomass conversion, each subjected to imperfect assimilation. This viscous energy supply may not only hamper the accumulation of biomass, it also may increase the extinction risk for large predator species. In contrast, small predators occupy a trophic position closer to the basis of the food web which provides them a liquid energy supply. The handicap of large predators may reduce the feeding pressure on the small predators. As a consequence, small predators grow to larger biomass densities and enhance the total direct feeding on the basal species. Thus, the smallest predators should dominate the total energetic budget of speciose predator communities. This apparently has negative effects for the basal community. The total biomass and the total respiration of basal species, both metrics for basal productivity, decrease with diversity.

Our findings answer to the long-established hypothesis of Strong (1992), who suggested that in diverse and highly interconnected communities trophic cascades should not occur (Strong, 1992; Pace *et al.*, 1999; Halaj and Wise, 2001; Duffy, 2002; Cardinale *et al.*, 2009). He expected, that any distinction into several trophic levels of consumers was lost in those ecosystems because of the enhanced feeding within the predator community. As a direct consequence, the cascading effect on the lower trophic level should be 'trickling'. The basal community should be released from feeding pressure (Halaj and Wise, 2001; Duffy, 2002; Cardinale *et al.*, 2009).

While our results corroborate the first part of this logic, showing a diverse predator community of low biomass, they reject the subsequent deduction that this must lead to enhanced biomass of the basal community. Instead, our findings suggests that increasing diversity and enhanced opportunities for intraguild predation do not *per se* release the basal community from feeding pressure and increase productivity. A diverse predator community might be more exploitative but, at the same time, less efficient.

Scope of the allometric model

The focus of this study is on the alteration of diversity within the predator community while the basal trophic level has a standardized species richness. The parameters and definitions for the model are derived from the community of deciduous forest floors. The rules for allometric

feeding in this system were parameterized empirically (Brose *et al.*, 2008; Vucic-Pestic *et al.*, 2010; Ehnes *et al.*, 2011; Chapter 2) and validated in microcosm experiments before (Kalinkat *et al.*, 2011; Schneider *et al.*, 2012; Chapters 3 and 4). We expect the derivations from this model system to hold for other ecosystems, terrestrial as well as marine, which show similar body mass structures and widespread intraguild predation (Riede *et al.*, 2011; Jacob *et al.*, 2011).

The model takes body mass as the only differentiating parameter for the particular set of feeding traits and physiological parameters of a species (Schneider *et al.*, 2012). This is a strict simplification of ecological systems, assuming that all predators of equal body mass *are* equal. We anticipate, however, that the model provides a much more realistic baseline for the investigation of systemic processes within food webs than a neutral species model (assuming that all species are equal) while adding only one predictive parameter. This enables an unprecedented integration of many levels of complexity in one single model framework that reproduces all of the mechanisms that were identified as drivers of the biodiversity–ecosystem functioning relationship:

- Allometry defines the prey range and feeding intensity of predators on the body-mass axis relative to their own body mass, analogous to classical niche concepts (Williams and Martinez, 2000). Thus, allometric feeding rates produce 'niche complementarity' (Petchey *et al.*, 2008*a*; Cardinale *et al.*, 2009).

- At the same time, the allometric niche differentiation predicts intraguild predation and subsequent 'indirect effects' (Ives *et al.*, 2005) within the food web. This means that the sign of one predator's effect on a focal species may depend on the allometrically constrained prey range and relative feeding rates on the other involved species (Schneider *et al.*, 2012). A randomly sized predator species thus could emerge negative or positive net effects on ecosystem functioning. By adding predator species to the system, new trophic levels may emerge, increasing the vertical diversity of the community (Duffy *et al.*, 2007).

- The allometric simulation of dynamic feeding rates returns cumulative interaction strengths over time. The more speciose a community becomes the more likely it is that a species is filling a new functional position and altering the attractor of the system substantially. This is analogous to an alteration in ecosystem function by increasing the likelihood of including a dominant species, as proposed by the concepts of 'sampling effects' and 'selection effects' (Loreau *et al.*, 2001; Ives *et al.*, 2005; Loreau, 2010*a*).

- This also means that species extinctions do not occur randomly but as a consequence of food web dynamics. Thus, functionally similar species may secure the total effect of the community and an increased diversity should yield 'insurance effects' (Yachi and Loreau, 1999).

In the presented form, the allometric food web model is parsimonious with parameters and

differentiates species' identity only by their body mass. However, individuals of different species are not only distinguishable by their size. Allometric models allow the addition of phylogeny and other body-mass independent traits (Eklöf *et al.*, 2011; Naisbit *et al.*, 2012). Furthermore, the model is well prepared for the integration of environmental factors such as temperature effects on physiological and ecological parameters (Brown *et al.*, 2004; Vucic-Pestic *et al.*, 2011; Binzer *et al.*, 2012) or nutrient enrichment (Binzer *et al.*, 2012), allowing to investigate the effects of global change on ecosystem functioning (Brose *et al.*, 2012; Binzer *et al.*, 2012).

In summary, the allometric model provides a framework that allows for mechanistic simulations of the biodiversity–ecosystem functioning relationship. Simply by increasing the number of allometrically defined species, horizontal and vertical diversity are varied in a way that is highly consistent with natural processes. The allometric rules on population level determine the food web topology and the attractor of the system which in turn determines species survival. Together, these properties emerge the higher level functions of the whole ecosystem.

Conclusion

The allometric model proposed in this study connects food web and predator–prey theory with the scope of multi-trophic diversity and ecosystem functioning. It does so with intricate simplicity. The approach overcomes the concept of vertical *vs.* horizontal diversity, which accords to the natural complexity of food webs, rich in feeding interactions across and within trophic levels. Since experimentation is strongly limited in manipulating large gradients of diversity, we anticipate that only network simulation can provide a smooth scaling from simple systems found in micro- and mesocosms to the complexity found in nature. We suggest integrative simulations of higher level ecosystem processes and functions on the basis of small scale mechanisms and network theory.

Our model revealed the following patterns: species persistence and functional diversity increase with predator species richness until saturation. Functionally unique species, however, are threatened more by extinction than redundant species. We found evidence, that increasing predator diversity does constrain the biomass of the predator community but this does not *per se* enhance basal productivity. The community is losing more energy to metabolism by selecting populations of small predators over larger ones. This reduces the efficiency of the predator community in building up biomass but enhances the total feeding rates which constrains the total basal biomass to lower stocks. The challenging bottom line of this study is that a highly diverse and interconnected predator community may be low in biomass but, at the same time, is able to suppress the basal community. Our results break new grounds in the understanding of community-wide trophic cascades and the consequences of predator loss for ecosystem functions.

Materials and methods

Food-web structure

The model food webs consist of a basal compartment (Fig. 7.2, **B**) and a predator compartment (Fig. 7.2, **P**). The initial predator species number, S_P, is varied from 1 to 100. The basal community is standardized to $S_B = 30$ species growing on two nutrients with species-specific efficiency. The $\log_{10}$ body masses of the species are drawn from independent normal distributions with mean $\mu_B = 5$ for basal species and $\mu_P = 7$ for predators, and standard deviation $\sigma = 4$ in both cases. For both basal and predator community, $\log_{10}$ body masses are limited to $\mu_{B,P} \pm 5$, constraining the smallest possible body mass of a basal species to 1 and the largest possible body mass of a predator species to 10^{12}.

Trophic relations depend on the body masses of predator and prey, which is expressed in the capture coefficient

$$b_{ij} = b_0 m_i^{\beta_i} m_j^{\beta_j} \left(\frac{m_i}{m_j R_{opt}} e^{1 - \frac{m_i}{m_j R_{opt}}} \right)^{\gamma} \tag{7.1}$$

of a predator species i on a prey species j. The rate of encounters between predator and prey increases according to a power law with the body masses of predator (m_i) and prey (m_j), accounting for their increasing movement speed ($\beta_i = 0.25$, $\beta_j = 0.25$, following Peters, 1983, with the constant $b_0 = 200$). The probability of a predator to actually capture a prey encountered is described by a hump-shaped curve with width $\gamma = 2$ (Persson *et al.*, 1998), centered around an optimal predator-prey body-mass ratio $R_{opt} = 100$ (Brose *et al.*, 2008; see Fig. 7.1*a*). A potential feeding link between any two species i and j is supposed to be active if the corresponding capture coefficient b_{ij} fulfills $b_{ij} \geq 0.05 \cdot \max_j(b_{ij})$, yielding food webs as depicted in Fig. 7.1*b*. Note that not only links between predators and basal species are possible, but also within the predator community, which promotes intraguild predation.

Feeding rates

The allometric model for the rate at which predator i feeds on a prey j (Brose *et al.*, 2006*a*; Schneider *et al.*, 2012) uses a multi-prey Holling-type functional response with variable Hill-coefficient (Holling, 1959*a*), and includes intra-specific predator interference (Beddington-DeAngelis type, Skalski and Gilliam, 2001). The feeding rate

$$F_{ij} = \frac{\omega_i b_{ij} B_j^q}{1 + c B_i + \omega_i h_i \sum_k b_{ik} B_k^q}, \tag{7.2}$$

is a function of the biomass densities of the predator (B_i) and the prey (B_j). It includes the capture coefficient b_{ij} (equation 7.1), the relative consumption rate ω_i, the handling time h_i,

the time loss due to predator interference c, and the Hill-coefficient q. The handling time,

$$h_i = h_0 m_i^{\eta_i}, \tag{7.3}$$

depends only on the body mass of the predator to the power of $\eta_i = -0.75$ (Yodzis and Innes, 1992) times the constant $h_0 = 0.4$. The predator interference c is the proportion of time that a predator spends with encountering con-specifics (Skalski and Gilliam, 2001). For each food-web replicate c is drawn from a normal distribution ($\mu_c = 1$, $\sigma_c = 0.1$) within the inclusive limits of 0.75 and 1.25. The hill coefficient q reduces the feeding rate for low prey densities and varies the functional response gradually between classic type II ($q = 1$) and type III ($q = 1$) (Holling, 1959*a*; Chapter 1). The value of q is drawn for each replicate from a normal distribution ($\mu_q = 1.5$, $\sigma_q = 0.2$) within the inclusive limits of 1 and 2. The relative consumption rate ω_i accounts for the fact that a predator has to split its consumption if it has more than one prey species. It is thus defined as $\omega_i = 1/(\text{number of prey species of } i)$.

Population dynamics

The model food webs are based on a dynamic nutrient model with two nutrients of different importance supplying the basal community. On top, a variable number of predators are feeding on the basal species and among each other as defined by the food-web structure. The change in species i's biomass density B_i is described by an ordinary differential equation of the form

$$\frac{dB_i}{dt} = r_i G_i B_i + e B_i \sum_j F_{ij} - \sum_k B_k F_{ki} - x_i B_i \,. \tag{7.4}$$

The first term describes growth due to the uptake of nutrients. The second term describes the summed gain by consumption of other species j times the conversion efficiency $e = 0.85$ that determines how much biomass of eaten prey is converted into predator biomass (Yodzis and Innes, 1992). The third term describes mortality due to predation, summed over all predators k of species i. Finally, each species has metabolic demands, $x_i = x_0 m_i^{-0.25}$, which depend on its body mass m_i and the constant $x_0 = 0.314$ (Yodzis and Innes, 1992).

The growth of a basal species is limited by its intrinsic growth rate r_i ($r_i = m_i^{-0.25}$ for basal species, (Brown *et al.*, 2004); $r_i = 0$ for predator species) and by the growth factor G_i which is determined dynamically by the concentration of the nutrient l that is most limiting to i:

$$G_i = \min_l \left(\frac{B_l}{K_{il} + B_l} \right). \tag{7.5}$$

For high nutrient concentrations the term in the minimum operator approaches 1. The half-saturation densities K_{il} determine the nutrient uptake efficiency and are assigned randomly for

each basal species i and each nutrient l (uniform distribution within the inclusive limits of 0.1 and 0.2). This generates niche differentiation of the basal species (Tilman, 1982; Huisman and Weissing, 1999; Brose, 2008). The change of nutrient concentration B_l is defined by

$$\frac{dB_l}{dt} = D(S_l - B_l) - \nu_l \sum_i r_i G_i B_i \,, \tag{7.6}$$

with a global turnover rate $D = 0.25$ that determines the rate by which nutrients are refreshed (Huisman and Weissing, 1999; Brose, 2008). The supply concentration S_l determines the maximal nutrient level drawn at random from a normal distribution ($\mu_S = 10$, $\sigma_S = 2$) and constrained to be larger than 0. The nutrient stock is diminished by the summed uptake by all basal species i. The loss of a specific nutrient l is limited by its relative content in the basal species' biomass ($\nu_1 = 1$, $\nu_2 = 0.5$).

The population dynamics were calculated by integrating the system of differential equations implemented in C using procedures of the GNU Scientific Library (4th order Runge-Kutta-Fehlberg method with 5th order error estimate; Galassi *et al.*, 2011). The initial biomasses of the species were drawn randomly from a uniform distribution within the limits of 0 and 10. Nutrient concentrations B_l were initialized with random values uniformly distributed between $S_l/2$ and S_l. The food webs were simulated until t = 150 000 to ensure that stationary dynamics were reached. Replicates that included predator-free basal species at the end of the simulation time were discarded from the data set. The uncontrolled growth of such an inedible basal species would dominate ecosystem function qualitatively (Thébault and Loreau, 2006). In total, 40 000 valid food webs were simulated.

Output parameters

The total biomass stocks of the predator community, B_P, and the basal community, B_B, were calculated as the average over an evaluation period of 10 000 time steps. Rates of biomass flow from basal to predator species, F_BP, and from predator to predator species (intraguild predation), F_{igp}, were calculated as average biomass transfer per time step over the evaluation period. The same was done for the total respiration rates of predators, X_P, and of basal species, X_B.

We defined functional diversity, *FD*, as the proportion of niche space that is covered by the potential feeding ranges of all predators (Fig. 7.2a). The feeding likelihood, $\mathcal{L}$, of a single predator i was normalized to maximal amplitude of 1 by dividing the capture coefficient b_{ij} by $b_0 m_i^{\beta_i} m_j^{\beta_j}$. The likelihood of a successful capture by a predator with mass m_i of an encountered prey item of body mass m_j is thus defined by

$$\mathcal{L}(m_j|m_i) = \left(\frac{m_i}{m_j R_{opt}} \mathrm{e}^{1-\frac{m_i}{m_j R_{opt}}} \right)^\gamma . \tag{7.7}$$

Each predator covers a certain area of niche space, given by the integral of $\mathcal{L}$ over the body-mass axis (Fig. 7.1*a*). The whole predator community covers the union of these integrals of all predators (numerator of *FD*; pale areas in Fig. 7.1*a*). The niche space is the maximal area that can be covered by the predators' feeding likelihoods (denominator of *FD*; dark area in Fig. 7.1*a*). It is defined as the whole range of the body-mass axis ($\log_{10} m_{max} - \log_{10} m_{min} = 12$) times 1 (max. of the likelihood curve), minus the body-mass range that cannot be accessed even by the largest predators with $\log_{10} m_i = 12$. The functional diversity is thus given by

$$FD = \frac{\int_{m_{min}}^{m_{max}} \underset{i}{\mathrm{ENV}} \mathcal{L}(m_j|m_i) \frac{1}{m_j \ln 10} dm_j}{10 + \int_{10^{10}}^{10^{12}} \mathcal{L}(m_j|10^{12}) \frac{1}{m_j \ln 10} dm_j}. \tag{7.8}$$

Here, $\underset{i}{\mathrm{ENV}}$ denotes the envelope over all feeding likelihood curves. To ensure that small and large predators contribute the same to functional diversity, integration was taken over $\log_{10} m_j$, which yields the factor $\frac{1}{m_j \ln 10}$. We derived the final functional diversity after the simulation of population dynamics, FD_{sim}, from the body masses of consumers that persisted the population dynamics. We addressed the question whether redundant or complementary species are more likely to persist by calculating the ratio between FD_{sim} and the functional diversity after random extinctions, FD_{rd}. For this we removed the same number of predator species that were lost during the simulation by random from the food web and calculated functional diversity of the remaining community (averaged over 100 repetitions).

Descriptive models

We applied nonlinear least squares (nls) and generalized linear modeling (glm) to illustrate the trends in the simulated data. The parameters species persistence, P, and final functional diversity, FD_{sim}, were described by a 4-parameter logistic function of initial predator species richness, S_P, using nls. Since these ignore the binomial error structure of proportion data we verified that the resulting parametric models are not distinguishable from nonparametric models with binomial error structure (generalized additive models; Zuur *et al.*, 2009; Wood, 2010; R Development Core Team, 2010). The functional diversity ratio FD_{sim}/FD_{rd} was described as a function of S_P using a linear least squares model. Finally, the metrics for basal and predator stocks and rates were modeled as functions of FD_{sim} by glm with gamma error structure using a logarithmic link (Zuur *et al.*, 2009). For the model of intraguild predation, replicates with value zero were omitted ($n = 289$; 0.7%).

Acknowledgements

We thank Amrei Binzer for comments on the manuscript. F.D.S. has been funded by Deutsche Bundesstiftung Umwelt (www.dbu.de).

Part III.

General discussion

Chapter 8.

Predator diversity and ecosystem functioning: a synthesis

Findings of this thesis

The research presented in this thesis re-builds the complexity that inherits diverse, multi-trophic predator communities on the basic assumption of allometry. In this final chapter, I conclude with a summary and draw a synthesis on the findings from six research studies which range from small scale predator–prey interactions to the large scale correlation between biodiversity and ecosystem functioning. In the following, I will discuss the results of the chapters of this thesis with regard to the four research questions.

(Q1) How can body mass explain the observed feeding rates of a predator on a prey?

The concepts of body-mass dependent feeding rates evolved rapidly during the last three years. The parameters of capture rate and handling time, which determine the density-dependent feeding rate of predators, have been related to allometric rules before (Brose, 2010*b*; Vucic-Pestic *et al.*, 2010; Rall *et al.*, 2011). Chapter 2 of this thesis goes one step further in understanding the dynamic behaviour of non-linear feeding rates. Here, I corroborated the body-mass dependency of the parameters of the functional response. The model defines handling time, h, as a positive exponential function of prey body mass and a negative exponential function of predator body mass. Thus, a large predator requires more time to handle relatively small prey (Fig. 2.1a, page 37). The capture rate, b, is maximized for prey of an optimal body-mass ratio and decreases for smaller as well as for larger prey (Fig. 2.1b). This hump-shaped feeding represents an optimal foraging trade-off. Very small prey species are difficult to find and provide only little energy, whereas large prey are rewarding but require more energy to subdue. An important novel finding of this study is the significant dependency of the capture coefficient, q, on body mass (Fig. 2.1c). This parameter can be modelled as a function of predator–prey body-mass ratio, predicting type-II functional responses for very large ratios and switching towards type-III functional responses for small ratios. This notion of a continuous variation of functional-response types

may enable a better understanding of predator feeding at low prey densities, which is critical for the stability of predator–prey systems. Indeed, the predictions achieved from this model produced an improved match to empirically observed predator–prey pairs than simpler models. Furthermore, I provided evidence that the higher number of parameters in this model is justified in comparison to models without a variable capture exponent.

The findings from Chapter 2 suggests the biological plausibility of allometric models for handling times and capture coefficients. Both dependencies were applied in the other studies of this thesis.

(Q2) Do these allometric feeding rates predict the effect of a predator in the context of a community?

In communities of multiple generalist feeders, indirect effects due to intraguild feeding are likely to occur. I observed the motif to occur in both microcosm experiments (Chapters 3, 4 and 5). The variable feeding rates within the motif rendered the net effect of a predator on a basal prey. It may be positive, if the cascading effect via the intraguild prey prevails, or it may be negative, if the direct feeding is predominating. Without knowledge on the food-web structure and the feeding rates, the effects of a particular species loss appears unpredictable (Chapter 3). A generalized model of allometric feeding rates, applied in a simulation of population dynamics was able to project the allometric feeding rates and predict the positive and negative, weak and strong net interaction strengths within the experimental community correctly (Chapter 4). With regard to absolute quantity, small bodied species should exert weak per capita effects, whereas large species should have strong per capita effects.

Furthermore, the successful qualitative prediction of positive or negative effects indicates the ability of allometric feeding rates to determine gradual intraguild predation, as a transition state between competition and straight food chains. It is worth mentioning that the model promoted in this thesis is largely mechanistic, in opposition to previous models which vary the strengths of intraguild predation by a phenomenological preference term (McCann and Hastings, 1997; Vandermeer, 2006; Kondoh, 2008).

Chapter 4 discusses the mismatch between the prediction and the observation for one of the predators, the lycosid spider *P. lugubris*. This mismatch is the consequence of body-mass independent species traits. Allometric models are not able to capture all of the variation in species-specific effects. Nonetheless, reducing the differentiation of species' feeding to one explanatory parameter – body mass – has got the potential to predict large parts of the interaction strengths in complex communities. The research question thus can be answered positively.

(Q3) How do these predictions scale with increasing predator diversity?

The study in Chapter 5 confirms the increased occurrence of intraguild predation in complex communities. The co-occurrence of multiple predators in the same community enables large predators to perform intraguild predation on others. This enables positive net effects, mediated via trophic cascades, whereas in the simple monoculture only direct feeding, and therefore only negative net effects are possible.

From the observed net interaction strengths in Chapters 3 and 4, a full mechanistic resolution of feeding interactions could be achieved because of the 'simplicity' of the food web. To resolve the feeding rates in a twelve species community of Chapter 5, the interaction strengths, as a metric which balances all direct and indirect feeding effects within the community, does not provide enough information. Instead I describe the net interaction strengths by simplifying linear models of population parameters. I corroborated the predictability of absolute interaction strengths (weak *vs.* strong) by population level characteristics of removed and target species, as it was proposed by Berlow *et al.* (2009). Furthermore, the quality and quantity of interaction strengths could be well predicted by the body mass of the predator and the population density of the target species. As was hypothesized by Berlow *et al.* (2009), the complexity of the surrounding community improved the predictability. The coefficient of determination doubled in the complex system compared to single predator communities. This counterintuitive finding promises a consolidating predictability of the net effect exercised by a diverse predator community on the lower trophic level.

A hypothesis from trophic cascade research suggests that suppressive effects on the lower trophic level in terrestrial systems should be dampened with increasing diversity because of enhanced intraguild predation (Strong, 1992; Pace *et al.*, 1999; Halaj and Wise, 2001). In both experiments reported in this thesis, the occurrence of intraguild predation was enabled with increasing diversity. Thus, the total suppression on the basal species level was diminished compared to the monoculture of the most exploitative predator. Further addition of predators with a high potential for intraguild predation, i.e. large predators, is likely to enhance these dampening predator effects. In contrast, I anticipate smaller species to enhance the direct feeding on the basal level. The hypothesis of dampened cascades may hold true for an increase in large predator species. However, the diversity range covered by the presented experiments is very narrow and thus does not allow a confident prediction of the development of prey suppression with increasing diversity.

(Q4) Can allometrically-defined predator species explain patterns at the ecosystem level?

The experiment in Chapter 6 was performed in field mesocosms in the marine subtidal. The described patterns in the response variables are thus less biased by experimental control but

include a higher residual error. The experimental treatment comprised a surgically precise manipulation of population body mass structure, which included the application of the allometric design and resulted in a gradient of average body mass. The experiment showed that with decreasing top-predator biomass the total community biomass and average individual body mass of the other species were increasing. Some species on lower trophic levels were affected by a gradual trophic cascade in response to average top-predator body mass.

The diversity experiments from chapters 3, 4 and 5, with three and five manipulated species, cover only low levels of diversity. It would require large-scaled experiments to describe the biodiversity–ecosystem functioning relationship from direct measurement. However, the complexity of natural ecosystems, which usually comprise hundreds to thousands of species, will never be tractable by experimental manipulation. Instead, the experiments reported in this thesis in the first place provide insight in the mechanisms of interactions among multiple predator species. The computational projection of these mechanisms to larger time-scales (Chapter 2) or larger scales of species richness (Chapter 7) by simulating population dynamics enables statements on the large-scale consequences of predator–prey interactions.

In Chapter 2, the empirically parameterized, allometric functional response model was employed in simple predator–prey population dynamics to project the persistence of both species over time. This provided a prediction of intrinsic stability for predator–prey pairs of particular body masses. The prediction showed a significant match with empirical body-mass data from predator–prey pairs observed in the field.

In Chapter 7, I finally apply a dynamic approach on a gradient of predator diversity to reproduce ecosystem functions. Here, based on allometric feeding rates, multiple predators of different body mass were assembled into communities and their total effect on the lower trophic level was simulated. This novel mechanistic approach on ecosystem functioning provides surprising insights in the mechanisms of community trophic cascades. Previous theory assumed that high predator diversity must induce low total predator biomass due to increased intraguild predation, and in consequence benefit total basal productivity due to released feeding pressure (Strong, 1992; Pace *et al.*, 1999; Halaj and Wise, 2001). I could show that this causal chain is erroneous. A highly diverse predator community with low total biomass can be more suppressive on the lower trophic level than a less diverse community. In diverse predator food webs, feeding withing the predator guild increased. As a consequence, the total biomass was directed into smaller predator species, which are less efficient in maintaining biomass due to their higher metabolic demands. The predator community became more exploitative but, at the same time, less efficient in maintaining energy. Finally, the basal productivity was lowest in diverse predator communities with low total biomass.

Thus, the allometric model allows the development of new mechanistic hypotheses for the relationship between biodiversity and ecosystem functioning while the application of an allometrically defined treatment design is able to produce compatible data.

A synthesis on allometrically defined predator identities

Rethinking species identity effects

Many papers in biodiversity–ecosystem functioning research that discuss the interactive effects of multiple species distinguish between the effect of biodiversity *per se* and the effects inherent to the particular species (Lawton, 1994; Duffy, 2002; Loreau *et al.*, 2001). For deviations of combined species effects from the summed effect of the species in monoculture 'species composition' effects are taken into account. This triumvirate of 'diversity effect', 'identity effects' and 'composition effects' has established as a statistical explanatory system for ecosystem functioning (Loreau and Hector, 2001; Fox, 2005; Bell *et al.*, 2009; Fox and Kerr, 2012). With respect to 'horizontal' variation of species richness *within* the trophic level this concept proved to be useful, because most composition effects reflect competition or facilitation between species. For multi-trophic diversity, however, indirect effects render the identity effects of a particular species strongly dependent on the presence and absence of the other predator species (Sih *et al.*, 1998; Worsfold *et al.*, 2009; Reiss *et al.*, 2011; Chapter 3).

The concept of a 'species identity effect' comes with some implications that are misguiding: It implies a fixed effect value of each species on the other elements of the community. Losing a particular species has a particular effect on the focal function. Thus, random species loss has unpredictable consequences. This was termed the idiosyncratic hypothesis (Lawton, 1994). The somehow fatalist notion was corrected by the concept of 'sampling effects', which assumes that each particular species has a particular set of species traits, which may be more or less suitable to the actual environment. With increasing diversity, the chance increases to include a highly suitable species, which may dominate the ecosystem-level effect ('sampling effect'; Huston, 1997; Tilman *et al.*, 1997). Thus, the observed pattern in ecosystem function with increasing diversity may be driven by an individual species. In this notion, the term 'species identity' can be defined as the entity that causes sampling effects. The 'identity effect' would be the total effect on ecosystem function that can be assigned to the presence of a particular species.

In Chapter 3, I translate this scaling of identity effects to multi-trophic communities by discussing the possibility of nested identity effects. Here, mites as the dominant predator species decreased the population density of springtails significantly. If centipedes were additively present, the effect of mites was dampened and the springtails were released from a feeding pressure. In absence of mites, the centipede had no significant effects. Additionally in Chapter 4, these feeding patterns could be predicted by a model of allometric functional responses. The general validity of this model for density-dependent feeding rates was highlighted in Chapter 2. Finally, the experiment of a more complex community presented in Chapter 5 corroborated the conditional character of species identity effects and their body-mass dependence. Intraguild predation was discussed here as a phenomenon of body-mass determined feeding that mediated the net interaction strength of a predator on a target basal species.

Altogether, this reveals the importance of food web structure and quantitative feeding rates for the determination of the net effect of a particular predator in a given food web context. I conclude, that the apparently idiosyncratic effects of species loss may be partially explained by allometric definitions of food web context and dynamic feeding interactions. At the same time, I admonish that allometry is no panacea for the prediction of species' identity effects. Many influences on species-specific trophic behaviour are not related to body mass. Species phenology, habitat preference or stoichiometry, to name but a few, will also contribute importantly to species differentiation. The species' phylogeny provides the biological frame in which feeding traits evolved. Therefore, recent investigations on food web structure suggest an integration of phylogeny in diet breadth models (Eklöf *et al.*, 2011; Stouffer *et al.*, 2011). In this vein, any body-mass independent effects can be incorporated into the allometric foraging model by adding a taxonomic factor to its parameters (Rall *et al.*, 2011). Here, trait based ecology promises a great set of methods to re-define the criteria for similarity and dissimilarity between species (McGill *et al.*, 2006; Reiss *et al.*, 2009). Finally, novel trait-based approaches might provide a more objective classification of species identity and functional groups (Reiss *et al.*, 2009; Rzanny and Voigt, 2012; Naeem *et al.*, 2012). The development of comprehensive trait data-bases might enable a more accurate prediction of species traits than can presently be achieved by body mass.

However,the study by Rall *et al.* (2011) indicates that body mass is a more efficient predictor for species feeding rates than taxonomy, because it requires far less assumptions in terms of model coefficients (Fig. 1.3). Thus, body mass should not be disregarded as one trait among many. Instead, it may provide a parsimonious null model for species' trait differentiation.

Rethinking experimental design

The experimental design for synthetic composition experiments necessarily influences the outcome of an experiment and the measured quantity of species effects. The density dependence of feeding rates will promote the effect of high or low predator or prey densities, especially in experiments that include trophic interactions. Therefore, experiments with multiple trophic levels will need a thorough *a priori* definition of densities to adjust the identity effect of the species to a 'realistic' value.

What defines a 'realistic' experimental identity effect? I assume, that it should be the aim of diversity experiments to approximate interaction effects as found in natural, unmanipulated communities. The closest manipulative approach would probably be an exclusion experiment, where the densities are not determined *a priori*. This approach, however, usually does not provide a full control of presence and absence of taxonomically resolved species. Therefore I anticipate, that in many cases the most realistic identity effects would be achieved by using field densities of the species and initialize a micro- or mesocosm experiment with those densities, as done in Chapter 5. This design was also used most successfully, for instance, to identify the

consequences of intraguild feeding in salt marsh communities (Finke and Denno, 2004). A deviation from field densities can be perceived as a bias of identity effects. Note, however, that the dynamic character of field densities provides some tolerance for the design of synthetic composition experiments.

In the experiments reported in this thesis, I propose an 'allometric design' that balances the abundance and biomass of the initial densities on basis of an allometric power law (Chapter 3 and 4; Griffiths *et al.*, 2008). I explained that a bias, either by individual density or biomass density, is inevitable when using differently sized predators (Box 2). In a prototype of an allometric design, I tried a negative $^3/_4$ power law with body mass to determine the initial densities of predators (Chapters 3 and 4). This yielded identity effects which were largely reproducible by allometric feeding rates in a dynamic simulation (Chapter 4). Nonetheless, the choice of the exponent may be too steep, as indicated by empirical investigations on local allometric mass–abundance scaling (White *et al.*, 2007). In Chapter 6, I therefore adopted an empirically documented mass–abundance scaling for the local habitat with an exponent of $-^1/_4$. Finally, the scaling should differ between trophic levels, due to the different energetic requirements and assimilation efficiencies (Brown *et al.*, 2004), as was documented by the natural abundances used in Chapter 5.

In many synthetic composition experiments, however, the initial abundances or biomass densities were standardized to a fixed value (Reiss *et al.*, 2009; Schmitz, 2007). This was intended as an *a priori* control of the per capita effects or per gram effects of the predator species, respectively. I remark that this implies a scaling of initial population density with body mass to the power of 0 (fixed-abundance) or -1 (fixed biomass), causing a maximal bias by biomass or abundance, respectively (Fig. 1.4 on page 22). Any such design should fail to produce 'natural' identity effects. In contrast, an allometric design proposes a valuable compromise.

The list of applied examples for allometric experimental designs is very short. Therefore, the hypothesis that allometric designs produce more 'natural' or 'realistic' identity effects still needs to be evaluated in comparative experiments and simulations.

Rethinking biodiversity-ecosystem functioning

Naeem (2002) described the research on biodiversity–ecosystem functioning as a paradigm of ecological science. The historical development of this research was initiated by the formulation of the notion that ecosystem functioning should be a function of biodiversity or, more general, a function of ecological properties of a number of species, individual traits, genes (Naeem *et al.*, 2002; Loreau, 2010*a*). The debate departed from a holistic view, by describing the relationship phenomenologically, but nowadays successively approach the mechanisms behind the correlation (Naeem *et al.*, 2002; Loreau, 2010*a*). However, research under this topic largely applied a one-sided view on the relationship, neglecting that a change in stability and

alterations in functioning will also lead to changes in species composition and species richness (but see Loreau, 2010*a*).

The diversity–stability debate complemented the biodiversity–ecosystem functioning debate, by perceiving species densities and species extinction as a consequence of the community dynamics (May, 1972; Loreau, 2000; McCann, 2000; Rooney and McCann, 2012). The integration of food web theory into this debate was able to provide a description of communities as highly connected networks of species populations (Dunne, 2006). In this understanding, species diversity is a consequence of individual species properties and environmental conditions.

In recent years, both notions converged successively (e.g. Loreau, 2000; Ives *et al.*, 2005; Thébault and Loreau, 2005, 2006). In this vein, this thesis aims at achieving a theoretical framework incorporating both perspectives in equal rights. Therefore, I apply concepts from allometric predator–prey and food-web theory to build plausible communities of differentiated predator species. Body mass serves as a universal determinant to define the feeding and population behaviour of predators. These are assembled in communities of different species number. This approach represents a reductionist view, because it assumes that all patterns on the higher ecosystem level emerge from interactions on the small population or individual level.

How does this connect to previous biodiversity–ecosystem functioning research? In microcosm experiments (Chapters 2–5), I investigate the ability of allometrically defined predators to express all major mechanisms that were proposed as drivers of the biodiversity–ecosystem functioning relationship. This includes niche-differentiation (or niche-complementarity), sampling effects of predator identities and indirect interactions induced by intraguild predation. The outcome of these studies was a mechanistic model for predator feeding that differentiates predators simply by their difference in body mass. This allometric model provides horizontal (diet breadth) and vertical (trophic level) differentiation at the same time. In Chapter 7, I employ this model in a mechanistic simulation of the relationship between functional diversity and ecosystem functioning. I found, that the increased diversity indeed promotes intraguild feeding. However, this did not diminish the total feeding of the predator community. The basal trophic level was not released from top-down pressure. The patterns obtained from this simulation provided a mechanistic insight into a long-lasting conundrum of diversity ecology: the community trophic cascade.

The metabolic theory of ecology furthermore incorporates temperature as a determinant of physiological rates (Brown *et al.*, 2004; Ehnes *et al.*, 2011; Binzer *et al.*, 2012). Therefore, this compatibility enables an easy integration of temperature into all of the modelling concepts described here. Also, interactions of top-down predator effects with bottom-up effects of nutrient enrichment can be investigated (Binzer *et al.*, 2012). The opportunities for global-change research are manifold (Woodward, 2010; Montoya and Raffaelli, 2010; Brose *et al.*, 2012). Therefore, I anticipate that this mechanistic perspective on diversity effects, which is not limited to body mass, is a promising road to our understanding of ecological complexity.

Part IV.

Appendix

References

Aljetlawi, A. A., Sparrevik, E., and Leonardsson, K. (2004). Prey-Predator Size-Dependent functional response: Derivation and rescaling to the real world. *Journal of Animal Ecology* 73:239–252.

Allesina, S. (2011). Predicting trophic relations in ecological networks: A test of the allometric diet breadth model. *Journal of Theoretical Biology* 279:161–168.

Allesina, S., Alonso, D., and Pascual, M. (2008). A general model for food web structure. *Science* 320:658–661.

Allesina, S. and Tang, S. (2012). Stability criteria for complex ecosystems. *Nature* 483:205–208.

Alpine, A. E. and Cloern, J. E. (1992). Trophic interactions and direct physical effects control phytoplankton biomass and production in an estuary. *Limnology and Oceanography* 37(5):946–955.

Atalah, J. and Crowe, T. P. (2010). Combined effects of nutrient enrichment, sedimentation and grazer loss on rock pool assemblages. *Journal of Experimental Marine Biology and Ecology* 388:51–57.

Balvanera, P., Pfisterer, A. B., Buchmann, N., He, J. S., Nakashizuka, T., Raffaelli, D., and Schmid, B. (2006). Quantifying the evidence for biodiversity effects on ecosystem functioning and services. *Ecology Letters* 9:1146–1156.

Bascompte, J. and Melian, C. J. (2005). Simple trophic modules for complex food webs. *Ecology* 86:2868–2873.

Beck, T., Joergensen, R. G., Kandeler, E., Makeschin, F., Nuss, E., Oberholzer, H. R., and Scheu, S. (1997). An inter-laboratory comparison of ten different ways of measuring soil microbial biomass C. *Soil Biology & Biochemistry* 29:1023–1032.

Beckerman, A. P., Petchey, O. L., and Warren, P. H. (2006). Foraging biology predicts food web complexity. *Proceedings of the National Academy of Sciences, U.S.A.* 103:13745–13749.

Bell, T., Lilley, A. K., Hector, A., Schmid, B., King, L., and Newman, J. A. (2009). A linear model method for biodiversity–ecosystem functioning experiments. *The American Naturalist* 174:836–849.

Berlow, E. L., Dunne, J. A., Martinez, N. D., Stark, P. B., Williams, R. J., and Brose, U. (2009). Simple prediction of interaction strengths in complex food webs. *Proceedings of the National Academy of Sciences, U.S.A.* 106:187–191.

Berlow, E. L., Navarrete, S. A., Briggs, C. J., Power, M. E., and Menge, B. A. (1999). Quantifying variation in the strengths of species interactions. *Ecology* 80:2206–2224.

Berlow, E. L., Neutel, A. M., Cohen, J. E., de Ruiter, P. C., Ebenman, B., Emmerson, M., Fox, J. W., Jansen, V. A. A., Jones, J. I., Kokkoris, G. D., Logofet, D. O., McKane, A. J., Montoya, J. M., and Petchey, O. (2004). Interaction strengths in food webs: issues and opportunities. *Journal of Animal Ecology* 73:585–598.

Beukema, J. J. (1991). Changes in composition of bottom fauna of a tidal-flat area during a period of eutrophication. *Marine Biology* 111:293–301.

Binzer, A., Brose, U., Curtsdotter, A., Eklöf, A., Rall, B. C., Riede, J. O., and de Castro, F. (2011). The susceptibility of species to extinctions in model communities. *Basic and Applied Ecology* 12:590–599.

Binzer, A., Guill, C., Brose, U., and Rall, B. C. (2012). The dynamics of food chains under climate change and nutrient enrichment. *Philosophical Transactions of the Royal Society B: Biological Sciences* in press, doi: 10.1098/rstb.2012.0230.

Bolker, B., (2008). *Ecological Models and Data in R*. Princeton University Press, Princeton, USA. ISBN 0-691-12522-8.

Bonsdorff, E., Blomqvist, E. M., Mattila, J., and Norkko, A. (1997). Coastal eutrophication: causes, consequences and perspectives in the archipelago areas of the northern baltic sea. *Estuarine, Coastal and Shelf Science* 44:63–72.

Borer, E. T., Halpern, B. S., and Seabloom, E. W. (2006). Asymmetry in community regulation: Effects of predators and productivity. *Ecology* 87:2813–2820.

Borer, E. T., Seabloom, E. W., Shurin, J. B., Anderson, K. E., Blanchette, C. A., Broitman, B., Cooper, S. D., and Halpern, B. S. (2005). What determines the strength of a trophic cascade? *Ecology* 86:528–537.

Brose, U. (2008). Complex food webs prevent competitive exclusion among producer species. *Proceedings of the Royal Society B: Biological Sciences* 275:2507–2514.

Brose, U. (2010*a*). Body-mass constraints on foraging behaviour determine population and food-web dynamics. *Functional Ecology* 24:28–34.

Brose, U. (2010*b*). Improving nature conservancy strategies by ecological network theory. *Basic and Applied Ecology* 11:1–5.

Brose, U., Cushing, L., Berlow, E. L., Jonsson, T., Banasek-Richter, C., Bersier, L. F., Blanchard, J. L., Brey, T., Carpenter, S. R., Cattin Blandenier, M. F., Cohen, J. E., Dawah, H. A., Dell, T., Edwards, F., Harper-Smith, S., Jacob, U., Knapp, R. A., Ledger, M. E., Memmott, J., Mintenbeck, K., Pinnegar, J. K., Rall, B. C., Rayner, T., Ruess, L., Ulrich, W., Warren, P., Williams, R. J., Woodward, G., Yodzis, P., and Martinez, N. D. (2005). Body sizes of consumers and their resources. *Ecology* 86:2545.

Brose, U., Dunne, J. A., Montoya, J. M., Petchey, O. L., Schneider, F. D., and Jacob, U. (2012). Climate change in size-structured ecosystems. *Philosophical Transactions of the Royal Society B: Biological Sciences* in press.

Brose, U., Ehnes, R. B., Rall, B. C., Vucic-Pestic, O., Berlow, E. L., and Scheu, S. (2008). Foraging theory predicts predator-prey energy fluxes. *Journal of Animal Ecology* 77:1072–1078.

Brose, U., Jonsson, T., Berlow, E. L., Warren, P., Banasek-Richter, C., Bersier, L. F., Blanchard, J. L., Brey, T., Carpenter, S. R., Cattin Blandenier, M. F., Cushing, L., Dawah, H. A., Dell, T., Edwards, F., Harper-Smith, S., Jacob, U., Ledger, M. E., Martinez, N. D., Memmott, J., Mintenbeck, K., Pinnegar, J. K., Rall, B. C., Rayner, T., Reuman, D. C., Ruess, L., Ulrich, W., Williams, R. J., Woodward, G., and Cohen, J. E. (2006*a*). Consumer-resource body-size relationships in natural food webs. *Ecology* 87:2411–2417.

Brose, U., Williams, R. J., and Martinez, N. D. (2003). Comment on "Foraging adaptation and the relationship between food-web complexity and stability". *Science* 301:918.

Brose, U., Williams, R. J., and Martinez, N. D. (2006*b*). Allometric scaling enhances stability in complex food webs. *Ecology Letters* 9:1228–1236.

Brown, J. H., Gillooly, J. F., Allen, A. P., Savage, V. M., and West, G. B. (2004). Toward a metabolic theory of ecology. *Ecology* 85:1771–1789.

Bruno, J. F., Boyer, K. E., Duffy, J. E., and Lee, S. C. (2008). Relative and interactive effects of plant and grazer richness in a benthic marine community. *Ecology* 89:2518–2528.

Bruno, J. F., Boyer, K. E., Duffy, J. E., Lee, S. C., and Kertesz, J. S. (2005). Effects of macroalgal species identity and richness on primary production in benthic marine communities. *Ecology Letters* 8:1165–1174.

Bruno, J. F. and O'Connor, M. I. (2005). Cascading effects of predator diversity and omnivory in a marine food web. *Ecology Letters* 8:1048–1056.

Buffan-Dubau, E. and Carman, K. R. (2000). Diel feeding behavior of meiofauna and their relationships with microalgal resources. *Limnology and Oceanography* 45(2):381–395.

Byrnes, J. E. and Stachowicz, J. J. (2009). The consequences of consumer diversity loss: different answers from different experimental designs. *Ecology* 90:2879–2888.

Byrnes, J. E., Stachowicz, J. J., Hultgren, K. M., Randall Hughes, A., Olyarnik, S. V., and Thornber, C. S. (2006). Predator diversity strengthens trophic cascades in kelp forests by modifying herbivore behaviour. *Ecology Letters* 9:61–71.

Cardillo, M., Mace, G. M., Jones, K. E., Bielby, J., Bininda-Emonds, O., Sechrest, W., Orme, C. D., and Purvis, A. (2005). Multiple causes of high extinction risk in large mammal species. *Science* 309:1239–1241.

Cardinale, B. J., Duffy, J. E., Srivastava, D. S., Loreau, M., Thomas, M. B., and Emmerson, M. C., (2009). Towards a food web perspective on biodiversity and ecosystem functioning. Pages 105–120 *in* Biodiversity, Ecosystem Functioning, & Human Wellbeing An Ecological and Economic Perspective. Oxford University Press, Oxford, UK, 2 edition. ISBN 978-0-19-954796-8.

Carman, K. R., Fleeger, J. W., and Pomarico, S. M. (1997). Response of a benthic food web to hydrocarbon contamination. *Limnology and Oceanography* 42(3):561–571.

Cattin, M., Bersier, L., Banasek-Richter, C., Baltensperger, R., and Gabriel, J. (2004). Phylogenetic constraints and adaptation explain food-web structure. *Nature* 427:835–839.

Cohen, J. E., (1978). *Food webs and niche space*. Princeton University Press, Princeton, USA. ISBN 978-0-691-08202-8.

Cohen, J. E. (1990). A stochastic theory of community food webs. VI. heterogeneous alternatives to the cascade model. *Theoretical population biology* 37:55–90.

Cohen, J. E., Beaver, R. A., Cousins, S. H., DeAngelis, D. L., Goldwasser, L., Heong, K. L., Holt, R. D., Kohn, A. J., Lawton, J. H., Martinez, N., *et al.* (1993). Improving food webs. *Ecology* 74:252–258.

Cottingham, K. L., Brown, B. L., and Lennon, J. T. (2001). Biodiversity may regulate the temporal variability of ecological systems. *Ecology Letters* 4:72–85.

Crain, C. M., Kroeker, K., and Halpern, B. S. (2008). Interactive and cumulative effects of multiple human stressors in marine systems. *Ecology letters* 11:1304–1315.

Crawley, M. J., (1992). *Natural enemies: the population biology of predators, parasites and diseases*. Blackwell Scientific.

Crawley, M. J., (2007). *The R Book*. John Wiley & Sons, West Sussex, UK. ISBN 978-0470510247.

Damuth, J. (1987). Interspecific allometry of population density in mammals and other animals: the independence of body mass and population energy-use. *Biological Journal of the Linnean Society* 31:193–246.

Daskalov, G. M., Grishin, A. N., Rodionov, S., and Mihneva, V. (2007). Trophic cascades triggered by overfishing reveal possible mechanisms of ecosystem regime shifts. *Proceedings of the National Academy of Sciences, U.S.A.* 104:10518–10523.

Daufresne, M., Lengfellner, K., and Sommer, U. (2009). Global warming benefits the small in aquatic ecosystems. *Proceedings of the National Academy of Sciences, U.S.A.* 106:12788 –12793.

de Ruiter, P. C., Neutel, A. M., and Moore, J. C. (1995). Energetics, patterns of interaction strengths, and stability in real ecosystems. *Science* 269:1257–1260.

De Troch, M., Chepurnov, V. A., Vincx, M., and Olafsson, E. (2008). The effect of *Fucus vesiculosus* on the grazing of harpacticoid copepods on diatom biofilms. *Journal of Sea Research* 60:139–143.

De Troch, M., Steinarsdóttir, M. B., Chepurnov, V., Ólafsson, E., *et al.* (2005). Grazing on diatoms by harpacticoid copepods: species-specific density-dependent uptake and microbial gardening. *Aquatic microbial ecology* 39.

DeAngelis, D. L. and Waterhouse, J. C. (1987). Equilibrium and nonequilibrium concepts in ecological models. *Ecological monographs* page 1–21.

Dell, A. I., Kokkoris, G. D., Banašek-Richter, C., Bersier, L. F., Dunne, J. A., Kondoh, M., Romanuk, T. N., and Martinez, N. D., (2005). How do complex food webs persist in nature? Pages 425–436 in *P. De Ruiter, V. Wolters, and J. C. Moore, eds. Dynamic Food Webs: Multispecies assemblages, ecosystem development, and environmental change*. Elsevier Academic Press Inc., Burlington, USA. ISBN 978-0-12-088458-2.

Dial, K. P., Greene, E., and Irschick, D. J. (2008). Allometry of behavior. *Trends in Ecology & Evolution* 23:394–401.

Digel, C., Riede, J. O., and Brose, U. (2011). Body sizes, cumulative and allometric degree distributions across natural food webs. *Oikos* 120:503–509.

Duffy, J. E. (2002). Biodiversity and ecosystem function: the consumer connection. *Oikos* 99:201–219.

Duffy, J. E., Cardinale, B. J., France, K. E., McIntyre, P. B., Thébault, E., and Loreau, M. (2007). The functional role of biodiversity in ecosystems: incorporating trophic complexity. *Ecology Letters* 10:522–538.

Dunger, W., (2008). *Tiere im Boden*. Westarp Wissenschaften, Hohenwarsleben, GER, 4 edition. ISBN 978-3-89432-424-7.

Dunne, J. A., (2006). The network structure of food webs in *J. A. Dunne and M. Pascual, eds. Ecological Networks: Linking Structure to Dynamics in Food Webs*. Oxford University Press, New York, USA. ISBN 978-0-19-518816-5.

Dunne, J. A. and Williams, R. J. (2009). Cascading extinctions and community collapse in model food webs. *Philosophical Transactions of the Royal Society B: Biological Sciences* 364:1711–1723.

Dunne, J. A., Williams, R. J., and Martinez, N. D. (2002*a*). Food-web structure and network theory: the role of connectance and size. *Proceedings of the National Academy of Sciences, U.S.A.* 99:12917.

Dunne, J. A., Williams, R. J., and Martinez, N. D. (2002*b*). Network structure and biodiversity loss in food webs: robustness increases with connectance. *Ecology Letters* 5:558–567.

Dunne, J. A., Williams, R. J., and Martinez, N. D. (2004). Network structure and robustness of marine food webs. *Marine Ecology Progress Series* 273:291–302.

Ehnes, R. B., Rall, B. C., and Brose, U. (2011). Phylogenetic grouping, curvature and metabolic scaling in terrestrial invertebrates. *Ecology Letters* 14:993–1000.

Eklöf, A. and Ebenman, B. O. (2006). Species loss and secondary extinctions in simple and complex model communities. *Journal of Animal Ecology* 75:239–246.

Eklöf, A., Helmus, M. R., Moore, M., and Allesina, S. (2011). Relevance of evolutionary history for food web structure. *Proceedings of the Royal Society B: Biological Sciences* 279:1588–1596.

Elton, C., (1927). *Animal Ecology*. University of Chicago Press, Chicago, USA, reprint 2001, 2nd edition. ISBN 978-0-226-20639-4.

Emmerson, M., Bezemer, T. M., Hunter, M. D., Jones, T. H., Masters, G. J., and Van Dam, N. M. (2004). How does global change affect the strength of trophic interactions? *Basic And Applied Ecology* 5:505–514.

Emmerson, M. and Yearsley, J. M. (2004). Weak interactions, omnivory and emergent food-web properties. *Proceedings Of The Royal Society Of London Series B-Biological Sciences* 271:397–405.

Emmerson, M. C., Solan, M., Emes, C., Paterson, D. M., and Raffaelli, D. (2001). Consistent patterns and the idiosyncratic effects of biodiversity in marine ecosystems. *Nature* 411:73–77.

Englund, G., Öhlund, G., Hein, C. L., and Diehl, S. (2011). Temperature dependence of the functional response. *Ecology Letters* 14:914–921.

Estes, J. A. and Palmisano, J. F. (1974). Sea otters: their role in structuring nearshore communities. *Science* 185:1058–1060.

Estes, J. A., Tinker, M. T., Williams, T. M., and Doak, D. F. (1998). Killer whale predation on sea otters linking oceanic and nearshore ecosystems. *Science* 282:473–476.

Fagan, W. F. and Denno, R. F. (2004). Stoichiometry of actual vs. potential predator-prey interactions: insights into nitrogen limitation for arthropod predators. *Ecology Letters* 7:876–883.

Finke, D. L. and Denno, R. F. (2004). Predator diversity dampens trophic cascades. *Nature* 429:407–410.

Finke, D. L. and Denno, R. F. (2005). Predator diversity and the functioning of ecosystems: the role of intraguild predation in dampening trophic cascades. *Ecology Letters* 8:1299–1306.

Fischer, M., Bossdorf, O., Gockel, S., Hänsel, F., Hemp, A., Hessenmöller, D., Korte, G., Nieschulze, J., Pfeiffer, S., Prati, D., Renner, S., Schöning, I., Schumacher, U., Wells, K., Buscot, F., Kalko, E. K., Linsenmair, K. E., Schulze, E., and Weisser, W. W. (2010). Implementing large-scale and long-term functional biodiversity research: The biodiversity exploratories. *Basic and Applied Ecology* 11:473–485.

Fisher, M. R. (1999). Effect of temperature and salinity on size at maturity of female blue crabs. *Transactions of the American Fisheries Society* 128:499–506.

Foelix, R. F., (1996). *Biology of Spiders*. Oxford University Press, New York, second edition.

Fontaine, C., Guimarães Jr, P. R., Kéfi, S., Loeuille, N., Memmott, J., van der Putten, W. H., van Veen, F. J. F., and Thébault, E. (2011). The ecological and evolutionary implications of merging different types of networks. *Ecology Letters* 14:1170–1181.

Fox, J. (2006). Using the price equation to partition the effects of biodiversity loss on ecosystem function. *Ecology* 87:2687–2696.

Fox, J. W. (2005). Interpreting the 'selection effect' of biodiversity on ecosystem function. *Ecology Letters* 8:846–856.

Fox, J. W. and Kerr, B. (2012). Analyzing the effects of species gain and loss on ecosystem function using the extended price equation partition. *Oikos* 121:290–298.

Fryxell, J. M., Mosser, A., Sinclair, A. R. E., and Packer, C. (2007). Group formation stabilizes predator–prey dynamics. *Nature* 449:1041–1043.

Gaines, S. D. and Denny, M. W. (1993). The largest, smallest, highest, lowest, longest, and shortest: extremes in ecology. *Ecology* 74:1677–1692.

Galassi, M., Davies, J., Theiler, J., Gough, B., Jungman, G., Booth, M., Rossi, F., and Alken, P., (2011). *GNU scientific library: reference manual*. Network Theory Limited. ISBN 978-0-9541617-0-5.

Gardner, J. L., Peters, A., Kearney, M. R., Joseph, L., and Heinsohn, R. (2011). Declining body size: a third universal response to warming? *Trends in Ecology & Evolution* 26:285–291.

Gellner, G. and McCann, K. (2012). Reconciling the Omnivory-Stability debate. *The American Naturalist* 179:22–37.

Greig, H. S., Kratina, P., Thompson, P. L., Palen, W. J., Richardson, J. S., and Shurin, J. B. (2012). Warming, eutrophication, and predator loss amplify subsidies between aquatic and terrestrial ecosystems. *Global Change Biology* 18:504–514.

Griffin, J. N., de la Haye, K. L., Hawkins, S. J., Thompson, R. C., and Jenkins, S. R. (2008). Predator diversity and ecosystem functioning: Density modifies the effect of resource partitioning. *Ecology* 89:298–305.

Griffin, J. N., OGorman, E. J., Emmerson, M. C., Jenkins, S. R., Klein, A. M., Loreau, M., and Symstad, A., (2009). Biodiversity and the stability of ecosystem functioning. page 78–94 *in* Biodiversity, Ecosystem Functioning, and Human Wellbeing. Oxford University Press, Oxford, UK, 2 edition. ISBN 978-0-19-954796-8.

Griffiths, G. J. K., Wilby, A., Crawley, M. J., and Thomas, M. B. (2008). Density-dependent effects of predator species-richness in diversity-function studies. *Ecology* 89:2986–2993.

Hairston, N. G., Smith, F. E., and Slobodkin, L. B. (1960). Community structure, population control, and competition. *The American Naturalist* 94:145–159.

Halaj, J. and Wise, D. H. (2001). Terrestrial trophic cascades: how much do they trickle? *The American Naturalist* 157:262–281.

Halpern, B. S., McLeod, K. L., Rosenberg, A. A., and Crowder, L. B. (2008). Managing for cumulative impacts in ecosystem-based management through ocean zoning. *Ocean & Coastal Management* 51:203–211.

Harding, L. W. and Perry, E. S. (1997). Long-term increase of phytoplankton biomass in chesapeake bay, 1950-1994. *Marine Ecology Progress Series* 157:39–52.

Harley, C. D. G., Randall Hughes, A., Hultgren, K. M., Miner, B. G., Sorte, C. J. B., Thornber, C. S., Rodriguez, L. F., Tomanek, L., and Williams, S. L. (2006). The impacts of climate change in coastal marine systems. *Ecology Letters* 9:228–241.

Hassell, M. P., (1978). *The Dynamics of Arthopod Predator-Prey Systems.* Number 13 in Monographs in Population Biology. Princeton University Press, Princeton, USA. ISBN 978-0-691-08215-8.

Hassell, M. P., Lawton, J. H., and Beddington, J. R. (1976). The components of arthropod predation: I. the prey death-rate. *Journal of Animal Ecology* 45:135–164.

Hassell, M. P., Lawton, J. H., and Beddington, J. R. (1977). Sigmoid functional responses by invertebrate predators and parasitoids. *Journal of Animal Ecology* 46:249–262.

Heithaus, M. R., Frid, A., Wirsing, A. J., and Worm, B. (2008). Predicting ecological consequences of marine top predator declines. *Trends in Ecology & Evolution* 23:202–210.

Hohberg, K. and Traunspurger, W. (2005). Predator–prey interaction in soil food web: functional response, size-dependent foraging efficiency, and the influence of soil texture. *Biology and fertility of soils* 41:419–427.

Holling, C. (1959*a*). The components of predation as revealed by a study of Small-Mammal predation of the european pine sawfly. *The Canadian Entomologist* 91:293–320.

Holling, C. (1959*b*). Some characteristics of simple types of predation and parasitism. *The Canadian Entomologist* 91:385–398.

Holt, R. D. (2002). Food webs in space: On the interplay of dynamic instability and spatial processes. *Ecological Research* 17:261–273.

Holt, R. D. and Polis, G. A. (1997). A theoretical framework for intraguild predation. *The American Naturalist* 149:745–764.

Hooper, D. U., Chapin, F. S., Ewel, J. J., Hector, A., Inchausti, P., Lavorel, S., Lawton, J. H., Lodge, D. M., Loreau, M., Naeem, S., Schmid, B., Setälä, H., Symstad, A. J., Vandermeer, J., and Wardle, D. A. (2005). Effects of biodiversity on ecosystem functioning: A consensus of current knowledge. *Ecological Monographs* 75:3–35.

Hooper, D. U., Solan, M., Symstad, A., Diaz, S., Gessner, M. O., Buchmann, N., Degrange, V., Grime, P., Hulot, F., Mermillod-Blondin, F., Roy, J., Spehn, E., and van Peer, L., (2002). Species diversity, functional diversity and ecosystem functioning. page 195–208 in *M. Loreau, S. Naeem, and P. Inchausti, eds. Biodiversity and Ecosystem Functioning: Syntheses and Perspectives.* Oxford University Press, New York, USA. ISBN 978-0-19-851570-8.

Huisman, J. and Weissing, F. J. (1999). Biodiversity of plankton by species oscillations and chaos. *Nature* 402:407–410.

Hunter, M. D. and Price, P. W. (1992). Playing chutes and ladders: heterogeneity and the relative roles of bottom-up and top-down forces in natural communities. *Ecology* 73:723–732.

Huston, M. A. (1997). Hidden treatments in ecological experiments: re-evaluating the ecosystem function of biodiversity. *Oecologia* 110:449–460.

IPCC Core Writing Team, Pachauri, R. K., and Reisinger, A., (2007). *Climate Change 2007: Synthesis Report. Contribution of Working Groups I, II and III to the Fourth Assessment Report of the Intergovernmental Panel on Climate Change.* IPCC, Geneva, Switzerland.

Ives, A. R., Cardinale, B. J., and Snyder, W. E. (2005). A synthesis of subdisciplines: predator-prey interactions, and biodiversity and ecosystem functioning. *Ecology Letters* 8:102–116.

Ives, A. R. and Carpenter, S. R. (2007). Stability and diversity of ecosystems. *Science* 317:58–62.

Jacob, U., Thierry, A., Brose, U., Arntz, W. E., Berg, S., Brey, T., Fetzer, I., Jonsson, T., Mintenbeck, K., Möllmann, C., Petchey, O. L., Riede, J. O., and Dunne, J. A., (2011). The role of body size in

complex food webs: A cold case. Pages 182–223 in *A. Belgrano, ed. The Role of Body Size in Multispecies Systems*, number 45 in Advances in Ecological Research. Academic Press, London, UK.

Jennings, S. and Mackinson, S. (2003). Abundance–body mass relationships in size-structured food webs. *Ecology Letters* 6:971–974.

Jeschke, J. M., Kopp, M., and Tollrian, R. (2002). Predator functional responses: discriminating between handling and digesting prey. *Ecological Monographs* 72:95–112.

Jeschke, J. M., Kopp, M., and Tollrian, R. (2004). Consumer-food systems: why type i functional responses are exclusive to filter feeders. *Biological Reviews* 79:337–349.

Jochum, M., Schneider, F. D., Crowe, T. P., Brose, U., and O'Gorman, E. J. (2012). Climate-induced changes in bottom-up and top-down processes independently alter a marine ecosystem. *Philosophical Transactions of the Royal Society B: Biological Sciences* in press, doi: 10.1098/rstb.2012.0237.

Kalinkat, G., Rall, B. C., Vucic-Pestic, O., and Brose, U. (2011). The allometry of prey preferences. *PLoS ONE* 6:e25937.

Kéfi, S., Berlow, E. L., Wieters, E. A., Navarrete, S. A., Petchey, O. L., Wood, S. A., Boit, A., Joppa, L. N., Lafferty, K. D., Williams, R. J., Martinez, N. D., Menge, B. A., Blanchette, C. A., Iles, A. C., and Brose, U. (2012). More than a meal... integrating non-feeding interactions into food webs. *Ecology Letters* 15:291–300.

Kempson, D., Lloyd, M., and Ghelardi, R. (1963). A new extractor for woodland litter. *Pedobiologia* 3:1–21.

Klassen, G. J. and Locke, A. (2007). A biological synopsis of the european green crab, *Carcinus maenas*. *Canadian Manuscript Report of Fisheries and Aquatic Sciences* 2818:1–75.

Kleiber, M. (1947). Body size and metabolic rate. *Physiological reviews* 27:511–541.

Koen-Alonso, M., (2007). A process-oriented approach to the multispecies functional response. page 1–36 in *N. Rooney, K. S. McCann, and D. Noakes, eds. From energetics to ecosystems: the dynamics and structure of ecological systems*, number 1 in The Peter Yodzis Fundamental Ecology Series. Springer, Dordrecht. ISBN 978-1-4020-5336-8.

Kohda, M., Shibata, J.-y., Awata, S., Gomagano, D., Takeyama, T., Hori, M., and Heg, D. (2008). Niche differentiation depends on body size in a cichlid fish: a model system of a community structured according to size regularities. *Journal of Animal Ecology* 77:859–868.

Kondoh, M. (2003). Foraging adaptation and the relationship between food-web complexity and stability. *Science* 299:1388–1391.

Kondoh, M. (2008). Building trophic modules into a persistent food web. *Proceedings of the Royal Society of London. Series B: Biological Sciences* 105:16631–16635.

Kumar, P. and United Nations Environment Programme (UNEP), (2010). *The Economics of Ecosystems and Biodiversity: Ecological and Economic Foundations*. Earthscan. ISBN 978-1-84971-212-5.

Laliberté, E. and Legendre, P. (2010). A distance-based framework for measuring functional diversity from multiple traits. *Ecology* 91:299–305.

Lang, B., Rall, B. C., and Brose, U. (2011). Warming effects on consumption and intraspecific interference competition depend on predator metabolism. *Journal of Animal Ecology* 81:516–523.

Laska, M. S. and Wootton, J. T. (1998). Theoretical concepts and empirical approaches to measuring interaction strength. *Ecology* 79:461–476.

Lawton, J. H. (1994). What do species do in ecosystems? *Oikos* 71:367–374.

Lawton, J. H. (1999). Are there general laws in ecology? *Oikos* 84:177–192.

Letourneau, D. K., Jedlicka, J. A., Bothwell, S. G., and Moreno, C. R. (2009). Effects of natural enemy biodiversity on the suppression of arthropod herbivores in terrestrial ecosystems. *Annual Review of Ecology, Evolution, and Systematics* 40:573–592.

Loeuille, N. and Loreau, M. (2005). Evolutionary emergence of size-structured food webs. *Proceedings of the National Academy of Sciences, U.S.A.* 102:5761 –5766.

Long, Z. T., Bruno, J. F., and Duffy, J. E. (2007). Biodiversity mediates productivity through different mechanisms at adjacent trophic levels. *Ecology* 88:2821–2829.

Loreau, M. (2000). Biodiversity and ecosystem functioning: recent theoretical advances. *Oikos* 91:3–17.

Loreau, M., (2010*a*). *From Populations to Ecosystems: Theoretical Foundations for a New Ecological Synthesis*. Princeton University Press, Princeton, USA. ISBN 978-0-691-12270-0.

Loreau, M. (2010*b*). Linking biodiversity and ecosystems: towards a unifying ecological theory. *Philosophical Transactions of the Royal Society B: Biological Sciences* 365:49–60.

Loreau, M. and Hector, A. (2001). Partitioning selection and complementarity in biodiversity experiments. *Nature* 412:72–76.

Loreau, M., Naeem, S., and Inchausti, P., eds., (2002). *Biodiversity and ecosystem functioning: synthesis and perspectives*. Oxford University Press, New York, USA. ISBN 978-0-19-851571-5.

Loreau, M., Naeem, S., Inchausti, P., Bengtsson, J., Grime, J. P., Hector, A., Hooper, D. U., Huston, M. A., Raffaelli, D., Schmid, B., Tilman, D., and Wardle, D. A. (2001). Biodiversity and ecosystem functioning: Current knowledge and future challenges. *Science* 294:804–808.

Macfadyen, A. (1961). Improved funnel-type extractors for soil arthropods. *Journal of Animal Ecology* 30:171–184.

Martinez, N. D. (1991). Artifacts or attributes? effects of resolution on the little rock lake food web. *Ecological Monographs* 61:367–392.

May, R. M. (1972). Will a large complex system be stable? *Nature* 238:413–414.

May, R. M. (1973*a*). Qualitative stability in model ecosystems. *Ecology* 54:638–641.

May, R. M., (1973*b*). *Stability and Complexity in Model Ecosystems*. Princeton University Press, Princeton. ISBN 0-691-08125-1.

McCann, K. and Hastings, A. (1997). Re-evaluating the omnivory-stability relationship in food webs. *Proceedings of the Royal Society of London. Series B: Biological Sciences* 264:1249–1254.

McCann, K., Hastings, A., and Huxel, G. R. (1998). Weak trophic interactions and the balance of nature. *Nature* 395:794–798.

McCann, K. S. (2000). The diversity-stability debate. *Nature* 405:228–233.

McGill, B. J., Enquist, B. J., Weiher, E., and Westoby, M. (2006). Rebuilding community ecology from functional traits. *Trends in Ecology & Evolution* 21:178–185.

McGrady-Steed, J., Harris, P. M., and Morin, P. J. (1997). Biodiversity regulates ecosystem predictability. *Nature* 390:162–165.

McLaughlin, O. B., Jonsson, T., and Emmerson, M. C., (2010). Temporal variability in predator–prey relationships of a forest floor food web. Pages 171–264 in *G. Woodward, ed. Ecological Networks*, volume 42 of *Advances in Ecological Research*. Academic Press, London, UK. ISBN 978-0-12-381363-3.

McNab, B. K., (2002). *The Physiological Ecology of Vertebrates: A View from Energetics*. Comstock Publishing Associates, Ithaca, NY. ISBN 978-0-8014-3913-1.

Meehan, T. D. (2006). Energy use and animal abundance in litter and soil communities. *Ecology* 87:1650–1658.

Mikola, J. and Setälä, H. (1998). No evidence of trophic cascades in an experimental microbial-based soil food web. *Ecology* 79:153–164.

Millennium Ecosystem Assessment, (2005). Ecosystems and human well-being: Synthesis. *in* Millennium Ecosystem Assessment. Island Press, Washington, USA. ISBN 1-59726-040-1.

Milo, R., Shen-Orr, S., Itzkovitz, S., Kashtan, N., Chklovskii, D., and Alon, U. (2002). Network motifs: Simple building blocks of complex networks. *Science* 298:824–827.

Montagna, P. A., Blanchard, G. F., and Dinet, A. (1995). Effect of production and biomass of intertidal microphytobenthos on meiofaunal grazing rates. *Journal of Experimental Marine Biology and Ecology* 185:149–165.

Montoya, J. M. and Raffaelli, D. (2010). Climate change, biotic interactions and ecosystem services. *Philosophical Transactions of the Royal Society B: Biological Sciences* 365:2013–2018.

Moulder, B. C. and Reichle, D. E. (1972). Significance of spider predation in the energy dynamics of forest-floor arthropod communities. *Ecological Monographs* 42:473–498.

Munyaneza, J. and Obrycki, J. J. (1997). Functional response of coleomegilla maculata (Coleoptera: coccinellidae) to colorado potato beetle eggs (Coleoptera: chrysomelidae). *Biological Control* 8:215–224.

Murdoch, W. W., Avery, S., and Smyth, M. E. B. (1975). Switching in predatory fish. *Ecology* 56:1094–1105.

Naeem, S. (2002). Ecosystem consequences of biodiversity loss: the evolution of a paradigm. *Ecology* 83:1537–1552.

Naeem, S., Duffy, J. E., and Zavaleta, E. (2012). The functions of biological diversity in an age of extinction. *Science* 336:1401–1406.

Naeem, S. and Li, S. (1997). Biodiversity enhances ecosystem reliability. *Nature* 390:507–509.

Naeem, S., Loreau, M., and Inchausti, P., (2002). Biodiversity and ecosystem functioning: the emergence of a synthetic ecological framework in *M. Loreau, S. Naeem, and P. Inchausti, eds. Biodiversity and Ecosystem Functioning: Synthesis and Perspectives*. Oxford University Press, New York, USA. ISBN 978-0-19-851571-5.

Naeem, S., Thompson, L. J., Lawler, S. P., Lawton, J. H., and Woodfin, R. M. (1994). Declining biodiversity can alter the performance of ecosystems. *Nature* 368:734–737.

Naisbit, R. E., Rohr, R. P., Rossberg, A. G., Kehrli, P., and Bersier, L. (2012). Phylogeny versus body size as determinants of food web structure. *Proceedings of the Royal Society B: Biological Sciences* published online, doi:10.1098/rspb.2012.0327.

Neutel, A., Heesterbeek, J. A., and de Ruiter, P. C. (2002). Stability in real food webs: weak links in long loops. *Science* 296:1120–1123.

Neutel, A. M., Heesterbeek, J. A. P., van de Koppel, J., Hoenderboom, G., Vos, A., Kaldeway, C., Berendse, F., and de Ruiter, P. C. (2007). Reconciling complexity with stability in naturally assembling food webs. *Nature* 449:599–602.

Oaten, A. and Murdoch, W. W. (1975). Functional response and stability in predator-prey systems. *American Naturalist* page 289–298.

O'Connor, N. E., Grabowski, J. H., Ladwig, L. M., and Bruno, J. F. (2008). Simulated predator extinctions: predatot identity affects survival and recruitment of oysters. *Ecology* 89:428–438.

Oelbermann, K., Langel, R., and Scheu, S. (2008). Utilization of prey from the decomposer system by generalist predators of grassland. *Oecologia* 155:605–617.

Oelbermann, K. and Scheu, S. (2010). Trophic guilds of generalist feeders in soil animal communities as indicated by stable isotope analysis (15N/14N). *Bulletin of entomological research* 100:511–520.

O'Gorman, E. J. and Emmerson, M. C., (2010). Manipulating interaction strengths and the consequences for trivariate patterns in a marine food web. page 301–419 in *G. Woodward, ed. Ecological Networks*, volume 42 of *Advances in Ecological Research*. Academic Press, London, UK. ISBN 978-0-12-381363-3.

O'Gorman, E. J. and Emmerson, M. C. (2011). Body mass–abundance relationships are robust to cascading effects in marine food webs. *Oikos* 120:520–528.

O'Gorman, E. J., Enright, R. A., and Emmerson, M. C. (2008). Predator diversity enhances secondary production and decreases the likelihood of trophic cascades. *Oecologia* 158:557–567.

O'Gorman, E. J., Fitch, J. E., and Crowe, T. P. (2012). Multiple anthropogenic stressors and the structural properties of food webs. *Ecology* 93:441–448.

O'Gorman, E. J., Jacob, U., Jonsson, T., and Emmerson, M. C. (2010). Interaction strength, food web topology and the relative importance of species in food webs. *Journal Of Animal Ecology* 79:682–692.

Oksanen, L., Fretwell, S. D., Arruda, J., and Niemela, P. (1981). Exploitation ecosystems in gradients of primary productivity. *The American Naturalist* 118:240–261.

Ólafsson, E., Modig, H., and van de Bund, W. (1999). Species specific uptake of radio-labelled phytodetritus by benthic meiofauna from the baltic sea. *Marine Ecology Progress Series* 177:63–72.

Otto, S. B., Berlow, E. L., Rank, N. E., Smiley, J., and Brose, U. (2008). Predator diversity and identity drive interaction strength and trophic cascades in a food web. *Ecology* 89:134–144.

Otto, S. B., Rall, B. C., and Brose, U. (2007). Allometric degree distributions facilitate food-web stability. *Nature* 450:1226–1229.

Pace, M. L., Cole, J. J., Carpenter, S. R., and Kitchell, J. F. (1999). Trophic cascades revealed in diverse ecosystems. *Trends in Ecology & Evolution* 14:483–488.

Paine, R. T. (1966). Food web complexity and species diversity. *The American Naturalist* 100:65–75.

Paine, R. T. (1980). Food webs: linkage, interaction strength and community infrastructure. *Journal of Animal Ecology* 49:667–685.

Parmesan, C., Yohe, G., *et al.* (2003). A globally coherent fingerprint of climate change impacts across natural systems. *Nature* 421:37–42.

Parsons, T. R., Maita, Y., and Lalli, C. M., (1984). *A manual of chemical and biological methods for seawater analysis*. Pergamon Press, Oxford, UK. ISBN 978-0-08-030287-4.

Persson, L. (1999). Trophic cascades: abiding heterogeneity and the trophic level concept at the end of the road. *Oikos* 85:385–397.

Persson, L., Leonardsson, K., de Roos, A. M., Gyllenberg, M., and Christensen, B. (1998). Ontogenetic scaling of foraging rates and the dynamics of a size-structured consumer-resource model. *Theoretical Population Biology* 54:270–293.

Peschel, K., Norton, R. A., Scheu, S., and Maraun, M. (2006). Do oribatid mites live in enemy-free space? evidence from feeding experiments with the predatory mite *Pergamasus septentrionalis*. *Soil Biology and Biochemistry* 38:2985–2989.

Petchey, O. L., (2007). Effects of environmental variability on ecological communities: testing the insurance hypothesis of biodiversity in aquatic microcosms in *D. A. Vasseur and K. S. McCann,*

eds. The impact of environmental variability on ecological systems, number 2 in The Peter Yodzis fundamental ecology series. Springer, Dordrecht, NL. ISBN 978-1-4020-5850-9.

Petchey, O. L. (2010). Maximum entropy in ecology. *Oikos* 119:577–577.

Petchey, O. L., Beckerman, A. P., Riede, J. O., and Warren, P. H. (2008*a*). Size, foraging, and food web structure. *Proceedings of the National Academy of Sciences, U.S.A.* 105:4191–4196.

Petchey, O. L., Beckerman, A. P., Riede, J. O., and Warren, P. H. (2011). Fit, efficiency, and biology: Some thoughts on judging food web models. *Journal of Theoretical Biology* 279:169–171.

Petchey, O. L., Eklöf, A., Borrvall, C., and Ebenman, B. (2008*b*). Trophically unique species are vulnerable to cascading extinction. *The American Naturalist* 171:568–579.

Petchey, O. L. and Gaston, K. J. (2002). Extinction and the loss of functional diversity. *Proceedings of the Royal Society of London. Series B: Biological Sciences* 269:1721–1727.

Petchey, O. L. and Gaston, K. J. (2006). Functional diversity: back to basics and looking forward. *Ecology Letters* 9:741–758.

Petchey, O. L. and Gaston, K. J. (2007). Dendrograms and measuring functional diversity. *Oikos* 116:1422–1426.

Petchey, O. L., McPhearson, P. T., Casey, T. M., and Morin, P. J. (1999). Environmental warming alters food-web structure and ecosystem function. *Nature* 402:69–72.

Petchey, O. L., O'Gorman, E., and Flynn, D. F., (2009). A functional guide to functional diversity measures. Pages 49–59 in *S. Naeem, D. E. Bunker, A. Hector, M. Loreau, and C. Perrings, eds. Biodiversity, ecosystem functioning, and human wellbeing: an ecological and economic perspective.* Oxford University Press, New York, USA. ISBN 978-0-19-954795-1.

Peters, R. H., (1983). *The Ecological Implications of Body Size.* Cambridge University Press, Cambridge, UK. ISBN 978-0-521-28886-6.

Pimm, S. L., (1982). *Food Webs*, volume 2002, University of Chicago Press, Chicago, USA. Chapman and Hall, New York, USA. ISBN 978-0-226-66832-1.

Pimm, S. L. (1984). The complexity and stability of ecosystems. *Nature* 307:321–326.

Pimm, S. L. and Lawton, J. H. (1978). Feeding on more than one trophic level. *Nature* 275:542–544.

Pinheiro, J., Bates, D., DebRoy, S., Sarkar, D., and R Development Core Team, (2011). nlme: Linear and nonlinear mixed effects models.

Polis, G. A. (1991). Complex trophic interactions in deserts: an empirical critique of food-web theory. *The American Naturalist* 138:123–155.

Polis, G. A. (1994). Food webs, trophic cascades and community structure. *Australian Journal Of Ecology* 19:121–136.

Polis, G. A. (1999). Why are parts of the world green? multiple factors control productivity and the distribution of biomass. *Oikos* 86:3–15.

Polis, G. A. and Holt, R. D. (1992). Intraguild predation - the dynamics of complex trophic interactions. *Trends In Ecology & Evolution* 7:151–154.

Polis, G. A., Sears, A., Huxel, G. R., Strong, D. R., and Maron, J. (2000). When is a trophic cascade a trophic cascade? *Trends in Ecology & Evolution* 15:473–476.

Polis, G. A. and Strong, D. R. (1996). Food web complexity and community dynamics. *The American Naturalist* 147:813–846.

Ponsard, S., Arditi, R., and Jost, C. (2000). Assessing top-down and bottom-up control in a litter-based soil macroinvertebrate food chain. *Oikos* 89:524–540.

Power, M. E. (1992). Top-down and bottom-up forces in food webs: do plants have primacy. *Ecology* 73:733–746.

Purvis, A., Gittleman, J. L., Cowlishaw, G., and Mace, G. M. (2000*a*). Predicting extinction risk in declining species. *Proceedings of the Royal Society of London. Series B: Biological Sciences* 267:1947–1952.

Purvis, A., Jones, K. E., and Mace, G. M. (2000*b*). Extinction. *BioEssays* 22:1123–1133.

R Development Core Team, (2010). *R: A language and environment for statistical computing, v 2.12.0.* R Foundation for Statistical Computing, Vienna, Austria. ISBN 3-900051-07-0.

R Development Core Team, (2011). *R: A language and environment for statistical computing, v 2.13.0.* R Foundation for statistical computing, Vienna, Austria. ISBN 3-900051-07-0.

Raffaelli, D., (2007). Food webs, body size and the curse of the latin binomial. page 53–64 in *N. Rooney, K. McCann, and D. Noakes, eds. From Energetics to Ecosystems: The Dynamics and Structure of Ecological Systems*, number 1 in The Peter Yodzis Fundamental Ecology Series. Springer, Dordrecht, NL. ISBN 978-1-4020-5336-8.

Rall, B. C., Brose, U., Hartvig, M., Kalinkat, G., Schwarzmüller, F., Vucic-Pestic, O., and Petchey, O. L. (2012). Universal temperature and body-mass scaling of feeding rates. *Philosophical Transactions of the Royal Society B: Biological Sciences* in press, doi: 10.1098/rstb.2012.0242.

Rall, B. C., Guill, C., and Brose, U. (2008). Food-web connectance and predator interference dampen the paradox of enrichment. *Oikos* 117:202–213.

Rall, B. C., Kalinkat, G., Ott, D., Vucic-Pestic, O., and Brose, U. (2011). Taxonomic versus allometric constraints on non-linear interaction strengths. *Oikos* 120:483–492.

Rall, B. C., Vucic-Pestic, O., Ehnes, R. B., Emmerson, M. C., and Brose, U. (2010). Temperature, predator–prey interaction strength and population stability. *Global Change Biology* 16:2145–2157.

Real, L. A. (1977). The kinetics of functional response. *The American Naturalist* 111:289–300.

Reiss, J., Bailey, R. A., Perkins, D. M., Pluchinotta, A., and Woodward, G. (2011). Testing effects of consumer richness, evenness and body size on ecosystem functioning. *Journal of Animal Ecology* 80:1145–1154.

Reiss, J., Bridle, J. R., Montoya, J. M., and Woodward, G. (2009). Emerging horizons in biodiversity and ecosystem functioning research. *Trends in Ecology & Evolution* 24:505–514.

Riede, J. O., Brose, U., Ebenman, B., Jacob, U., Thompson, R., Townsend, C. R., and Jonsson, T. (2011). Stepping in elton's footprints: a general scaling model for body masses and trophic levels across ecosystems. *Ecology Letters* 14:169–178.

Rogers, D. (1972). Random search and insect population models. *Journal of Animal Ecology* 41:369–383.

Romanuk, T. N., Vogt, R. J., and Kolasa, J. (2006). Nutrient enrichment weakens the stabilizing effect of species richness. *Oikos* 114:291–302.

Rooney, N., McCann, K., Gellner, G., and Moore, J. C. (2006). Structural asymmetry and the stability of diverse food webs. *Nature* 442:265–269.

Rooney, N. and McCann, K. S. (2012). Integrating food web diversity, structure and stability. *Trends in Ecology & Evolution* 27:40–46.

Royama, T. (1971). A comparative study of models for predation and parasitism. *Researches on Population Ecology* 13:1–91.

Rzanny, M. and Voigt, W. (2012). Complexity of multitrophic interactions in a grassland ecosystem depends on plant species diversity. *Journal of Animal Ecology* 81:614–627.

Sarnelle, O. and Wilson, A. E. (2008). Type III functional response in daphnia. *Ecology* 89:1723–1732.

Savage, V. M., Gillooly, J. F., Brown, J. H., West, G. B., and Charnov, E. L. (2004). Effects of body size and temperature on population growth. *The American Naturalist* 163:429–441.

Savage, V. M., Webb, C. T., and Norberg, J. (2007). A general multi-trait-based framework for studying the effects of biodiversity on ecosystem functioning. *Journal of Theoretical Biology* 247:213–229.

Schaefer, M. (1990). The soil fauna of a beech forest on limestone: trophic structure and energy budget. *Oecologia* 82:128–136.

Scheu, S. (1992). Automated measurement of the respiratory response of soil microcompartments - active microbial biomass in earthworm feces. *Soil Biology & Biochemistry* 24:1113–1118.

Scheu, S. and Falca, M. (2000). The soil food web of two beech forests (*Fagus sylvatica*) of contrasting humus type: stable isotope analysis of a macro- and a mesofauna-dominated community. *Oecologia* 123:285–296.

Scheu, S. and Schaefer, M. (1998). Bottom-up control of the soil macrofauna community in a beechwood on limestone: Manipulation of food resources. *Ecology* 79:1573–1585.

Scheu, S. and Setälä, H., (2002). Multitrophic interactions in decomposer food-webs in *T. Tscharntke and B. A. Hawkins, eds. Multitrophic Level Interactions*. Cambridge University Press, Cambridge, UK. ISBN 978-0-521-08418-5.

Schmid, B., Balvanera, P., Cardinale, B. J., Godbold, J., Pfisterer, A. B., Raffaelli, D., Solan, M., and Srivastava, D. S., (2009). Consequences of species loss for ecosystem functioning : meta-analyses of data from biodiversity experiments. Pages 14–29 in *S. Naeem, D. E. Bunker, A. Hector, M. Loreau, and C. Perrings, eds. Biodiversity, Ecosystem Functioning, & Human Wellbeing An Ecological and Economic Perspective*. Oxford University Press, Oxford, UK, 2 edition. ISBN 978-0-19-954796-8.

Schmitz, O. J. (2007). Predator diversity and trophic interactions. *Ecology* 88:2415–2426.

Schmitz, O. J., Hambäck, P. A., and Beckerman, A. P. (2000). Trophic cascades in terrestrial systems: a review of the effects of carnivore removals on plants. *The American Naturalist* 155:141–153.

Schmitz, O. J., Krivan, V., and Ovadia, O. (2004). Trophic cascades: the primacy of trait-mediated indirect interactions. *Ecology Letters* 7:153–163.

Schneider, F. D., Scheu, S., and Brose, U. (2012). Body mass constraints on feeding rates determine the consequences of predator loss. *Ecology Letters* 15:436–443.

Sheldon, R. W., Prakash, A., and Sutcliffe Jr, W. H. (1972). The size distribution of particles in the ocean. *Limnology and Oceanography* page 327–340.

Sheridan, J. A. and Bickford, D. (2011). Shrinking body size as an ecological response to climate change. *Nature Climate Change* 1:401–406.

Shurin, J. B., Borer, E. T., Seabloom, E. W., Anderson, K., Blanchette, C. A., Broitman, B., Cooper, S. D., and Halpern, B. S. (2002). A cross-ecosystem comparison of the strength of trophic cascades. *Ecology Letters* 5:785–791.

Shurin, J. B., Gardner, J. L., Greig, H. S., Kratina, P., and Thompson, P. L. (2012). Warming shifts top-down and bottom-up control of pond food web structure and function. *Philosophical Transactions of the Royal Society B: Biological Sciences* in press: 10.1098/rstb. 2012.0243.

Sih, A. (1984). Optimal behavior and density-dependent predation. *The American Naturalist* 123:314–326.

Sih, A., Englund, G., and Wooster, D. (1998). Emergent impacts of multiple predators on prey. *Trends in Ecology & Evolution* 13:350–355.

Sinclair, A. R. E., Mduma, S., and Brashares, J. S. (2003). Patterns of predation in a diverse predator-prey system. *Nature* 425:288–290.

Skalski, G. and Gilliam, J. (2002). Feeding under predation hazard: testing models of adaptive behavior with stream fish. *The American Naturalist* 160:158–172.

Skalski, G. T. and Gilliam, J. F. (2001). Functional responses with predator interference: viable alternatives to the holling type II model. *Ecology* 82:3083–3092.

Smith, V. H., Tilman, G. D., and Nekola, J. C. (1999). Eutrophication: impacts of excess nutrient inputs on freshwater, marine, and terrestrial ecosystems. *Environmental pollution* 100:179–196.

Soetaert, K., Petzoldt, T., and Setzer, R. W. (2010). Solving differential equations in R: package deSolve. *Journal of Statistical Software* 33:1–25.

Solan, M., Godbold, J., Symstad, A., Flynn, D. F. B., and Bunker, D. E., (2009). Biodiversity-ecosystem function research and biodiversity futures: early bird catches the worm or a day late and a dollar short? Pages 30–45 in *S. Naeem, D. E. Bunker, A. Hector, M. Loreau, and C. Perrings, eds. Biodiversity, ecosystem functioning, and human wellbeing: an ecological and economic perspective*. Oxford University Press, New York, USA. ISBN 978-0-19-954795-1.

Sole, R. V. and Montoya, M. (2001). Complexity and fragility in ecological networks. *Proceedings of the Royal Society of London. Series B: Biological Sciences* 268:2039–2045.

Solomon, M. E. (1949). The natural control of animal populations. *The Journal of Animal Ecology* 18:1–35.

Spitze, K. (1985). Functional response of an ambush predator: *Chaoborus americanus* predation on *Daphnia pulex*. *Ecology* 66:938–949.

Steiner, C. F. (2001). The effects of prey heterogeneity and consumer identity on the limitation of trophic-level biomass. *Ecology* 82:2495–2506.

Stouffer, D. B., Camacho, J., Jiang, W., and Amaral, L. A. N. (2007). Evidence for the existence of a robust pattern of prey selection in food webs. *Proceedings of the Royal Society of London. Series B: Biological Sciences* 274:1931–1940.

Stouffer, D. B., Rezende, E. L., and Amaral, L. A. N. (2011). The role of body mass in diet contiguity and food-web structure. *Journal of Animal Ecology* 80:632–639.

Strong, D. R. (1992). Are trophic cascades all wet? differentiation and Donor-Control in speciose ecosystems. *Ecology* 73:747–754.

Thébault, E. and Loreau, M. (2003). Food-Web constraints on Biodiversity–Ecosystem functioning relationships. *Proceedings of the National Academy of Sciences, U.S.A.* 100:14949–14954.

Thébault, E. and Loreau, M. (2005). Trophic interactions and the relationship between species diversity and ecosystem stability. *The American Naturalist* 166:E95–E114.

Thébault, E. and Loreau, M. (2006). The relationship between biodiversity and ecosystem functioning in food webs. *Ecological Research* 21:17–25.

Tilman, D., (1982). *Resource Competition and Community Structure*. Princeton University Press, Princeton, USA. ISBN 978-0-691-08302-5.

Tilman, D. (1999). The ecological consequences of changes in biodiversity: a search for general principles. *Ecology* 80:1455–1474.

Tilman, D. and Downing, J. A. (1994). Biodiversity and stability in grasslands. *Nature* 367:363–365.

Tilman, D., Knops, J., Wedin, D., Reich, P., Ritchie, M., and Siemann, E. (1997). The influence of functional diversity and composition on ecosystem processes. *Science* 277:1300–1302.

Tilman, D., Lehman, C. L., and Bristow, C. E. (1998). Diversity-Stability relationships: Statistical inevitability or ecological consequence? *The American Naturalist* 151:277–282.

Twomey, M., Brodte, E., Jacob, U., Brose, U., Crowe, T. P., and Emmerson, M. C. (2012). Idiosyncratic species effects confound size-based predictions of responses to climate change. *Philosophical Transactions of the Royal Society B: Biological Sciences* in press.

Van De Pol, M., Ens, B. J., Heg, D., Brouwer, L., Krol, J., Maier, M., Exo, K. M., Oosterbeek, K., Lok, T., Eising, C. M., *et al.* (2010). Do changes in the frequency, magnitude and timing of extreme climatic events threaten the population viability of coastal birds? *Journal of Applied Ecology* 47:720–730.

Vandermeer, J. (2006). Omnivory and the stability of food webs. *Journal of Theoretical Biology* 238:497–504.

Vonesh, J. R. and Bolker, B. M. (2005). Compensatory larval responses shift trade-offs associated with predator-induced hatching plasticity. *Ecology* 86:1580–1591.

Vucic-Pestic, O., Ehnes, R. B., Rall, B. C., and Brose, U. (2011). Warming up the system: higher predator feeding rates but lower energetic efficiencies. *Global Change Biology* 17:1301–1310.

Vucic-Pestic, O., Rall, B. C., Kalinkat, G., and Brose, U. (2010). Allometric functional response model: body masses constrain interaction strengths. *Journal of Animal Ecology* 79:249–256.

Wahlström, E., Persson, L., Diehl, S., and Bystrom, P. (2000). Size-dependent foraging efficiency, cannibalism and zooplankton community structure. *Oecologia* 123:138–148.

Wardle, D. A. (1999). Is "Sampling effect" a problem for experiments investigating biodiversity-ecosystem function relationships? *Oikos* 87:403–407.

Weitz, J. S. and Levin, S. A. (2006). Size and scaling of predator–prey dynamics. *Ecology Letters* 9:548–557.

Werner, E. E. and Peacor, S. D. (2003). A review of trait-mediated indirect interactions in ecological communities. *Ecology* 84:1083–1100.

West, G. B., Brown, J. H., and Enquist, B. J. (1997). A general model for the origin of allometric scaling laws in biology. *Science* 276:122–126.

West, G. B., Brown, J. H., and Enquist, B. J. (1999). The fourth dimension of life: fractal geometry and allometric scaling of organisms. *Science* 284:1677–1680.

White, E., Ernest, S., Kerkhoff, A., and Enquist, B. (2007). Relationships between body size and abundance in ecology. *Trends in Ecology & Evolution* 22:323–330.

Williams, R. J. and Martinez, N. D. (2000). Simple rules yield complex food webs. *Nature* 404:180–183.

Williams, R. J. and Martinez, N. D. (2004*a*). Limits to trophic levels and omnivory in complex food webs: Theory and data. *The American Naturalist* 163:458–468.

Williams, R. J. and Martinez, N. D. (2004*b*). Stabilization of chaotic and non-permanent food web dynamics. *European Physical Journal B: Condensed Matter and Complex Systems* 38:297–303.

Wollrab, S., Diehl, S., and De Roos, A. M. (2012). Simple rules describe bottom-up and top-down control in food webs with alternative energy pathways. *Ecology Letters* 15:935–946.

Wood, S. N. (2010). Fast stable restricted maximum likelihood and marginal likelihood estimation of semiparametric generalized linear models. *Journal of the Royal Statistical Society: Series B (Statistical Methodology)* 73:3–36.

Woodward, G., (2010). *Ecological Networks*. Number 42 in Advances in Ecological Research. Academic Press, London, UK. ISBN 978-0-12-381363-3.

Woodward, G., Blanchard, J., Lauridsen, R. B., Edwards, F. K., Jones, J. I., Figueroa, D., Warren, P. H., and Petchey, O. L., (2010). Individual-Based food webs: Species identity, body size and sampling effects. Pages 211–266 in *G. Woodward, ed. Integrative Ecology: From Molecules to Ecosystems*, number 43 in Advances in Ecological Research. Academic Press, London, UK. ISBN 978-0-12-385005-8.

Woodward, G., Ebenman, B., Ernmerson, M., Montoya, J. M., Olesen, J. M., Valido, A., and Warren, P. H. (2005). Body size in ecological networks. *Trends in Ecology & Evolution* 20:402–409.

Woodward, G. and Hildrew, A. G. (2002). Body-size determinants of niche overlap and intraguild predation within a complex food web. *Journal of Animal Ecology* 71:1063–1074.

Wootton, J. T. (1997). Estimates and tests of per capita interaction strength: diet, abundance, and impact of intertidally foraging birds. *Ecological Monographs* 67:45–64.

Wootton, J. T. and Emmerson, M. (2005). Measurement of interaction strength innature. *Annual Review of Ecology, Evolution, and Systematics* 36:419–444.

Worm, B., Lotze, H. K., Hillebrand, H., Sommer, U., *et al.* (2002). Consumer versus resource control of species diversity and ecosystem functioning. *Nature* 417:848–851.

Worsfold, N. T., Warren, P. H., and Petchey, O. L. (2009). Context-dependent effects of predator removal from experimental microcosm communities. *Oikos* 118:1319–1326.

Yachi, S. and Loreau, M. (1999). Biodiversity and ecosystem productivity in a fluctuating environment: The insurance hypothesis. *Proceedings of the National Academy of Sciences, U.S.A.* 96:1463–1468.

Yodzis, P. (1981). The stability of real ecosystems. *Nature* 289:674–676.

Yodzis, P. (1998). Local trophodynamics and the interaction of marine mammals and fisheries in the benguela ecosystem. *Journal of Animal Ecology* 67:635–658.

Yodzis, P. (2000). Diffuse effects in food webs. *Ecology* 81:261–266.

Yodzis, P. (2001). Must top predators be culled for the sake of fisheries? *Trends in Ecology & Evolution* 16:78–84.

Yodzis, P. and Innes, S. (1992). Body size and consumer-resource dynamics. *The American Naturalist* 139:1151–1175.

Yvon-Durocher, G., Montoya, J. M., Trimmer, M., and Woodward, G. (2011). Warming alters the size spectrum and shifts the distribution of biomass in freshwater ecosystems. *Global Change Biology* 17:1681–1694.

Zook, A. E., Eklöf, A., Jacob, U., and Allesina, S. (2010). Food webs: Ordering species according to body size yields high degree of intervality. *Journal of Theoretical Biology* 271:106–113.

Zuur, A. F., Ieno, E. N., Walker, N., Saveliev, A. A., and Smith, G. M., (2009). *Mixed Effects Models and Extensions in Ecology with R.* Springer Science+Business Media, New York, USA. ISBN 978-0-387-87457-9.

Acknowledgements / Danksagungen

Zuerst danke ich meinem Doktorvater **Ulrich Brose** für dreieinhalb Jahre Betreuung. Ich danke für die Gelegenheit über dieses spannende Thema zu promovieren; fürs gnadenlose Geradekommentieren meiner unausgereiften Texte und vor allem Titel; für aufbauende Worte und Lob; für die uneingeschränkte Gestaltungsmöglichkeit meiner Projekte; kurz: für die besten Arbeitsbedingungen, die man sich als Doktorand wünschen kann.

Dank an die **Deutsche Bundesstiftung Umwelt**, die mich drei Jahre lang mit einem Promotionsstipendium unterstützt hat.

Kay Hamacher und **Nico Blüthgen** danke ich für das Bereitstellen eines Arbeitsplatzes am Fachbereich Biologie in Darmstadt.

Björn Rall möchte ich danken für viele Diskussionen, geduldige Erklärungen und so manchen nützlichen R-Code. Ohne dich hätte ich mich nicht so ohne Weiteres ans Programmieren herangetraut.

Mit den Diplomarbeiten von **Malte Jochum** und **Thomas Schimmer**, sowie der Examensarbeit von **Anna Schmehl** durfte ich drei großartige Abschlussarbeiten mitbetreuen. Es hat sehr viel Spaß gemacht, mit euch zusammenzuarbeiten.

Eine ganze Menge Leute waren als HiWis oder Praktikanten an den Experimenten beteiligt. Vielen Dank dafür!

Ganz besonderer Dank gebührt **Dora Volovei** und **Petra Hosumbek**. Ohne euch wären die Laborexperimente und vieles Andere undenkbar gewesen. Wirklich!

I am grateful to the co-authors of the chapters of this thesis, especially to **Malte Jochum** and **Eoin O'Gorman** for taking me to the Lough Hyne.

Thanks to all proof-readers of the chapters of the chapters in this thesis and of course to all other colleagues of Uli's singular working group. I hope this is just the beginning of many years of collaboration and shared research projects.

Ich danke **Amrei Binzer** und **Birgit Lang** für die Wohnung in Göttingen.

Ebenso danke ich **Gregor Kalinkat** und **Roswitha Ehnes**, dafür dass wir es gemeinsam an der Uni in Darmstadt ausgehalten haben, auch ohne eine *eigene* Arbeitsgruppe; Dieser Mangel wurde vollständig behoben durch **Franzi**, **Phillip**, **Steffi**, **Sabine**, **Patrick**, **Frank** und dem Rest der AG Hamacher. Die letzten zwei Jahre wären sehr trostlos gewesen ohne euch. Danke für alles.

Zuletzt möchte ich natürlich denen danken, ohne die ich überhaupt nicht da wäre, wo ich heute bin; **allen Freunden**, die während dem Studium und neben dem Studium immer da waren; **meinen Eltern**, auf deren uneingeschränkte Unterstützung ich immer Vertrauen konnte und können werde; **meiner Oma**, die sich so sehr über diesen Abschluss freut.

Und natürlich **Rike**. Ich liebe dich sehr.

Ehrenwörtliche Erklärung

Ich erkläre hiermit ehrenwörtlich, dass ich die vorliegende Arbeit entsprechend den Regeln guter wissenschaftlicher Praxis selbstständig und ohne unzulässige Hilfe Dritter angefertigt habe. Sämtliche aus fremden Quellen direkt oder indirekt übernommenen Gedanken sowie sämtliche von Anderen direkt oder indirekt übernommenen Daten, Techniken und Materialien sind als solche kenntlich gemacht. Die Arbeit wurde bisher bei keiner anderen Hochschule zu Prüfungszwecken eingereicht.

Florian Dirk Schneider
Darmstadt, 07.09.2012

Curriculum Vitae

Dipl.-Biol. Florian Dirk Schneider

Personal Details

Date of Birth:	05.12.1981
Place of Birth:	Darmstadt
Marital Status:	unmarried

Work Experience

Since March ’11 — **Scientific assistant** at Georg-August-University Göttingen (GER), group of Prof. Dr. Ulrich Brose (Systemic Conservation Ecology)

- Mentoring of undergraduate research (Diploma-theses)

March ’09 - Feb. ’11 — **Scientific assistant** at Technische Universität Darmstadt (GER), group of Dr. Ulrich Brose (Ecological Networks)

- Tutorial in student courses
- Mentoring of undergraduate research (Diploma-theses)

Dec. ’07 - Dec. ’08 — Undergraduate **student assistant** at the Centre for Interdisciplinary Study Programs (CISP), Technische Universität Darmstadt

- Artwork and management for information media and web presence
- Tutorials in interdisciplinary student courses (project management)
- Technical management of guest lectures

Higher Education

March ’09 - present — PhD at Technische Universität Darmstadt (GER), group of Dr. Ulrich Brose (Ecological Networks)

- Research topic: "**Predator diversity and ecosystem functioning: An allometric approach**"
- Funded by a PhD-fellowship of Deutsche Bundesstiftung Umwelt (www.DBU.de)

Oct. '02 - Jan. '09	Diploma in Biology at Technische Universität Darmstadt (GER) • Diploma thesis: "Effects of predator diversity and intra-guild predation on ecosystem function" • result: "very good", 1.0 • Major subjects: Ecology, Environmental Science, and Botany

Civil Service

Sept. '01 - June '02	Civil Service at Verband Christlicher Pfadfinderinnen und Pfadfinder (VCP), Landesverband Hessen, in Bad Nauheim (GER)

School Education

1992 - 2001	Secondary school, Ernst-Göbel-Schule, Höchst im Odenwald (GER), • Abitur, result: 2.2
1988 - 1992	Primary school, Höchst im Odenwald (GER)

Additional Skills

Software:	*Operating Systems:* Microsoft Windows XP & 7, Linux (Ubuntu) *Office Tools:* Microsoft Office Word, Excel, Power Point; Open Office Writer, Calc, ImPress *Graphical Tools:* Adobe Photoshop, Adobe Illustrator, InkScape, ImageJ *Layout Tools:* Adobe Indesign, LaTeX *Programming Tools:* Eclipse, TinnR, R-studio, Subversion client and server *Programming languages:* R (proficiency), C and C++ (working knowledge), Html and Javascript (basic knowledge) *Further Software:* ArcGis & ArcView
Languages:	German (first language) English (fluent)

Voluntary Work

I was voluntary member of district and state leading committees (until 2007) of the Verband Christlicher Pfadfinderinnen und Pfadfinder (VCP, the largest protestant scouting organization in Germany). There, I headed several project groups, amongst other things developing an environmental program and a quality management for the training of group leaders.

Memberships

I am a member of the Gesellschaft für Ökologie (GfÖ), the ecological society of Germany, Austria and Switzerland.

List of publications and contributions

Publications in peer-reviewed journals

Schneider, F.D., Scheu, S., Brose, U. (2012) Body mass constraints on feeding rates determine the consequences of predator loss, *Ecology Letters*, 15:436–443, doi: 10.1111/j.1461-0248.2012.01750.x

Jochum, M., **Schneider, F.D.**, Crowe, T.P., Brose, U., O'Gorman E.J. (2012) Climate-induced changes in bottom-up and top-down processes independently alter a marine ecosystem, *Philosophical Transactions of the Royal Society B: Biological Sciences*, in press, doi: 10.1098/rstb.2012.0237

Brose, U., Dunne, J.A., Montoya, J.M., Petchey, O.L., **Schneider, F.D.**, Jacob, U. (2012) Climate change in size-structured ecosystems, *Philosophical Transactions of the Royal Society B: Biological Sciences*, in press

Schneider, F.D., Brose, U. (2012) Beyond diversity: how nested predator effects control ecosystem functions, *Journal of Animal Ecology*, conditionally accepted

Manuscripts in preparation

Schneider, F.D., Brose, U., Rall, Björn C., Guill, C., How predator diversity drives ecosystem functioning in complex food webs, in preparation

Rall, B.C., Binzer, A., Kéfi, S., **Schneider, F.D.**, Woodward, G., Brose, U., Body-masses balance weak and strong interactions to stabilize food webs, in preparation

Kalinkat, G., **Schneider, F.D.**, Schmehl, A., Schimmer, T., Vucic-Pestic, O., Guill, C., Digel, C., Brose, U., Rall, B.C. , Generalized allometric functional responses facilitate predator-prey stability, in preparation

Schneider, F.D., Brose, U., Size-structured intraguild predation simplifies the prediction of interaction strengths in complex food webs, in preparation

Conference talks

Schneider, F.D. (2012) When predators eat predators - complexity in multi-trophic food webs, DBU Fachkolloquium - Invertebraten, Ulm, GER, 13.–15.02.2012

Schneider, F.D., Brose, U., Guill., C. (2011) Allometric identity effects in multi-predator food webs, *Annual Meeting of the British Ecological Society*, Sheffield, UK, 12.–14.09.2011

Schneider, F.D., Brose, U., Guill., C. (2011) Allometric identity effects in multi-predator food webs, *Annual Meeting of the Gesellschaft für Ökologie*, Oldenburg, GER, 05.–09.09.2011

Schneider, F.D. (2011) Körpermassen als Standardgröße der Ökologie, DBU Fachkolloquium - Invertebraten, Göttingen, GER, 14.–16.03.2011

Schneider, F.D., Brose, U. (2010) Computational prediction of food web inter-action strength in an experimental forest floor community, *Annual Meeting of the Gesellschaft für Ökologie*, Gießen, GER, 30.08.–03.09.2010

Poster contributions to conferences

Schneider, F.D. (2011) Deep Thought – A scientific comic tribute to Douglas Adams, *4th Sizemic Workshop*, Hamburg, GER, 13.–15.04.2011

Schneider, F.D., Brose, U. (2010) Nested sampling effects in complex food webs: decrypting the biodiversity-function relationship, *Annual Meeting of the British Ecological Society*, Leeds, UK, 7.–9.09.2010

Schneider, F.D., Brose, U. (2010) Interaction strengths of litter-dwelling, generalist predators in a microcosm food web, *Multitrophic Interactions Workshop*, Göttingen, GER 25.–26.03.2011

"Shhh," said Loonquawl with a slight gesture, "I think Deep Thought is preparing to speak!"

"Good morning," said Deep Thought at last.

"Er...good morning, O Deep Thought," said Loonquawl nervously, "do you have...er, that is..."

"An answer for you?" interrupted Deep Thought majestically. "Yes. I have."

The two men shivered with expectancy. Their waiting had not been in vain.

"To Everything? To the great Question of Life, the Universe and Everything?"

"Yes."

"Tell us!"

"All right," said Deep Thought. "The Answer to the Great Question..."

"Yes...!"

"Of Life, the Universe and Everything..." said Deep Thought.

"Yes...!"

"Is..."

"Yes...!!!..."

"Forty-two," said Deep Thought, with infinite majesty and calm.

The Hitchhiker's Guide to the Galaxy – Douglas Adams